ABSTRACT

Title of Document: A MOLECULAR AND ISOTOPIC APPROACH TO EXAMINE THE ROLE OF TERRESTRIAL ORGANIC MATTER IN THE CARBON CYCLE OF THE ARCTIC OCEAN

Laura Lee Belicka, Doctor of Philosophy, 2009

Directed By: Professor H. Rodger Harvey, Marine, Estuarine, and Environmental Sciences

The organic carbon cycle in the Arctic Ocean is complicated by the delivery and redistribution of terrigenous material through rivers, sea-ice, and erosion. This dissertation combines an isotopic and molecular biomarker approach to assess the role that terrestrial organic carbon plays in the Arctic organic carbon cycle, with a focus on a comparison of geochemical proxies for the quantification of organic matter, an analysis of the sources and transformation of organic carbon to particulate organic matter (POM) and sediments, and an experimental investigation on the kinetics of recycling.

Estimates for preserved terrestrial organic components varied considerably for identical sediment samples, suggesting that proxies account for different sources of terrestrial material (i.e., soil versus vascular plants). In spite of the variability, an estimated 12-43% of the organic carbon preserved in surface sediments was terrestrial in origin. This contrasted sharply with surface and halocline POM, in which marine

inputs dominated despite spatial variability. With depth, POC composition reflected the increasing significance of inputs from secondary production and microbial degradation, as well as continental material. Acid-volatile sulfide (AVS) and redox-sensitive elements coupled with $\delta^{13}C$ and lipid biomarkers demonstrated a transition from intense metabolism of labile marine organic matter in shelf sediments to slower sedimentary metabolism from occasional delivery of labile organic matter in the basin. Experimental determinations of the kinetics of microbial recycling revealed striking contrasts in marine and terrestrial organic carbon lability. Marine organic matter was recycled on very short timescales compared to terrestrial organic matter, corresponding to results of sedimentary and particle analyses. A simplified box model of organic carbon cycling in the Chukchi/Alaskan Beaufort Sea region reveals that 0.9 Mt and 0.7 Mt of marine and terrestrial organic matter, respectively, are buried in shelf sediments, while an additional 0.2 Mt marine and 0.1 Mt of terrestrial organic carbon are buried in basin sediments annually, confirming that land-derived organic matter plays a large role in carbon dynamics in Arctic systems, even on non-river dominated margins.

A MOLECULAR AND ISOTOPIC APPROACH TO EXAMINE THE ROLE OF TERRESTRIAL ORGANIC MATTER IN THE CARBON CYCLE OF THE ARCTIC OCEAN

By

Laura Lee Belicka

Dissertation submitted to the Faculty of the Graduate School of the
University of Maryland, College Park, in partial fulfillment
of the requirements for the degree of
Doctor of Philosophy
2009

Advisory Committee:
Professor H. Rodger Harvey, Chair
Professor Neil Blough
Research Associate Professor Jeffrey Cornwell
Dr. Robie W. Macdonald
Professor Allen R. Place
Professor Diane K. Stoecker

Acknowledgements

I extend my sincerest thanks to my research advisor, Dr. H. Rodger Harvey, for his guidance and support throughout my time at the Chesapeake Biological Laboratory. I could not have finished this dissertation without his encouragement and kindness. I am extremely grateful for the amazing and diverse opportunities that I was involved with as a member of the Harvey Lab, ranging from research cruises in the Arctic Ocean to conferences in Spain. These opportunities not only helped to build my experience and confidence levels as a young scientist, but also sparked a love for travel and adventure that will remain long past graduate school. I am also very grateful to my additional committee members: Drs. Neil Blough, Jeffrey Cornwell, Robie Macdonald, Allen Place, and Diane Stoecker. I would like to acknowledge Dr. Neil Blough for agreeing to serve as the Dean's Representative for my dissertation defense. Dr. Jeffrey Cornwell is acknowledged for his assistance and technical support with the ^{210}Pb measurements. I also thank Drs. Allen Place and Diane Stoecker for their advice and support throughout the graduate school process. Dr. Robie Macdonald provided stimulating and challenging conversation throughout my graduate student career, and was of particular assistance with Chapter 4 of this dissertation. I am grateful to Kathy Wood and the entire Nutrient Analytical Services Laboratory for CHN analysis, to David Morris and Dr. Stephen Macko at the University of Virginia for δ^{13}C analysis, the NOSAMS lab at Woods Hole Oceanographic Institution for Δ^{14}C analysis, and also to the National Science Foundation and the CBL Graduate Education Committee for funding for this research.

I also thank past and present members of the Harvey Lab. I am grateful to have worked with Se-Jong Ju and Antonio Mannino, as they both have been instrumental in my training as a geochemist, but I am even more grateful to have them both as friends. I am also lucky to have had such wonderful lab-mates, and specifically acknowledge the friendship and research assistance that Rachael Dyda, Jessica Faux, Amy Griffin, Eli Moore, Rachel Pleuthner, Lori Roth Stansberry, Angela Squier, and Karen Taylor provided over the years. Rachel and Karen are especially acknowledged for their assistance with an experimental trial during the summer of 2008. Two summer REU students, Abby Grabitz and Charlie Morgan, are also thanked for their laboratory assistance.

A wonderful support system of friends and family has helped me along the way. I especially thank Carrie Miller, Susan Klosterhaus, Rebecca Pirtle-Levy, Arianne Balsom, and Christine Bergeron for their friendship and wonderful memories from Solomons and around the world. I am also very grateful for my yoga pals—Deanna McQuarrie Hanks, Kathy Wood, and Becca Wingate—the daily practice was definitely a high point during the writing phase. Lastly, I owe most of my success in life to my family, and I am especially grateful for my husband, Jason Snyder; my dog, Leia; my sister, Lisa Keranen; and my parents and step-parents, Linda and Ron Bashore and David and Jeanne Belicka, for their constant love and support.

Table of Contents

List of Tables

List of Figures

Chapter 1:

Chapter 2:

Chapter 3:

Chapter 4:

Chapter 5:

Chapter 6:

.

Chapter 1: Introduction

1.1. Research Overview

The Arctic Ocean has received much attention in the past two decades as the sensitivity of polar regions to climate change has become increasingly apparent. Accumulating evidence reveals decreasing sea-ice cover and thickness (Cavalieri et al., 1997; Hilmer and Lemke, 2000; Johannessen et al., 1999; Maslanik et al., 1996; Rothrock et al., 1999), increasing length of sea-ice melt season (Belchansky *et al.*, 2004; Smith, 1998), and shifting predominance from multiyear to first-year ice. Correlations between the Arctic Oscillation (AO)/North Atlantic Oscillation (NAO) and the circulation of water and sea-ice (Maslowski *et al.*, 2000) demonstrate linkages between large scale and local physical processes. Similarly, observations linking surface air temperature and hydrological changes to increasing mobilization of permafrost-bound organic carbon (Frey and Smith, 2005) have highlighted important changes in terrestrial organic carbon delivery. Despite these observations, incomplete historical records and large spatial and temporal variability often blur distinctions of documented climate changes, and many uncertainties remain as to how the atmospheric, oceanic, and terrestrial biospheres of the Arctic will respond to climate change.

What is clear, however, is that the Arctic is a complex system where understanding the impacts of the warming climate will require examination of a variety of interconnected feedback mechanisms linked to both the hydrologic cycle (including precipitation, runoff, and sea-ice) and the organic carbon cycle. These cycles are strongly

intertwined—sea-ice cover and stratification of the water column from spring runoff and ice melt exert control over the timing, location, and intensity of phytoplankton blooms, which subsequently impact higher trophic levels. Yet when conditions are favorable, some of the highest global levels of primary production have been measured on the broad continental shelves of the Arctic Ocean. Imprinted over this marine input is a strong terrestrial signal from large rivers that enter the Arctic. In fact, of all the ocean basins the Arctic is most influenced by continental runoff—representing only 1% of global ocean volume, it receives 10% of global freshwater discharge (Opsahl *et al.*, 1999). Recent studies suggest that unlike most oceanic systems, a large proportion of this terrestrial organic carbon becomes preserved in offshore sediments (Belicka *et al.*, 2004; Stein *et al.*, 2004; Yunker *et al.*, 2005). Through analysis of the modern and historical inputs of organic carbon using molecular biomarkers, we can improve source and sink estimates for Arctic carbon budgets and begin to understand how both natural and anthropogenic climate changes affect the biogeochemical cycles in this complex, sensitive environment.

The broad theme of this dissertation is the organic carbon cycle of the Arctic Ocean and how the input of terrigenous material affects the recycling and sequestration of organic carbon. My specific goals are fourfold: (i) to compare established methods for the quantification of terrestrial carbon in Arctic sediments and evaluate the implications of differences between methods for regional carbon budget development; (ii) to analyze the processes controlling the production and early diagenetic transformation of suspended particulate organic matter and the consequences of these processes for long-term carbon sequestration; (iii) to evaluate the timescales and patterns of sedimentary organic matter processing and storage; and (iv) to experimentally investigate the differential recycling

kinetics between terrestrial and marine organic matter substrates. I have utilized a coupled analytical approach using molecular organic biomarkers and isotopic analysis with both experimentally-derived and field collected samples to probe central issues of carbon cycling necessary to understand the global ramifications of Arctic climate change.

1.2. Scientific Background

1.2.1. The Global Carbon Cycle

There has been a surge in carbon cycle research over the past few decades because of the uncertainties regarding how the atmosphere, ocean, and terrestrial biosphere will respond to increasing anthropogenic emissions. The pre-industrial carbon cycle, as reconstructed by Siegenthaler and Sarmiento (1993), assumed balanced fluxes between the atmosphere, land biota, soil, rivers, and oceans through gas exchange, photosynthesis, and respiration. With the onset of the industrial revolution and our unabated burning of fossil fuels and deforestation, the carbon cycle is no longer in a steady-state and an imbalance exists between the increased atmospheric CO_2 and its sinks in the ocean and terrestrial biosphere.

In the organic compartment of the global carbon cycle, dissolved organic carbon (DOC) in the ocean is the largest carbon reservoir (Fig. 1.1), while terrestrial and marine primary production provide carbon stock for secondary production and metabolism. Although land plant biomass is far greater, terrestrial and marine plants produce similar quantities of organic carbon, estimated at 50-65 and 43.5 Gt C yr^{-1}, respectively (Behrenfeld and Falkowski, 1997). Rivers link the terrestrial and oceanic biospheres, transporting an estimated 0.8 Gt yr^{-1} of terrestrial particulate and dissolved organic

carbon to the global ocean. Microbial degradation recycles an estimated 99.5% of marine primary production and 50% of terrestrial organic matter that enters the ocean (Hedges *et al.*, 1997), but a small fraction (0.2 Gt C yr^{-1}; Fig. 1.1), becomes buried in marine sediments.

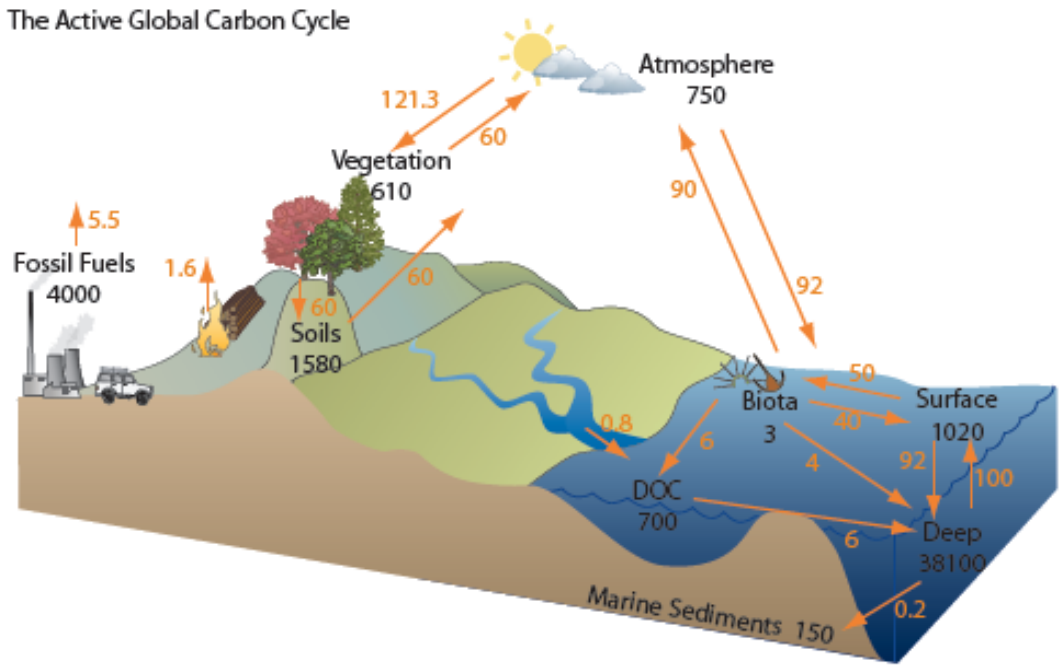

Figure 1.1. The active global carbon cycle, redrawn from Balino et al. (2001) and Siegenthaler and Sarmiento (1993). Reservoirs (Gt) and **Fluxes (Gt yr^{-1})** of carbon. Symbols courtesy of the UMCES Integration and Application Network (*ian.umces.edu/symbols/*).

Factors such as water depth, light availability, primary production/input rates, and remineralization rates impact the long-term preservation of organic matter in oceanic sediments. On continental shelves, the shallow water depths reduce organic matter recycling compared to deep water during the short fall of a particle to the sediment-water interface, despite the fact that microbial degradation is quickest in the upper water

column (Meyers, 1997). Coastal regions typically receive high levels of nutrients and detritus from runoff that can support high levels of primary productivity, sometimes resulting in similarly high rates of organic matter burial. As a result of these factors, continental shelves and margins have some of the highest levels of deposition, accounting for an estimated 80% of global sedimentary preservation of organic carbon (Hedges and Keil, 1995).

1.2.2. The Arctic: Oceanographic Setting

Oceanographic currents and water column stratification strongly influence the availability of nutrients for primary productivity. Capping central Arctic waters is the nitrate-deplete Polar Mixed Layer (PML) (Codispoti et al., 2005), occupying the upper 0-50 m and enhanced through summer ice melt and strong river inputs of freshwater. Below the PML lies the halocline, extending to approximately 225 m, which for the western Arctic can be characterized by an upper halocline (UHL) associated with waters of Pacific origin with a lower salinity (~33.1) and higher nutrient concentrations than the Atlantic-derived lower halocline (LHL) with an average salinity of 34.2-34.6 (Codispoti et al., 2005; Jones and Anderson, 1986). A warm Atlantic layer (AWL) lies between ~200-800 m, and Arctic Ocean Deep Water (AODW) comprises the deep basins of the central Arctic (Bates et al., 2005b). Two long-term surface circulation patterns are present and act to help redistribute organic matter trapped in sea-ice: 1) the anticyclonic Beaufort gyre in the Canada Basin and 2) the Transpolar Drift of Siberian water masses towards the Fram Strait (Rigor et al., 2002). Additionally, advective processes involving Pacific waters are especially important for the Chukchi and western Beaufort regions of

the western Arctic Ocean (Codispoti et al., 2005), the principal study areas of this dissertation. In particular, the delivery of nutrient-rich water northward through Bering Strait supports the extremely high productivity found in the western Bering Strait and shallow Chukchi Sea (Hill and Cota, 2005). A sea-surface pressure gradient between the Pacific and Arctic Oceans and an atmospheric pressure difference across the strait itself drives a northward 0.8 Sv annual mean inflow through Bering Strait (Coachman and Aagaard, 1966; Roach et al., 1995; Woodgate et al., 2005), which is subsequently topographically split into four main outflow pathways: Herald Valley, the Central Channel, Barrow Canyon, and Long Strait (Weingartner et al., 2005; Woodgate et al., 2005). The distinct water mass characteristics of these outflow pathways (i.e., nutrient-rich Anadyr waters in the western outflow compared to nutrient-replete waters along the eastern boundary, (Codispoti et al., 2005; Walsh et al., 1989)) strongly influence primary productivity throughout the western Arctic Ocean.

1.2.3. Sources and Transport of Organic Carbon in the Arctic

With its broad continental shelves and major rivers (Fig. 1.2) contributing organic matter from terrestrial ecosystems and its high levels of seasonal primary production, the Arctic Ocean provides an ideal location to study the complexities of organic carbon dynamics. Yet only in the past few decades, with the development of ice camps and ice-capable ships have scientists begun to realize the global significance of the Arctic Ocean. Formerly viewed as an isolated region devoid of life, with continuous ice cover and overwhelming darkness for half the year, recent measurements of high levels of primary

productivity and observations of rapid and measurable climate change have shifted attitudes and spawned major research programs.

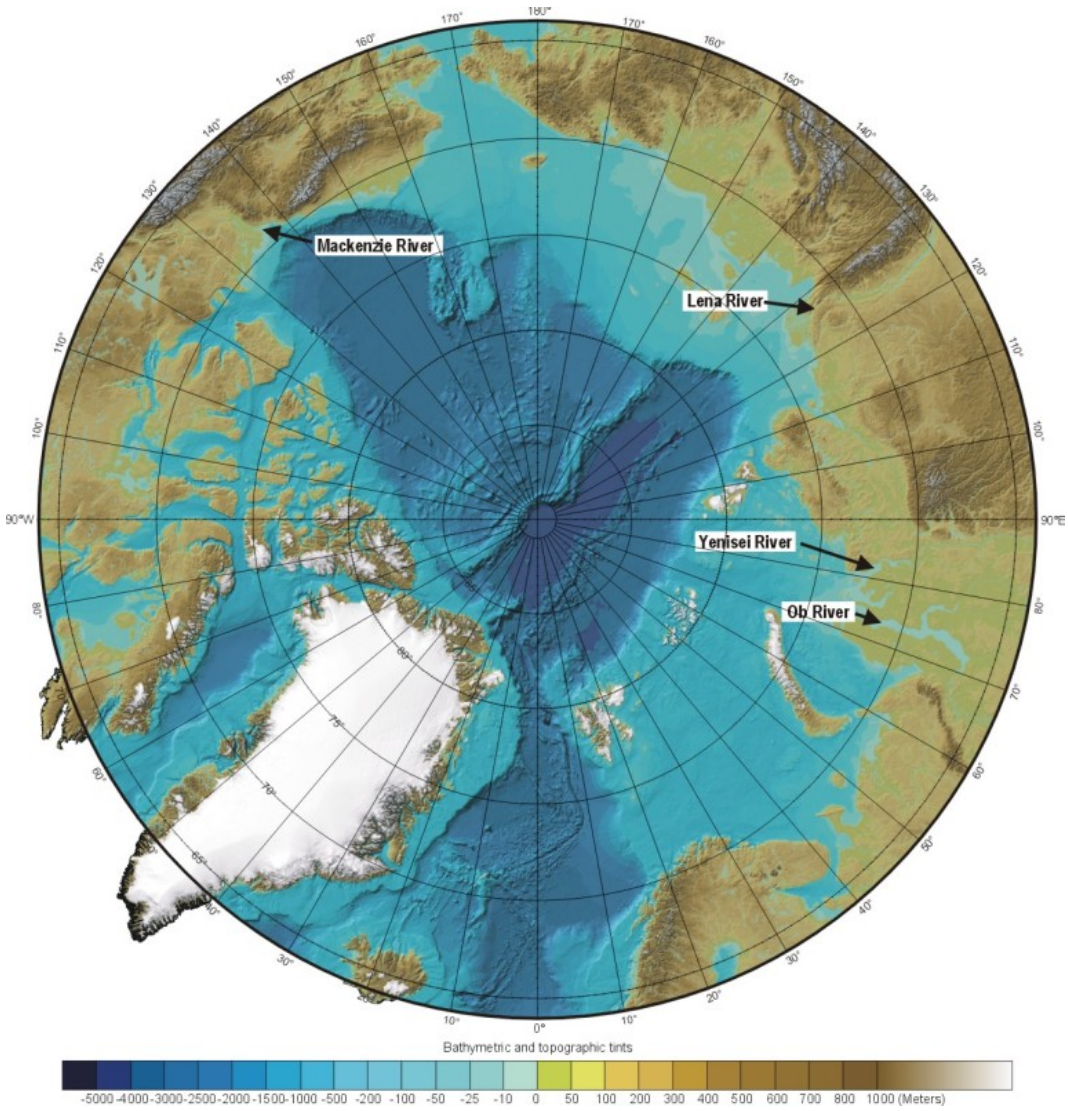

Figure 1.2. Map of the Arctic Ocean, showing bathymetry, major river outflows, basins and seas discussed in this dissertation. Image modified from http://www.ngdc.noaa.gov/mgg/bathymetry/arctic/images/IBCAO_ver1map_letter_low.jpg.

We now know that primary production in the Arctic is substantially higher than previously believed. Most of this production is centered over the broad, shallow shelf seas (Fig. 1.2) that make up nearly 50% of the area of the Arctic Ocean (Jakobsson, 2002). Although highly variable both spatially and temporally, primary production rates in the open waters of the Chukchi Sea reach as high as 2.57 g C m^{-2} day^{-1}, while rates within and just beneath the ice itself average 0.033 g C m^{-2} day^{-1} (Gosselin *et al.*, 1997). Likewise, Hill and Cota (2005) estimate an average daily production of 0.783 g C m^{-2} day^{-1} for the shelf of the Alaskan Chukchi and Beaufort Seas during summer, while spring bloom conditions near the Barrow Canyon region, studied as part of the this work, support daily levels as high as 8 g C m^{-2} day^{-1}(Hill and Cota, 2005). This suggests an annual rate of approximately 70.5 g C m^{-2} for the western Arctic shelves, with localized hot-spots supplying as much as 470 g C m^{-2} yr^{-1} (Hill and Cota, 2005). Comparing these values to the average *global* annual oceanic primary productivity of 128 g C m^{-2} yr^{-1} (estimated using an annual photosynthetic rate of 43.5 Pg C yr^{-1} with an ocean area of 3.39×10^{14} m^2 (Behrenfeld and Falkowski, 1997)), the Arctic is clearly an important contributor. Levels of primary productivity are controlled to a great extent by light and nutrient availability. The sudden abundance of light during ice break-up in spring stimulates water column photosynthesis (Fig. 1.3), and typically the spring bloom follows the basin-ward migration of the ice edge (Wang et al., 2005). Algae living on and in the ice can also be important contributors to primary production, especially in the central Arctic, but snow cover reduces photosynthetically available radiation (PAR), limiting productivity.

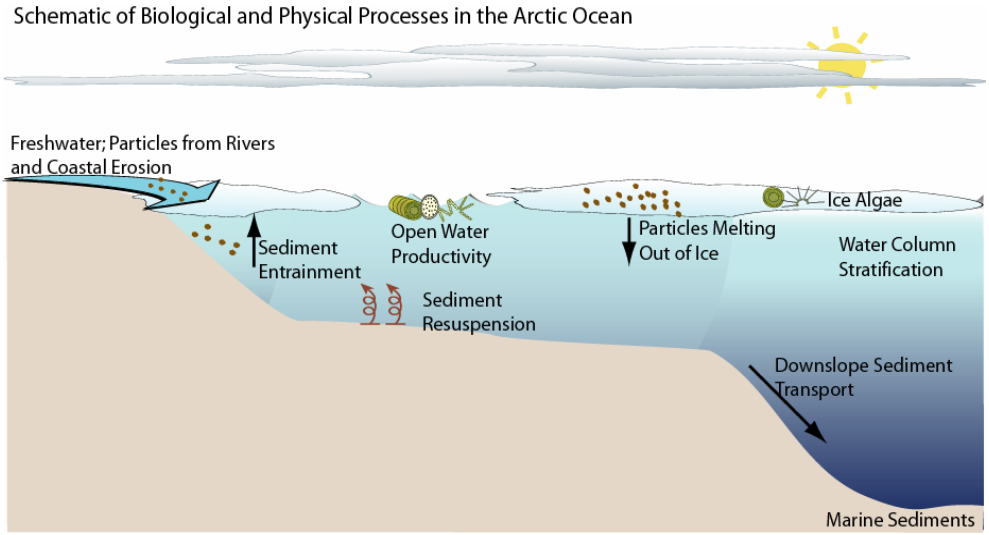

Figure 1.3. Schematic of biological and physical processes that affect the cycling of organic matter in the Arctic Ocean. Modified from Stein and Macdonald (2004b). Symbols courtesy of the UMCES Integration and Application Network (*ian.umces.edu/symbols/*).

Despite the abundance of marine organic carbon from primary productivity, large quantities of both particulate and dissolved terrestrial organic carbon are also delivered to Arctic waters, largely from four major rivers (outflow locations shown on Fig. 1.2). These include the Yenesei, Lena, and Ob Rivers in the Laptev and Kara Sea watersheds, and the Mackenzie River in Canada, which deliver a combined freshwater flow of 1879 km^3 yr^{-1} and a combined total suspended particulate matter flux of 164.9 x 10^6 t yr^{-1} (Gordeev *et al.*, 1996; Holmes *et al.*, 2002). In terms of organic carbon, this translates to a total organic carbon (TOC) flux of about 30 x 10^6 t yr^{-1} for the entire Arctic Ocean, with nearly 85% of this flux entering the Eurasian sector (Rachold *et al.*, 2004). This flux is highly seasonal, with up to 80% of the delivery occurring during freshet in June and July (Rachold *et al.*, 2004) as rivers thaw and the snow-pack melts. In the Yenesei, Lena, and Ob rivers, dissolved organic carbon is the bulk of the TOC flux. In the Mackenzie River, however, the high concentrations of suspended material lead to particulate organic matter concentrations that are twice as high as the dissolved phase

(Rachold *et al.*, 2004). Coastal erosion also provides a significant quantity of terrestrial carbon to the Arctic, estimated in some locations to be greater than the delivery from rivers, yet this parameter remains poorly quantified in most regions. Some of this eroded material may be from melting permafrost deposits, releasing old organic matter back into the active carbon cycle (Guo *et al.*, 2004).

Entrainment of material into sea-ice also provides a mechanism for transport and redistribution of organic carbon (Fig. 1.3) throughout the Arctic basin (Eicken, 2004). Sea-ice can carry large quantities of particulate organic matter, on the order of tens to hundreds of milligrams per liter (Eicken, 2004), which can later be deposited into the central Arctic basin during summer melting. Because of widespread ice cover and bathymetric isolation, this delivery of sediments and organic matter through sea-ice is proposed to be a significant, if not the dominant sedimentation mechanism in the central Arctic (Bischof and Darby, 1997). Once deposited in sediments, turbidity currents can then transport both autochthonous carbon and eroded terrestrial debris from the shelves and slopes to the central Arctic basin (Grantz *et al.*, 1999).

1.2.4. Organic Matter Source Determination

Based on the inputs of organic matter discussed above, the Arctic organic carbon cycle can be characterized as a complex interplay of a freshly-produced marine organic carbon pool and a terrestrial organic carbon pool composed of recalcitrant, possibly ancient, eroded continental material. Although biochemically distinct, with accumulating evidence suggesting that the labile marine component is rapidly recycled while the recalcitrant terrestrial component remains for burial (Belicka et al., 2004; Goñi et al.,

2000; Stein and Macdonald, 2004a; Yunker et al., 2005), these two pools are linked through the processes of the hydrological cycle. Yet, continued climate changes will likely affect the marine and terrestrial source components differently (Stein and Macdonald, 2004b). Distinguishing between these two organic pools both in the modern and historical Arctic provides insight on the impacts of production, recycling, and sequestration of organic carbon in a changing climate.

Multiple indicators preserved in sediments can provide tools for differentiating between the marine and terrestrial pools of organic carbon. These proxies supply diverse information on both sources and processing of organic matter (Meyers, 1997), and range from measures of bulk fractions to individual molecules. Carbon to nitrogen ratios of bulk organic matter, for example, give general distinctions between marine and terrestrial carbon, as terrestrial plants contain far more cellulose and less protein than algae, resulting in C to N ratios greater than 15-20 (Hedges et al., 1986; Meyers, 1997). Stable carbon and nitrogen isotopic composition can also give a general indication of organic matter composition (Fogel and Cifuentes, 1993; Hedges et al., 1988b) since the overall isotopic composition of the organic fraction reflects the photosynthetic pathway utilized in organic matter synthesis and subsequent degradation reactions (Table 1.1). Terrestrial plants typically use the C_3 pathway with atmospheric CO_2 as their carbon source, resulting in bulk plant material with a $\delta^{13}C$ around -27‰ (Fogel and Cifuentes, 1993). C_4 terrestrial plants, such as maize and some grasses, use an additional enzyme (PEP carboxylase) to RuBisCO and separate carbon fixation to bundle sheath cells in the plant's interior to minimize energy losses from photorespiration (Fogel and Cifuentes, 1993). This process results in a smaller isotope effect than the C_3 pathway, producing

less isotopic fractionation and bulk isotopic values ranging from -8 to -18‰ (Fogel and Cifuentes, 1993). Although marine algae use the C_3 pathway, they employ an active transport mechanism to concentrate inorganic carbon, as HCO_3^-, resulting in $\delta^{13}C$ values between -20‰ and -22‰ (Meyers, 1997).

Table 1.1. Typical ranges of $\delta^{13}C$ values for types of organic matter.

Type of Organic Matter	Typical Range (‰)[a]
Terrestrial C_3 Plants	-23 to -30
Terrestrial C_4 Plants	-8 to -18
Terrestrial CAM Plants	-11 to -33
Temperate Marine POM	-18 to -24
Saltmarsh C_3 Plants	-29 to -23
Saltmarsh C_4 Plants	-15 to -12
Arctic Water Column POM	~ -27 to -20
Arctic Ice POM	~ -27 to -8

[a]Data complied from Fogel and Cifuentes (1993); Meyers (1997); Ostrom and Fry (1993); and Tremblay et al. (2006).

These bulk measures provide general information about the origin of preserved sedimentary organic matter, but an analysis of individual molecular compounds preserved in the material can add substantial specificity to source determinations, and can likewise provide information on the transformations organic matter undergoes post-burial. This "molecular biomarker" approach has gained popularity through the ability of individual compounds to be assigned to their molecular precursors and the enhanced preservation of some structures relative to fossil remains. Lipids in particular have been widely used as molecular biomarkers because of their superior ability over inorganic tracers to both conserve biological information and also reflect environmental and diagenetic alterations (Meyers, 1997).

Despite their value, few studies have thus far utilized lipid biomarkers to address carbon cycling in the Arctic. In the western Arctic, Belicka et al. (2002 and 2004) and Yunker et al. (2005) used this approach with the purpose of determining the suite of compounds most useful for tracking the fate of marine and terrestrial organic carbon, and to then apply these markers to understand differences in preservation of organic carbon between the Beaufort and Chukchi Seas in the western Arctic. Similarly, Goñi et al. (2000) and Yunker et al. (1993a, b; 1995; 2002) have focused on biomarker patterns in sediments and particles from the Mackenzie Delta area of the Canadian Beaufort Sea. Guo and Macdonald (2006) sampled organic matter from the Yukon River with the aim of characterizing the composition, reactivity, and flux of organic carbon in this system. In the eastern Arctic, the most comprehensive work has been completed by Stein and colleagues for the Laptev and Kara Seas (Fahl and Stein, 1997; Fahl and Stein, 1999; Knies and Stein, 1998; Schubert and Stein, 1996; Schubert and Stein, 1997; Stein et al., 2004; Stein and Fahl, 2000; Stein et al., 1999; Stein et al., 1994a; Stein et al., 1994b; Stein et al., 1994c; Stein and Stax, 1996) where they used core samples for Holocene reconstructions of the eastern Arctic Ocean using a combination of hydrogen indices, hydrocarbon concentrations, and isotopic signatures of bulk sediments and foraminifera. Although all these studies are beginning to address the dynamics of organic carbon cycling in the Arctic, data are still sparse in comparison to other ocean basins. Comparisons between Arctic regions are likewise hampered by a lack of related measurements among multiple geographic areas.

1.2.5. Quantification of Preserved Organic Matter Components

In addition to their use as organic matter source indicators, many proxies are often utilized in quantification approaches for marine and terrestrial organic matter inputs. For example, stable carbon isotopes have been used to quantify the fractions of marine or terrestrial carbon in sediments or POM by assigning isotopic values for two end members (one for marine carbon, and one for terrestrial carbon) and assuming linear mixing between these two types of carbon (Goñi et al., 2000; Hedges et al., 1988b; Prahl et al., 1994). Lipid biomarkers have also been used to quantify the fractions of marine and terrestrial organic matter in sediments, as in the ALKOC method (Fernandes and Sicre, 2000; Prahl and Carpenter, 1984). This method exploits the relationship between total organic carbon and concentrations of odd carbon number long-chain *n*-alkanes, typically derived from the decarboxylation of long-chain even-carbon fatty acids used as protective coatings on leaves of terrestrial plants (Killops and Killops, 1993). The BIT index approach (Hopmans et al., 2004) is a ratio of branched glycerol dialkyl glycerol tetraether (GDGT) lipids, which are though to be produced by organisms that typically live in terrestrial environments, to their sum plus the amount of crenarchaeol, a GDGT of marine planktonic archaeal origin. In this regard, a BIT index of 1 corresponds to a fully terrestrial origin, while a BIT index of 0 corresponds to a lack of fluvial input (Hopmans et al., 2004). Statistical approaches such as principal component analysis combined with regression techniques have also been used to model the terrigenous and marine content of individual lipids preserved in sediment samples (Goñi et al., 2000; Yunker et al., 2005; Yunker et al., 1995). Relative amounts of organic carbon derived from each source are then summed and divided by total biomarker input to estimate preserved components.

1.3. Research Objectives and Approach

Potential changes to the Arctic with climate warming, including continued sea-ice loss and increasing coastal erosion as two examples, will likely affect the marine and terrestrial carbon pools differently (Stein and Macdonald, 2004b). Therefore, the effects of these changes may best be understood by tracking the sources and sinks of the two distinct components, instead of focusing on bulk organic matter cycling. Distinguishing the balance between marine and terrestrial organic matter, both presently and throughout the past, is therefore the key to understanding and predicting future effects of climate change on the Arctic system. This dissertation takes an integrated, multi-proxy approach—utilizing molecular biomarkers and stable isotopic composition—to address the role of the terrestrial organic matter pool in the carbon cycle of the Arctic Ocean. It is designed in four parts to quantify the abundances of terrestrial organic matter in western Arctic waters and sediments and to understand how the prevalence of terrestrial carbon in this ocean system affects the recycling and long-term preservation of organic carbon.

Chapter 2 investigates new and established methods for the quantification of preserved terrestrial organic matter components in sedimentary environments and evaluates the implications of these approaches for the development of regional carbon budgets. The construction of carbon budgets for the Arctic is a crucial step in understanding how past and future climate change may affect biogeochemical cycles. While regional budgets are beginning to be developed for the Arctic (see (Macdonald et al., 1998; Stein and Macdonald, 2004a), estimates of the marine and terrestrial organic matter components in sediments are lacking in many Arctic locations. Compounding the

problem, researchers working in different regions have typically utilized different proxies for the quantification of marine/terrestrial inputs (Stein and Macdonald, 2004a), and these different proxies may result in diverse estimates of marine or terrestrial components, limiting the ability to compare data between regions of the Arctic. The following research question was investigated:

1) How inconsistent are methods for the quantification of terrestrial organic carbon components for a given sedimentary environment?

The task of quantifying each component in a carbon budget is especially important for the Arctic due to the regions' sensitivity to global climate change and the potential for enhanced terrestrial organic carbon inputs with continued Arctic warming to alter carbon sequestration. If methods presently utilized for this task result in varying estimates of specific components, or if they systematically quantify separate sub-pools of organic matter, the ability to incorporate these measurements into carbon budgets is limited.

To address these research inquiries, four established methods for quantifying terrestrial organic matter in sediments (Two end-member stable isotopic mixing models, *n*-alkane ratio (ALKOC), lipid biomarkers with PCA and regression scaling, and the BIT index) were investigated with the intention of determining the differences between each method and understanding the implications of these differences for regional carbon budgets. Each approach was performed on 19 surface sediment samples ranging from shelf to basin environments in the Chukchi and Alaskan Beaufort Seas. Additionally, terrestrial organic matter samples collected from the North Slope of Alaska were analyzed to calibrate the isotopic end-members and to encompass the range of terrigenous

carbon inputs from fluvial and coastal erosion sources. In addition to evaluating the robustness of each established proxy, this exercise will also provide much needed data on the spatial distribution of organic matter.

Chapter 3 explores the sources and spatial variability of suspended particulate organic matter (POM) in summer western Arctic waters. As POM largely provides the source of organic carbon ultimately preserved in sediments, the transformation and retention of POM were also investigated. The following research questions were addressed in this exploration:

1) Does the molecular composition of suspended particulate organic matter reflect the complex balance between marine primary productivity and the delivery of terrestrial materials via rivers and erosion?
2) Is the molecular biomarker "fingerprint" of particulate organic matter from deep waters distinct from that of shallow POM as a result of microbial degradation during sinking and particle transport?

The lipid biomarker composition of 53 samples of suspended POM collected from varying depths in summer Arctic waters was determined and is presented in Chapter 3. Principal components analysis was employed to explore relationships between biomarkers and between similar observations. Two deep basin stations were chosen for an in-depth analysis of the transformation of organic matter during sinking. Both $\delta^{13}C$ and $\Delta^{14}C$ of the POM are included as ancillary measures for the understanding of these processes.

Sediments of the world's oceans are the ultimate repository of the inorganic and organic material in the global carbon cycle and therefore hold key clues to past conditions and environments. Chapter 4 presents an analysis of lipid biomarkers in three sediment cores in the Alaskan Beaufort Sea region of the western Arctic Ocean to evaluate timescales and patterns of sedimentary organic matter processing along a shallow to deep water continuum. These measures also include the addition of stable isotopic composition and trace metal concentrations to examine sedimentary condition. The following research inquiries were addressed:

1) Do organic biomarkers of terrestrial origin present in sediments directly reflect inputs of land-derived material and do their concentrations change over time in response to changing environmental conditions of the Arctic?
2) Do trace elements sensitive to sediment oxidation state demonstrate episodic pulses of organic matter in the western Alaskan Beaufort Sea similar to those found by Gobeil et al. (2001) for the deep Arctic Ocean?
3) Can ^{210}Pb be utilized to calculate sedimentation rates in the shallower regions of the Alaskan Beaufort Sea?

The final segment of this research (Chapter 5) is based on accumulating evidence that large portions of land-derived organic carbon are preserved relative to marine carbon in the modern Arctic (Belicka et al., 2004; Goñi et al., 2000; Stein and Macdonald, 2004a; Yunker et al., 2005; Yunker et al., 1995). This literature implies that marine carbon is recycled rapidly in the Arctic water column, leaving the more recalcitrant terrestrial organic matter to be preserved in sediments. With climate warming, inputs of

this recalcitrant material will likely increase. Permafrost deposits in many regions of the Arctic and sub-Arctic over the past few decades have experienced changes including greater variability in thicknesses of the active layers, increasing surface and deep permafrost temperatures, and downward thawing in some regions of 0.1 m yr^{-1} (Osterkamp and Romanovsky, 1999), and this implies that increasing amounts of relict terrestrial carbon are being transported to the Arctic Ocean (Davidson et al., 2000; Freeman et al., 2001; Frey and Smith, 2005). It remains unclear how this relict carbon will impact the organic carbon cycle in the Arctic Ocean. The character and reactivity of natural particulate organic matter being transported through rivers and sea-ice to the Arctic Ocean were investigated and presented in Chapter 5. For this experimental investigation, algal and terrestrial organic matter substrates were added to microcosms containing Arctic water with associated microbial assemblages. The microcosms were sampled over time to determine rates of marine and terrestrial organic matter microbial degradation (Chapter 5). These following research questions were investigated:

1) What is the difference in recycling rates between marine and terrestrial organic substrates in Arctic waters?
2) What is the effect of increasing temperature on the kinetics of microbial degradation of both marine and terrestrial organic substrates?
3) Does POM eroded from Alaskan coastal deposits contain labile organic matter that can undergo microbial degradation?

1.4. Research Significance

The source of organic carbon has a substantial influence on its potential for preservation. This dissertation research has been designed to determine the sources of terrestrial and marine organic carbon to the Arctic Ocean to improve carbon budgets and to understand the differences in recycling of these carbon substrates. As part of the recently completed Shelf-Basin Interactions Program (SBI) Part II, we have begun to look at the recycling of organic materials both experimentally and through field observations. This research implies that marine-derived organic carbon is rapidly recycled in the water column, with terrestrial carbon becoming an increasing proportion of the material preserved in the sedimentary record. By quantifying the rates of degradation of marine and terrestrial organic matter and by examining the historical record for changes in the balance between these two main organic matter pools, this research begins to fill a critical gap in our understanding of the modern carbon cycle and how it has been linked to the hydrological cycle over geologic timescales.

Chapter 2: The Sequestration of Terrestrial Organic Carbon in Arctic Ocean Sediments: A Comparison of Methods and Implications for Regional Carbon Budgets

2.1. Abstract

A variety of approaches have been developed to estimate the fraction of terrestrial or marine organic carbon present in aquatic sediments. The task of quantifying each component is especially important for the Arctic due to the regions' sensitivity to global climate change and the potential for enhanced terrestrial organic carbon inputs with continued Arctic warming to alter carbon sequestration. Yet it is unclear how each approach compares in defining organic carbon sources in sediments as well as their impact on regional or pan-Arctic carbon budgets. Here, we investigated four methods: (1) two end-member mixing models utilizing bulk stable carbon isotopes; (2) the relationship between long-chain *n*-alkanes and organic carbon (ALKOC); (3) principal components analysis combined with regression scaling of a large suite of lipid biomarkers; and (4) ratios of branched and isoprenoid glycerol dialkyl glycerol tetraether lipids (the BIT Index) to calculate the fraction of terrestrial organic matter preserved in Arctic marine sediments.

Estimated terrestrial organic carbon content between approaches showed considerable variation for identical sediment samples. The BIT index resulted in the lowest estimates for terrestrial organic matter, suggesting that this proxy may represent a different fraction of terrestrial organic matter; i.e., peat or soil organic matter, as opposed to markers such as *n*-alkanes or long-chain fatty acids which measure higher plant wax

inputs. Because of the patchy inputs of *n*-alkanes to this region from coastal erosion in the western Arctic, the ALKOC approach was not as effective as when applied to river-dominated margins found in the eastern Arctic. The difficulties in constraining a marine $\delta^{13}C$ end-member limit the applicability of stable isotope mixing models in polar regions. The lipid-based PCA approach resulted in higher proportions of terrestrial organic matter than bulk organic carbon proxies, suggesting possible differences in composition between the bulk organic carbon and the lipid component, but was presently the most appropriate technique for estimating terrestrial carbon inputs in the western Arctic. Terrestrial organic matter inputs to the Chukchi and western Beaufort Seas using the average of the four methods at each site ranged from 12-43%, indicating that land-derived organic matter plays a substantial role in carbon dynamics in the western Arctic Ocean.

2.2. Introduction

Carbon budgets provide a means to quantify the sequestration and recycling of organic matter in the world's oceans as well as an understanding of the linkages between carbon reservoirs. For a sensitive environment like the Arctic Ocean, they can also provide a conceptual understanding of how future climate change may affect biogeochemical cycling. In a typical open ocean setting, primary productivity and the uptake and recycling of generated organic matter are the overriding processes. In the Arctic, however, the terrestrial organic carbon reservoir is a significant contributor (Belicka et al., 2004; Goñi et al., 2000; Yamamoto et al., 2008). Large quantities of both particulate and dissolved terrestrial organic carbon are delivered to Arctic waters, mainly from the Yenesei, Lena, and Ob Rivers in the Laptev and Kara Sea watersheds, and the

Mackenzie River in Canada, which together deliver a freshwater flow of 1879 km^3 yr^{-1} and a combined total suspended particulate matter flux of 164.9 x 10^6 t yr^{-1} (Gordeev et al., 1996; Holmes et al., 2002). Although highly seasonal, this tallies to an organic carbon (TOC) flux of about 30 x 10^6 t yr^{-1} for the entire Arctic Ocean, with nearly 85% of this flux entering Eurasian waters (Rachold et al., 2004). In the Yenesei, Lena, and Ob rivers, dissolved organic carbon is the bulk of the TOC flux. In the Mackenzie River, however, the high concentrations of suspended material lead to particulate organic matter concentrations that are twice as high as the dissolved phase (Rachold et al., 2004). Coastal erosion also provides a significant quantity of terrestrial carbon to the Arctic, estimated in some locations to be greater than the delivery from rivers (Rachold et al., 2004).

Local and regional carbon budgets are being developed for the Arctic (Macdonald et al., 1998; Stein and Macdonald, 2004a); yet estimates of organic carbon reservoirs in the water column and sediments are lacking in many Arctic locations. The marine organic carbon component is better constrained, as primary productivity and microbial respiration have been measured over the wide continental shelves of the Arctic (Arnosti et al., 2005; Bates et al., 2005a; Booth and Horner, 1997; Gosselin et al., 1997; Hill and Cota, 2005). Nevertheless, the high temporal and spatial variability combined with the difficulty of estimating production and recycling in the waters and ice of the central Arctic basin make it challenging to extrapolate measurements to basin-wide estimates. The terrestrial organic carbon component and its retention in the system are poorly defined. Riverine delivery of terrestrial organic matter can be measured in large rivers;

yet the redistribution of this material by entrainment in sea-ice as well as its remineralization rates are poorly understood.

Molecular organic markers and stable carbon isotopes are well established proxies for tracing both the sources and processing of organic matter (Meyers, 1997). The utility of these proxies, however, is limited to their source specificity. For a robust analysis, researchers have often utilized a suite of organic markers as opposed to a single class of lipids (Belicka et al., 2002; Canuel and Zimmerman, 1999; Goñi et al., 2000); and in several cases have coupled biomarker analysis with stable carbon isotopic measurements (Drenzek et al., 2007; Tolosa et al., 2003). These geochemical proxies are often combined to estimate terrestrial and marine organic matter fractions sequestered in water column particles and sediments. For example, two end-member mixing models of stable carbon isotopes exploit the differences in $\delta^{13}C$ between land plants and marine algae, providing an estimate of the fractions of marine and terrestrial organic matter in sediments (see Hedges et al., 1988a; Prahl et al., 1994; Meyers, 1997). Lipid biomarkers have also been applied in varying degrees of complexity. Techniques can involve a single class of compounds, such as odd carbon number long-chain *n*-alkanes, (Bouloubassi et al., 1997; Fernandes and Sicre, 2000; Prahl and Carpenter, 1984) to estimate terrestrial organic matter content of ocean margin sediments. More complex statistical approaches which combine regression of multiple lipid structures with principal components analysis (PCA) have also been used (Goñi et al., 2000; Yunker et al., 2005; Yunker et al., 1995). This approach incorporates a linear regression on the biomarker loadings from the PCA, and source end members are assigned to each end of the regression line. The regression line acts as a mixing line between molecular biomarkers

that are solely derived from marine organic matter versus those derived from terrestrial organic matter. For markers that are less specific and fall between the two end-members, a relative contribution of each organic matter compartment is calculated by projecting the biomarker in PCA space onto the mixing line using the geometric distance formula. The concentration of individual biomarkers is then scaled to reflect the contribution of that biomarker to marine or terrestrial carbon and summed to estimate terrestrial carbon preservation.

Novel proxies have also recently suggested—including the BIT index (**B**ranched and **I**soprenoid **T**etraether Index), which diverges from the more standard approaches in that it utilizes compounds produced by organisms believed resident of terrestrial environments, rather than rely on the proxies specific to the terrestrial organic matter itself (Hopmans et al., 2004). The biological origin of these compounds, the glycerol dialkyl glycerol tetraethers (GDGTs), is not yet known; however, the abundance of several of the branched compounds in peat samples supports their terrestrial origin (Hopmans et al., 2004).

Each of these proxies may result in a disparate estimate of the marine or terrestrial organic carbon component (Stein and Macdonald, 2004b). If these proxies arrive at substantially different estimates of terrestrial or marine contents, it limits the ability to compare carbon budgets and models of carbon cycling among regions of the Arctic. Here, we investigate four methods for quantifying terrestrial organic matter in sediments: (1) A two end-member stable isotope mixing model; (2) The *n*-alkane ratio (ALKOC) method; (3) Lipid biomarkers with PCA and regression scaling; and (4) The BIT index to compare differences in the estimated terrestrial organic carbon content between each

method. For valid comparison, measurements were made using each approach on 19 surface sediment samples ranging from shelf to basin environments on the Chukchi/Alaskan Beaufort Sea. In addition, a variety of terrestrial samples collected from the North Slope of Alaska were analyzed to determine the range of terrigenous carbon from fluvial and coastal erosion inputs. The strong influence of terrestrial organic matter from rivers and erosion and the potential global impacts of a changing carbon cycle make the Arctic a relevant location to investigate the comparability of terrestrial organic matter proxies. Results of these analyses over spatial scales also provide much needed data on the distribution of organic matter and its shelf-basin exchange in a region where climate change has already been observed.

2.3. Materials and Methods

2.3.1. Study Area and Sampling

Surface samples were taken from nineteen undisturbed sediment cores collected during the Shelf-Basin Interactions Program (SBI) process cruises in 2002 and 2004 aboard the USCGC *Healy* (Table 2.1). Sample sites were chosen in shelf to basin transects in the Chukchi and Alaskan Beaufort Seas (Fig. 2.1). Cores were taken with a Pouliot box corer with an area of 0.06 m^2, and sectioned in 1 cm intervals in the upper 10 cm of sediment, and 2 cm intervals below. Surface samples described here are the 0-1 cm sample of each core. Sediment sections were stored in pre-cleaned plastic or glass I-Chem jars and immediately frozen until chemical analysis. Prior to chemical analysis, each sediment section was thawed and thoroughly homogenized.

Table 2.1. Locations of surface sediment (0-1 cm) stations and bulk geochemical parameters observed for the Arctic sediments analyzed.

Station Name	Station Number	Longitude (W)	Latitude (N)	Depth (m)	Org. C (%)	TN (%)	C:N	$\delta^{13}C$ (‰)	$\delta^{15}N$ (‰)
STN 1	HLY02-01-001	168° 52.9’	67° 27.2’	52	1.686	0.093	21.15	-19.98	6.56
STN 2	HLY02-01-002	167° 28.0’	70° 38.0’	50	1.310	0.178	8.59	-18.40	5.87
WHS-2	HLY02-01-006	160° 34.0’	72° 50.5’	58	0.931	0.132	8.23	-20.24	7.31
WHS-5	HLY02-01-009	160° 06.7’	73° 16.8’	1198	0.958	0.138	8.10	-20.05	4.08
WHS-6	HLY02-01-010	159° 49.8’	73° 26.7’	1855	0.953	0.128	8.69	-19.91	2.63
WHS-7	HLY02-01-011	159° 33.2’	73° 36.7’	2443	1.042	0.139	8.75	-18.23	5.28
WHS-12	HLY04-03-052	157° 51.2’	73° 54.1’	3748	0.931	0.150	7.24	-19.19	7.56
EHS-4	HLY02-01-019	158° 44.2’	72° 36.3’	86	1.560	0.248	7.34	-18.34	7.83
EHS-6	HLY02-01-017	158° 28.5’	72° 51.1’	426	1.400	0.156	10.47	-19.34	6.99
EHS-9	HLY02-01-014	158° 08.8’	73° 06.1’	2158	1.080	0.145	8.69	-18.20	4.65
EHS-11	HLY02-01-012	157° 31.9’	73° 26.2’	2861	1.691	0.193	10.22	-20.25	4.97
EHS-12	HLY04-03-051	156° 45.9’	73° 47.9’	3778	0.666	0.146	5.32	-20.04	5.97
BC-3	HLY02-01-037	155° 45.3’	71° 39.0’	183	1.047	0.137	8.92	-20.58	2.03
BC-4	HLY02-01-031	154° 49.2’	71° 55.7’	401	1.634	0.178	10.71	-18.60	6.89
BC-5	HLY02-01-032	154° 27.8’	72° 04.2’	1317	1.809	0.183	11.53	-18.30	6.41
BC-7	HLY02-01-034	154° 29.9’	72° 32.0’	2934	1.273	0.152	9.77	-16.74	5.14
EB-2	HLY02-03-023	152° 33.2’	71° 27.4’	89	0.921	0.128	8.40	-22.07	4.97
EB-4	HLY02-03-021	152° 24.7’	71° 39.0’	498	1.871	0.209	10.44	-20.86	4.34
EB-7	HLY02-03-018	151° 59.1’	72° 19.3’	3264	1.588	0.183	10.12	-19.82	5.08

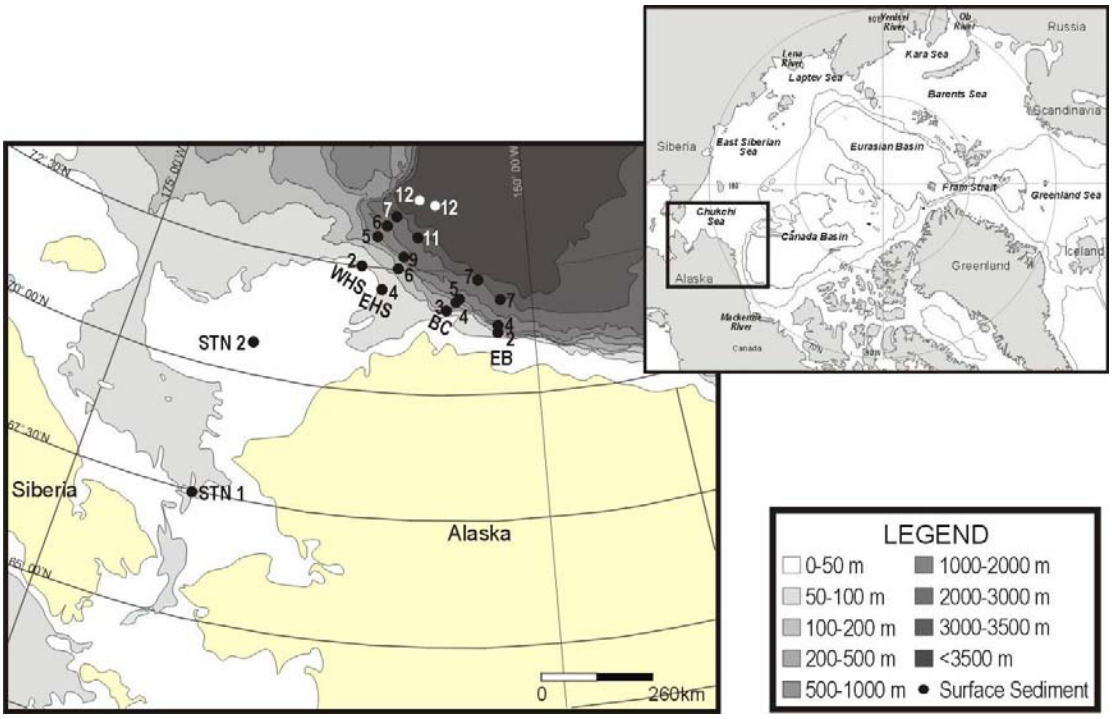

Figure 2.1. Map of the western Arctic Ocean, showing the sampling stations along four shelf to basin transects. WHS: West Hanna Shoal; EHS: East Hanna Shoal; BC: Barrow Canyon; EB: East of Barrow Canyon. Inset shows location of samples relative to entire Arctic region.

2.3.2. Chemical Analyses

Bulk Sedimentary Composition

Sediment organic carbon and nitrogen content (after removal of $CaCO_3$ by acidification with HCl) was determined with an elemental analyzer (EA) coupled through continuous flow with an OPTIMA stable isotope ratio mass spectrometer (GV, Manchester, UK). Internal laboratory reference gases for carbon and nitrogen were calibrated against the respective international standards NBS-19 and atmospheric N_2. Isotopic results were reported in delta notation (δ) as per mil deviations (‰) from the corresponding international standards of Pee Dee Belemnite (PDB) and atmospheric N_2 (air). Analytical precision for carbon and nitrogen was within ±0.2‰.

Lipid Biomarker Analysis

To quantify non-tetraether lipid biomarkers, 5-10 g of wet sediments were extracted three times with a mixture of methylene chloride:methanol (2:1) in solvent-rinsed glass test tubes with sonication for 2 minutes as described in Belicka et al. (2002). Partitioning of lipids was achieved by addition of Nanopure water and centrifugation at 1200 rpm for 5 minutes. The extraction was repeated twice, the three extracts were combined, and excess solvent was removed by rotary evaporation. Saponification was performed by reaction at 70 °C for 30 minutes after addition of a solution of 0.5 N KOH in methanol to dried extracts. Neutral lipids were partitioned three times with a 9:1 mixture of hexane:diethyl ether followed by fatty acid partitioning after acidification with HCl to pH<2. Neutral lipids were dried and derivatized at 50 °C for 15 minutes with bis-(trimethylsilyl)trifluoroacetamide amended with 25% pyridine. Fatty acids were dried and methylated at 70 °C for 30 minutes with boron trifluoride in methanol. Nonadecanoic acid and 5α-cholestane added prior to saponification served as internal standards for the polar and non-polar phases, respectively. Polar and neutral lipids were quantified by capillary gas chromatography (GC) with flame ionization detection. Gas chromatography-mass spectrometry was performed with an Agilent 5973N GC-MS for lipid identification with electron ionization mode. The instrument methods and column parameters were identical to those described in Belicka et al. (2002). Repeated sedimentary lipid extraction analysis for fatty acids and sterols averaged ±20.5%.

Glycerol dialkyl glycerol tetraether lipids (GDGTs) were analyzed using the method of Hopmans et al. (2004) with minor modifications. Briefly, approximately 20 g wet sediments were extracted three times with a mixture of methylene chloride:methanol (9:1, v/v). The total lipid extract was then partitioned into apolar and polar fractions

using alumina oxide column chromatography with hexane:methylene chloride (9:1, v/v) and methylene chloride:methanol (1:1, v/v), respectively, as eluents. The polar fraction was dried either by rotary evaporation or under N_2, redissolved ultrasonically in a mixture of hexane:propanol (99:1, v/v), and filtered through a 0.2 μm pore size, 13 mm diameter Teflon filter in a Swinny stainless steel filter holder using a luer-lock syringe. GDGTs were analyzed using an Agilent 1100 Series High Performance Liquid Chromatography system coupled to an Agilent 1100 Series SL Ion Trap Mass Spectrometer equipped with an atmospheric pressure chemical ionization source. Separation was achieved on a Rainin Microsorb-MV NH_2 column (4.6 x 250 mm; 5μm particle size) and a 4.0 x 3.0 mm (L x i.d.) Phenomenex Security Guard NH_2 column. The sample run time was 50 minutes with a constant flow rate of 1.0 mL/min, beginning with an isocratic hold at 99% hexane 1% propanol for 5 minutes, followed by a linear gradient to 1.8% propanol over 45 minutes. A post-run cleaning was achieved by a reverse gradient back to 1% propanol, followed by a 10 minute flush of 99:1 hexane:propanol. Positive ion spectra were produced by scanning an *m/z* range from 950-1450 under the conditions of Hopmans et al. (2004). Concentrations of 5 major GDGTs were quantified by comparison of the $[M+H]^+$ peaks to an external standard curve constructed with 1,2-di-O-phytanyl-*sn*-Glycerol (Avanti Polar Lipids), with identical APCI-MS conditions except with full scanning from m/z 650-1450.

2.3.3. Calculations of Terrestrial Organic Carbon Content

Four methods of estimating the terrestrial organic carbon fraction (%Terr OC) in sediment samples were compared. The first method, a two-end-member isotopic mixing

model based on $\delta^{13}C$ (equation 1), utilized a $\delta^{13}C_{terrestrial}$ end-member of -27.76‰, the average of three terrestrial organic matter substrates collected on land near the study site (see results section for description of samples and isotopic composition).

$$\text{Terr OC (\%)} = [(\delta^{13}C_{sample} - \delta^{13}C_{marine}) / (\delta^{13}C_{terrestrial} - \delta^{13}C_{marine})] * 100 \quad (1)$$

For the $\delta^{13}C_{marine}$ end-member, a value of -17.5‰ was used, an intermediate of heavy isotopic values found characteristic of ice algal species during bloom conditions (-14.2, -13‰, Gradinger, in press, Tremblay, 2006) and Arctic marine particulate organic matter (-27 to -18, Goericke and Fry, 1994 and references therein).

The second method employed the relationship between long-chain *n*-alkanes and organic carbon content (Equation 2). ALKOC is the slope of a linear correlation between *n*-alkanes and organic carbon content), as proposed by Prahl and Carpenter (1984) and subsequently used by Fernandes and Sicre (2000) in the Kara Sea.

$$\text{Terr OC (\%)} = [((C_{25\text{-}31} \text{ (ug/g sed)} / \text{OC (g/g sed)})\text{sample}) / \text{ALK OC}] * 100 \quad (2)$$

In the third technique, we used detailed molecular-level analysis of lipid biomarkers together with principal components analysis (Yunker et al., 2005) developed for nearby locations in the western Arctic. In this analysis, a linear regression was performed on the biomarker loadings from the PCA, and represented a transition from marine/labile markers to stable/terrestrial markers. For molecular organic biomarkers derived from both marine and terrestrial organic matter, their relative contribution from these two diverse sources were estimated by projecting its position in PCA space onto the

regression mixing line (see Yunker et al., (2005)). The relative contribution of each biomarker to marine/terrestrial sources is provided (Table 2.2). The concentration of individual biomarkers in each sample is then scaled to reflect the contribution of that biomarker to marine or terrestrial carbon, and a total sum of terrestrial biomarkers is compared to the total biomarker concentration in order to calculate %Terr OC.

Fourthly, the BIT Index was calculated based on determination of the relative abundances of three branched GDGTs (I, II, and III) compared with the isoprenoid GDGT crenarchaeol ((IV; equation 3), as determined by the area of the $[M+H]^+$ peak for each compound (Hopmans et al., 2004). Roman numerals refer to the GDGT structures shown in Fig. 2.2.

$$BIT = [I + II + III]/[I + II + III + IV] \quad (3)$$

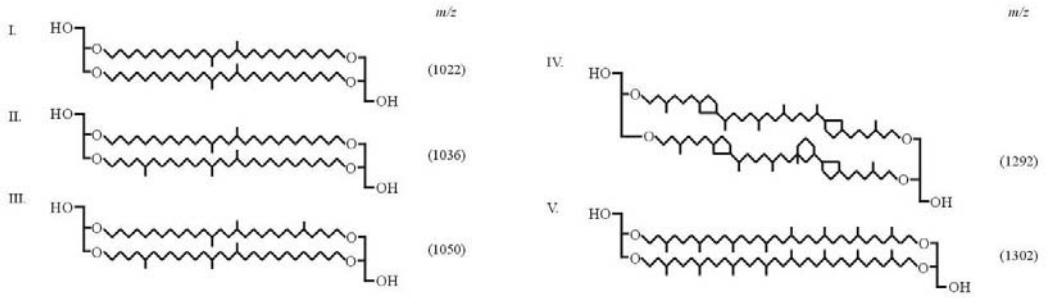

Figure 2.2. Glycerol dialkyl glycerol tetraether lipid structures quantified in this study. Structures I-IV are utilized for construction of the BIT Index, as described in detail in the text.

Table 2.2. Individual lipids used in PCA and the modeled fractional contribution of each biomarker from terrestrial organic matter.

Compound	Fraction Terrestrial	Compound	Fraction Terrestrial	Compound	Fraction Terrestrial
n-alkanes		Other Neutrals		Fatty Acids (cont.)	
C_{17}	0.94	Phytol	0.50	C23:0n	0.56
C_{18}	0.96	α-amyrin	1.00	C24:0n	0.54
C_{19}	0.91			C25:0n	0.36
C_{20}	0.88	Sterols		C26:0n	0.36
C_{21}	0.88	24-norcholesta-5,22-dien-3β-ol ($C_{26}\Delta^{5,22}$)	0.54	C27:0n	0.27
C_{22}	0.85	24-nor-5α-cholest-22-en-3β-ol ($C_{26}\Delta^{22}$)	0.75	C28:0n	0.34
C_{23}	0.84	Cholesta-5,22-dien-3β-ol ($C_{27}\Delta^{5,22}$)	0.81	16:1ω9	0.20
C_{24}	0.85	Cholest-22-en-3β-ol ($C_{27}\Delta^{22}$)	0.79	16:1ω7	0.11
C_{25}	0.79	Cholest-5-en-3β-ol ($C_{27}\Delta^{5}$)	0.66	16:1ω5	0.03
C_{26}	0.86	Cholesta-5,24-dien-3β-ol ($C_{27}\Delta^{5,24}$)	0.61	17:1ω8	0.02
C_{27}	0.84	24-methylcholesta-5,22-dien-3β-ol ($C_{28}\Delta^{5,22}$)	0.82	17:1ω6	0.29
C_{28}	0.79	24-methylcholest-22-dien-3β-ol	0.74	18:1ω9	0.01
C_{29}	0.79	Cholest-7-en-3β-ol ($C_{27}\Delta^{7}$)	0.23	18:1ω7	0.01
C_{30}	0.74	24-methylcholesta-5,24(28)-dien-3β-ol ($C_{28}\Delta^{5,24(28)}$)	0.76	20:1ω9	0.11
C_{31}	0.69	24-methylcholest-5-en-3β-ol ($C_{28}\Delta^{5}$)	0.53	20:1ω7	0.15
		24-methylcholest-24(28)-en-3β-ol ($C_{28}\Delta^{24(28)}$)	0.50	16:2	0.22
		23,24-dimethylcholest-22-en-3β-ol	0.81	18:2	0.29
		24-ethylcholest-5-en-3β-ol ($C_{29}\Delta^{5}$)	0.94	18:2	0.19
n-alkanols		4α,24-dimethylcholestan-3β-ol	0.54	20:4	0.15
C_{14}	0.77	24-ethylcholesta-5,24(28)Z-dien-3β-ol ($C_{29}\Delta^{5,24(28)Z}$)	0.77	20:5	0.29
C_{15}	0.89	24-ethylcholest-7-en-3β-ol ($C_{29}\Delta^{7}$)	0.89	14:0i	0.42
C_{16}	0.54	4α,23,24-trimethylcholest-22-en-3β-ol ($C_{30}\Delta^{22}$)	0.57	15:0i	0.06
C_{17}	0.81	24-propylcholesta-5,24(28)-dien-3β-ol ($C_{30}\Delta^{5,24(28)}$)	0.30	15:0a	0.08
C_{18}	0.67	4α,23,24-trimethylcholest-8(14)-en-3β-ol ($C_{30}\Delta^{8(14)}$)	0.71	16:0i	0.44
C_{19}	0.70			17:0br	0.22
C_{20}	0.71	Fatty acids		17:0i	0.06
C_{21}	0.80	C14:0n	0.26	17:0a	0.00
C_{22}	0.72	C15:0n	0.11	C20 DCA	0.26
C_{23}	0.65	C16:0n	0.01	C21 DCA	0.34
C_{24}	0.79	C17:0n	0.12	C22 DCA	0.25
C_{25}	0.79	C18:0n	0.17	C23 DCA	0.32
C_{26}	0.63	C20:0n	0.36	C24 DCA	0.40
C_{27}	0.53	C21:0n	0.40	C25 DCA	0.34
C_{28}	0.60	C22:0n	0.50	C26 DCA	0.52

2.4. Results

2.4.1. Bulk Sedimentary Characterization

Total organic carbon (OC) ranged from 0.5 to 2% in surface sediments (Fig. 2.3a). Sediments to the eastern side of the sampling zone (Barrow Canyon (BC) and East Barrow (EB) transects, Fig. 2.1) contained higher concentrations of sedimentary OC than those from transects near the east and west sides of Hanna Shoal (EHS and WHS, respectively). Concentrations of sedimentary OC showed no consistent pattern with water depth (Fig. 2.3a). The atomic C:N ratios in most sediments ranged from 7-11.5 (Fig. 2.3b) and were similar to those found in other Arctic Ocean sediments (Belicka et al., 2002; Goñi et al., 2000; Naidu et al., 2000) with two stations as exceptions. Station 1, just north of the Bering Strait, had a very high C:N ratio of 21.2 and Station EHS-12, in the deep Arctic basin, had a much lower C:N ratio of 5.3 (Fig. 2.3b). The C:N ratio was, on average, higher in the BC and EB transects and no shelf-to-basin gradients were observed, similar to trends in total organic carbon concentration. Bulk sedimentary $\delta^{13}C$ was enriched overall compared to sediments to the both the south and east in the Chukchi and Canadian Beaufort Seas (Goñi et al., 2000; Naidu et al., 1993), but most depleted in the BC and EB transects (Fig. 2.3c) The spatial distribution of $\delta^{15}N$ was highly variable, but overall surface sediment $\delta^{15}N$ ranged from 2.03 to 7.83 ‰ (Fig. 2.3d).

To constrain the terrestrial organic carbon $\delta^{13}C$ end-member for this region of the Arctic, three samples from rivers on the Alaskan mainland were collected and analyzed: (1) Ikpikpuk River suspended particulate organic matter ($\delta^{13}C$ = -27.30‰); (2) Ikpikpuk River Delta sediment consisting of peat and woody debris in a light sandy matrix ($\delta^{13}C$ = -28.32‰); and (3) Kokolik River suspended particulate organic matter ($\delta^{13}C$ = -27.67‰).

Based on the average of these analyses, a $\delta^{13}C_{terrestrial}$ value of -27.76‰ was used. As explained in the methods section above, the $\delta^{13}C_{marine}$ value was defined as -17.5‰, yielding a wide range of estimates of %Terr OC from 7-44% in our two end-member mixing model.

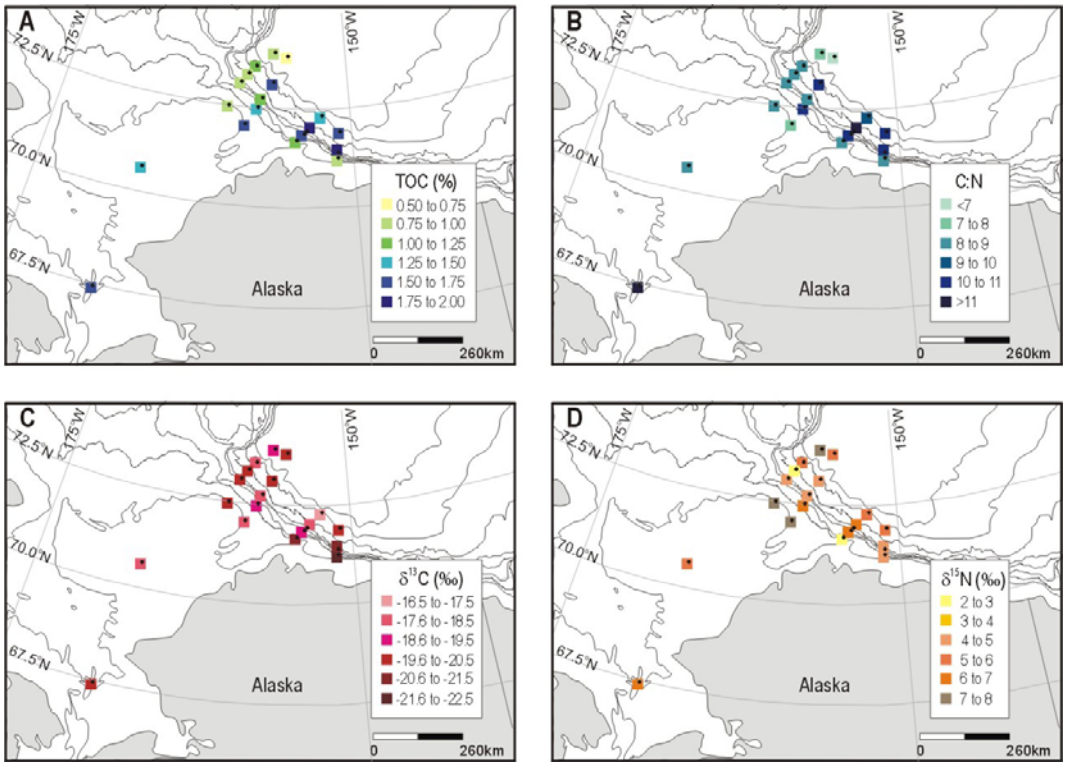

Figure 2.3. Total organic carbon (TOC, %), atomic C:N, $\delta^{13}C$ (‰), and $\delta^{15}N$ (‰) among surface sediments of the 19 sites examined in the western Arctic Ocean.

2.4.2. Lipid Biomarker Distribution

A variety of lipid compounds were present in Chukchi and Beaufort Sea surface sediments. Because the focus of this study is on comparing methods for calculating terrestrial and marine organic matter components, a detailed spatial analysis of the more than 90 individual lipids quantified is beyond the scope of this paper. Instead, we focus on diagnostic groups of markers most useful for assigning organic sources.

Concentrations of individual markers used in the PCA calculation are presented in the appendices (Tables A2.1, A2.2, A2.3, and A2.4).

Most sediments contained a mix of both marine and terrestrial lipids; in general, lipid concentrations were highest in shallow sediments from shelf locations. The total concentration of sedimentary long-chain ($>C_{25}$) *n*-alkanes observed was spatially variable (Table A2.1), but in most stations exhibited the strong odd over even predominance indicative of terrestrial material (Eglinton and Hamilton, 1969). Two notable exceptions were stations WHS-6 and WHS-7, where concentrations of odd and even carbon *n*-alkanes were similar (Table A2.1). The sum of $C_{25\text{-}31}$ odd-carbon *n*-alkanes ($\Sigma ALK_{25\text{-}31}$) was only weakly correlated to sedimentary organic carbon content ($r = 0.65$, Fig. 2.4a). Water depth (shelf versus basin samples) did not show significant trends with either long-chain *n*-alkane concentration (Fig. 2.4a) or $\delta^{13}C$ (Fig. 2.4b). Using the ALKOC ratio (equation 2), the %Terr OC estimates ranged from 9 to 94 % for the nineteen locations.

A representative marine lipid (C16:0n fatty acid) and a representative terrestrial lipid (α-amyrin) are displayed (Fig. 2.5) to illustrate the abundance of both marine and terrestrial organic matter sources in the EB and BC transects (see Tables A2.1-A2.4 for individual lipid concentrations). Despite the enriched $\delta^{13}C$ values of the EHS and WHS transect sediments and their pelagic location, lipids indicative of terrestrial organic matter (including long-chain *n*-alkanes and *n*-alcohols, α-amyrin, and the sterols 24-ethylcholesta-5,22-dien-3β-ol and 24-ethylcholest-5-en-3β-ol) were common in surface sediments. These compounds were, on average, lower than concentrations found in the EB and BC sediments; yet, concentrations of most marine markers were also lower near Hanna Shoal. As a result, the Hanna Shoal transects (EHS and WHS) contained

proportionally more lipids derived from terrestrial material than the EB and BC transects. Utilizing regression techniques together with principal components analysis for the suite of lipid biomarkers quantified (Tables 2.2, A2.1-A2.4), the fractional terrestrial estimates ranged from 20 to 50%.

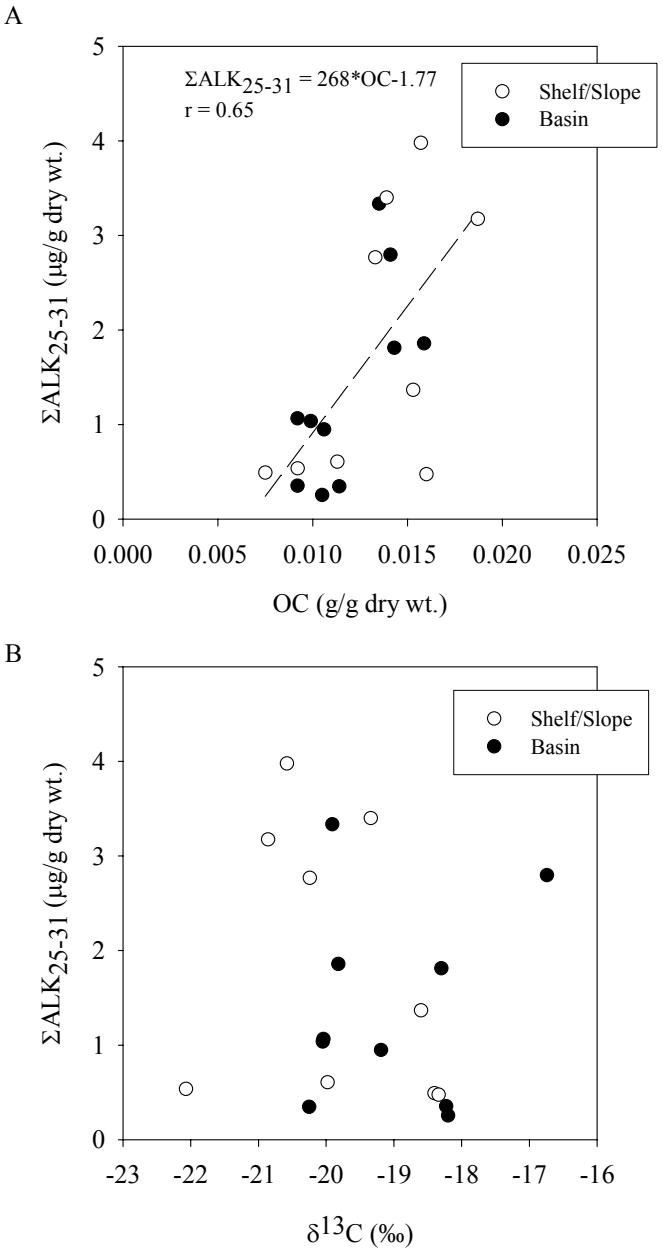

Figure 2.4. Sum of $C_{25\text{-}31}$ odd-carbon number *n*-alkanes versus total organic carbon content (a) and $\delta^{13}C$ composition (b) in shelf and slope (<500 m) and basin (>500 m) environments.

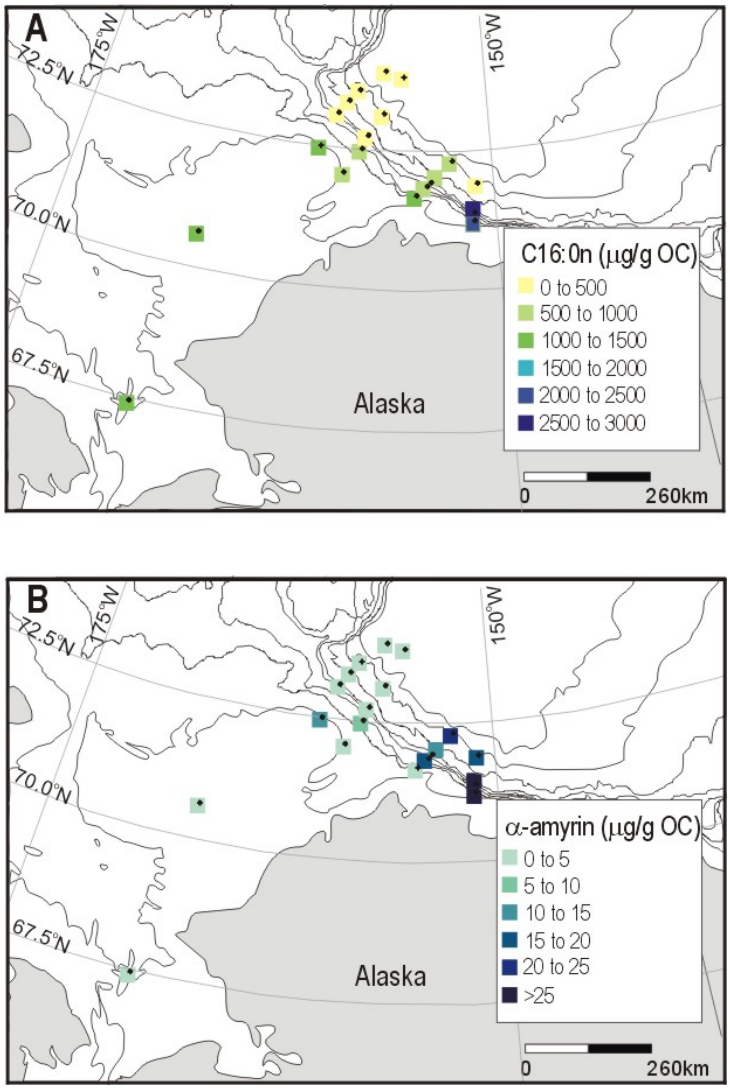

Figure 2.5. The variation in concentrations observed for the C16:0n fatty acid and α-amyrin in surface sediments from the 19 sites examined. Concentrations showed significant declines westward for both markers.

2.4.3. Tetraether Lipids and the BIT Index

Five glycerol dialkyl glycerol tetraether (GDGT) lipids were quantified in all surface sediments excepting Station 2 where adequate sedimentary material for analysis was unavailable (Table A2.5). For this discussion we focus on general trends and the BIT index method of quantification for terrestrial organic matter components.

Crenarchaeol (IV), the group 1.1 Crenarchaeota specific compound (Sinninghe Damsté et al., 2002), and the ubiquitous, non-specific compound (V) were the most abundant GDGTs found in sediments (Table A2.5, Fig. 2.6). Unlike most other lipid biomarkers, crenarchaeol concentrations were high in the Hanna Shoal transects, especially at WHS-2 (Fig. 2.6), and were low in the EB sediments. The branched GDGT compounds (I, II, and III, Fig. 2.2), thought to derive from bacteria living in terrestrial environments (Weijers et al., 2006; Weijers et al., 2007), were generally more abundant in the BC and EB sediments than in the East or West Hanna Shoal sediments (Fig. 2.6). Calculated BIT indices were overall quite low, ranging from 0.03-0.46 (Fig. 2.7).

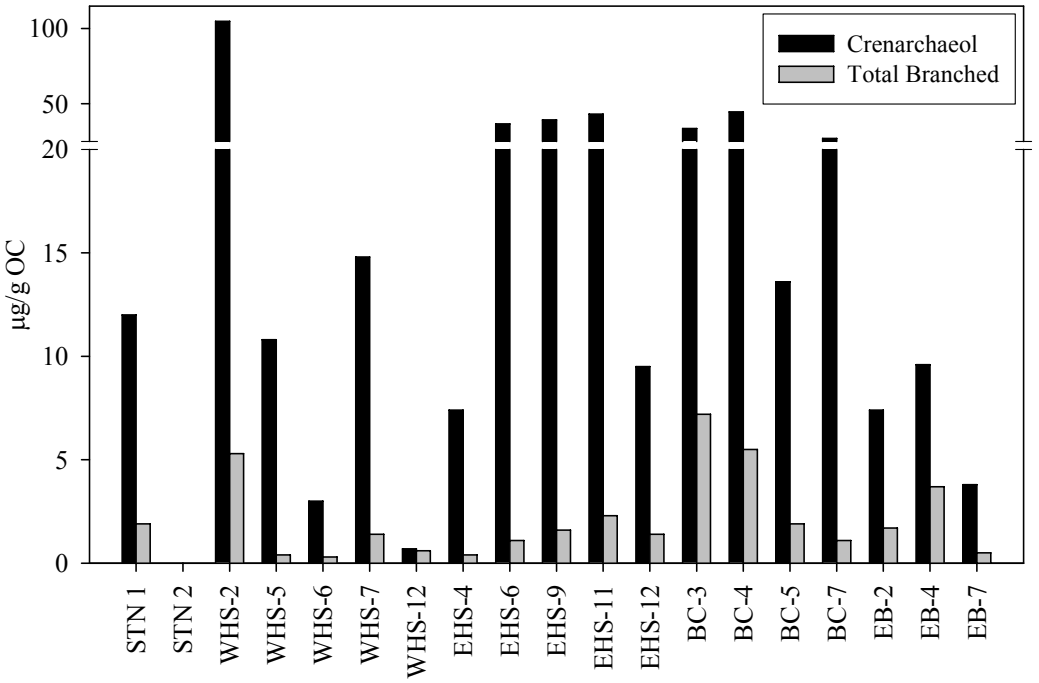

Figure 2.6. Concentrations of crenarchaeol (structure IV) and total branched GDGTs (structures I, II, and III) in surface sediments along shelf to basin transects in the western Arctic Ocean.

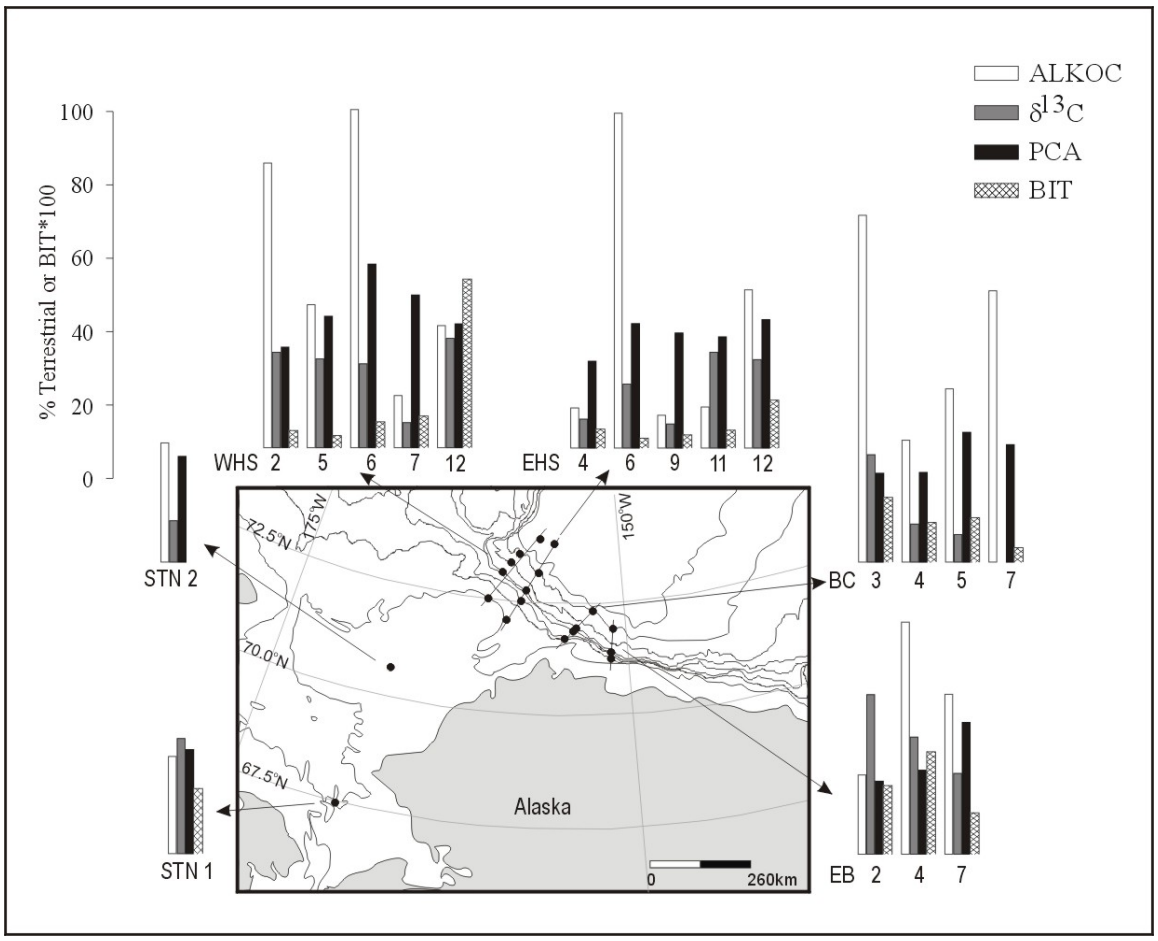

Figure 2.7. Comparison of the four methods for calculation of preserved terrestrial organic matter in surface sediments of the western Arctic Ocean. Note the axis reflects estimated preserved terrestrial organic carbon (in % for ALKOC, $\delta^{13}C$ and PCA methods) or the BIT index (multiplied by 100).

2.5. Discussion

2.5.1. Spatial Trends in Bulk Organic Carbon and Lipid Biomarker Preservation

In general, bulk sedimentary organic carbon increased towards the BC and EB transects (Fig. 2.3a), suggesting that burial efficiency of organic matter is greater in the eastern region of the study area, either from higher levels of primary productivity or lower organic carbon remineralization in the water column and sediments (Meyers, 1997). In concurrent studies of water column processes in the western Arctic (Grebmeier

and Harvey, 2005), the area around Barrow Canyon was characterized by exceptionally high rates of primary productivity, estimated to reach a maximum of 430 g C m^{-2} yr^{-1} (Hill and Cota, 2005), as well as the highest rates of export productivity for this study region (Moran et al., 2005). The Barrow Canyon feature appears to act as a focusing zone to funnel organic matter to the central canyon sediments, resulting in the elevated OC concentrations. The sedimentary distribution of total organic matter presented here closely reflects trends of water column particulate organic carbon (POC) presented by Bates et al. (2005b), with the highest concentrations of POC found in summertime over the BC and EB transects and the lowest OC from the EHS and WHS transects, and suggests a tight coupling between the pelagic and benthic realms. High concentrations of suspended organic matter were observed in tongues extending off the shelf into the basin in the SBI region (Bates et al., 2005b), which may also contribute to elevated sedimentary organic matter at the continental slope stations as compared to shallow shelf or deep basin environments. As a result, the sedimentary environment of the Barrow Canyon region may play an important role in the shelf to basin exchange of organic matter. Recent studies indicate that the flow of nutrient rich waters through Barrow Canyon is an important mechanism to deliver nutrients to the basin (Weingartner et al., 2005)—part of this off shelf flow may include nutrients regenerated from recently deposited sediments.

Atomic C:N ratios were also generally higher in the EB and BC transects (Fig. 2.3b). These sites are closer to the Alaskan shoreline, and the elevated C:N ratio in these sediments is likely reflecting terrestrial inputs from several small rivers and coastal erosion. This input of land-derived organic matter to the Barrow Canyon region is also

suggested by the sedimentary $\delta^{13}C$, which was lightest in the BC and EB transects (Fig. 2.3c). The heavy $\delta^{13}C$ values in the transects to the east and west of Hanna Shoal are indicative of widespread marine material, and the lack of proximity of Hanna Shoal to either the Alaskan or Russian coastline limits direct inputs of terrestrial organic materials. In contrast to the trends in $\delta^{13}C$ distribution, the $\delta^{15}N$ composition was more variable and less spatially distinct (Fig. 2.3d), ranging from 2.03-7.83 ‰, similar to values of 5.4 to 8.2 ‰ found in surface sediments of the central Arctic Ocean (Schubert and Calvert, 2001). This large variability in $\delta^{15}N$ is likely representing the balance between inputs of land-derived materials, which express relatively depleted $\delta^{15}N$ compositions as a result of minimal fractionation, and phytoplankton utilization of nitrate (Schubert et al., 2001). A $\delta^{15}N$ analysis separating the bound and organic forms of nitrogen, as in Schubert and Calvert (2001), may help resolve these processes.

Lipid biomarker concentrations generally paralleled organic matter distribution, with high concentrations of marine (diatom) markers (14:0n, 16:0n, 16:1ω7, 20:5) in the EB and BC sediments, consistent with the high levels of primary productivity noted in this location. However, the terrestrial markers including the $C_{29}\Delta^5$ sterol and the triterpenoid α-amyrin were also very high in the BC and EB sediments, suggesting that the sediments east of Barrow Canyon appear to be a deposition center for both sources of organic matter in the western Arctic Ocean. Unlike most other lipids quantified, long-chain *n*-alkane concentrations were not enhanced in the EB sediments, possibly indicating a different source of these markers compared to $C_{29}\Delta^5$ and α-amyrin.

Crenarchaeol (IV) and the non-specific tetraether (V) were the most abundant GDGTs in sediments (Table A2.5, Fig. 2.6). In contrast to most other lipid biomarkers

noted above, crenarchaeol concentrations were high in the Hanna Shoal transects, especially at WHS-2 (Fig. 2.6). Higher crenarchaeol abundances have been found with increasing pH in soils (Weijers et al., 2006); however, it is unclear why sediments near Hanna Shoal would potentially have more basic pH levels than East Barrow sediments. Branched GDGTs (I, II, and III) are assumed to be produced by bacteria as opposed to archaea, largely because of their branched alkyl chains and their 1,2-di-*O*-alkyl-*sn*-glycerol stereochemical configuration at C-2 in the glycerol backbone (Weijers et al., 2006; Weijers et al., 2007). It has been suggested that the organisms that produce branched GDGTs thrive in peat bogs (Herfort et al., 2006). The BC and EB sediments, where these markers were most abundant, are in close proximity to the Alaskan coastline which undergoes tremendous amounts of erosion. This coastline is also characterized by peat-rich deposits, and elevated concentrations of branched GDGTs in the BC and EB sediments may reflect mobilization of peat deposits into the Arctic Ocean.

2.5.2. Terrestrial Organic Carbon Fractions among the Methods

Of the four approaches studied here, the two end-member mixing model and the PCA/regression analysis resulted in intermediate estimates for the fraction of terrestrial organic carbon components, with very high estimates seen for the ALKOC ratio method and low terrestrial carbon values seen for the BIT index.

The $\delta^{13}C$ two end-member mixing model is the only technique among the four analyzed that incorporates bulk organic carbon, and it is also very sensitive to the assigned isotopic end-member values. The chosen terrestrial $\delta^{13}C$ value for our mixing model of -27.7‰ closely matches standard isotopic values of land plants that utilize the

C_3 photosynthetic pathway (-26 to -28‰)—this pathway is most common in northern latitudes where C_4 or CAM plants do not thrive (Naidu et al., 2000). The range of reported $\delta^{13}C$ values for land-derived organic matter entering the Arctic Ocean is thus rather narrow. Sinking organic particles at the mouth of the Yenesei River had average $\delta^{13}C$ values of around -26.9 ‰ (Gaye et al., 2007), while those at the mouth of the Mackenzie River ranged from -25.4 to -26.0 ‰ (Drenzek et al., 2007; Goñi et al., 2000). In a recent analysis of POC from three Alaskan Rivers, Guo et al. (2007) found $\delta^{13}C$ to range from -26.79 to -28.90 ‰. Samples of peat and suspended organic matter collected at the Ikpikpuk and Kokolik river mouths were nearly identical to these additional Alaskan river particulate samples and ranged from -27.30 to -28.32 ‰.

Several authors have noted the difficulty in assigning a marine $\delta^{13}C$ end-member for polar waters, in part because of the increasing solubility of CO_2 with decreasing temperatures, differences in cell sizes and growth rates, and potential inputs of sea-ice algae, which may have limited access to dissolved inorganic carbon substrates (Gradinger, in press; Laws et al., 1995). The $\delta^{13}C$ composition of Arctic sea-ice algae recently sampled from this study region ranged from -25 to -14.2‰ (Gradinger, in press), with samples from the Canadian Arctic very similar, ranging from -24.9 to -13.2‰ (Tremblay et al., 2006). Both studies found increasing $\delta^{13}C$ values with increases in sea-ice biomass, an observation that supports DIC limitation leading to reduced isotopic fractionation. A wide range in isotopic composition of water column marine phytoplankton has also been reported for the Arctic (-16.7 to -30.4‰, (Goericke and Fry, 1994)); however for this study region, Gradinger (in press) found water column phytoplankton $\delta^{13}C$ to vary between -26.1 to -22.4‰.

If we assume that the water column and ice phytoplankton $\delta^{13}C$ measured by Gradinger (in press) are representative of marine organic matter in this area, the heavy isotopic composition of most sediment samples in this study (-16.74 to -22.07‰) suggests substantial retention of carbon in sediments from ice algae. Additionally, we can also infer that the bulk preserved organic matter contains substantial inputs of marine origin, reflected by the estimates of terrestrial organic matter calculated using the mixing model (7-44%; Fig. 2.7). This assumption also relies on little to no input from plants using the C_4 photosynthetic pathway, which encompasses plants common in arid and tropical regions assumed to be negligible in the Arctic (Naidu et al., 2000 and references therein).

While $\delta^{13}C$ can be used to make these general claims about organic matter sources in Arctic sediments, the large variability in reported $\delta^{13}C$ values for both water column and ice phytoplankton and the difficulty in determining potential inputs from sea-ice algae in Arctic sediments are problematic and inhibit quantitative ability of $\delta^{13}C$ mixing models. Additional constraints on the isotopic variability of ice and water column Arctic phytoplankton are necessary to improve the usefulness of this approach.

The three other approaches (ALKOC ratio, PCA scaling, and BIT index) rely on preserved organic markers, in particular, lipids. Lipid biomarkers, specific to their molecular precursors, impart modern or historical organic matter source information. Long-chain ($>C_{25}$) odd carbon *n*-alkanes, for example, derived from protective wax coatings on higher plant leaves, generally indicate terrestrial organic matter inputs. With the exception of stations WHS-6 and WHS-7, surface sediments in the study region showed a strong odd over even predominance (OEP) indicative of terrestrial material

(Eglinton and Hamilton, 1969). Petrogenic inputs may be contributing to the *n*-alkane distribution at the two WHS sites; however, bacterial degradation of the odd-chain alkanes has also been proposed as an explanation for a lack of OEP (Yunker et al., 1994).

In river-dominated margins like the Columbia River, or the Laptev or Kara Seas in the Arctic, there exists a relatively constant ratio of long-chain *n*-alkanes to organic carbon, often termed the ALKOC ratio (Fernandes and Sicre, 2000; Prahl et al., 1994). For the Laptev and Kara Seas, this ratio is 750 and 451, respectively (Fernandes and Sicre, 2000; Stein and Fahl, 2004). In contrast, the ALKOC for the western Arctic was 268 (Fig. 2.4), reflecting lower concentrations of *n*-alkanes per organic carbon content in the western Arctic than in the eastern Arctic. By dividing the organic carbon normalized long-chain *n*-alkane concentration by the ALKOC ratio, one can obtain an estimate of the fraction of terrestrial material preserved in sediments. For this study region, the ALKOC routinely appears to overestimate preserved terrestrial organic components compared to the other techniques for most sampling stations (Fig. 2.7). This method makes two assumptions—first, that *n*-alkanes are delivered at the mouth of the river to the coast in a fixed ratio and second, that a change in the ALKOC ratio in shelf sediments is caused by simple dilution with marine organic matter that does not contain long-chain *n*-alkanes (Fernandes and Sicre, 2000; Prahl and Carpenter, 1984; Prahl et al., 1994). The weak correlation between long-chain *n*-alkanes and organic matter concentration (Fig. 2.4a) and the lack of relationship between water depth (distance from shoreline) and *n*-alkane concentration (Fig. 2.4b) in this study region suggest that these assumptions do not hold true for this area of the Arctic Ocean. Unlike the Laptev and Kara Seas, which are strongly influenced by a major river system, the eastern Chukchi and Alaskan Beaufort

Seas contain numerous small rivers distributed along the coastline. The Colville River alone delivers an estimated 170,000 t yr^{-1} of particulate organic carbon to this region (Macdonald et al., 2004a). Estimates of coastal erosion along the Beaufort Sea coast range from 0.5 to 6 m yr^{-1} (Are et al., 2008; Lantuit and Pollard, 2008) and may even reach a maximum of 18 m yr^{-1} (Harper, 1990), demonstrating that this delivery pathway also plays a major role in carbon dynamics in this region. Although the ALKOC ratio was found to be quite useful for regions such as the Kara Sea where the simple dilution of river-derived terrestrial organic matter occurs (Fernandes and Sicre, 2000), the patchy distribution of terrestrial organic matter inputs in the western Arctic preclude its quantitative use.

For most transects, the PCA approach resulted in higher estimates of preserved terrestrial organic matter at deep water stations. While at first glance the trend of increased terrestrial organic matter offshore may seem counterintuitive, especially for the WHS and EHS locations that are far removed from any direct source of terrestrial organic matter, several lines of evidence support this observation. First, terrestrial organic matter delivered to the pelagic WHS and EHS sediments likely arrives via melting sea-ice. A study by Eicken et al. (2005) in the region concluded that major ice transport trajectories, both observed and simulated, followed an east to west path, resulting in transport of particulate matter by sediment laden sea-ice towards the western-most transects. Furthermore, sediments were entrained into the ice by resuspension at water depths <20 m (Eicken et al., 2005), suggesting considerable incorporation of terrestrial organic matter at shallow depths near the coastline where erosion rates are high. Cooper et al. (2005) have found rapid (~3 month timescales) deposition of sea-ice rafted particulate

matter to surface sediments in the study area, particularly on the shelf but also extending into deeper waters which highlights the ability for sea-ice to provide an effective mechanism for particle export (Cooper et al., 2005). In the deep waters of the WHS and EHS regions, net daily production was still quite low in summertime compared to the BC and EB regions, despite high productivity on the shelf (Hill and Cota, 2005). In the absence of high levels of primary production, much of this marine organic matter is likely recycled in the water column prior to deposition, effectively leading to enhanced terrestrial organic matter preservation in deeper waters. Although the BC and EB transects were characterized by high levels of marine primary productivity as discussed above, the PCA-based estimation still showed increased levels of terrestrial organic matter at the basin stations. This is likely reflecting decreased levels of primary productivity from longer sea-ice coverage, as well as inputs of coastal erosion that extend to the basin. The narrow Alaskan Beaufort shelf likely exerts more influence on the basin than the broad shelf near Hanna Shoal. It is possible that the terrestrial organic matter delivered to the BC and EB sediments arrives mainly via sediment slumping or water column transport, as opposed to the sea-ice rafting characteristic of the Hanna Shoal region.

The PCA approach is robust in that it utilizes a large number of individual lipids (94 compounds in this case) from marine and terrestrial organic matter sources, and does not have the difficulties of choosing end-members or the problems of spatial variability as described for the $\delta^{13}C$ mixing model and ALKOC methods. Because it relies on only preserved lipids, however, it may introduce bias into terrestrial organic matter estimates if the lipid distribution is not representative of the bulk organic matter inputs and therefore

more accurately reflects the preservation of terrestrial organic matter rather than estimate delivery of terrestrial organic matter.

The BIT index resulted in the lowest estimates of terrestrial organic matter with most stations representing typical open ocean marine environments (Herfort et al., 2006; Hopmans et al., 2004). Out of the four proxies, the BIT index also showed the greatest differences between the western (EHS and WHS) and eastern (EB and BC) transects. In the western transects the BIT index increased offshore, indicating increased preserved terrestrial organic matter offshore in the basin similar to the results of the PCA-based approach as discussed above. In contrast, in the BC and EB transects the opposite trend as the PCA approach was found, with decreasing estimates of preserved terrestrial material with water depth. Because the GDGT compounds are thought to occur from bacteria living in the terrestrial environment, as opposed to the terrestrial material itself, and from several observations that have noted the abundance of branched GDGT compounds in peat bogs (Herfort et al., 2006; Hopmans et al., 2004; Weijers et al., 2006), it may be that the BIT index tracks inputs of peat carbon, whereas the lipid markers utilized in the PCA could represent higher-plant derived organic matter. This issue requires further evaluation as more information of the provenance of these markers comes to light.

2.5.3. Implications for Arctic organic carbon budgets

The large difference between terrestrial organic matter approximations (Fig. 2.7) demonstrates that estimates are not directly comparable. This conclusion has broad implications for the development of pan-Arctic carbon budgets and as well attempts to

follow the relative fate of marine and terrestrial organic matter components in other aquatic settings. Each quantification technique clearly has benefits and drawbacks, but caution must be taken when attempting to compare organic matter dynamics in various regions of the Arctic using these distinctly different proxies.

This point can be illustrated with a simple carbon budget calculation. Consider, for example, station EB-4, located in the eastern sampling section and likely receiving terrestrial organic matter inputs from both rivers (including the Colville) and coastal erosion. Holocene sedimentation rates for this region are not well constrained (Macdonald et al., 2004a); however, on the inner shelf near the Colville Delta, an average sediment accumulation rate of 1 g cm^{-2} yr^{-1} was observed (Naidu et al., 1999). While it is likely that the delta region receives much higher sedimentary fluxes than the continental slope (EB-4), considerable amounts of POC were found to escape deltaic sedimentation through entrainment in sea-ice during the spring thaw and subsequently undergoing burial farther offshore (Macdonald et al., 2004a and references therein). If we conservatively assume that 10% of this material reaches water depths of 500 m near EB-4, we obtain an estimated sediment accumulation rate of 100 mg cm^{-2} yr^{-1} in the EB-4 region, which is similar to the average mass accumulation rate (133 mg cm^{-2} yr^{-1}) measured by Baskaran and Naidu (1995) for the adjacent Chukchi Sea. Utilizing the ALKOC method of preserved terrestrial organic matter (63.3%) and the organic carbon concentration (1.871%), we would estimate that surface sediments at EB-4 receive approximately 1.18 mg cm^{-2} yr^{-1} of terrestrial organic carbon. In contrast, if we were to use the result from the PCA-based model and assume that only 23% of the organic matter preserved in sediments was terrestrial in origin, we would conclude that less than half as

much (0.43 mg cm^{-2} yr^{-1}) of terrestrial organic carbon is deposited in sediments. This nearly three-fold discrepancy is also a concern when attempting to determine sedimentary reserves of marine organic matter by difference, as well as when extrapolating in a carbon budget to determine the fraction of terrestrial organic matter that has been respired or exported.

The two end-member stable carbon isotopic mixing model and the ALKOC approach were not found to be suitable for the western Arctic based on the difficulties in assigning marine organic matter end-members and varied inputs from both small rivers and coastal erosion as discussed above. The BIT index approach may be promising; however, more information on the provenance of the branched and isoprenoid GDGT compounds is needed to confirm that the BIT index does indeed reflect terrestrial (including peat-derived) organic matter inputs. Because it is a multi-marker approach, the PCA based method likely provides the best current method of estimating preserved terrestrial organic matter in the Chukchi and Alaskan Beaufort Sea region of the Arctic Ocean. Based on this approach, estimates of the fraction of terrestrial organic matter ranged from 20 to 50%. While such measures reveal that marine-derived organic matter is a strong input to the productive Chukchi and western Beaufort Seas, terrestrial organic matter plays a surprisingly important role in the organic carbon cycle. Implicit in these estimates is the assertion that unlike the traditional model of open ocean carbon dynamics where inputs are largely marine-derived and rapidly recycled, the abundant terrestrial organic carbon delivered to Arctic sediments is sequestered over much longer timescales. Few estimates of the differences in remineralization rates between marine versus terrestrial organic substrates exist for Arctic regions, but generalized pan-Arctic carbon

cycle box models suggest marine organic matter on Arctic shelves is oxidized up to 70 times faster than shelf terrestrial organic matter (Stein and Macdonald, 2004a). The difference in recycling between marine and terrestrial sources and its implications for the rate of carbon turnover in sediments necessitate a quantitative evaluation of preserved terrestrial and marine components in modern and historical Arctic sediments for modeling of the Arctic carbon cycle.

2.6. Conclusions

Current methods used to estimate fractions of terrestrial organic matter in marine sediments show considerable variation for identical sediment samples. This limits our ability to incorporate these types of estimates into pan-Arctic carbon budgets. The BIT index resulted in lower estimates for terrestrial organic matter than the other techniques, suggesting that this proxy may represent a different fraction of terrestrial organic matter; i.e., peat or soil organic matter, as opposed to markers such as n-alkanes or long-chain fatty acids which measure higher plant wax inputs. The lipid-based PCA approach resulted in higher proportions of terrestrial organic matter than bulk organic carbon proxies, suggesting that organic matter fractions such as amino acids and carbohydrates may be contributing marine organic matter to sediments, but is likely the most appropriate proxy for terrestrial organic matter in the western Arctic. Overall, average terrestrial organic matter inputs to the Chukchi and western Beaufort Seas using the multi-marker PCA approach ranged from 20-50%, highlighting the importance of terrestrial organic matter in Arctic Ocean sediments, even on non-river dominated continental margins. The potential for increasing inputs of both fresh and ancient terrestrial organic matter with continued Arctic warming argues that Arctic sediments

may play an increasingly important role in the sequestration of carbon in the future. Models which incorporate elemental cycling will require refinement to account for the multiple pools of organic matter and the potential for large differences in recycling rates.

Chapter 3: Tracking Particulate Organic Matter Recycling in the Western Arctic Ocean: Implications for the Deposition and Long-Term Storage of Organic Carbon

3.1. Abstract

Chemical characterization of suspended particulate organic matter demonstrated considerable spatial heterogeneity in organic carbon abundance in the western Arctic. The lipid composition of surface and intermediate particles reflected the abundant labile marine material present after the spring phytoplankton bloom and contained little to no molecular evidence of terrestrial organic matter inputs. In contrast, deep water offshore particles contained relatively higher concentrations of long-chain fatty acid markers indicative of land-derived material, suggesting that lateral transport of allochthonous inputs augment the organic matter inventory in the Arctic basin. The average age of basin suspended particulate organic matter increased with water depth, indicating that fresh marine components are rapidly recycled in the upper water column while older, more recalcitrant material remains for export and burial.

3.2. Introduction

The broad continental shelf areas of the western Arctic Ocean support some of the highest global levels of marine primary productivity (Gosselin et al., 1997; Wheeler et al., 1996), yet details of the production, recycling, and ultimate fate of this organic carbon remain unresolved. The complexity of the Arctic system, demonstrated by strongly intertwined physical and biogeochemical cycles (Grebmeier, 1993), leads to much of this

uncertainty. Sea-ice cover with corresponding light limitation and stratification of the water column from spring runoff and ice melt exert control over the timing, location, and intensity of phytoplankton blooms, which subsequently impact food supplies for benthic populations and higher trophic levels (Hill and Cota, 2005). Continental run-off via rivers and erosion strongly influences the Arctic Ocean (Rachold et al., 2004), adding nutrients, mineral grains, and terrigenous particulate and dissolved organic matter. Recent studies have focused on Arctic sediments to understand organic carbon dynamics in this sensitive polar setting (Belicka et al., 2004; Drenzek et al., 2007; Guo et al., 2004; Yamamoto et al., 2008), yet suspended particulate organic matter (POM) provides the primary source of organic materials and acts as an integrator of the biological, chemical, and physical processes operating in the water column (Budge and Parrish, 1998; Canuel and Zimmerman, 1999; Volkman et al., 1998; Wakeham and Beier, 1991; Wakeham et al., 1980). Unlike sedimentary investigations, which offer clues of organic carbon dynamics integrated over long time scales, suspended particle analysis provides a snapshot perspective of water column biogeochemical and physical conditions and shorter timescale transformation processes.

The decadal-long multidisciplinary western Arctic Shelf-Basin Interactions Program (SBI) was initiated with a primary goal of understanding how global climate change affects physical and biogeochemical processes in shelf, slope, and basin environments. Here, as part of the SBI Program, we present a lipid biomarker analysis of particulate organic matter from the western Arctic Ocean in order to characterize the sources and transformation of organic matter in the summer Arctic water column.

3.3. Methods

3.3.1. Study area and Sampling

Samples were collected during two summer process cruises for the SBI Program in 2002 and 2004 aboard the USCGC *Healy*. The majority of samples reported here were taken during the 2002 sampling cruise (July 17-August 21), while two basin locations, EHS-12 and EB-8 were taken during 2004 (July 19-August 23) to augment the 2002 collections. The sampling scheme for the SBI Program was designed to investigate the exchange of water masses and suspended materials between shelf and basin environments (Grebmeier and Harvey, 2005), and focused on transects extending from the Chukchi/Alaskan Beaufort Shelves to the Canada Basin. Here, we report on primary samples along the East Barrow Canyon (EB) and Barrow Canyon (BC) transects, as well as selected stations from East Hanna Shoal (EHS), the Bering Strait (BS), and Alaskan Coastal Water (ACW) locations (Fig. 3.1).

Water samples were collected with 30 L Niskin bottles mounted on a rosette with CTD package. Suspended particulate matter was collected onto pre-combusted GF/F filters (0.7 μm) by closed-system vacuum filtration to avoid contamination. The filters were packed in pre-combusted aluminum foil packets and stored at -20 °C aboard the ship. Upon return to the laboratory, samples were stored at -70 °C until analysis.

3.3.2. Chemical Analyses

Particulate organic carbon (POC) and total particulate nitrogen (PN) were determined with an Exeter Analytical 440-XA elemental analyzer following vapor-phase acidification with concentrated HCl. Total lipids were extracted from the particulate

organic matter using a modified Bligh and Dyer (1959) extraction method, as previously described (Belicka et al., 2002). Briefly, filters were extracted quantitatively using multiple organic solvents, saponified under alkaline conditions, and partitioned into neutral and polar fractions. Fractions were then derivatized prior to chromatographic analysis to form the respective methyl esters (polar) or trimethylsilyl (neutral) derivatives. Gas chromatography with flame ionization detection and gas chromatography with mass selective detection were employed for identification and quantification, respectively.

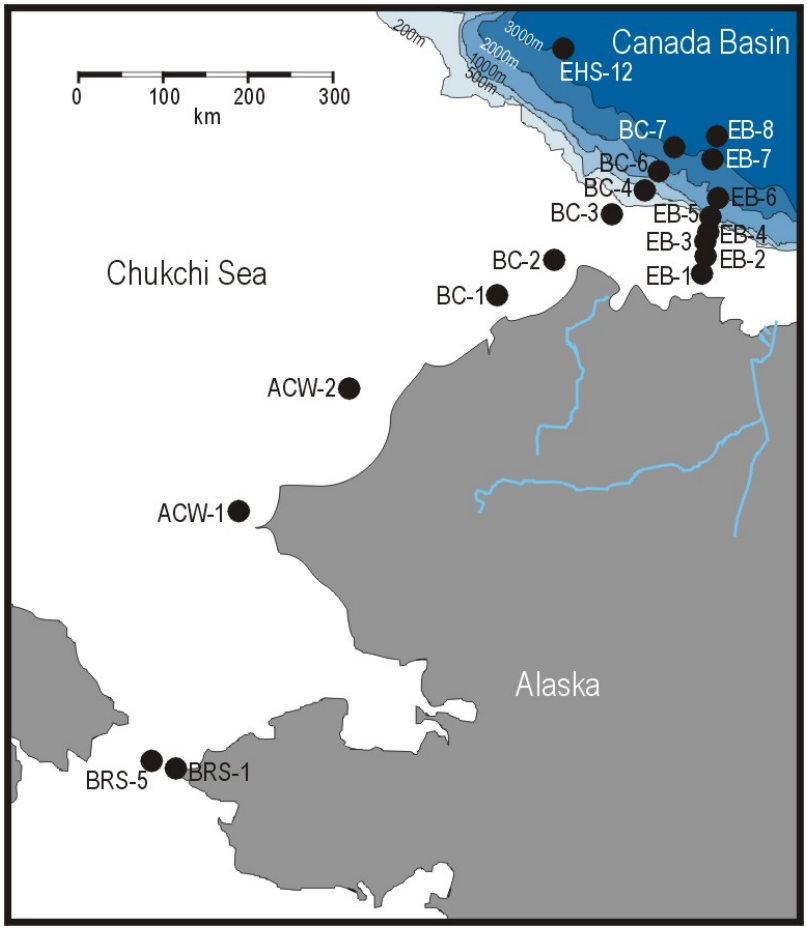

Figure 3.1. Map of stations where particulate organic matter (POM) samples were collected in the western Arctic Ocean.

3.3.3. Data Analyses

To explore the spatial variability in bulk organic matter properties, samples were classified based on total station water depth (shelf versus basin location) and sample depth (surface, halocline, deep water; Table 3.1). This classification resulted in five regions: (1) Shelf Surface Waters (POM collected landward of 200 m isobath, from ≤ 40 m water depth, n=13); (2) Shelf Halocline Waters (landward of 200 m isobath, 41-200 m water depth, n=7); (3) Basin Surface Waters (seaward of 200 m isobath, ≤ 40 m, n=7); (4) Basin Halocline Waters (seaward of 200 m isobath, 41-200 m, n=13); and (5) Basin Deep Waters (seaward of 200 m isobath, >200 m, n=13).

Selected POM samples as well as surface sediment intervals (presented in Chapter 2) from the EB-7 and EHS-12 stations were sent to the National Ocean Sciences Accelerator Mass Spectrometry (NOSAMS) facility for $\delta^{13}C$ and $\Delta^{14}C$ analysis (Table 3.2). Unfortunately, the 800 m sample from EB-7 did not contain sufficient quantities of organic carbon for radiocarbon analysis. In order to obtain an estimate of deep water carbon isotopic composition, one particulate organic matter sample was taken from 1000 m depths at a nearby station (EB-8, Fig. 3.1) during a subsequent cruise (HLY04-03; summer 2004). In all cases, $\Delta^{14}C$ is corrected for fractionation effects using measured $\delta^{13}C$ values from the same sample. Values of $\Delta^{14}C$ were calculated from the NOSAMS f_m (fraction modern) reported values using equation 1 (Stuiver and Polach, 1977) where $\lambda = 1/8267$ and y_m is the year measured:

$$\Delta^{14}C = (f_m * e^{\lambda*(1950-ym)} - 1)*1000 \qquad (1)$$

Table 3.1. Station identification, total water depth, sample depths, and location and water mass classifications for particulate organic matter samples collected in the western Arctic Ocean.

Station Number	Name	Water Depth (m)	Sample Depth (m)	Location	Water Mass
HLY-02-03-007	ACW-1	45	10	Shelf	Surface
			38	Shelf	Halocline
HLY-02-03-008	ACW-2	32	10	Shelf	Surface
			28	Shelf	Surface
HLY-02-03-010	BC-1	79	15	Shelf	Surface
			60	Shelf	Halocline
HLY-02-03-012	BC-2	117	15	Shelf	Surface
			50	Shelf	Halocline
HLY-02-03-013	BC-3	179	24	Shelf	Surface
			65	Shelf	Halocline
			150	Shelf	Halocline
HLY-02-03-014	BC-4	524	22	Basin	Surface
			100	Basin	Halocline
HLY-02-03-016	BC-6	1753	25	Basin	Surface
			50	Basin	Halocline
			170	Basin	Halocline
			300	Basin	Deep
			800	Basin	Deep
			1500	Basin	Deep
HLY-02-03-017	BC-7	3122	42	Basin	Halocline
			90	Basin	Halocline
			170	Basin	Halocline
			1000	Basin	Deep
			2000	Basin	Deep
			3000	Basin	Deep
HLY-02-03-001	BRS-1	99	15	Shelf	Surface
HLY-02-03-002	BRS-5	51	15	Shelf	Surface
HLY-02-03-024	EB-1	48	14	Shelf	Surface
			35	Shelf	Surface
HLY-02-03-023	EB-2	86	25	Shelf	Surface
			90	Shelf	Halocline
HLY-02-03-022	EB-3	171	35	Shelf	Surface
			80	Shelf	Halocline
			120	Shelf	Halocline
HLY-02-03-021	EB-4	410	20	Basin	Surface
			120	Basin	Halocline
HLY-02-03-020	EB-5	832	30	Basin	Surface
			113	Basin	Halocline
			170	Basin	Halocline
			300	Basin	Deep
			800	Basin	Deep
HLY-02-03-019	EB-6	2202	15	Basin	Surface
			30	Basin	Surface
			45	Basin	Halocline
			133	Basin	Halocline
			500	Basin	Deep
HLY-02-03-018	EB-7	2953	30	Basin	Surface
			130	Basin	Halocline
			800	Basin	Deep
HLY-04-03-051	EHS-12	3700	50	Basin	Halocline
			524	Basin	Deep
			1000	Basin	Deep
			3669	Basin	Deep

All statistical analyses were performed with SAS version 9.1 (SAS Institute, Inc.). Analysis of variance (ANOVA) followed by Tukey's Honestly Significant Difference test were utilized to attempt to compare between the means of POC, PN, C:N, and total fatty acids (TFA) within each water type classification. When assumptions of normality and heterogeneity of variance were not met, data were normalized with a logarithmic transformation. A significance level of <0.05 was used for all analyses. Principal components analysis with varimax rotation of concentration-normalized lipid biomarker data was employed to reduce the dimensionality and examine the relationship between molecular compounds and between observations. For lipid biomarkers not detected in a given sample, a value of ¼ of the minimum amount detected for that variable in the entire sample set was assigned to alleviate gaps in the data. Individual fatty acids (in μg/g OC) were normalized to total fatty acid concentration and individual sterols were likewise normalized to total sterol concentration prior to statistical analysis to remove bias from the large differences in concentration between samples and also between these two types of markers. Variables not present in 33% or more of samples were removed from the analysis. The final dataset for the analysis therefore consisted of 53 observations (samples) and 36 variables (biomarkers).

Table 3.2. Results of carbon isotopic analysis of POM and surface sediment samples from the East Barrow and East Hanna Shoal basin stations.

Station Name	Depth (m)	$\delta^{13}C$ (‰)	f_m	$\Delta^{14}C$ (‰)	Age (^{14}C Years)	NOSAMS Accession #
EB-7 POM	30	-22.34	1.0085	2.0	>Modern	OS-39127
EB-7 POM	130	-23.97	0.9551	-51.0	370 ± 55	OS-41431
EB-8 POM	1000	-25.76	0.8338	-171.7	1460 ± 75	OS-48936
EB-7 Sed[a]	Surface Sed	-23.64	0.4668	-536.1	6120 ± 30	OS-40759
EHS-12 POM	50	-26.77	0.9678	-38.6	260 ± 35	OS-48365
EHS-12 POM	1000	-25.93	0.7833	-221.9	1960 ± 85	OS-48930
EHS-12 Sed[a]	Surface Sed	-23.39	0.3333	-668.9	8820 ± 40	OS-48216

[a]See Chapter 2 for surface sediment collection details. Also note EB-8 POM details in methods section above.

3.4. Results

3.4.1. Bulk particulate organic matter abundance and distribution

Particulate organic carbon (POC) and particulate nitrogen (PN) concentrations ranged from 6.9 to 782 μg/L and 0.6 to 193 μg/L, respectively (Fig. 3.2). Both were present in the highest concentrations between 15-30 m corresponding to the average depth of the chlorophyll max (not shown), although concentrations throughout the upper 100 m were highly variable. Below 200 m, concentrations of POC and PN were low and fairly constant (Figs. 3.2a and 3.2b). Atomic C:N ratios ranged from 4.7 to 17.7 and increased with depth, although deep waters showed considerable variability (Fig. 3.2c).

Regional and water mass groupings of the samples showed general differences for POC, PN, and C:N between shelf and basin locations and surface, halocline, and deep waters (Fig. 3.3). Surface waters from both the shelf and basin contained the highest average POC and PN, although the variability was quite high, especially for shelf samples (Fig. 3.3a, b). The average C:N ratios were low and similar for both shelf and basin surface waters, at 6.7 and 6.25, respectively. Halocline water C:N ratios were also quite similar, averaging 7.3 for the shelf and 7.7 for the basin samples. The C:N ratio in the deep waters of the basin was considerably higher, with an average value of 11.8.

POC, PN, and C:N did not meet the criteria for normal distribution and heterogeneity of variance necessary for analysis of variance (ANOVA) so a statistical difference between groupings for these variables could not be determined. However, upon logarithmic transformation, POC and PN data were normally distributed. One-way analysis of variance of the log transformed data supported statistically significant differences in the means of POC and PN between groupings.

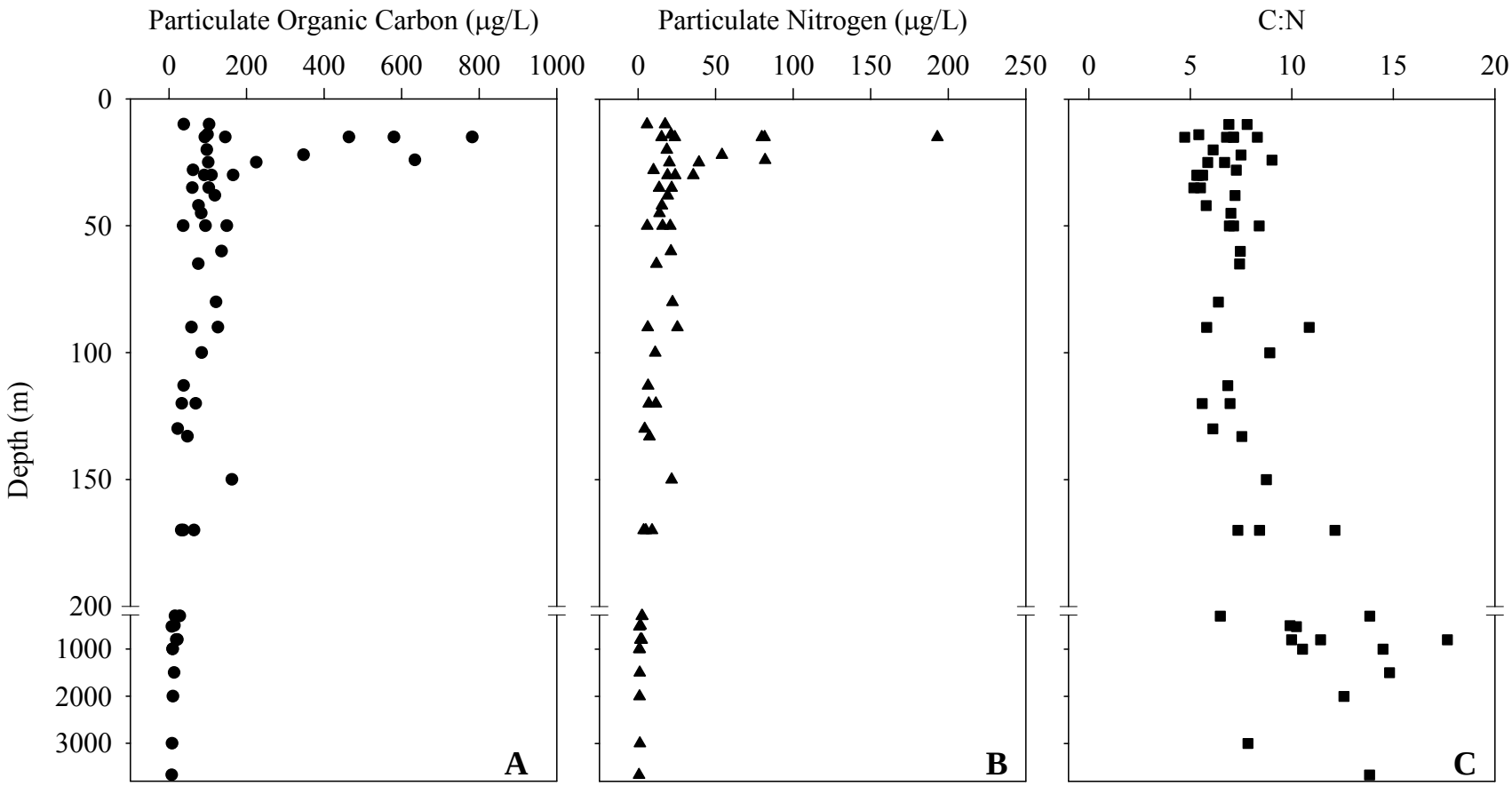

Figure 3.2. Particulate organic carbon (a), particulate nitrogen (PN), and atomic C:N ratio (c) in suspended particle samples from the western Arctic Ocean.

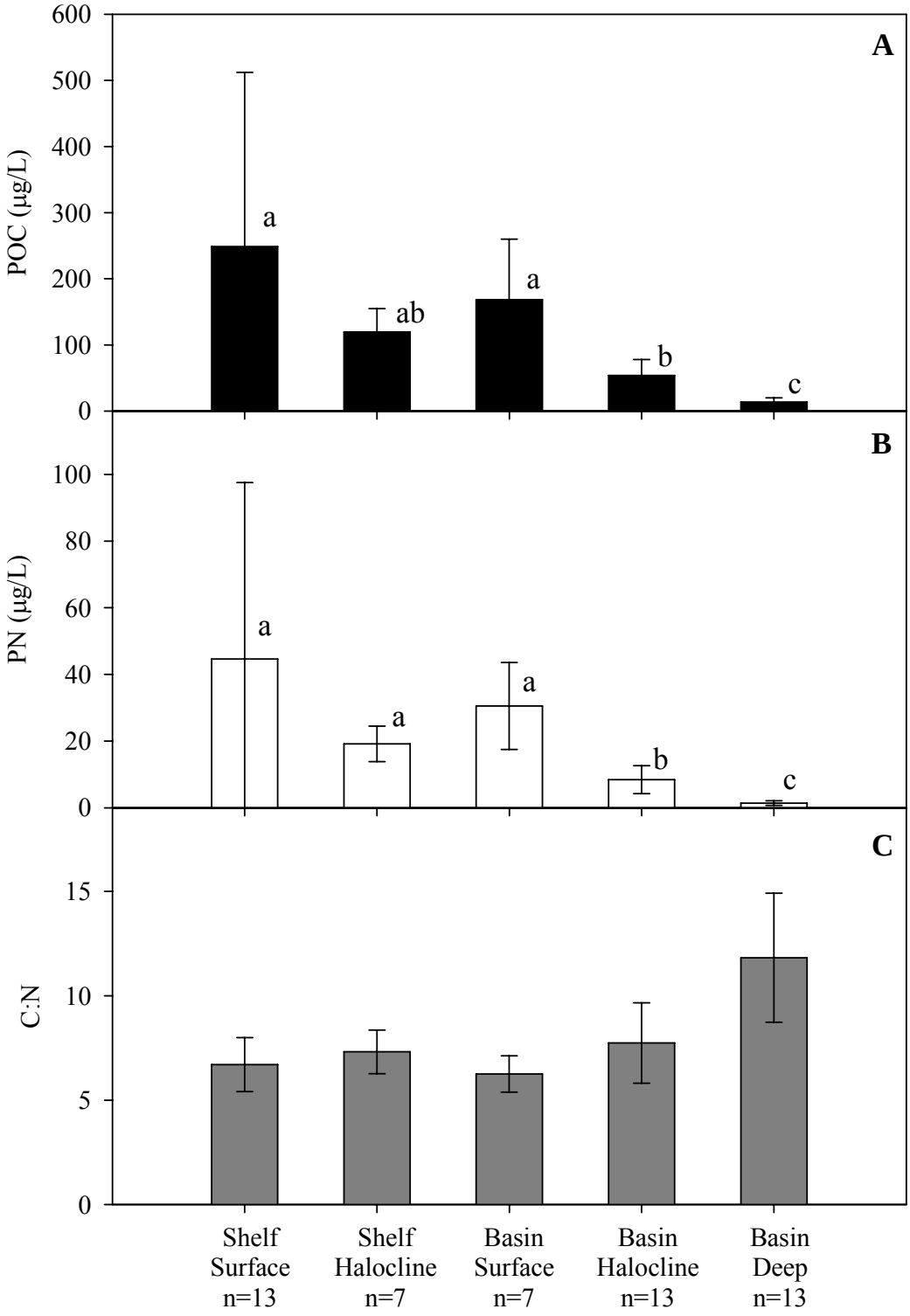

Figure 3.3. Particulate organic carbon (A) particulate nitrogen (B) and atomic C:N ratio (C) in grouped POM samples from the western Arctic Ocean (average ± standard deviation).

3.4.2. Lipid biomarker concentration and distribution

Total fatty acid concentration (TFA) ranged from 0.2 to 131 μg L^{-1} or 8.3 to 472.0 μg mg OC^{-1} and was highly variable with water depth (Fig. 3.4, Table A3.1). Short-chain (C_{12}-C_{20}) saturated and monounsaturated acids were the largest components of the total fatty acids and displayed similar concentrations throughout the water column (Fig. 3.4). Polyunsaturated fatty acids (PUFA) were most abundant between 15-50 m, but were negligible below 200 m. Interestingly, long-chain saturated fatty acids (>C_{20}, LCFA) were low or undetectable in surface waters, but deep waters (i.e., >1000 m) contained substantially higher concentrations of these acids (Fig. 3.4, Table A3.1). Branched fatty acids mirrored total fatty acid concentrations in deep waters (r = 0.95) and halocline waters (r = 0.84), but concentrations were highly variable in surface waters and did not correspond to total fatty acid concentrations (r = 0.25, Fig. 3.4).

Sterol concentrations were much lower than total fatty acids, ranging from 0.01-2.7 μg L^{-1} or 0.1-30.2 μg mg^{-1} OC, and were also less variable with depth (Fig. 3.5, Table A3.2). For nearly all samples, the following six sterols were most abundant: 24-norcholesta-5,22-dien-3β-ol ($C_{26}\Delta^{5,22}$), cholesta-5,22-dien-3β-ol ($C_{27}\Delta^{5,22}$), cholest-5-en-3β-ol ($C_{27}\Delta^{5}$, cholesterol), 24-methylcholesta-5,22-dien-3β-ol ($C_{28}\Delta^{5,22}$), 24-methylcholesta-5,24(28)-dien-3β-ol ($C_{28}\Delta^{5,24(28)}$), and 24-ethylcholesta-5,24(28)Z-dien-3β-ol ($C_{29}\Delta^{5,24(28)Z}$). Cholesterol concentrations were highly variable in the upper water column, but increased with depth and cholesterol comprised nearly half of the total sterol concentration in samples below 800 m (Fig. 3.5). Inputs of the $C_{26}\Delta^{5,22}$, $C_{27}\Delta^{5,22}$, $C_{28}\Delta^{5,22}$, and $C_{28}\Delta^{5,24(28)}$ were very similar in distribution (with all pair-wise combinations significantly correlated at $p<0.0001$), so only $C_{28}\Delta^{5,24(28)}$ is shown on Fig. 3.5 for brevity.

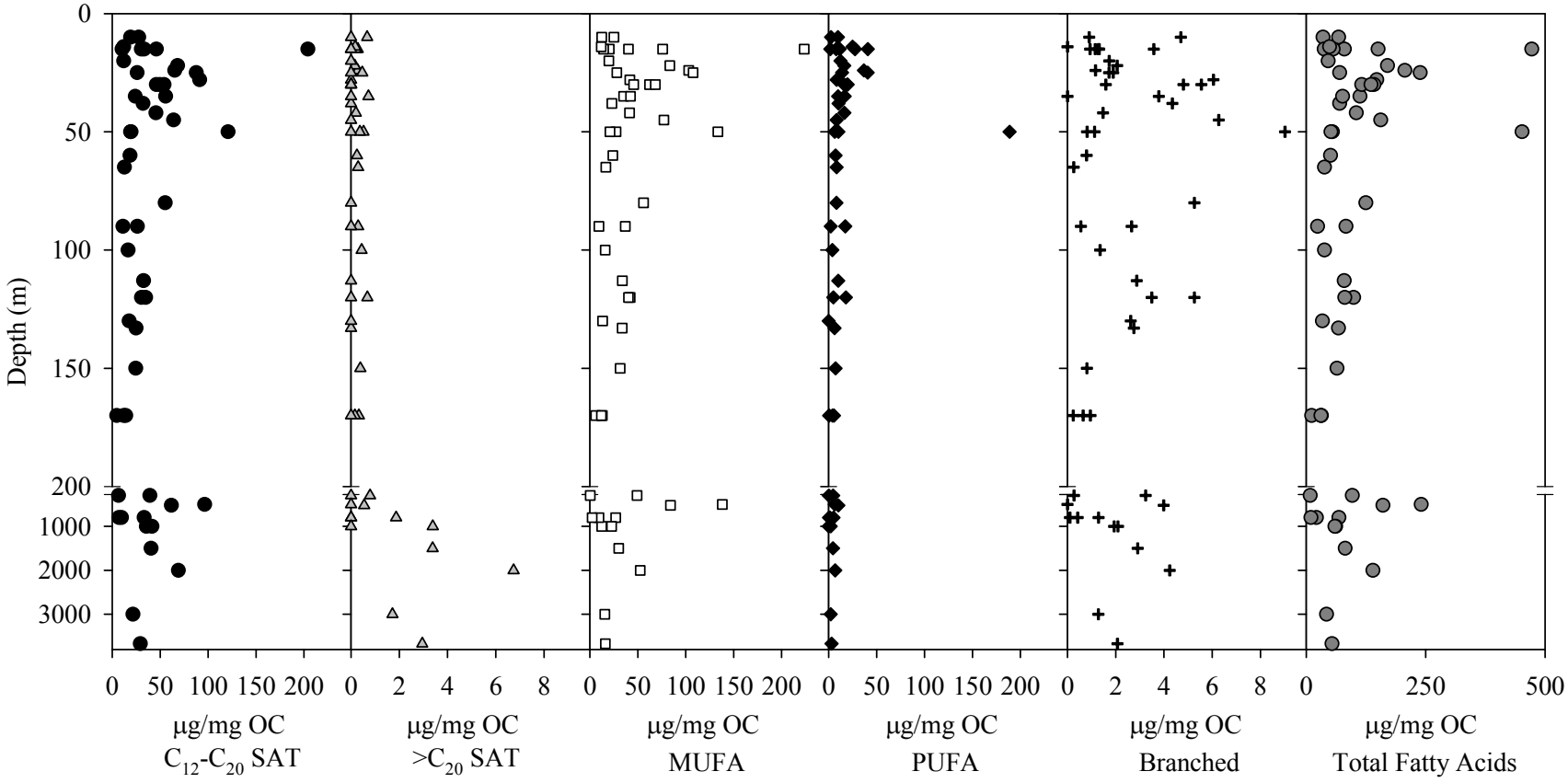

Figure 3.4. Total and groups of fatty acids (in µg/mg OC) in particulate organic matter samples from the western Arctic Ocean.

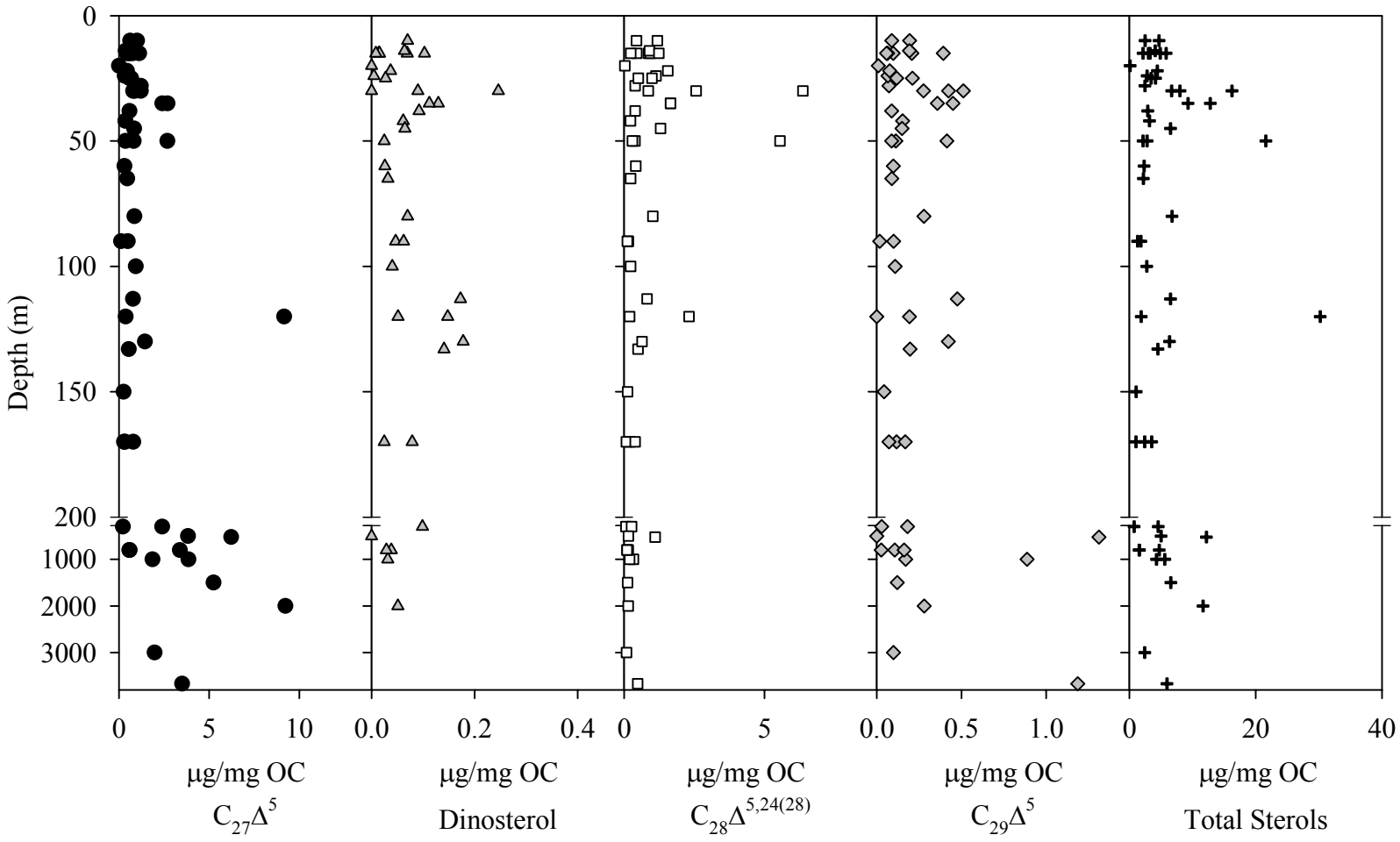

Figure 3.5. Total and selected sterol concentrations (µg/mg OC) in water column particulate organic matter from the western Arctic Ocean.

These sterols displayed varying concentrations in the upper water column with little remaining below 200 m, similar to water column profiles of short-chain saturated and monounsaturated fatty acids (Figs. 3.4 and 3.5). Both 4α,23,24-trimethylcholest-22-en-3β-ol (dinosterol) and 24-ethylcholest-5-en-3β-ol ($C_{29}\Delta^5$) made smaller contributions to total sterol concentrations in the majority of samples; however, $C_{29}\Delta^5$ did not substantially decrease with water depth and some of the highest concentrations of this marker were found below 800 m, similar to the distribution of long-chain saturated fatty acids.

Averaged by region, basin surface waters contained the highest concentrations of particulate total fatty acids (Fig. 3.6), although variability was high, especially for the basin sample classifications. Interestingly, average total fatty acids were quite similar for shelf surface and halocline and basin halocline and deep waters (Fig. 3.6). ANOVA indicated no significant difference between the means of log-transformed total fatty acids between groupings, even for basin surface sediments. Representative grouped or individual lipids for organic matter of marine (PUFAs), bacterial (Branched), and terrestrial ($C_{29}\Delta^5$) origin are shown in Fig. 3.6. Not surprisingly, concentrations of PUFAs were reduced in deep basin waters. Yet, the average concentrations in basin surface and halocline waters appear at least as high as those on the shelf despite their variability. Branched fatty acid concentrations were relatively constant for each group. Concentrations of the $C_{29}\Delta^5$ sterol were slightly higher in some deep water stations, resulting in the higher average concentrations for deep water POM overall (Fig. 3.6).

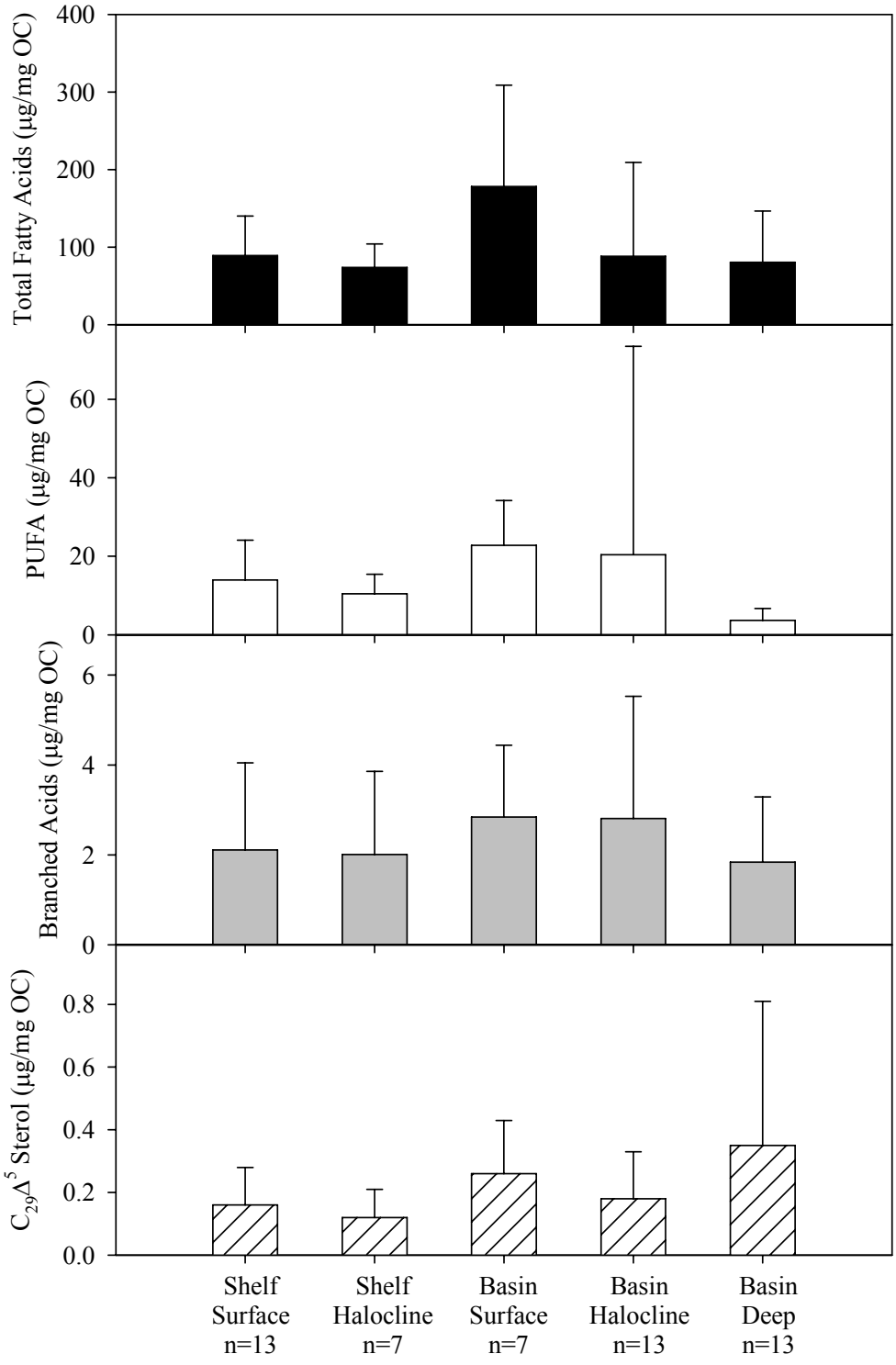

Figure 3.6. Selected biomarkers in grouped samples of particulate organic matter from the western Arctic Ocean

3.4.3. Principal Components Analysis

Principal components analysis (PCA) was employed to explore the relationship between the suite of diagnostic organic biomarkers and location. Analysis found that factors 1 and 2 together accounted for 37% of the variance in the overall data set and revealed controlling parameters of organic matter composition throughout the western Arctic Ocean. Markers of phytoplankton (C16:1ω7, C20:5, C14:0n, $C_{28}\Delta^{5,24(28)}$, $C_{28}\Delta^{5,22}$, and $C_{26}\Delta^{5,22}$) had strong negative loadings on factor 1. In contrast, typical bacteria markers (C15:0n, C17:0n, C18:1ω9, and branched C_{15} acids) as well as cholesterol had strongly positive loadings on factor 1 (Fig. 3.7). The $C_{29}\Delta^5$ sterol, commonly considered a vascular plant marker, but also a minor sterol in some marine algae, also had a positive loading on factor 1. Thus, about 25% of the overall data variability, seen as factor 1, separates biomarkers by organic matter source (planktonic material versus bacteria/vascular plant inputs). Unfortunately, long-chain fatty acids were not detected across an adequate number of observations (stations) to be included in the PCA, and thus we could not verify the separation of terrestrial biomarkers suggested by the $C_{29}\Delta^5$ sterol from other source origins. Factor 2 accounted for 12% of the data variability and was less well-defined; but, as noted by the strongly negative loadings of poly- and monounsaturated fatty acids, may be separating fresh material from material undergoing microbial metabolism seen by strong positive factor 2 loadings for C_{17} fatty acids.

Score plots demonstrated distinct differences for particulate organic matter samples from varying water depths. Both shelf and basin surface water POM had strongly negative loadings for factor 1, whereas basin deep water POM showed only positive factor 1 loadings.

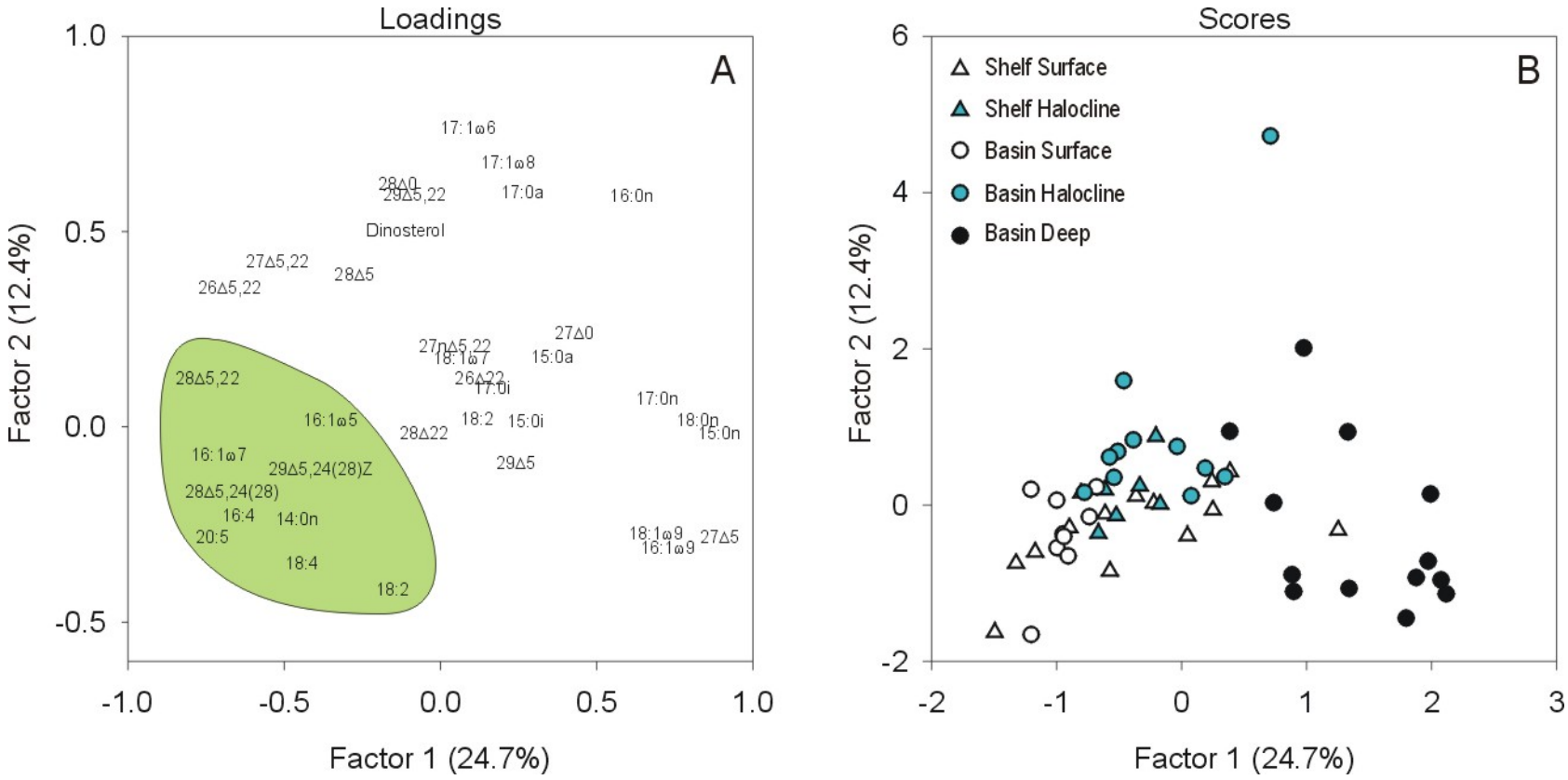

Figure 3.7. Loadings (A) and scores (B) from principal components analysis of water column particle samples from the western Arctic Ocean. Shaded area represents markers indicative of fresh algal material from primary productivity (see discussion in text).

Halocline sample scores were varied and often intermixed between surface and deep samples (Fig. 3.7). Factor 1 strongly supports the grouping of samples into surface, halocline, and deep waters, but did not support separation between shelf and basin locations.

To explore carbon recycling and its sequestration in the deep basin, the EB-7 and EHS-12 stations were investigated further. Surface waters in the basin contained fresh, modern phytoplankton material, as evidenced by high concentrations of lipid biomarkers of primary productivity (shaded region in PCA, Fig 3.7) and modern radiocarbon ages (Fig. 3.8). Descending through the water column, an aging of the POM was observed and was accompanied by the rapid loss of lipid markers of primary productivity (Fig. 3.8). By approximately 1000 m water depth, the POM from both basin stations had average radiocarbon ages between 1460 and 1960 years before present. In contrast to the exponential loss of primary productivity markers with depth in the basin, the $C_{29}\Delta^5$ sterol concentrations were variable, with no consistent loss with water depth (Fig. 3.8).

3.5. Discussion

Lipid biomarkers and bulk radiocarbon composition of particulate organic matter reveal an Arctic water column where abundant, but spatially variable, phytoplankton inputs in surface waters are quickly recycled, evolving towards older, more recalcitrant material with increasing water depth. Surface waters were highly variable with respect to total POC content, C:N ratios, and lipid biomarker concentrations, highlighting the strong heterogeneity on spatial scales in the western Arctic Ocean.

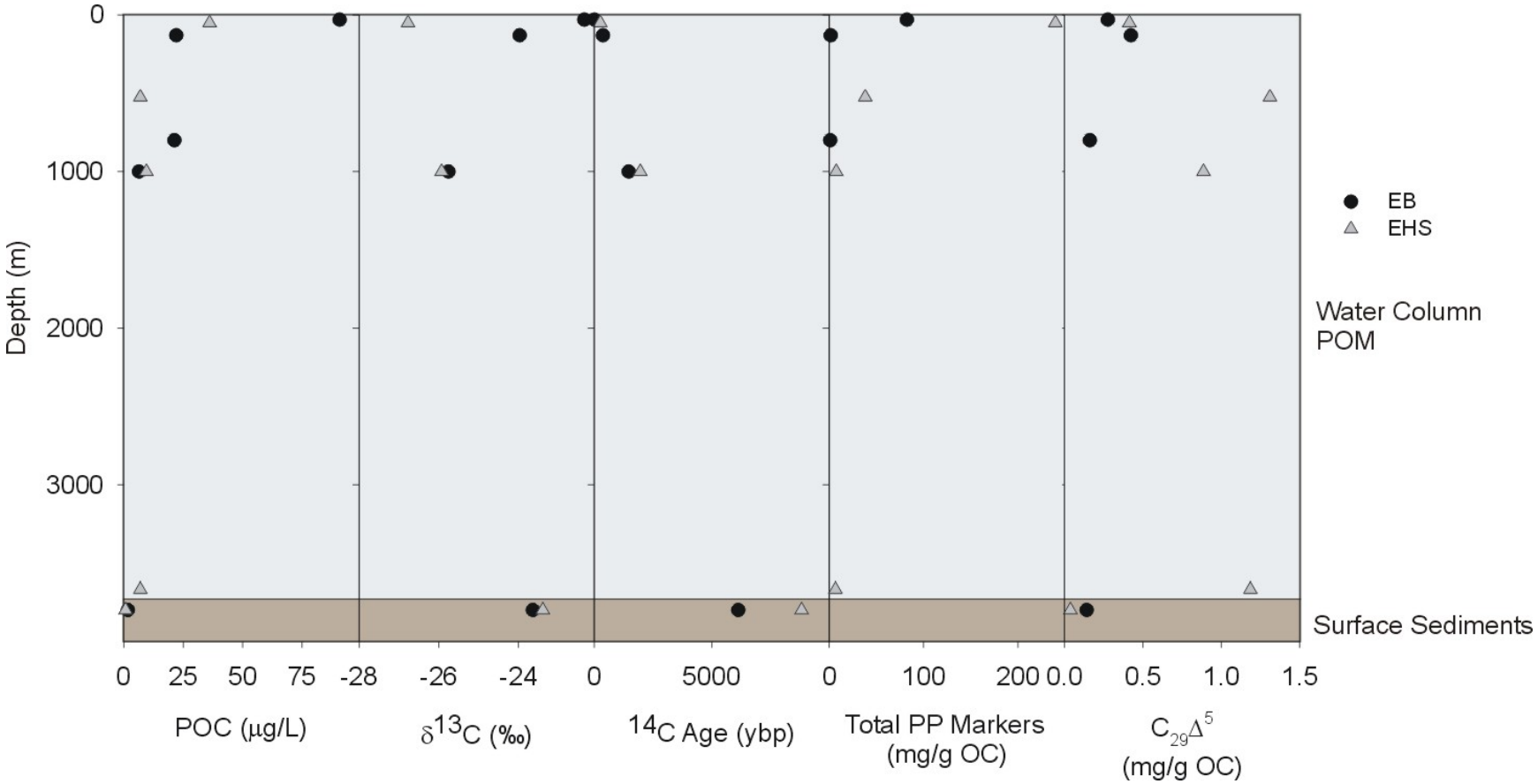

Figure 3.8. Particulate organic matter (POC), stable carbon isotopic composition ($\delta^{13}C$), radiocarbon age as calculated from $\Delta^{14}C$ (years before present, ybp), sum of individual biomarkers characteristic of primary productivity (mg/g OC; see Fig. 3.7), and $C_{29}\Delta^5$ sterol concentrations in particulate organic matter (POM) and surface sediments at the EB-7 and EHS-12 basin stations.

Even after grouping by location and water mass (Figs. 3.3 and 3.6), variability in POC, PN, and lipid concentrations was considerable, implying that the shelf versus basin and water-depth classifications were not accounting for the large differences in organic matter abundance and composition. Instead, strong environmental forcing factors, such as the lateral advection of POM via sea-ice and currents (i.e. Hwang et al. (2008), nutrient availability, and ice and snow cover-induced light limitation (Hill and Cota, 2005) appear to control the abundance and composition of particulate organic carbon in the western Arctic Ocean.

In general, the highest concentrations of POC and PN were observed in the upper 40 m of water of both shelf and basin stations, and corresponded to the presence of a deeper chlorophyll maximum (~25m) than was observed during the preceding spring months (10-15 m) (Hill and Cota, 2005), and indicating widespread phytoplankton production in the nutricline during the summer months when near surface nitrate and ammonium concentrations are near zero (Codispoti et al., 2005). The effect of nutrient availability was also particularly apparent in the southernmost, sea-ice free sampling stations (BRS and ACW stations, Fig. 3.1), where nutrient-rich Anadyr waters led to an 8-fold increase in POC concentration along the western flank of the Bering Strait compared to the nutrient-poor eastern Bering Strait and Alaskan Coastal Water regions (Codispoti et al., 2005).

Surface water POM also exhibited a large range in C:N ratio (4.73-9.03), where the higher values could indicate contributions from terrestrial organic matter since vascular plants are typically more nitrogen-depleted than algal material and have C:N ratios greater than 20 (Meyers, 1997). However, the lack of long-chain even carbon

saturated fatty acids (LCFA) and low concentrations of the $C_{29}\Delta^5$ sterol imply little vascular plant inputs in surface waters. Instead, the higher C:N atomic ratios likely reflect the quality of organic matter. Bates et al. (2005b) found an increase in particulate C:N from spring to summer in the western Arctic, potentially reflecting a shift to nitrogen-poor production as phytoplankton assemblages changed to a diatom-centered community post-bloom. Indeed, the clustering of lipid biomarkers representing fresh phytoplankton material (14:0n, 16:1ω7, 16:4, 20:5, 18:4, $C_{28}\Delta^{5,24(28)}$) towards negative loadings for factors 1 and 2 revealed during PCA were most closely associated with shelf and basin surface water samples (Fig. 3.7). Diatoms are known to synthesize high concentrations of both 16:4 and 20:5 and the sterol $C_{28}\Delta^{5,24(28)}$ is typically thought of as a specific marker for centric diatoms including those comprising the genera *Thalassiosira* and *Skeletonema* (Volkman, 2006). Similarly, both *Melosira arctica* and *Nitzschia frigida* associations collected from ice stations in the Barents Sea contained abundant 14:0n, 16:1ω7, and 20:5, as well as 16:0n (Falk-Petersen et al., 1998), and these four lipids along with 18:1ω9 were the dominant five fatty acids in sinking particulate organic matter characterized by centric and pennate diatoms from Trinity Bay in Newfoundland (Budge and Parrish, 1998). Thus, diatoms appear to be major contributors to upper water column marine organic matter in western Arctic summers—a conclusion supported by phytoplankton pigment abundances indicative of important contributions of diatoms and haptophytes to the community in shelf surface waters and also at the base of the euphotic zone over basin waters (Hill et al., 2005).

Typically, the Arctic basin is thought of as far less productive than the shelf environment, due to heavy ice cover, so the lack of PCA separation between shelf and

basin surface water (<40 m) stations and the absence of a significant difference of log-normalized POC and PN between shelf surface and basin surface stations is noteworthy. Although we cannot directly address temporal variability because only a snapshot of summer POM composition is presented here, the timing of sampling may explain the close relationship between shelf and basin surface waters. Firstly, POM samples were taken over a 40-day cruise, and ice cover conditions constantly shifted in response to melting and wind. The relatively high concentrations of POC and marine-derived lipids observed for basin surface samples could indicate that basin locations were experiencing bloom conditions due to ice break-up and subsequent increased light availability. If this process is the cause of the high concentrations of POC and algal lipids, especially the high average labile polyunsaturated fatty acids (Fig. 3.6) in basin surface and halocline waters, it is likely that production is not occurring right at the surface where dissolved nitrate was nearly always in summer, but rather slightly deeper in the nutricline (Codispoti et al., 2005).

However, it remains difficult to separate marine inputs derived from localized basin primary productivity from those resulting from the shelf-basin exchange of organic matter. Satellite imagery, combined with wide-scale nutrient depletion in the upper surface waters during summer sampling, suggests that the spring phytoplankton bloom occurred prior to the summer sampling trip, sometime between mid-June to mid-July (Hill and Cota, 2005). Previous comparisons between spring and summer total POC support this suggestion and infer that considerable organic carbon accumulated between the two cruises as a result of the bloom (Bates et al., 2005b; Hill and Cota, 2005). In light of this observation, the summer POC concentrations measured here are likely lower

than what would characterize typical bloom conditions. In addition, tongues of elevated POM extending offshore were observed at depths of 25-35 meters in Barrow Canyon (Bates et al., 2005b), suggesting that the measurements of biomarkers in basin surface waters presented here may instead represent lateral transport of shelf-derived organic matter to the Arctic basin, as opposed to representing basin productivity itself.

Halocline waters (40-200 m) were characterized by lower concentrations of POC and PN as well as lower variability than surface waters. Similar to that found for surface samples, the principal components analysis did not separate shelf halocline samples from basin halocline samples, and with one exception (EB-7 at 130 m depth), halocline particle samples largely clustered between the surface samples and deep water samples (Fig. 3.7). The average C:N ratios for both shelf and basin halocline waters were slightly higher than their surface water counterparts, suggesting loss of proteinaceous components (Meyers, 1997). Changing proportions of autochthonous versus allochthonous sources of organic matter could also increase the average atomic C:N ratio; however, as noted for surface waters, the lack of long-chain even carbon saturated fatty acids suggests little input from vascular plant material. With the exception of bacterial branched fatty acids, total and individual fatty acids were lower in concentration in halocline particles. While it must be noted that not all bacteria produce these branched fatty acids (Canuel, 2001) and bacteria are capable of changing the individual fatty acids they synthesize depending on available carbon substrates (Harvey et al., 2006), the increasing relative abundance of these compounds and the distinct separation of most halocline samples in the PCA in conjunction with increasing C:N ratios suggest that suspended particles are undergoing increased microbial degradation at intermediate water depths compared to surface waters.

In all likelihood, both increased terrestrial inputs to bottom waters and increased degradation of sinking material appear responsible for the composition of POM at depth in the Arctic basin. The deep water (200-3700 m) POM was clearly distinguished from surface or halocline water particles in the PCA (Fig. 3.7), and was characterized by low and relatively consistent concentrations of POC and PN. Although we could not determine a statistical significance, average atomic C:N ratio was the highest observed for all site groupings, nearing a value of 12, and as discussed above, may indicate mixed autochthonous and allochthonous sources or the continual degradative loss of proteinaceous material. The most abundant concentrations of long-chain, even-carbon saturated fatty acids ($>C_{20}$ SAT (LCFA); Fig. 3.4), associated with vascular plant source material (Volkman, 2006), were found in deep water particles, and similarly, substantial abundances of the $C_{29}\Delta^5$ sterol were also present in deep particles and did not decrease with water depth as seen for the diatom sterols $C_{28}\Delta^{5,22}$ and $C_{28}\Delta^{5,24(28)}$. These markers, in conjunction with the higher C:N ratios, argue for terrigenous inputs to the deep water column. Additionally, a corresponding lack of polyunsaturated fatty acids and substantially decreased concentrations of monounsaturated fatty acids relative to surface water particles implies that the lipid composition reflects a loss of these more labile components consistent with degradation (Tolosa et al., 2003). Associated with the elevated concentration of LCFAs in deep particles, cholesterol concentrations in deep particles exceeded surface concentrations. This observation implies increasing inputs of material from secondary productivity (i.e., marine snow, fecal pellets) with depth.

The distinct presence of LCFA terrestrial markers in deep basin waters is curious considering the near complete absence of these compounds in surface and halocline

waters. Several processes could result in this discrepancy. First, the timing of sample collection could play an important role in this observation. The terrestrial organic matter evidenced at depth could be from early melting, and rapid sinking, of material that was entrained the previous autumn season. Cooper et al. (2005) have found rapid (~3 month timescales) deposition of sea-ice rafted particulate matter to surface sediments in the study area, particularly on the shelf, but also extending into deeper waters which highlights the ability for sea-ice to provide an effective mechanism for particle export (Cooper et al., 2005). Interestingly, Bates et al. (2005b) measured C:N ratios in both suspended particulate organic matter trapped on 0.7μm GF/F filters as measured here, as well as large particle (>53μm) samples trapped on nitex screens and later transferred to GF/F filters. Although collected largely from surface waters, large particles in summertime were characterized by substantially higher C:N ratios (8-60) than in suspended particles (6.16±0.67) from surface waters (Bates et al., 2005b). Although we cannot confirm that enrichment of terrestrial carbon is linked to large particles, it presents a mechanism for transport of terrestrial material to rapidly reach deep waters. Alternatively, the elevated concentrations of LCFA in deep particles may result from advective transport in the water column. Evidence for lateral transport of continental material exists for both the Canada Basin (Hwang et al., 2008) and the Laptev Sea (Fahl and Nöthig, 2007).

To explore carbon recycling and its sequestration in the Arctic basin, as well as investigate the effects of lateral transport of organic matter from shallow to deep environments, two basin stations, EHS-12 (3669 m) and EB-7 (3264 m), were chosen for more in-depth analysis. The intent here is not to directly compare abundances of lipid

biomarkers given the temporal differences in sampling, but instead to examine potential changes in the molecular and isotopic composition of particles throughout their descent to sediments of the Arctic basin.

As noted earlier, basin surface waters were characterized by fresh, modern phytoplankton material, as evidenced by modern radiocarbon ages, high concentrations of lipid biomarkers of primary productivity, and relatively heavy bulk carbon stable isotopic composition (EB-7 POM only; Fig. 3.8). Additionally, an ageing of the particulate organic matter accompanied the loss of modern, labile carbon descending through the water column such that POM at depths of 1000 m from both stations had ages of 1460 and 1960 years before present. As a measure of the bulk organic material, it is conceivable, and in fact highly likely, that the radiocarbon age is being affected by older organic matter delivered by rivers or erosion. This is not to say that erosional, perhaps ancient permafrost material, is not present in surface waters where the radiocarbon age was modern. Contemporary phytoplankton material with a contemporary radiocarbon signal could easily mask the presence of minor ancient carbon components. However, as suspended POM slowly sinks through the water column, the most labile (i.e., youngest) components are degraded rapidly and more recalcitrant (typically older) material remains.

Typically, suspended particles (<20 μm diameter) sink very slowly through the water column, with rates usually <1 m day^{-1} while larger particles, (>20 μm) sink at rates of hundreds of meters per day (Tolosa et al. 2003 and references therein). Because of this sinking rate discrepancy, the larger particles are more consistently found in sediment trap collections and also tend to represent fresher material than the suspended particles that is typically trapped on filter material and has remained exposed to microbial activity longer

in the water column. The data presented here is solely suspended POM trapped on filters, however data from Hwang et al. (2008) on settling POC caught in a deep (3067 m) sediment trap from a parallel location in the Canada Basin (75° N, 150° W latitude and 3824 m total water depth, compared with our EB-7 station located at 72° 19' N, 151° 59.1' W 32) is appropriate for comparison. Interestingly, the average ^{14}C age of sinking particles at this depth was 1900 ^{14}C years (Hwang et al., 2008), remarkably similar to our range of 1460-1960 ^{14}C years at a water column depth of 1000 m. Similarly, $\delta^{13}C$ for the sediment trap particles ranged from -24 to -26‰ over the span of a year (Hwang et al., 2008)—the suspended POM at 1000 m collected here averaged -26‰ and the coupled $\delta^{13}C$ and $\Delta^{14}C$ results argue for similar composition between large and small sinking particulate organic matter in the Canada Basin.

Hwang et al. (2008) conclude that lateral transport is responsible for the continental character of the sinking particulate organic matter in the Canada Basin. Similarly, Fahl and Nöthig (2007) have argued that lateral transport of shelf terrigenous material is responsible for between 42-64% of the particle flux at water depths of 1500 m on the Lomonosov Ridge in the central Arctic Ocean. The lack of terrigenous markers in surface and halocline waters discussed above would suggest that lateral transport, at depth, instead of sea-ice rafting, could provide the main transport mechanism for the delivery of land-derived materials to deep waters in the western Arctic. Nevertheless, because our POM samples were only taken during a single year in July and August, compared to surface sediments which integrate signals from several years at the very least, we cannot exclude the presence of land-derived material in upper water column waters in other seasons or years.

A simple two end-member mixing model using $\Delta^{14}C$ can be constructed to quantify the losses of fresh marine material in the Arctic basins (Fig. 3.9). Here, the terrestrial $\Delta^{14}C$ end-member was determined based on the average of radiocarbon measurements from Kokolik River suspended particles (-309.3‰; NOSAMS Accession Number OS-39257) and Ikpikpuk River peat (-353.9‰; NOSAMS Accession Number OS-39574, see Chapter 2 for details) and was defined as $\Delta^{14}C_{terr}$ = -331.6‰. The marine carbon end-member was defined as the radiocarbon content of EB-7 30m POM ($\Delta^{14}C$ = +2‰ (modern), OS-39127). The mixing model highlights the changing character of POM through the upper 1000 m of water and with the biomarker data, confirms the rapid loss of marine components with depth.

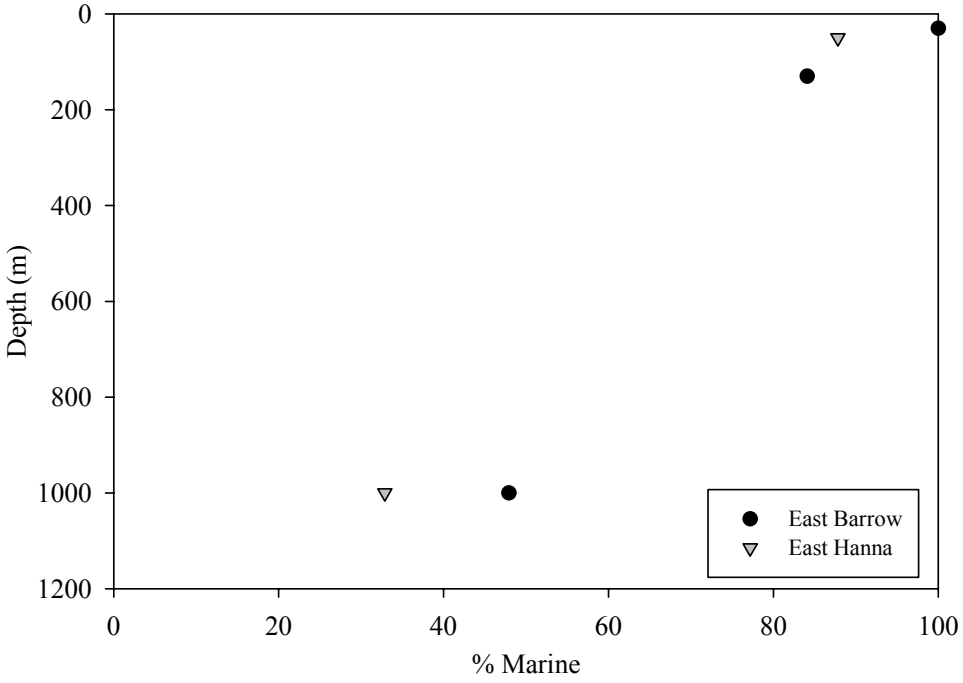

Figure 3.9. Loss of labile, marine organic matter with depth in Arctic basin waters as calculated through a two end-member mixing model using $\Delta^{14}C$ composition.

Discerning the balance of sea-ice rafting or deep-water lateral advection as the mechanisms for the transport of continental material to the Arctic interior remains to be completed. Yet, the definitive ageing of the POM with depth in the water column, and the increasing "terrestrial" signal and corresponding rapid decrease in marine-derived biomarkers, confirm the labile material is quickly recycled during descent such that the material that remains for deposition in sediments contains a substantial component of recalcitrant, aged terrestrial organic matter.

3.6. Summary and Conclusions

A molecular-level characterization of suspended POM demonstrated the extreme spatial heterogeneity of organic carbon content as a result of nutrient availability and sea-ice cover. Surprisingly, surface and halocline POM contained little to no molecular evidence of terrestrial organic matter, suggesting a disconnect between sedimentary material, which contains large fractions of preserved terrigenous material (Chapter 2), and water column POM. Deep water particles contained the highest concentrations of long-chain fatty acid markers indicative of land-derived material, suggesting that lateral transport of continental material occurs either at depth or via sea-ice rafting and subsequent sinking. Regardless of the transport mechanism, POM aged with increasing water depth, confirming that labile marine components are recycled quickly in the upper water column. The POM in deep waters and that delivered to sediments therefore is largely older and much more recalcitrant, suggesting that Arctic sediments contain little organic matter in the global carbon cycle that is easily remobilized.

Chapter 4: Trace Element and Molecular Markers of Organic Carbon Dynamics along a Shelf-Basin Continuum in Sediments of the Western Arctic Ocean

4.1. Abstract

Molecular organic biomarkers together with trace element composition were investigated in sediments from a region east of Barrow Canyon in the western Arctic Ocean to determine sources and recycling of organic carbon in a continuum from the shelf to the basin. Algal biomarkers (polyunsaturated and short-chain fatty acids, $C_{28}\Delta^{5,24(28)}$ sterol, dinosterol) highlight the substantial contribution of organic matter from marine primary productivity in shelf environments, while redox markers such as AVS, Mn, and Re indicate intense metabolism of this material leading to anoxia. Sea-ice algal inputs may fuel some of this intense metabolism, as noted by the enriched stable carbon isotopic composition of shelf sediments compared to previous reported values. In addition to the inputs from labile marine organic matter, shelf sediments also receive considerable inputs from terrestrial organic carbon. Slope sediments were a site of focusing of organic matter both of terrestrial and marine origin with evidence for slumping as a mechanism of this focusing. Sedimentary metabolism was not quite as intense as on the shelf, indicated by lower levels of AVS from sulfate reduction; however, sufficient labile organic matter reaches slope sediments to create suboxic and anoxic conditions, at least intermittently. Basin sediments also showed evidence for episodic delivery of labile marine organic carbon inputs despite the strong physical controls of water depth and sea-ice cover. In general, however, the basin was characterized by generally low organic carbon delivery and sluggish sedimentary

metabolism. Preserved lipid biomarkers were used in accordance with a principal components analysis model to estimate fractions of preserved recalcitrant (of terrestrial origin) and labile (of marine origin) organic matter in the sediments. Overall, 20-56% of the preserved organic matter was estimated as terrestrial in origin. Terrestrial components increased substantially with depth in the shelf core, attributed to both increased delivery of land-derived components during past time periods as well as the intense metabolic removal of more labile marine inputs. Notably, although total biomarker concentrations were lower in basin sediments, the relative preserved terrestrial organic matter in the deep basin sediments was similar to that found on the shelf. Clearly, a mechanism for the shelf-basin exchange of organic carbon must exist to transport land-derived material to deep basin sediments.

4.2. Introduction

With its many large rivers, substantial coastal erosion rates, and sea-ice as a material transport vector, the Arctic Ocean embodies a large potential repository for terrestrial organic matter. Through four main rivers (Yenesei, Lena, Ob, and Mackenzie), the Arctic receives a terrestrial organic carbon (TOC) flux of about 30 x 10^6 t yr^{-1} (Rachold et al., 2004). Superimposed on this background of terrestrial organic matter is a spatially variable marine component, largely driven by seasonal primary productivity centered over the broad, shallow shelf seas that make up nearly 50% of the area of the Arctic Ocean (Jakobsson, 2002). Although on an annual scale the input of marine organic matter (250 x 10^6 t yr^{-1}) dwarfs the terrestrial carbon input, recent studies document terrestrial organic matter as a substantial component of organic carbon in

Arctic Ocean sediments (Belicka et al., 2002; Belicka et al., 2004; Birgel et al., 2004; Goñi et al., 2000; Schubert and Stein, 1996; Schubert and Stein, 1997; Stein and Macdonald, 2004a). Given the dominance of marine organic matter production versus terrestrial inputs, the marine component appears to be largely recycled with selective preservation of terrestrial organic matter.

The fluxes of both marine and terrestrial organic matter to the Arctic are expected to change with continued climate warming and alterations to the hydrological cycle. Two basic alteration scenarios can be envisioned: 1) enhanced primary productivity as the ice clears from the shelves earlier in the spring and 2) a similar increase in terrestrial organic matter loading as permafrost-bound material melts and erodes. Alternatively, it has been suggested that in the absence of an autumn recharge of nutrients by physical or biological factors, it is unlikely that increased ice retreat would lead to enhanced annual marine carbon sequestration (Walsh et al., 2005). Many questions remain, and understanding the implications of these changes requires isolating the rapid production and recycling of marine organic matter from the slower delivery and incorporation of recalcitrant terrestrial organic matter.

Molecular organic biomarkers have long served as proxies for both the sources and processing of organic matter in natural systems (Meyers, 1997; Volkman, 2006; Volkman et al., 1998). Lipid biomarkers both alone and coupled with hydrogen indices and bulk and compound-specific isotopic composition have been utilized to examine the sources of organic matter to the Eurasian Arctic (Belyaeva and Eglinton, 1997; Birgel et al., 2004; Boucsein et al., 2002; Fahl and Stein, 1997; Schubert and Stein, 1997; Stein and Fahl, 2000). In the Canadian Arctic, Goñi et al. (2000) examined biomarker patterns

in sediments and particles from the Mackenzie Delta area of the Canadian Beaufort Sea. Guo and Macdonald (2006) sampled organic matter from the Yukon River to characterize the composition, reactivity, and flux of organic carbon transiting this system. Our previous efforts (Belicka et al., 2004; Yunker et al., 2005) combined molecular structures with multivariate statistical approaches (principal components analysis) to determine those organic biomarkers most useful for tracking marine and terrestrial organic matter to western Arctic sediments. Here, we build and expand upon those results to evaluate the timescales and patterns of marine and terrestrial organic matter cycling in Arctic sediments from the Alaskan Beaufort Sea east of Barrow Canyon. For the marine carbon pool, we couple those molecular markers most informative for marine primary and secondary carbon inputs (fatty acids) with trace elements sensitive to sediment oxidation state as well as ^{210}Pb to evaluate of the input and longevity of marine organic matter. More recalcitrant markers, including hydrocarbons, amyrins, and specific sterols are used to provide insight into long-term terrestrial organic matter storage.

4.3. Materials and Methods

4.3.1. Study area and sampling

Sediment cores were collected during the summer Shelf-Basin Interactions Program (SBI) process cruise in 2002 (July 17 – August 21) aboard the USCGC *Healy* along a shelf to basin transect (East Barrow (EB); Fig. 4.1) in the Alaskan Beaufort Sea (for a program overview, see Grebmeier and Harvey, (2005)). Cores were taken with a Pouliot box corer, and sectioned in 1 cm intervals in the upper 10 cm of sediment, and 2 cm intervals from 10-20 cm. Several cm of sediment along the edges of each core were

discarded. Sediment sections were stored in pre-cleaned plastic or glass I-Chem jars with Teflon-lined lids and immediately frozen at -20 °C on the ship. Upon return, samples were held at -70 °C until chemical analysis in the shore-based laboratory.

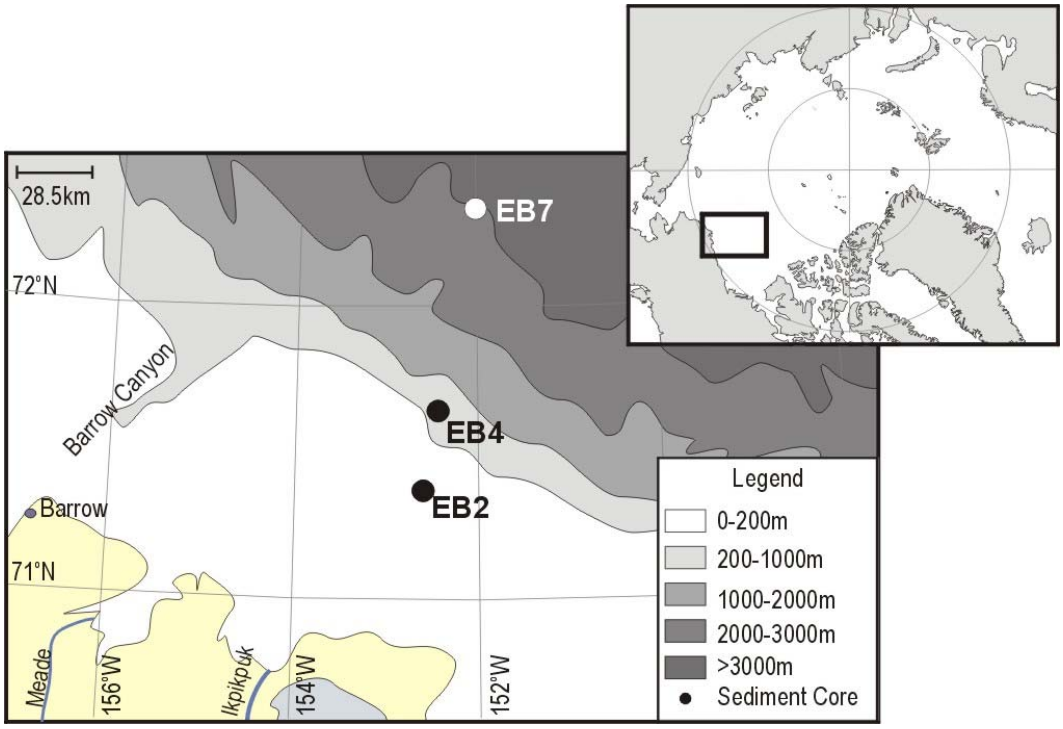

Figure 4.1. Map of the Chukchi and Alaskan Beaufort Seas, showing sampling stations along the shelf-basin transect east of Barrow Canyon (EB).

The EB transect line examined here is located along the western edge of the Alaskan Beaufort Sea, approximately 75 km east of the axis of Barrow Canyon. The continental shelf along this section of the Alaska coastline is narrow, and supplied with terrestrial organic matter from multiple small rivers and coastal erosion. Substantial

sedimentary material in this area is also exported from the shelf by sea-ice (Reimnitz et al., 1993), and this poorly understood process appears to be increasing in the both the Chukchi and Beaufort Seas (Eicken et al., 2005). Compared to the well-studied Mackenzie shelf to the east, few studies have addressed organic carbon cycling on the Alaskan Shelf, focusing mainly on bulk sedimentary OC and $\delta^{13}C$ (Naidu et al., 2000; Naidu et al., 1993).

4.3.2. Chemical Analyses

Bulk Sedimentary CHN and Carbon Isotopic Composition

Sediments were first acidified with 30% HCl to remove carbonates, then loaded into sample tins. Bulk organic carbon and nitrogen content and stable isotope composition were measured using a Fisons NA 1500-R Series 2 Elemental Analyzer coupled to a VG Optima Isotope Ratio Mass Spectrometry (EA/IRMS) with continuous flow. Data are reported as per mil $\delta^{13}C$ using the PeeDee Belemnite carbonate standard and per mil $\delta^{15}N$ using atmospheric air.

Lipid Biomarker Analysis

Detailed methods for lipid biomarker extraction are described in Belicka et al. (2002). Briefly, sediments were extracted three times with a mixture of CH_2Cl_2:MeOH (1:1) in solvent-rinsed glass test tubes with sonication. Total lipid extracts were saponified with 0.5 N KOH in methanol at 70 °C for 30 minutes. Neutral lipids were partitioned three times with a 9:1 mixture of hexane:diethyl ether followed by fatty acid partitioning after acidification with HCl to pH<2. Neutral lipids were dried and

derivatized at 50 °C for 15 minutes with bis-(trimethylsilyl)trifluoroacetamide amended with 25% pyridine. Fatty acids were dried and methylated at 70 °C for 30 minutes with boron trifluoride in methanol. Nonadecanoic acid and 5α-cholestane added prior to saponification served as internal standards for the polar and non-polar phases, respectively. Polar and neutral lipids were separated and quantified by capillary gas chromatography (GC) with flame ionization detection. Gas chromatography-mass spectrometry was utilized for lipid identification. The instrumental set-up and methods were identical to those described in Belicka et al. (2002); however, a J&W DB-5ms column (60 m length x 0.32 mm internal diameter x 0.25 μm film thickness) was used.

^{210}Pb Analysis

Sediments were dried overnight at 45 °C for ^{210}Pb analysis. A NIST standard of ^{209}Po was added to the dried sediments to determine ^{210}Po recovery. Sediments were digested first with concentrated nitric acid until foaming ceased, then with concentrated hydrochloric acid for 1.5 hours. The digest was then centrifuged at 3000 rpm for 10 minutes, and dried at 60-80 °C overnight. Samples were redissolved in 2 mL HCl and evaporated to dryness two more times sequentially to remove residual nitric acid. A solution of 0.1 N HCl with ascorbic acid was added, and polonium was plated onto silver planchets overnight at 60-80 °C. Alpha spectroscopy was used to measure ^{210}Pb, and gamma counting was used to measure ^{226}Ra on selected samples.

Trace Metal Analysis

AVS was determined on wet samples, using the protocol described by Allen et al. (1993). Briefly, sediments were acidified with hydrochloric acid, and the evolving

sulfide was trapped in a sodium hydroxide solution and subsequently determined by colorimetric analysis (Allen et al., 1993). The analytical precision, determined by replicate analysis (n=5) of one sample, was 10 % at a concentration of 0.2 μmol g^{-1} (dry weight).

Sediment sub-samples were freeze-dried and homogenized by grinding. Aliquots (~250 mg) deposited in Teflon beakers were heated for one hour at approximately 100°C on a hot plate with 10 mL of HNO_3, and then, after the addition of 4 mL of $HClO_4$, for two supplementary hours. After cooling, 5 mL of HF were added to the mixtures to complete the digestion at room temperature for 15 hours. The acids were then evaporated to near dryness and the residue dissolved in 1 mL of concentrated HNO_3 and diluted to 50 mL. The solutions were then analyzed with both ICP-OES (Inductively Coupled Plasma-Optical Emission Spectrometry; Mn) and ICP-MS (Inductively Coupled Plasma-Mass Spectrometry; Ag, Cd, Mo, Re, and U) using external calibrations. The precision (± standard deviation) and accuracy (SRM value minus sample mean) of the analyses were determined by replicate analysis (n=5) of the standard reference sediments PACS-2 (Ag – ±4.7%, -6%; Cd – ±4.9%, 12 %; Mn – ± 3.5%, -6.3%; Mo – ±4.8%, -11%; Re – ±2.1%, nd; U – ±7.0, 4.7%).

4.4. Results

4.4.1. Bulk sedimentary organic matter

Total sedimentary organic carbon (OC) ranged between 0.73% and 1.87% (Fig. 4.2). Slope sediments (EB-4) were enriched in organic carbon compared to the other

cores, while shelf sediments (EB-2) contained the lowest concentrations of organic carbon. EB-4 sedimentary OC was very consistent in the upper 8 cm at approximately 1.7%, but became more variable in the lower core depths. Sediments from the basin at EB-7 contained intermediate OC concentration between the shelf and slope sediments, with average values around 1.4% in the upper 10 cm and 1.2% in the lower depths of the sediment core. Atomic C:N ratio varied between 8 and 14 for all cores. In the shallow shelf location (EB-2), the C:N ratio was relatively constant in the upper 5 cm, averaging 8.75 ± 0.30 (average ± standard deviation), but was highly variable below 5 cm. A strong increase from 8 to 14 was found between the 16-18 and 18-20 cm core segments. This increase in C:N ratio at depth was also present in the EB-4 sediment core, as well as a similar excursion to a C:N of 13.41 at 8-9 cm, which also had the highest C:N ratios of all three investigated sediment cores. The C:N ratio at EB-7 was very consistent with core depth, with an average of 9.95 ± 0.26 (Fig. 4.2). Stable carbon isotopic composition ($\delta^{13}C$) ranged from –18.6 to –24.6 ‰ in the shelf, slope, and basin cores, with the heaviest values found in the deeper sections of the basin (EB-7) core (Fig. 4.2). In EB-4 sediments, a sharp decrease to light values (-24.6 ‰) was found at the 9-10 cm interval, just below the high peak in C:N ratio at 8-9 cm. Stable nitrogen isotopic composition ($\delta^{15}N$) in the three cores was highly variable, ranging from 1.83 to 5.33 ‰ in shelf sediments, with the lowest values found in the mid-range sediment depths (~8-10 cm; Fig. 4.2). Slope (EB-4) sediments contained slightly higher $\delta^{15}N$ values with a range from 2.86 to 6.86 ‰, with no consistent downcore trends. Stable nitrogen isotopic composition was also highly variable in the basin core (EB-7), fluctuating between 1.48 and 9.13 ‰ with depth.

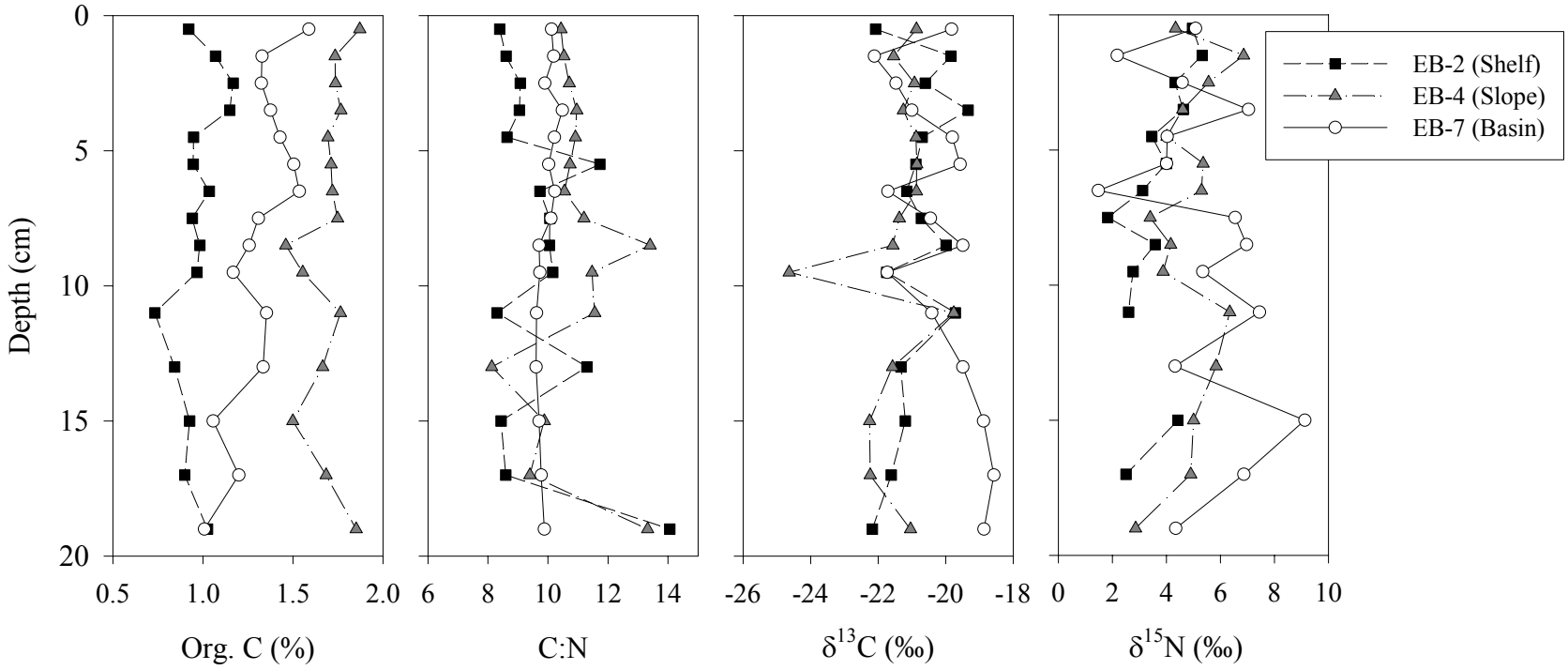

Figure 4.2. Bulk parameters, including organic carbon (%), atomic C:N ratio, $\delta^{13}C$ (‰), and $\delta^{15}N$ (‰) in shelf, slope, and basin sediments in the EB sediments of the Alaskan Beaufort Sea.

4.4.2. Molecular biomarker distributions

A large suite of biomarkers of diverse origin was observed in sediment cores and individual concentration data for all markers are presented in the supplementary information (Tables A4.1-A4.10). Here, we focus on individual and grouped markers that provide organic matter source and process information (Table 4.1).

Fatty Acids

Total fatty acid concentrations in the shelf core ranged from 1.1 to 17.9 mg/g OC, with minimum concentrations found in the 7-8 cm layer (Fig. 2.3a, Table A4.1). Surface sediments contained the highest concentrations, but a subsurface peak was present at 3-4 cm where total fatty acids reached 9.3 mg/g OC. Below 4-5 cm, total fatty acids decreased and varied between 1-4 mg/g OC. Concentrations of total fatty acid were highest in slope sediments (EB-4) reaching 28 mg/g OC (Table A4.2) at 2-3 cm, but dropped below 3 cm, ranging from 2.8 to 7.4 mg/g OC. Total fatty acid concentrations were substantially lower in the basin (EB-7) core sediments, ranging from 0.5 to 2.8 mg/g OC (Table A4.3). Similar to the shelf core, a subsurface maximum in total fatty acids was present at 3-4 cm (Fig. 4.3a).

In both the shelf and slope cores, concentrations of low molecular weight (C_{12}-C_{22}) saturated, as well as monounsaturated (MUFAs) and branched fatty acids (Figs. 4.3a and 3b) mirrored the total fatty acid profile (Table 4.2). Polyunsaturated fatty acids (PUFAs) similarly matched the short-chain saturated concentration profiles in the shelf ($r=0.93$) and slope ($r=0.99$) cores, but this correspondence was dampened in the shelf core below 5 cm (Fig. 4.3a).

Table 4.1. Sources of grouped and individual fatty acid and neutral lipid biomarkers in Arctic Ocean sediments.

Biomarker	Carbon Range	Dominant Source	Reference
n-alkanes			
	C_{15}, C_{17}, C_{19}	Algae	Han et al. (1968)
	C_{20}-C_{36} with odd predominance	Vascular plant	
	C_{20}-C_{35} with no odd/even predominance	Petroleum	Volkman et al., 1997
n-alcohols			
	C_{14}-C_{22} saturated and monounsaturated	Zooplankton	Sargent (1981)
	C_{22}-C_{32} with even predominance	Vascular Plant	Volkman (2006)
n-alkanoic acids			
	C_{12}-C_{18} saturated, even	Ubiquitous	
	C_{13}-C_{17} branched	Bacteria	Perry et al. (1979)
	C_{23}-C_{30} saturated, even predominance	Vascular plant	Volkman et al. (1989)
	C_{18}-C_{22} polyunsaturated (PUFA)	Marine Algae, Zooplankton	Dalsgaard et al. (2003)
	C_{22+} dicarboxylic	Vascular Plants	Wakeham (1999)
Sterols			
	24-methylcholesta-5,22E-dien-3β-ol ($C_{28}\Delta^{5,22}$)	Diatoms, Haptophytes, Cryptophytes	Volkman (1986), Goad et al. (1983)
	24-methylcholesta-5,24(28)-dien-3β-ol ($C_{28}\Delta^{5,24(28)}$)	Centric Diatoms	Barrett et al. (1995)
	4α,23,24-trimethyl-5α-cholest-22E-en-3β-ol (dinosterol)	Select dinoflagellates, minor contributions from diatoms	Volkman et al. (1993)
	24-ethylcholesta-5,22E-dien-3β-ol ($C_{29}\Delta^{5,22}$)	Higher plants, some microalgae contribution	Volkman (1986)
	24-ethylcholest-5-en-3β-ol ($C_{29}\Delta^{5}$)	Higher plants, some microalgae contribution	Volkman (1986)
Terpenoids			
	a-amyrin, b-amyrin, taraxerol	Higher Plants	Volkman (2006)

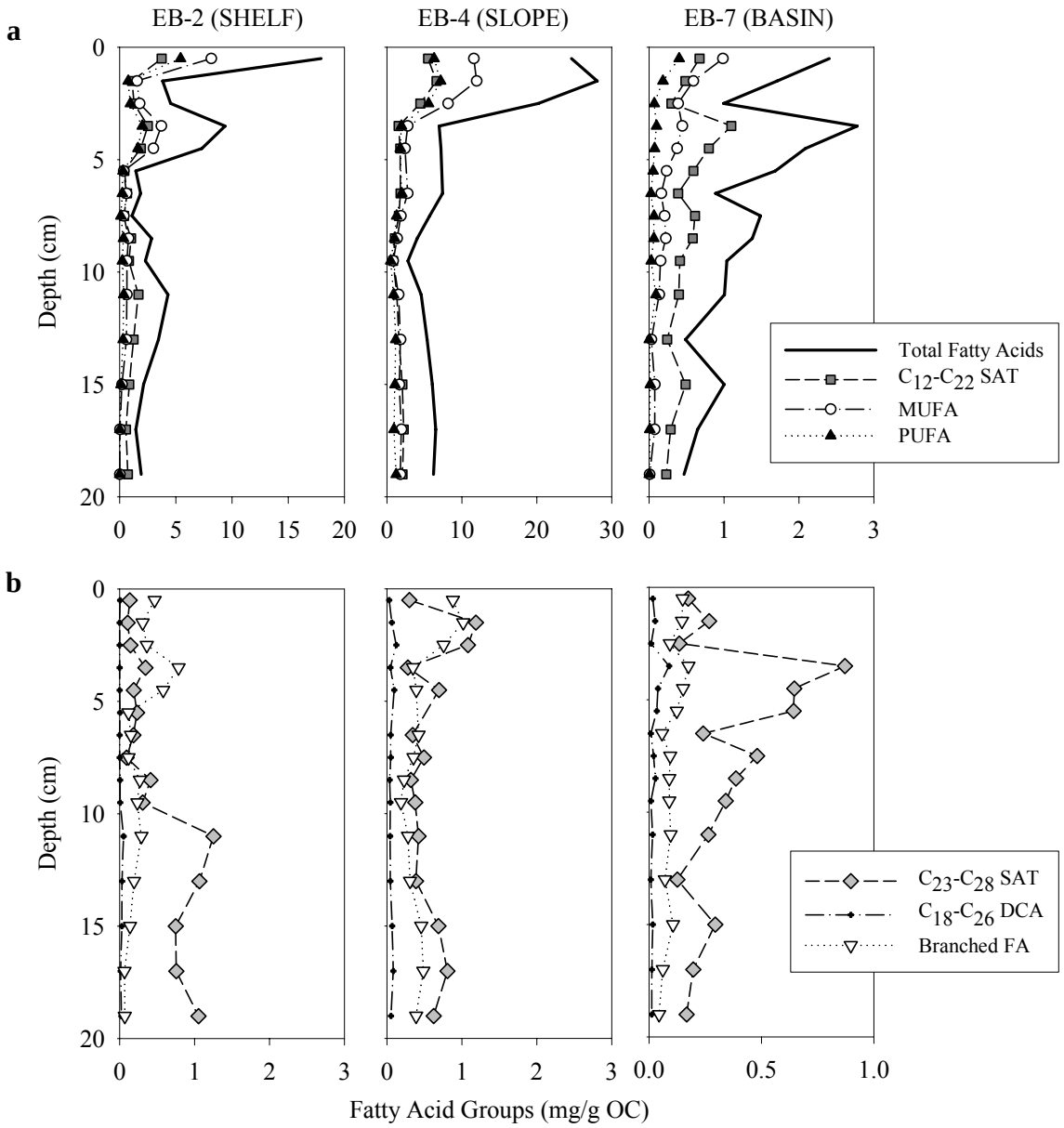

Figure 4.3. Total fatty acid, short-chain saturated (C_{12}-C_{22} SAT), monounsaturated (MUFA), and polyunsaturated (PUFA) concentrations (a) and concentrations of long-chain saturated (C_{23}-C_{28} SAT), mid- to long-chain saturated dicarboxylic acids (C_{18}-C_{26} DCA), and branched fatty acids (Branched FA) (b) in sediment cores from a transect of shelf to basin sediments in the Alaskan Beaufort Sea.

A similar correspondence was noted between the PUFAs and MUFAs in shelf and slope sediments (r=0.97 and r=0.99, respectively; Table 4.2). In contrast, long-chain fatty acids (>C_{22}) were lower in concentration than their shorter-chain counterparts, and did not closely mimic the total fatty acid trend (Fig. 4.3b, Table 4.2). In shelf sediments, long-chain fatty acids increased below 8 cm to higher concentrations than short-chain saturates. In the basin, short and long-chain fatty acids were present in similar concentrations throughout the entire core and matched the trend in total fatty acid concentrations (r=0.94 and r=0.71, respectively). Polyunsaturated fatty acids were low with only trace amounts below 3 cm (Fig. 4.3).

Neutral Lipids

In all sediments, *n*-alkanes showed a strong odd-even predominance (OEP) with concentrations dominated by longer chain (>C_{23}) homologues (Tables A4.4-A4.6). Even carbon *n*-alcohols were also abundant, but unlike the *n*-alkanes, long-chain alcohols were present in similar concentrations as the shorter-chain (C_{16}, C_{18}) alcohols (Tables A4.4-A4.6). Similar to the fatty acids, concentrations of *n*-alkanes and *n*-alcohols were highest in slope sediments, especially in the upper 4 cm of the core, and down-core profiles of these two biomarker classes closely mirrored one another at all three sites (Fig. 4.4). Concentrations of long-chain *n*-alkanes and *n*-alcohols were well correlated throughout the entire shelf core (r=0.92), and demonstrated a strong increase in concentration beginning around 8 cm (Figs. 4.3 and 4.4).

Table 4.2. Correlation coefficients for grouped fatty acids in shelf, slope, and basin sediments.

	SCFA	LCFA	MUFA	PUFA	DCA	BR	TFA
EB-2 (Shelf)							
SCFA	1.00	-0.13	0.94*	0.93*	0.01	0.78	0.98*
LCFA		1.00	-0.40	-0.37	0.87	-0.33	-0.26
MUFA			1.00	0.99*	-0.28	0.70	0.99*
PUFA				1.00	-0.28	0.63	0.98*
DCA					1.00	-0.06	-0.16
BR						1.00	0.71
TFA							1.00
EB-4 (Slope)							
SCFA	1.00	0.61	0.98*	0.97*	0.25	0.99*	0.99*
LCFA		1.00	0.47	0.52	0.77	0.63	0.55
MUFA			1.00	0.99*	0.16	0.96*	1.00*
PUFA				1.00	0.24	0.95*	0.99*
DCA					1.00	0.31	0.24
BR						1.00	0.97*
TFA							1.00
EB-7 (Basin)							
SCFA	1.00	0.86*	0.51	0.40	0.89*	0.85*	0.94*
LCFA		1.00	0.09	-0.04	0.88*	0.63	0.70
MUFA			1.00	0.95*	0.31	0.72	0.76
PUFA				1.00	0.18	0.62	0.66
DCA					1.00	0.77	0.80
BR						1.00	0.92*
TFA							1.00

Pearson correlation coefficients. Highly significant correlations ($p<0.001$) are marked with an asterisk. SCFA: Short-chain (C_{12}-C_{22}) saturated fatty acids; LCFA: long-chain (C_{23}-C_{28}) saturated fatty acids; MUFA: monounsaturated fatty acids; PUFA: polyunsaturated fatty acids; DCA: mid- to long-chain (C_{18}-C_{27}) dicarboxylic acids; BR: branched saturated fatty acids; TFA: sum of total fatty acids.

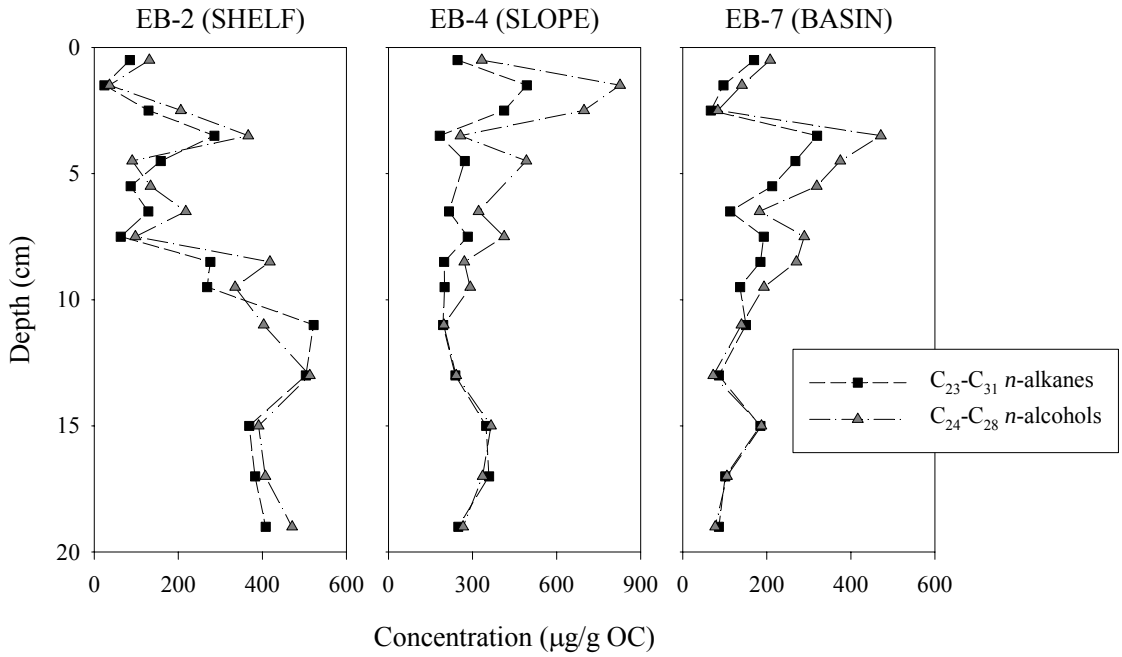

Figure 4.4. Concentrations of long-chain *n*-alkanes (C_{23}-C_{31}) and *n*-alcohols (C_{24}-C_{28}) in shelf, slope, and basin sediments of the Alaskan Beaufort Sea.

A diverse suite of sterols was identified in sediments (Tables A4.7-A4.9). Twenty-seven sterols were found in most sediment intervals, with summed total sterol concentrations ranging from 192-1311 μg/g OC, 783-2880 μg/g OC, and 160-1023 μg/g OC in shelf, slope, and basin cores, respectively. In all samples, however, six structures accounted for over half of the total sterol concentration and included cholest-5-en-3β-ol ($C_{27}\Delta^5$ or cholesterol), 24-methylcholesta-5,22-dien-3β-ol ($C_{28}\Delta^{5,22}$), 24-methylcholesta-5,24(28)-dien-3β-ol ($C_{28}\Delta^{5,24(28)}$), 24-methylcholest-5-en-3β-ol ($C_{28}\Delta^5$), 24-ethylcholest-5-en-3β-ol ($C_{29}\Delta^5$,), and 4α,23,24-trimethylcholest-22-en-3β-ol (dinosterol), Fig. 4.5). In the shelf sediments (EB-2), total sterol concentrations fluctuated with depth, and loosely followed the general depth profile of the fatty acids with highest concentrations at the

sediment-water interface (1311 μg/g OC) and a subsurface peak (1180 μg/g OC) at 3-4 cm. Markers of primary and secondary productivity, such as cholesterol and $C_{28}\Delta^{5,22}$, and the terrestrial sterol $C_{29}\Delta^{5}$ were the most abundant sterols in the upper 5 cm of the core. Below 5 cm, however, $C_{29}\Delta^{5}$ was the most concentrated sterol (Figs. 4.5), with variable cholesterol concentrations throughout the entire core. The variations in concentrations of 24-ethylcholest-5-en-3β-ol ($C_{29}\Delta^{5}$) sterol and α-amyrin were similar to high molecular weight *n*-alkane and *n*-alcohol profiles in all cores, but, did not show as high an increase in the shelf core below 8 cm where the long-chain *n*-alkanoic acids, *n*-alkanes, and *n*-alkanols increased (Figs. 4.3, 4.4, and 4.5). The EB-4 (slope) sediments contained higher concentrations of total sterols than EB-2 or EB-7, and $C_{29}\Delta^{5}$ was the most concentrated sterol in all core intervals, with cholesterol, $C_{28}\Delta^{5,22}$, and $C_{28}\Delta^{5,24(28)}$ also abundant (Fig. 4.5). With depth in the sediment, inputs of the major sterols did not proportionally change in slope sediments, and the sterol profiles closely mimicked downcore trends in fatty acids (Figs. 4.3 and 4.5). In sediments from the deeper waters at the basin station (EB-7), $C_{29}\Delta^{5}$ and $C_{28}\Delta^{5}$ were the most abundant sterols (Fig. 4.5). Notably, absolute concentrations of α-amyrin and $C_{29}\Delta^{5}$ are similar in the basin core as the shelf core (Fig. 4.5).

Trace Element Composition and ^{210}Pb

Trace element species measured in the sediments of the three sites are shown in Table A4.10. Across the transect, Al, Fe, Ba, Cr, Ni, Cu, Zn, and Co showed generally small differences between cores and little variation with sediment core depth (Table A4.10).

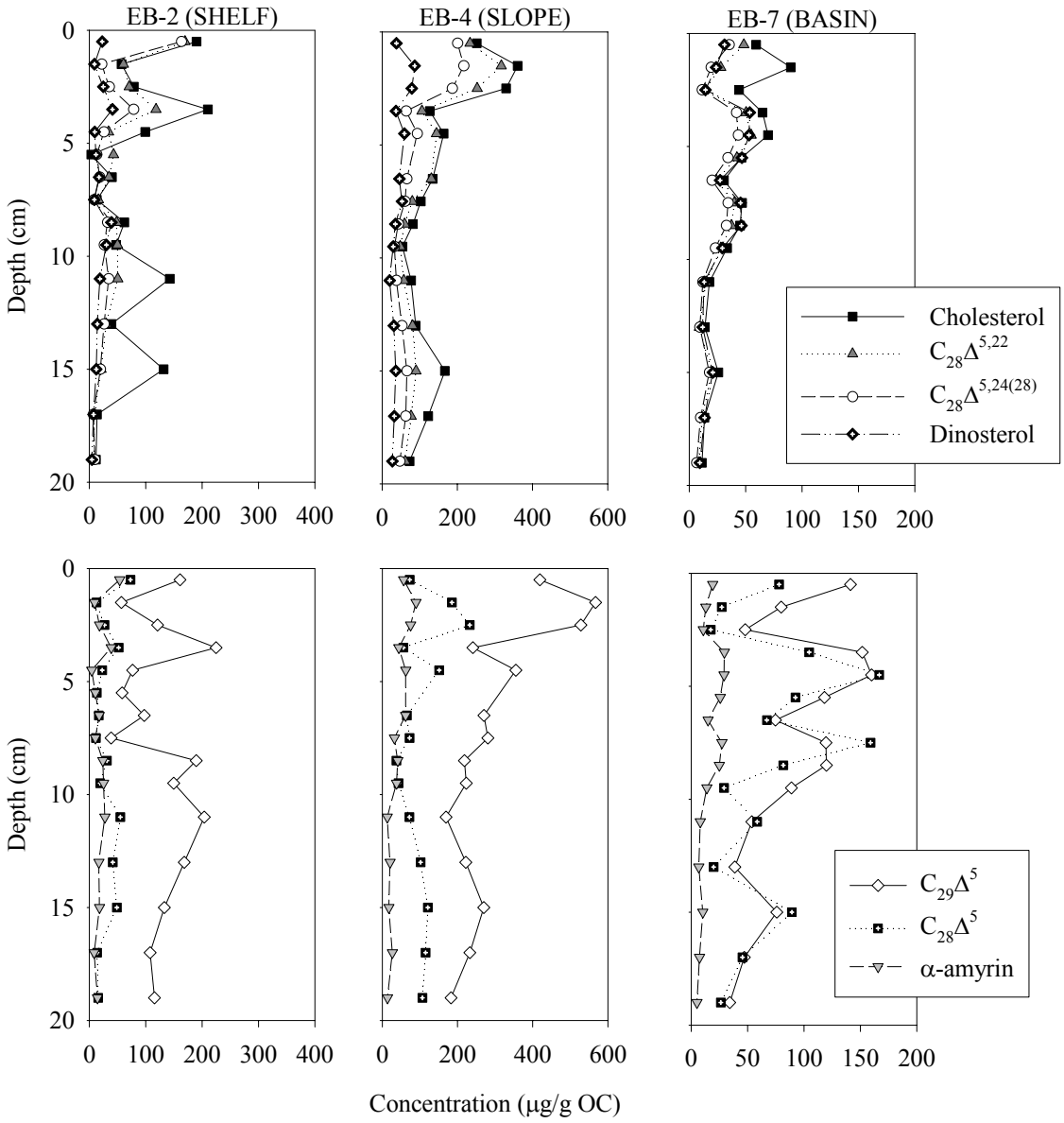

Figure 4.5. Concentrations of cholest-5-en-3β-ol (cholesterol), 24-methylcholesta-5,22-dien-3β-ol ($C_{28}\Delta^{5,22}$), 24-methylcholesta-5,24(28)-dien-3β-ol ($C_{28}\Delta^{5,24(28)}$), and 4α,23,24-trimethylcholest-22-en-3β-ol (Dinosterol) (a) and 24-ethylcholest-5-en-3β–ol ($C_{29}\Delta^{5}$), 24-methylcholest-5-en-3β–ol ($C_{28}\Delta^{5}$), and α-amyrin (b) in shelf, slope, and basin sediments of the Alaskan Beaufort Sea.

Remaining elements, which are affected by sediment redox conditions, however, showed considerable differences along the shelf-basin transect and with sediment depth (Fig. 4.6). In the shallow sediments from the shelf, AVS was detected just below the surface, and reached a maximum of 591 μmol/g at 8-9 cm. Concentrations of Mn and Re did not show enrichment in these sediments, remaining relatively constant downcore (Fig. 4.6). Concentrations of Mn and Re were similar to the shelf sediments at the slope site, but AVS was first detected at a deeper depth in the core and at lower concentrations (maximum of 40 μmol/g) than on the shelf. In basin sediments, a distinct enrichment of Mn was present in the top 3 cm. Below this surface Mn enrichment, a Re peak was present at 6-7 cm, followed by a sharp increase in AVS to a maximum of 129 μmol/g at 7-8 cm. Below this horizon, AVS concentrations dropped off, but remained detectable (Fig. 4.6).

^{210}Pb in the shelf core (EB-2) was low with an excess activity ($^{210}Pb_{ex}$) in surface sediment of 0.38 dpm g^{-1}. Total ^{210}Pb activity in the shelf core reached supported levels (1.53 dpm g^{-1}) by 7 cm (Table 4.3, Fig. 4.6). In slope (EB-4) sediments, ^{210}Pb concentrations were highly variable, with a secondary subsurface peak present below 10 cm. Supported concentrations of ^{210}Pb were not quantified for these sediments; however, total ^{210}Pb activity in the surface interval was 3.66 dpm g^{-1}.

In the basin core, $^{210}Pb_{ex}$ concentrations were high with a surface activity of 24.7 dpm g^{-1}, and decreased exponentially, reaching a supported concentration (2.96 dpm g^{-1}) below 8 cm. In order to calculate sedimentary ^{210}Pb inventories, ^{210}Pb activities were estimated for non-measured sediment intervals by linear interpolation.

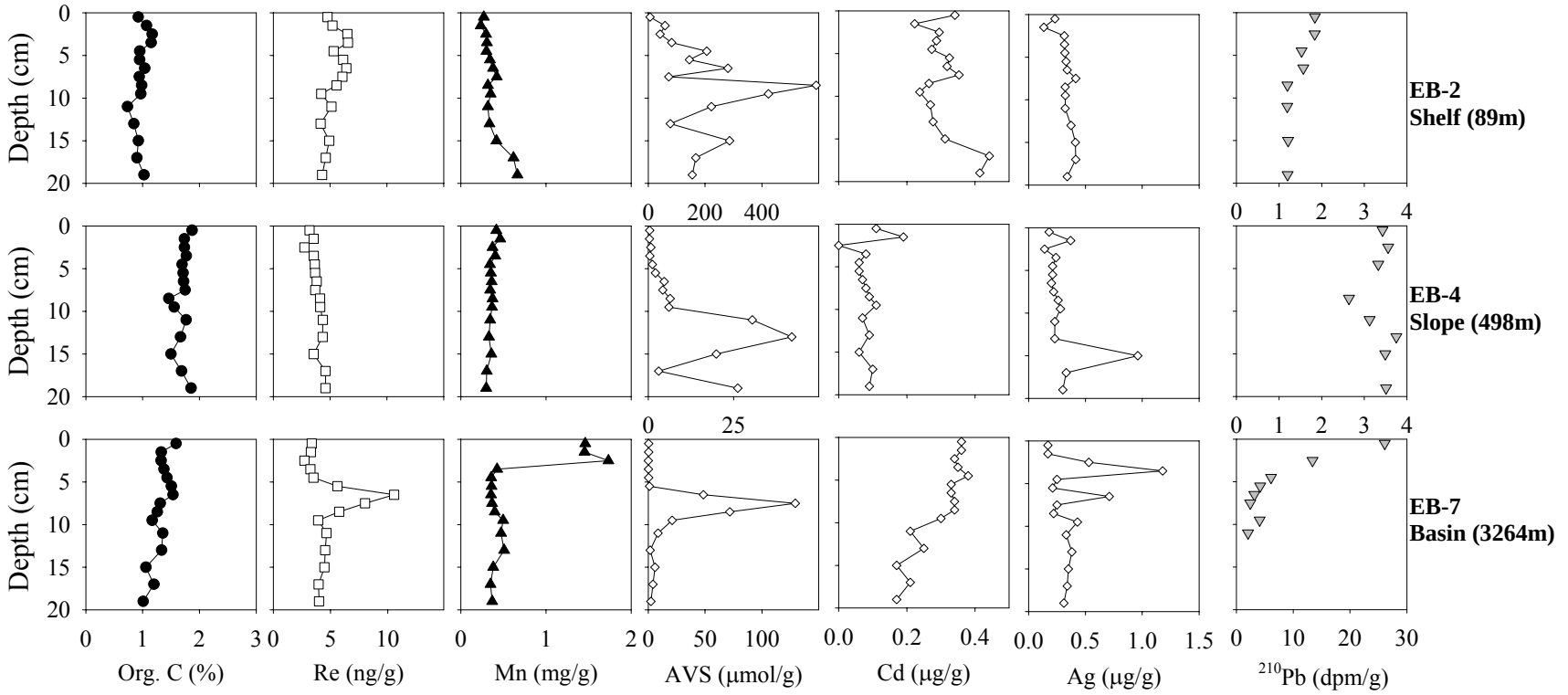

Figure 4.6. Concentrations of organic carbon (%), Re (ng/g), Mn (mg/g), AVS (µmol/g), and ^{210}Pb (dpm/g) in shelf, slope, and basin sediments of the Alaskan Beaufort Sea.

Table 4.3. Profiles of excess ^{210}Pb in sediments from the shelf, slope, and basin of the Alaskan Beaufort Sea

Horizon (cm)	$^{210}Pb_{total}$ (dpm g^{-1})	$^{210}Pb_{supported}$ (dpm g^{-1})	$^{210}Pb_{excess}$ (dpm g^{-1})	Sediment Density (g cm^{-3})	$^{210}Pb_{excess}$ (g cm^{-2})	$^{210}Pb_{excess}$ Inventory (dpm cm^{-2})
EB-2 (Shelf)						
0-1	1.91	1.53	0.38	0.67	0.25	
1-2	1.89[a]		0.36	0.90	0.32	
2-3	1.87		0.34	1.02	0.35	
3-4	1.72[a]		0.19	0.98	0.18	
4-5	1.56		0.03	1.09	0.03	
5-6	1.58[a]		0.05	1.07	0.05	
6-7	1.60		0.07	1.14	0.07	
7-8				1.15		
8-9	1.22		-	1.13		
9-10				1.17		
10-12	1.21		-	1.21		
12-14				1.19		
14-16	1.23		-	1.15		
16-18				1.17		
18-20	1.22		-	1.13		1.26
EB-4 (Slope)						
0-1	3.66			0.43		
1-2				0.32		
2-3	3.86			0.36		
3-4				0.58		
4-5	3.46			0.67		
5-6				0.65		
6-7				0.67		
7-8				0.72		
8-9	2.74			0.72		
9-10				0.75		
10-12	3.24			0.69		
12-14	3.90			0.66		
14-16	3.63			0.67		
16-18				0.76		
18-20	3.64			0.71		
EB-7 (Basin)						
0-1	27.66	2.96	24.70	0.48	11.88	
1-2	20.83[a]		17.87	0.59	10.53	
2-3	14.00		11.04	0.59	6.55	
3-4	10.19[a]		7.23	0.60	4.36	
4-5	6.38		3.42	0.59	2.03	
5-6	4.38		1.42	0.59	0.83	
6-7	3.29		0.33	0.63	0.20	
7-8	2.53		-	0.65	-	
8-9	3.41[a]		0.45	0.63	0.28	
9-10	4.29		1.33	0.56	0.75	
10-12	3.22[a]		0.26	0.53	0.27	
12-14	2.15		-	0.56		
14-16	-		-	0.55		
16-18	-		-	0.54		
18-20	-		-	0.55		37.69

[a]Values for intermediate depths not directly measured were estimated by linear interpolation.

^{210}Pb activities were then converted from dpm g^{-1} to dpm cm^{-2} by estimating sediment density from measured porosities (Table 4.3). For cores EB-2 and EB-7 where ^{226}Ra activities were measured and used to calculate supported ^{210}Pb (Table 4.3), sedimentary inventories of 1.26 and 37.69 dpm cm^{-2}, respectively, were calculated by summing concentrations of $^{210}Pb_{ex}$ throughout the core (Table 4.3).

4.5. Discussion

4.5.1 Organic carbon dynamics: The transition from shallow to deep sedimentary environments

The continental shelf region

Lipid biomarkers together with bulk sedimentary properties and trace element compositions can help decipher organic carbon cycling in the region east of Barrow Canyon in the Alaskan Beaufort Sea. Along the transition from the shallow continental shelf to the deep basin, the sediments reflect a highly dynamic environment where physical and biological processes are strongly linked.

The narrow Alaskan Beaufort Shelf, influenced by numerous small rivers and high coastal erosion rates, is thought to be a far less productive region than the broad, shallow shelves of the Chukchi Sea to the west where nutrient-rich waters from the Bering Sea support high marine primary productivity (Grebmeier et al., 1995; Naidu et al., 1993; Walsh et al., 1989). Yet concurrent studies from the Shelf-Basin Interactions program have shown that the areas near Barrow Canyon and the East Barrow transect line (this study region) are represented by high rates of primary (Hill and Cota, 2005) and net community productivity (Bates et al., 2005a) and consequently high concentrations of suspended particulate organic matter (POM) and sinking large-particle (>53 μm) POM

(Bates et al., 2005b). For example, in Barrow Canyon daily primary productivity rates reached 8.2 g C m^{-2} day^{-1} during the spring bloom, and 2 g C m^{-2} day^{-1} for the remaining summer months (Hill and Cota, 2005). These rates are comparable to the daily primary productivity measurements made in the ice-free western Chukchi shelf region of 2.6 g C m^{-2} day^{-1} (Gosselin et al., 1997), and demonstrate that areas in the Alaskan Beaufort Sea are certainly important locally and may be significant for the marine organic carbon budget of the Arctic Ocean.

In shelf sediments of the EB transect, bulk organic matter reflects the overlying highly productive waters and shallow depth. Atomic C:N ratios between 8 to 14 suggest predominantly marine material, with the higher values possibly the result of degradation of more protein-rich components during early diagenesis (Meyers, 1997) or of mixing with terrestrial organic matter (Bordowskiy, 1965; Hedges et al., 1986). The range of stable carbon isotopic composition in the shelf core, -19 to -22 ‰, is also typical of marine organic matter inputs (Fogel and Cifuentes, 1993; Meyers, 1997) and is greatly enriched compared to the marine end-member suggested previously for the Alaskan Beaufort Sea (C:N ratio of 6-7 and a $\delta^{13}C$ of -24 to -23.4 ‰; (Naidu et al., 2000)). This apparent enrichment in bulk $\delta^{13}C$ in outer shelf (89 m water depth) sediments could reflect at least three possible scenarios: (1) the outer shelf receives negligible terrestrial organic matter inputs, suggesting a marine organic matter end-member value for the Alaskan Beaufort Sea of -20.8 ‰ (average in EB-2 sediment core), higher than the previously suggested -24 to -23.4 ‰; (2) the outer shelf receives substantial inputs of marine organic matter with highly enriched isotopic composition (i.e., sea-ice algae or kelp communities). Sea-ice algae has been shown to have highly variable stable carbon

isotopic composition as discussed below, and Naidu et al. (2000) found kelp communities in the Alaskan Beaufort Shelf region with $\delta^{13}C$ values ranging from -13.6 to -16.5 ‰. Finally, (3) the outer shelf region of the Alaskan Beaufort Sea receives its marine organic matter inputs from the Chukchi Sea to the east, which has been shown to have a more enriched (~ -21‰) marine organic carbon composition (Naidu et al., 2000). Given these large differences, however, it is apparent that the difficulty in constraining marine $\delta^{13}C$ and C:N values in the Arctic Ocean limits our ability to provide confident quantitative estimates of the sources for bulk sedimentary composition. Without greater spatial distribution of samples on the outer shelf, any of the three scenarios are plausible.

The first scenario of negligible terrestrial organic inputs to the outer shelf appears implausible considering the high levels of coastal erosion (Are et al., 2008) and previous work specifically identifying that terrestrial organic carbon is an important fraction in the particles and sediments elsewhere in the region (Belicka et al., 2002). Likewise, lipid biomarker data discussed below confirms the presence of terrestrial organic compounds in these sediments. The observed isotopic composition of the outer shelf sediments therefore suggests the presence of a strongly enriched source of marine organic matter (scenario 2). Measurements of fresh marine phytoplankton have shown considerable variability in the Arctic, and sea-ice algae in particular, growing in restricted ice pockets or meltwater ponds, can be highly enriched in $\delta^{13}C$ (Gradinger, in press; Tremblay et al., 2006). Nevertheless, $\delta^{13}C$ values were depleted below the 7-8 cm depth, which could suggest a stronger component of terrestrial organic matter contributing to sediments in this region of the Arctic during earlier time periods. This suggestion also appears to be corroborated by the deplete $\delta^{15}N$ values below 8 cm (Fig. 4.2); however, this trend was

not evident in the C:N ratio, which showed no increase below 8 cm. The C:N is not always indicative of source, as multiple samples of terrestrial organic matter from the Mackenzie River were found to have strongly depleted $\delta^{13}C$ but a relatively low C:N ratio (Naidu et al., 2000). Bound, inorganic nitrogen estimated by the intercept of a plot of organic carbon versus total nitrogen (Schubert and Calvert, 2001) was nearly zero (0.007%) in these sediments and would therefore not be a source of bias of C:N in this core.

The presence of a sediment mixed layer of 3 cm or deeper in the shelf sediments is shown by the ^{210}Pb data (Fig. 4.6). The sedimentary inventory of ^{210}Pb (1.26 dpm cm^{-2}; penetration to 7 cm) is lower than those found by Baskaran and Naidu (1995) and Smith et al. (2003) for sediments from similar water depths on the Chukchi Sea shelf (range of 2.98 to 13.9 dpm cm^{-2}) and substantially lower than those calculated by Lepore et al. (in press) for the nearby Barrow Canyon sediments (range of 15.46 to 33.84 dpm cm^{-2}). It is apparent that a large degree of heterogeneity exists in the delivery of ^{210}Pb to Arctic sediments.

The atmospheric flux of ^{210}Pb is known to be low throughout the Arctic due to both reduced precipitation compared to temperate and tropical regions and limited radon exhalation from scarce soils and permafrost (Dibb, 1992; Hermanson, 1990). This atmospheric flux into the ocean is likely to be spatially variable, depending to some degree on ice cover and location of melting, and annual estimates have ranged from 0.025 dpm cm^{-2} for the Canada Basin interior (Moore and Smith, 1986) to 0.22 dpm cm^{-2} in southern Alaska (Preiss et al., 1996). Clearly the high inventories of ^{210}Pb in sediments of the Barrow Canyon (Lepore et al., in press) indicate enhanced focusing of

atmospherically-derived ^{210}Pb compared to the sediments east of Barrow Canyon presented here, likely as a result of inputs from sea-ice melting. Observations from Eicken et al. (2005) demonstrate abundant sediment-laden sea-ice in the Barrow Canyon region, with most sites showing between 50-100% of the area as occupied by sediment-laden ice during the months of May-June. Observations were not made in the region east of Barrow Canyon; however, the overall drift pattern of sediment-laden sea-ice followed a westward trajectory (Eicken et al., 2005), suggesting the possibility for increased focusing of particulates from the ice as it drifts westward and melts. The Barrow Canyon sediments to the west studied by Lepore et al. (in press) did have high sedimentary focusing factors (average of 6.2), yet sediment budgets did not suggest that particulate matter from the west (near the Hanna Shoal) was being transported to Barrow Canyon (Lepore et al., in press). Unfortunately, sediments to the east were not investigated and it remains conceivable that sediments (and scavenged ^{210}Pb) from the East Barrow region are trapped by the nearby Barrow Canyon, thus starving the EB shelf.

The abundant AVS in the shelf core together with the lack of Mn enrichment in surface sediments indicate that labile organic carbon metabolism is sufficiently strong in these sediments to create anoxic conditions, at times to the sediment surface, and sulfate reduction just below the sediment surface (Fig. 4.6). Clearly the shelf region receives sufficient fluxes of labile organic matter to consume oxygen completely up to the sediment-water interface at least part of the year. Preserved lipid structures in the shelf sediments generally support redox-element evidence for pulses of marine organic matter inputs, yet also provide specific evidence for additional organic inputs from terrestrial organic matter not apparent from simple bulk organic matter proxies. The high

abundance of PUFAs (predominantly the 20:5 diatom marker, but also 16:4, 18:4, and 22:6) in the upper 5 cm of shelf sediments (Fig. 3) supports the rapid mixing of relatively fresh, ungrazed marine organic matter into sediments as might occur during post-bloom deposition. Concentrations of short-chain saturated and monounsaturated fatty acids closely tracked the PUFAs downcore, suggesting a similar source and a similar rate of diagenetic processing in the upper 10 cm of the core.

It is significant in the shelf sediments that terrestrial biomarkers, like the long-chain saturated fatty acids, increase with depth below about 8 cm in contrast to marine markers like the shorter-chain saturated and monounsaturated fatty acids, which decrease with depth (Figs. 4.3 and 4.4). This increase in long-chain fatty acids was mirrored in the concentrations of other alkanoic compounds; for example, long-chain saturated fatty acid concentrations were well correlated with both long-chain *n*-alkanes (r=0.95) and long-chain *n*-alcohols (0.82) in the shelf core. These long-chain compound series (*n*-alkanoic acids, *n*-alkanes, and *n*-alkanols) have long been used as terrestrial markers, based on their abundance in the epicuticular waxes of higher plant leaves (Eglinton and Hamilton, 1969), and it is tempting to infer that terrestrial organic matter inputs to the shelf were higher during earlier times represented by depths below 10 cm in this core. Yet, two other well-known, stable terrigenous organic markers, α-amyrin and the $C_{29}\Delta^5$ sterol, show no dramatic increases in the deeper sediments of this core (Fig. 4.5). Based on compound-specific isotopic composition, it has been suggested that substantial proportions of long-chain *n*-alkanoic acids found in sediments might actually be of marine origin (Birgel et al., 2004; Naraoka and Ishiwatari, 2000). The measurement of both $\delta^{13}C$ and $\Delta^{14}C$ in long-chain fatty acids in sediments from the nearby eastern

Beaufort Sea (Drenzek et al., 2007), however, clearly shows these compounds to be thousands of years older than short-chain counterparts, which led these authors to conclude that the long-chain fatty acids must have spent considerable time in terrestrial soils before being eroded into rivers or the ocean.

If these markers are terrestrial in origin, there must be two terrestrial organic matter pools—a fresh, rapidly cycled modern pool, and a much older and only recently mobilized terrestrial soil pool. The proximity to the shoreline would argue for a fraction of fresh terrestrial material, yet the high coastal erosion rates on the narrow Alaskan Beaufort shelf, estimated between 0.5 to 6 m yr^{-1} (Are et al., 2008; Lantuit and Pollard, 2008), allows for considerable inputs from eroding permafrost deposits, one potential source for ancient vascular plant material given that average radiocarbon ages of exposed peat deposits from the Kokolik and Ikpikpuk Rivers range from 2900 to 3400 years (Chapter 2). The existence of these two pools of varied age may explain the uneven concentrations of the terrestrial biomarkers despite their likely similar diagenetic loss rates.

The presence of two terrestrial organic matter pools with apparently varied recycling times in marine sediments was also proposed by Gordon and Goñi (2004), who found hydrodynamics to play a strong role in the distribution of organic matter in the Gulf of Mexico. Organic matter preserved within the river channel and inner shelf region was composed of a modern, coarser land-plant material fraction, while Gulf of Mexico sediments from the outer shelf contained finer-grained particles composed of aged, soil-derived organic carbon along with additions of modern, marine organic matter from primary productivity (Gordon and Goñi, 2004). In addition to hydrodynamic sorting of

particles, atmospheric transport could be responsible for fractionating between two terrestrial organic matter pools. Long-chain *n*-alkanes, *n*-alkanols, and *n*-alkanoic acids have been shown to be transported long distances in atmospheric aerosols, as opposed to phytosterols and amyrins which were minor components in atmospheric particulates (Simoneit, 1989; Yunker et al., 1994). The increase in the alkanoic compounds with no corresponding increase in ringed structures below 8 cm in this shelf core suggests that atmospheric delivery of fine particulates was relatively more important during this time period.

The Shelf-Break/Continental Slope Region

The high loadings of organic matter, including abundant marine polyunsaturated fatty acids, in sediments from deeper waters (~500 m) on the continental slope (Figs. 4.2 and 4.3) together with the presence of AVS and the lack of surface enrichment of Mn (Fig. 4.6) point to high fluxes and recycling of organic matter at this location. Labile organic fluxes are lower those found on the shelf, as indicated by AVS, which shows lower concentrations distributed deeper in the core (Fig. 4.6). The presence of AVS below about 5 cm demonstrates that sulfate has become an oxidant for metabolism of labile organic carbon, and that sufficient metabolism occurs near the surface to use up all oxygen and manganese oxygen carriers. The loss of oxygen is fueled by organic degradation of high levels of labile carbon supplied from marine primary productivity, a situation that appears to have existed at this core site throughout the time period the sediments have been accumulating.

Concentrations of algal polyunsaturated fatty acids were substantially higher on the slope than on the shelf (Fig. 4.3). Similar to the shelf environment, the presence of

these labile markers reflects the input of fresh marine organic matter to the sediments. The sharp drop-off in short-chain saturated and polyunsaturated fatty acids below 4 cm in the sediments suggests that organic matter is rapidly recycled in upper sediments. Yet, the substantially higher concentrations of short-chain saturated and polyunsaturated fatty acids at the slope station show that slope waters are also areas with substantial primary productivity. Its location near the shelf-break/marginal ice zone, or its proximity to Barrow Canyon, which can receive high nutrient water masses draining the Herald Valley region (Woodgate et al., 2005) or, during current reversals, nutrient-rich Atlantic water from below the pycnocline (Hill and Cota, 2005), might elevate primary productivity rates and subsequent marine organic matter deposition. Furthermore, the slope may receive labile organic carbon both directly from primary production as described above, and indirectly through the focusing of resuspended sediment over the shelf with export to the slope (O'Brien et al., 2006). The higher concentrations of polyunsaturated fatty acids in slope sediments together with the lower metabolic rate evident in the AVS distribution may simply reflect slower metabolism or more episodic inputs rather than increased inputs of labile organic matter.

It is important to note that concentrations of recalcitrant terrestrial markers, including long-chain *n*-alkanols, *n*-alkanes, and *n*-alkanoic acids, were substantially higher in the slope sediments, especially in the upper 10 cm. This evidence, combined with its elevated concentration of marine carbon, implies that the slope region could be a site of organic matter focusing supported by export of organic remains and sediments from the nearby shelf (O'Brien et al., 2006). Focusing is also evident in the very high sedimentary chlorophyll *a* concentrations at the mouth of Barrow Canyon (Pirtle-Levy et

al., in press) and in the high levels of faunal biomass found in the trough of the canyon; together they suggest delivery of organic matter from shelf regions drives strong benthic activity in the BC region (Dunton et al., 2005; Feder et al., 1994). Baroclinic instabilities eastward of the Colville River, evidenced by regularly spaced regions of higher chlorophyll a concentrations, provide one possible advective mechanism for the focusing of shelf-derived organic matter to the slope region (Macdonald et al., 2004a).

An estimate of the supported contribution of ^{210}Pb was not measured for this sediment core, so an inventory could not be determined. The presence of a subsurface maximum of ^{210}Pb around 15 cm, however, does suggests that slope sediments have experienced rapid mixing, perhaps from bioturbation or gravity flows. Slumping may have brought older, ^{210}Pb-poor sediments downslope, resulting in the minimum ^{210}Pb concentrations around 10 cm. Further evidence for the slumping of older material was found with radiocarbon dating. The average radiocarbon age of the organic matter at the surface and at 20 cm was 6200 ± 35 and 6190 ± 40 radiocarbon years—at 10 cm, on the other hand, the average age of the organic matter was 9170 ± 40 years (NOSAMS Accession Numbers OS-40707 (0-1 cm), OS-40708 (9-10 cm), and OS-40709 (18-20 cm)). This material may have originated from deeper shelf sediments that were transported to the slope during a storm or turbidite flow, or, it may represent the input of ancient material that had been exposed and eroded from the continent. The minimum δ^{13}C value of -24.63 ‰ and a relatively high C:N ratios in the 10 cm depth range supports a terrestrial origin of this slumped material, and the relatively low δ^{15}N values (~3 ‰) could support a terrestrial origin, although a separation of δ^{15}N into bound and organic components would help support this interpretation (Schubert et al., 2001).

The Basin Region

In spite of plentiful concentrations of organic carbon (1.0-1.5%) present in the basin (3264 m) sediments, total fatty acid concentrations were much lower than in shelf and slope sediments, and low PUFA concentrations suggests substantial sedimentary reworking of labile organic matter. This is also evidenced by the higher $\delta^{15}N$ values observed in deeper sediment sections, representing preferential loss of nitrogen-rich components during oxic recycling (Lehmann et al., 2002). Concentrations of long-chain saturated fatty acids were of similar magnitudes to their shorter-chain homologues, a situation not found in shelf or slope sediments. These trends in the lipid biomarkers reflect low inputs of labile carbon, with recalcitrant, terrestrial-derived organic matter accounting for a much larger fraction of preserved organic matter. This is supported by concentrations of biomarker classes, with short-chain saturated fatty acids up to 20x higher in concentration on the slope compared to the basin. Redox-sensitive elements also support the notion that metabolism is slow in these sediments: the enrichment of Mn in the top 3 cm of basin sediments indicates an oxic mixed layer where organic matter metabolism is slow, likely due to limited flux of labile carbon to deep basin waters beneath perennial ice cover.

Regardless of the physical limitations of sea-ice cover and water depth characteristics of the basin, relatively labile organic matter must have been rapidly delivered to the sediments as noted by the AVS-rich zone between 6-9 cm (Fig. 4.6). This episodic enrichment of labile organic matter could have been derived from a turbidite flow or from an algal bloom or sea-ice algae, but given the rapid metabolism the typical algal unsaturated fatty acids are absent. Indeed, no change in concentration of

unsaturated fatty acids was observed in the sediment layers above the suboxic zone. Increases in the concentration of terrestrial organic markers, including long-chain saturated fatty acids, *n*-alcohols, *n*-alkanes, and $C_{29}\Delta^5$ were readily apparent between 3-6 cm (Figs 4.3, 4.4, and 4.5) but were matched by slight increases in the more typical marine markers cholesterol, $C_{28}\Delta^{5,24(28)}$, and $C_{28}\Delta^{5,22}$. This evidence, along with the strong correlation between long-chain and short-chain saturated fatty acids (r=0.86; Table 4.2) may be indicative of a turbidite origin, which coming from shallower waters would likely contain both terrestrial and marine organic proxies. More likely, though, the corresponding changes in concentration of both marine and terrestrial organic matter throughout the entire core suggests that the relative inputs between these carbon pools have not changed, or, that the lipid composition of these sediments is highly consistent and set prior to deposition, such as that found in pre-aged organic matter inputs (Drenzek et al., 2007).

In contrast to shelf sediments, basin sediments contained a large inventory of ^{210}Pb (37.69 dpm cm^{-2}), which compare well with other Arctic basin sediments (Gobeil et al., 2001). The high inventory of ^{210}Pb together with the depth of the water column here in the basin (3264 m) suggests that the source of excess ^{210}Pb is from water column ^{226}Ra rather than atmospheric deposition, which is known to be low in the Arctic (see discussion above). Combined with previous low estimates of Arctic basin sedimentation (~0.2 mm kyr^{-1}; Darby et al. (1997), Huh et al. (1997)), implies that the ^{210}Pb profiles is largely controlled by diffusive mixing from bioturbation (see Crusius and Kenna (2007)) and sedimentation rates are below the applicability of ^{210}Pb. Recent studies, however, have suggested Arctic sedimentation rates are higher than previously reported. Jakobsson

et al. (2003) determined rates near the Lomonosov Ridge to be on the order of 3 cm kyr^{-1}, and Pirtle-Levy et al. (in press), using ^{137}Cs, suggested a much higher rate of 175 cm kyr^{-1} in a sediment core taken in the East Barrow Canyon region (EB-6, 2227 m water depth. This rate appears quite high for a deep water setting such as the basin offshore of Barrow Canyon, especially when considering the slow sedimentation suggested by the ^{210}Pb and biomarker data presented here. However, the episodic delivery of labile organic matter suggested by the AVS record in basin sediments argues that sea-ice cover and water depth do not strictly limit the deposition of material to basin sediments and mechanisms such as turbidite flows of sea-ice rafting may supplement sediment accumulation. Previous assumptions of a deep Arctic with extremely slow sedimentation and little to no labile organic matter inputs may need to be revisited.

4.5.2. The relative abundances of terrestrial and marine organic matter in sediments

The combination of biomarker profiles and redox-sensitive elements clearly demonstrates that Arctic Ocean sediments receive a sufficient supply of labile organic carbon at times to consume all available O_2. Yet below the upper few centimeters of sediment, the concentration of measured organic matter proxies did not substantially decrease, demonstrating the potential for long-term carbon preservation in these sedimentary reservoirs. Because of the difficulties in constraining the marine $\delta^{13}C$ value in the Arctic, the relative proportions of marine and terrestrial organic matter using 2-end-member stable carbon isotope mixing models as in Prahl et al. (1994) are ineffective. However, by scaling lipid biomarkers to represent relative contributions from labile/marine versus recalcitrant/terrestrial sources, we can estimate the amount from each source preserved in sediments over time. Yunker et al. (2005) developed a

multivariate approach using molecular organic markers in 6 sediment cores from the Chukchi and Beaufort Seas, and together with regression techniques estimated the relative proportion of marine/labile material and recalcitrant/terrestrial material for each individual lipid marker. Compounds such as α-amyrin, produced only by vascular plants, could be scaled as 0 % marine/labile organic matter (and conversely 100 % recalcitrant/terrestrial organic matter. Compounds such as phytol with multiple origins from both marine and terrestrial sources required a less constrained estimate of 50 % from each potential reservoir [for details of the full multivariate analysis, see Yunker et al. (2005)]. Based on this scaling, we can estimate the relative proportions of labile and recalcitrant organic matter preserved in the sediment cores from the Alaskan Beaufort Sea (Fig. 4.7).

The fraction of the recalcitrant component of preserved organic matter ranged from 20-56%. Coupled lipid biomarkers and redox-sensitive elements presented above demonstrated that these sediments receive adequate labile organic matter which enhances sedimentary metabolism, at least episodically for the slope and basin and more regularly on the shelf, driving sediments to anoxia and increased proportions of preserved recalcitrant material with increasing depth for each core. The relative increase in recalcitrant material with sediment depth was least pronounced for the basin core, corresponding to the likely episodic nature of labile carbon delivery and subsequent O_2 drawdown. Interestingly, although total biomarker concentrations were lower in the basin sediments, the proportion of the recalcitrant organic matter in sediments from 3000 m water depth was as high as that found on the shelf. This necessitates a well-developed transport mechanism to deliver terrestrial organic matter to basin sediments, with sea-ice

rafting, atmospheric transport during ice-free conditions, and sediment slumping as possibilities. Lateral transport is also a known transport mechanism in the Arctic, evidenced by the terrestrial character of sinking particles in the Canada Basin (Hwang et al., 2008) and along the Lomonosov Ridge (Fahl and Nöthig, 2007) and by resuspension events creating bottom and mid-water nepheloid layers (O'Brien et al., 2006).

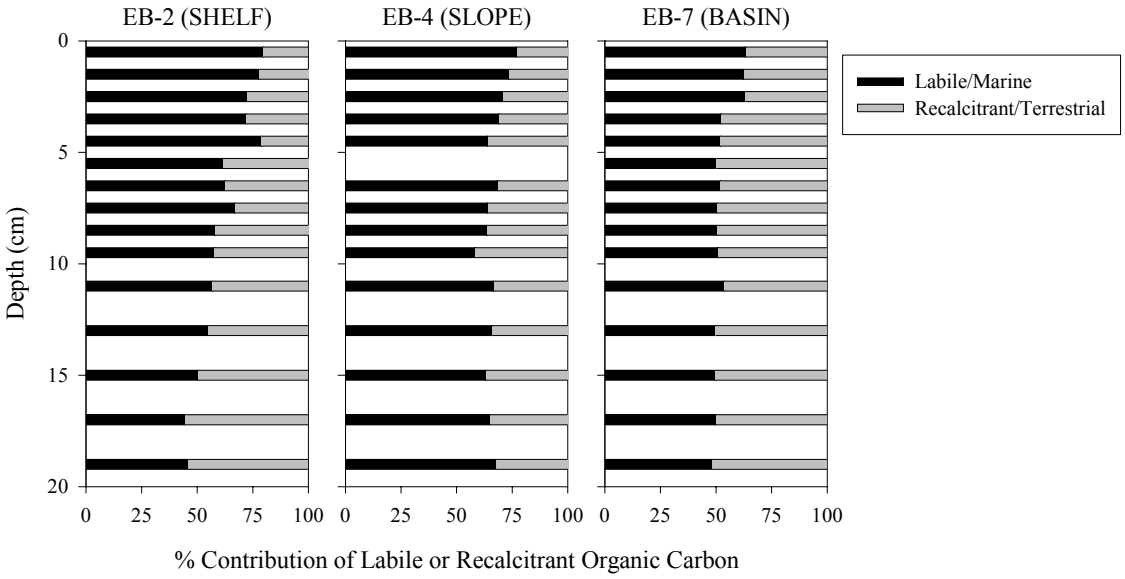

Figure 4.7. Relative contribution of labile/marine organic matter versus recalcitrant/terrestrial sources in preserved organic matter of the Alaskan Beaufort Sea.

4.6. Conclusions

Combined lipid biomarker and redox-sensitive elements demonstrate that sediments along the shelf-to-basin continuum in the western Arctic Ocean, receive sufficient labile organic matter inputs to consume all available O_2. Production of AVS

was highest in the shelf environment, indicating that intense metabolism of organic matter, at least partly involving sulfate reduction, occurs here, and the enriched isotopic composition of sediments suggest important inputs from sea-ice algae fuel this metabolism. The abundance of long-chain *n*-alkanes, *n*-alcohols, and *n*-alkanoic acids in sediments highlight the presence of an additional terrestrial pool of organic carbon, which increases in significance with sedimentary depth as the intense metabolism removes more labile components of the organic fraction. Discrepancies between markers of terrestrial origin argue for inputs from two pools of land-derived organic matter—material with a more modern, vascular-plant source and an older, recently mobilized permafrost source. Along the continental slope, higher concentrations of biomarkers of both terrestrial and marine organic matter were observed. Despite the less intense sedimentary metabolism noted here by lower concentrations of AVS which could lead to greater levels of organic preservation, concentrations of recalcitrant markers were in greater abundance than on the shelf, suggesting that the slope is a site of organic matter focusing. In spite of the physical limitations that sea-ice cover and water depth exert on carbon fluxes to the benthos in the deep Arctic basin, episodic pulses of labile material must reach basin sediments as noted by the redox-sensitive elemental profiles in the EB-7 core. In addition to evidence of labile organic matter reaching sediments at >3200 m water depth, strong evidence for terrestrial organic matter inputs were found in the basin sediments, corroborating recent evidence for abundant land-derived organic carbon in locations far removed from coastlines (Belicka et al., 2002; Stein and Macdonald, 2004b; Yamamoto et al., 2008). Sedimentation rates for both shallow and deep regions of the Arctic remain difficult to constrain, and future efforts should focus on this issue.

Chapter 5: Microbial Degradation of Marine versus Terrestrial Organic Matter in Polar and Sub-Polar Waters: Experimental Investigations and Kinetics

5.1. Abstract

The microbial degradation of marine and terrestrial organic matter substrates in polar and sub-polar waters was investigated through shipboard degradation experiments with the intention of determining the timescales of the turnover of organic carbon and the effect of temperature on remineralization kinetics. Overall, marine organic matter was recycled very quickly, at rates comparable to, and in some cases greater than, those found for temperate environments. Experiments suggest that removal rates of marine organic matter are sufficiently high enough to completely remove organic carbon from algal inputs on seasonal timescales. In contrast, the timescales for turnover of terrestrial organic matter are substantially longer than those measured for labile marine organic matter. While total POC was not removed over the timescales of the experiments, several classes of lipids were found to decay, albeit at rates 1.5-6.6 times slower than for identical compounds from marine organic substrates. This argues for a physical or biological protection mechanism within the terrestrial organic matter that enhances preservation. The effect of temperature on degradation rates was inconsistent—further investigations should focus on the fate and changing inputs of marine and terrestrial organic carbon in a warmer future polar environment.

5.2. Introduction

Accumulating evidence demonstrates that large portions of terrestrial carbon are preserved in the modern Arctic Ocean despite the dominance of marine carbon inputs (Belicka et al., 2004; Goñi et al., 2000; Stein and Macdonald, 2004a; Yunker et al., 2005; Yunker et al., 1995). These observations, along with the evidence for changing particulate organic matter composition with increasing depth in the water column (Chapter 3), imply that marine carbon is rapidly remineralized in the Arctic water column, with the more recalcitrant terrestrial organic matter preserved in sediments. Changing climate conditions, however, have the potential to substantially alter the inputs and balance of these two sources of organic carbon in the Arctic Ocean. Permafrost deposits in many regions of the Arctic and sub-Arctic over the past few decades have experienced changes including greater variability in thicknesses of the active layers, increasing surface and deep permafrost temperatures, and downward thawing in some regions of 0.1 m yr^{-1} (Osterkamp and Romanovsky, 1999). This implies that increasing amounts of relict terrestrial carbon are now being mobilized and are available for transport to the Arctic Ocean (Davidson et al., 2000; Freeman et al., 2001; Frey and Smith, 2005). The remarkably low summer sea-ice cover observed, in particular, during 2005, 2007, and 2008 (NSIDC, 2008) reflects a changing physical regime with the possibility for a longer phytoplankton growing season and increasing net marine primary productivity (Macdonald et al., 2004b). The implications of these changes for the Arctic microbial community and higher trophic levels as well as potential changes to carbon storage reservoirs in the global carbon cycle remain unclear.

Multiple studies on the fate of organic matter in the marine environment have addressed the recycling of plant-derived material under both oxic and anoxic conditions (Arnarson and Keil, 2005; Harvey and Johnston, 1995; Harvey and Macko, 1997; Harvey et al., 1995; Kristensen and Holmer, 2001; Lee, 1992; Lehmann et al., 2002; Sun et al., 1993). The effect of climate warming on microbial recycling in terrestrial ecosystems has also recently been investigated (Biasi et al., 2005), suggesting a temperature-dependent shift to more recalcitrant carbon substrates. Yet the potential for recycling of increased terrestrial organic matter inputs has not been addressed.

The overarching theme of this chapter relies on the suggestion that inputs of recalcitrant, possibly ancient terrestrial organic matter to the Arctic Ocean will increase with continued climate warming. The impact of this material on the organic carbon cycle is unknown. Here, we investigate the character and reactivity of this recently remobilized organic carbon reservoir through incubation experiments designed to quantify microbial degradation rates and compare these rates with recycling rates of labile marine organic substrates in Arctic and sub-Arctic waters. Because of their frequent use as organic matter source indicators in geochemical studies, we focus largely on the lipid pool; however, amino acid and carbohydrate lability in terrestrial organic matter substrates are similarly investigated.

5.3. Materials and Methods

5.3.1. Experimental Design

Experimental shipboard incubation experiments were conducted in multiple years aboard scheduled expeditions and cruises of opportunity in the Arctic Ocean and Bering

Seas. The experimental design evolved over time in response to the benefits and drawbacks of completed trials, yet each trial shared the same basic set-up (Fig. 5.1). In general, near-surface waters (typical from 8 m depth) were filtered to 0.7-1.0 μm in order to remove phytoplankton and larger grazers, but retain the natural microbial consortia. Filtered water was placed in 10 – 20 L carboys depending on the experiment and specific substrates (marine, terrestrial, mix) were added and dispersed via shaking. The natural microbial consortia were allowed to degrade the material over timescales of 1-2 months under oxic conditions in the absence of light. Particulate organic matter in the microcosm was removed at designated sampling times to evaluate degradation of both total organic carbon and specific lipid markers present in the organic matter. In one incubation (Ikpikpuk River peat, 2004), analysis was expanded to include measures of the amino acid and carbohydrate fractions. Specific experimental trials are outlined in Table 5.1 below.

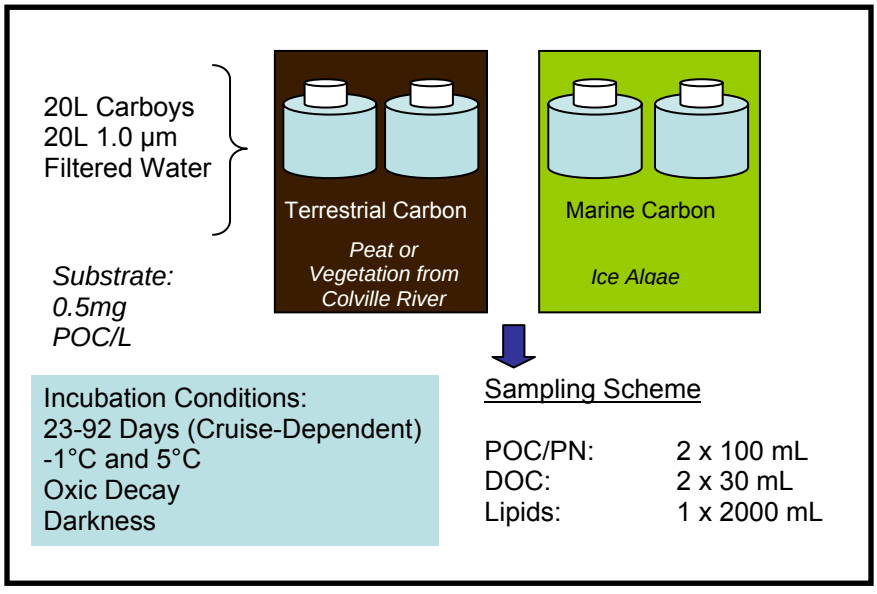

Figure 5.1. Schematic of organic matter degradation basic experimental set-up.

Table 5.1. Summary of substrate addition, approximate initial carbon load following substrate addition, incubation temperature(s), and length of incubation for multiple sets of shipboard incubations in the Arctic Ocean and Bering Seas.

Year	Location	Substrate	Initial OC (mg/L)	Temperature(s) (°C)	Length (days)
2002	Arctic Ocean	Sea-ice Algae	20	-1	92
2004	Arctic Ocean	Ikpikpuk River Peat	27	-1	82
		Ikpikpuk River Dirty Snow	0.450	-1	69
2007	Bering Sea	*Melosira arctica* (ice algae)	0.5 to 1	-1 5	25
		Ikpikpuk River Peat	10	-1 5	25
		1:10 Mix (*M. arctica* : Ikpikpuk Peat)	20	-1 5	25
2008	Bering Sea	Colville River Peat	4	1.7 5	23

Summary of Experimental Trials

I. Ice Algae Degradation 2002

The microbial decomposition of sea-ice algae was investigated during the spring and summer of 2002 on two research cruises for the Shelf Basin Interactions (SBI) Program aboard the USCGC *Healy* (HLY-02-01: 5 May – 15 June 2002 and HLY-02-03: 16 July – 26 August 2002). An assemblage of sea-ice algae was collected near station HLY-02-01-007 (WHS-3) on 18 May 2002 at an approximate position of 73° 2.19N, 160° 23.03W and total water depth of 150 m. A floe of visibly colonized sea-ice was overturned and the sea-ice algal assemblage was scraped off of the underside of the floe. This sea-ice assemblage served as the organic carbon substrate for the degradation experiment. Water for the incubation experiment was collected from the shipboard uncontaminated science sea-water system from a depth of 8 m. Low surface water chlorophyll allowed the avoidance of filtration and algal additions were placed in 20 L of the whole seawater. The microcosm was wrapped in black plastic to simulate dark

conditions and incubated at -1 °C for the experimental duration. The carboy was shaken and aerated frequently to avoid oxygen depletion. After 13 days, the sample was split in half. One half was returned to the incubation temperature. The remaining half was frozen to cause cell rupture, then returned to the incubator and treated in the exact manner of the remaining half. Because results were similar for both the original and frozen/thawed fraction, only the original results are presented here. Samples were taken on days 5, 13, 20, 25, 63, and 92 via either water collection with subsequent centrifugation or via vacuum filtration onto pre-combusted glass fiber filters (GF/F) and analyzed for POC, PN, and lipid biomarker composition.

II. Terrestrial Organic Matter Degradation 2004

During the spring and summer 2004 process cruises for the SBI Program (HLY-04-02: 15 May – 23 June 2004; HLY-04-03: 16 July – 26 August 2004), two experimental incubations were investigated. The first experiment was conducted in conjunction with incubations investigating the phylogenetic and lipid synthesis responses of Arctic bacterioplankton communities to organic matter additions (see Dyda (2005) for full description). While experiments were conducted using multiple substrates, only the peat substrate experiment was examined and will be presented here. Briefly, Arctic waters (8 m sampling depth) were collected near station HV-2 (70° 41.908N, 167° 12.096W, 56 m total water depth) on 20 May 2004. Water was filtered to 0.2 μm to remove all microbial and planktonic particulate matter, and 18 L of this filtered water was added to a 20 L carboy. To re-introduce natural microbial assemblages, 2 L of 1.0 μm filtered water were added for a total volume of 20 L. The terrestrial organic matter

substrate used for this incubation was collected from the banks of the Ikpikpuk River on the North Slope of the Alaskan mainland on 4 June 2002, and was characterized as small woody debris with interspersed peat material. Prior to addition, the peat was dried at 50 °C and screened to remove particles <10 μm to ensure easy separation of the peat substrate. Approximately 3 g of dried peat was added to each carboy, for an approximate initial carbon load of 27 mg POC L^{-1}. The carboy was covered in black plastic and incubated at a temperature of -1 °C. The carboy was agitated and aerated daily. Because the primary purpose of this incubation was the phylogenetic and lipid synthesis response of Arctic bacterioplankton during growth, total particulate organic matter samples were not taken over time. Instead, only samples of the initial (T=0 days) and final (T=82 days) peat substrate were taken for characterization of organic carbon, total nitrogen, $\delta^{13}C$, $\Delta^{14}C$, lipid biomarker distributions, amino acid composition, and total carbohydrate content.

A second experimental incubation was initiated following the collection of snow with visible particulate inclusions (hereto referred to as "dirty snow") from the banks of the Ikpikpuk River on 8 June 2004. The dirty snow was melted at 5 °C, and a volume of 2 L of the snowmelt was preserved by re-freezing. On 13 June 2004, Arctic waters were collected via the science sea-water system in the Barrow Canyon region of the western Arctic Ocean (BC-5: 72° 06.23N, 154° 27.64W; 1536 m total water depth) and filtered to 1.0 μm so that only the microbial consortia remained. A volume of 18 L was added to a carboy, and the 2 L of reserved dirty snowmelt was added as the terrestrial organic matter substrate. The carboy was incubated at -1 °C in total darkness. Particulate matter was

sampled by vacuum filtration on days 0, 37, 60, and 69 and was analyzed for POC, PN, and lipid biomarker composition.

Unfortunately, during the gap between the spring and summer cruises (representing days 33-56 of the peat incubation and days 10-33 of the "dirty snow" incubation), the environmental chamber housing both the peat and dirty snow carboy experiments shipboard experienced a broken thermostat and the chamber warmed considerably. Because we were required to disembark between the two expeditions, the difficulty with the thermostat was not noticed for several days. The incubation chamber likely warmed to 20 °C for 3-7 days based on reports from shipboard personnel. The carboys were also not shaken or aerated during this time period. However, none of the experimental containers exhibited signs of anoxia upon return to the ship and were agitated and aerated regularly throughout the remaining incubation period.

III. Marine and Terrestrial Organic Matter Degradation 2007

An additional set of degradation experiments were carried out on a cruise for SLIPP (St. Lawrence Island Polynya Program; HLY-07-02) in the summer of 2007 in the Bering Sea. This set of degradation experiments was the most comprehensive, investigating both the effect of organic substrate and also temperature. At each temperature (-1 °C and 5 °C), a total of six carboys were incubated: (1 and 2) Ice Algae additions in duplicate; (3 and 4) Ikpikpuk River peat additions in duplicate; and (5 and 6) Mixture of ice algae and peat additions in duplicate (Table 5.1). The experiment was initiated on 17 May 2007. Water for the incubation was taken from the uncontaminated science seawater system (8 m depth) from a position of 58° 02.918N, 169° 24.045W in a

total water depth of 121 m. Incubation water was filtered to 1.0 μm, and 20 L each was placed into 14 carboys. Substrates were added as described above and carboys were agitated to promote mixing. Carboys were wrapped in black plastic and incubated at their appropriate temperature (-1 °C and 5 °C). Sampling by vacuum filtration occurred on days 0, 5, 10, and 25 and POC, DOC, and lipid composition were analyzed.

IV. Terrestrial Organic Matter Degradation 2008

A final experimental degradation was performed during the summer of 2008 on cruise HLY-08-03 as part of the Bering Sea Ecosystem Study (BEST) Program. Water was collected using Niskin bottles from 20.8 m (below chlorophyll *a* maximum) at station HLY-08-03-004 (UP-3) at 54° 25.858N, 165° 09.358W and filtered through GF/F filters (0.7 μm) to remove phytoplankton and grazers. Approximately 17 L of the 0.7 μm-filtered water was added to four carboys and a volume of 1 L of unfiltered water was included to enhance the microbial consortia. A terrestrial substrate consisting of peat was used which had been collected from the Colville River on 29 July 2004, sieved to <600 μm and homogenized by grinding. This addition was made to the four carboys for an approximate initial carbon load of 4 mg/L. Two carboys were incubated at 1.7 °C and two carboys were incubated at 5 °C to determine the effect of temperature on the microbial degradation of terrestrial organic carbon. Particulate organic matter samples were taken by vacuum filtration onto GF/F filters on days 0, 7, 14, and 23 and analyzed for POC, PN, and lipid composition. On day 13 of the incubation, the environmental chamber in which the 1.7 °C microcosm was stored failed, and the temperature of the chamber warmed to 20 °C. Upon discovery of the anomaly, the microcosm was moved

to the 5 °C chamber until repair. The microcosm experienced higher temperatures for a period less than 24 hours.

5.3.2. Chemical Analyses

Sedimentary Carbon, Nitrogen, and Lipid Analysis

Samples were either dried in an oven at 40 °C or lyophilized to constant weight. CHN analysis was performed with an Exeter Analytical Elemental Analyzer. Individual lipid biomarker analysis followed the standard methods presented elsewhere in this dissertation (Chapter 3, modification of Bligh and Dyer (1959)). Briefly, lipids were extracted from POM on GF/F filters using organic solvents with sonication. Following an alkaline hydrolysis, fatty acids were derivatized to methyl esters and sterols were converted to trimethylsilyl ethers for quantification with capillary gas chromatography (GC) and structural identification with GC-mass spectrometry.

Amino Acid Analysis

To account for a larger fraction of the total organic material, amino acids analysis was also conducted. Approximately 30 mg of dried peat substrate was hydrolyzed in glass vials at 110 °C with 6 N HCl, using a modified liquid phase method of Grutters et al. (2000). A solid-phase extraction purification and derivatization followed, utilizing the EZ:Faast method developed by the Phenomenex Corporation (Torrance, California), which employs gas chromatography-mass spectrometry for both quantification and identification of individual structures. Concurrent analysis of pure bovine serum albumin

(BSA) and the addition of methyl-leucine as an internal standard allowed for quantification and detector-response correction for individual amino acids.

Carbohydrate Analysis

Particulate carbohydrates were quantified using the MBTH (3-methyl-2-benzothiazolinone hydrazone hydrochloride) method (Johnson and Sieburth, 1977; Pakulski and Benner, 1992). Glucose standards (in H_2SO_4; concentration range of 0-8 mg) were created and treated identically as samples for quantification. Samples and standards were placed in serum vials and pretreated with 1 mL 12M H_2SO_4, swirled, sealed, and stored at room temperature for two hours, then diluted 10-fold and hydrolyzed for 3 hours at 100 °C. Following a cooling period, 250 μL aliquots of each sample were removed and placed in 5 test tubes each, resulting in triplicate analysis plus duplicate sample blanks per sample/standard. Solutions were further diluted with water and neutralized with NaOH. Carbohydrates were then reduced to alditols with the addition of KBH_4, and tubes were incubated in the dark at room temperature for four hours. The reduction reaction was terminated by the addition of HCl with agitation, and all samples and standards were frozen overnight. The following day, samples were thawed and 1 mL aliquots were transferred to new vials. The triplicate analyses for both samples and standards were oxidized by the addition of periodic acid for ten minutes, followed by addition of $NaAsO_2$ to terminate oxidation. Duplicate sample/standard blanks received a 1:1 periodic acid:$NaAsO_2$ solution. All solutions were subsequently acidified and 200 μL MBTH was added with heating at 100 °C for 3 minutes. Following addition of $FeCl_3$ and acetone, samples were quantified by spectrophotometric

measurement of absorption at 635 nm (Johnson and Sieburth, 1977; Pakulski and Benner, 1992).

5.4. Results

5.4.1. Marine organic matter degradation: Sea-Ice Algae Experiments

During oxic decay of a sea-ice algal assemblage in 2002, total particulate organic carbon (POC) and nitrogen (PN) showed an initial decline over the first five days, then an increase, followed by a rapid decrease between days 20-92 (Fig. 5.2). Organic carbon was lost at a greater rate than total nitrogen, resulting in a decrease in the atomic C:N ratio from approximately 8 to 6 (Fig. 5.2). Similarly, during the 2007 degradation of the sea-ice diatom *Melosira arctica* at both -1 °C and 5 °C, a loss of POC was observed in the first five days of degradation, followed by an increase back to the initial concentration by day ten (Fig. 5.3). Because the microcosm replicates, designated as A and B for each temperature, received slightly different initial organic matter loadings, they will be presented as separate results throughout this chapter instead average concentrations between the two separate microcosms. Concentrations of DOC throughout the 2007 incubation are shown in Table A5.1. Over the next fifteen days, POC concentrations dropped slightly, yet the exponential decrease observed in the longer 2002 incubation was not apparent, possibly due to the shorter incubation time (Fig. 5.3). PN in the *M. arctica* degradation responded differently in each microcosm, yet a net loss over the full 25 day experiment was observed for all treatments (Fig. 5.3).

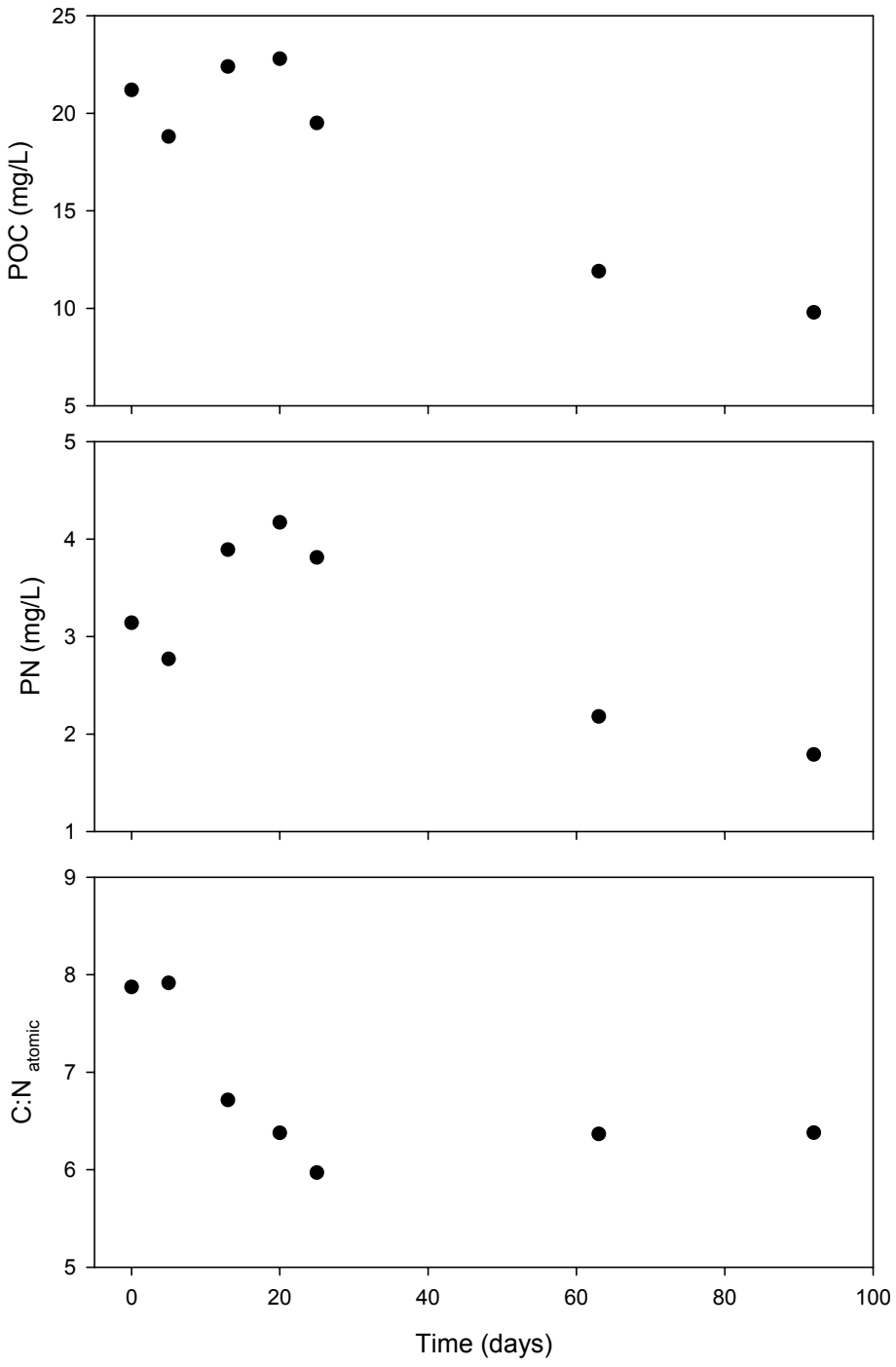

Figure 5.2. Particulate organic carbon (POC) and particulate nitrogen (PN) in mg/L and atomic C:N ratio during the 2002 92-day oxic decay of a sea-ice algal assemblage.

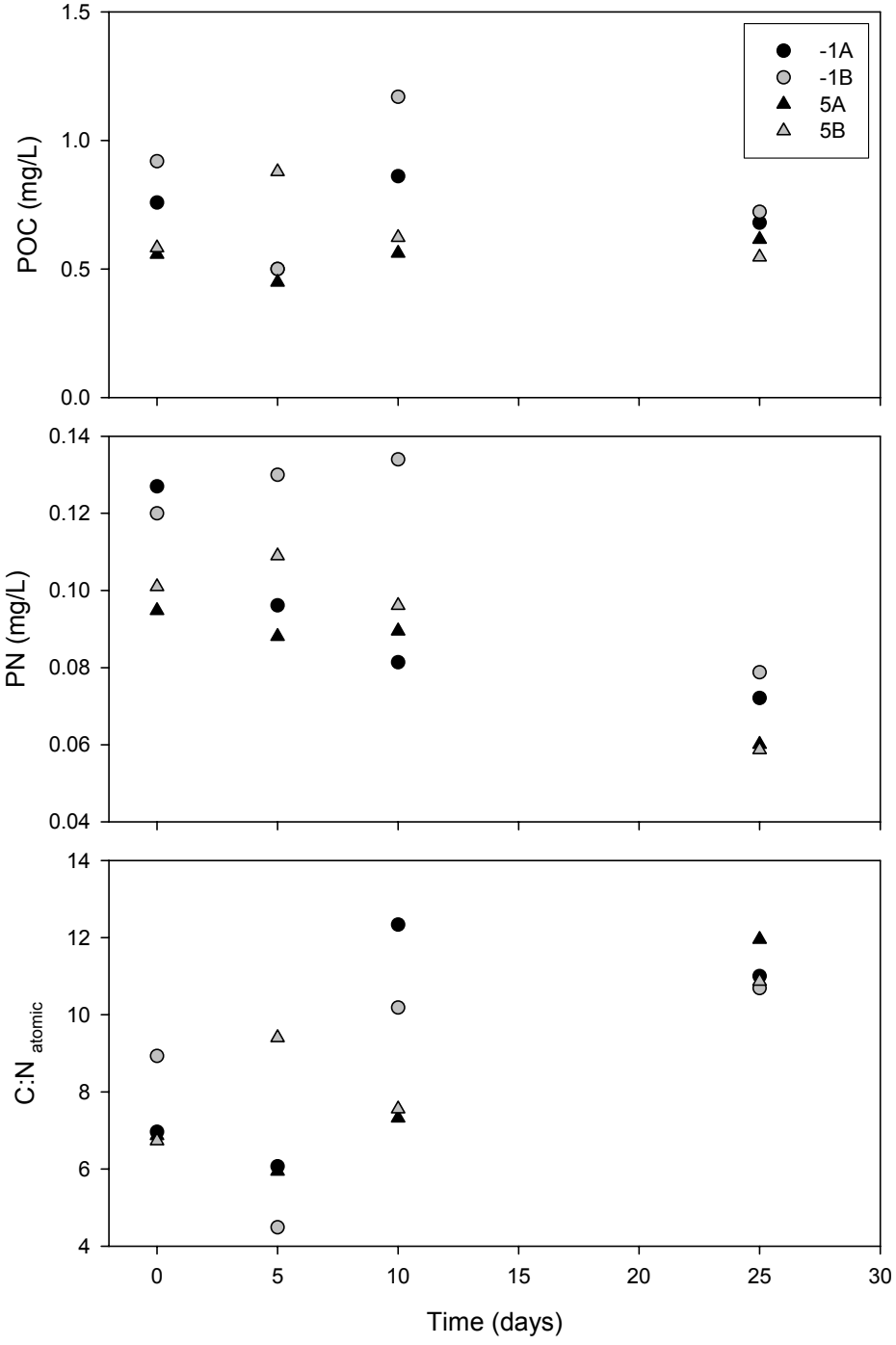

Figure 5.3. Total particulate organic carbon (POC) and particulate nitrogen (PN) in mg/L and atomic C:N ratio throughout the 2007 25-day *M. arctica* degradation experiments at temperatures of -1° C (circles) and 5° C (triangles).

Unlike the 2002 experiment, however, the atomic C:N ratio increased throughout the experiment, indicating a greater loss of nitrogen-rich components. Lipids decreased rapidly during both the 2002 and 2007 incubations of marine algal carbon (Figs. 5.4 and 5.5, respectively). In the 2002 degradation, total fatty acid loss began immediately and continued throughout the first two months of the incubation, leveling off after the day 63 sampling time point (Fig. 5.4). Saturated (C_{14}-C_{22}) and monounsaturated fatty acids (MUFA) were present in similar concentrations in the 2002 sea-ice algae assemblage, and loss rates were similar over the first 13 days. Polyunsaturated fatty acid (PUFA) concentrations also decreased rapidly to near zero by day twenty of the incubation experiment. In addition to decreasing concentrations of all lipid groups, the distribution of lipids shifted throughout the incubation. Initially, PUFAs comprised 12% of the total fatty acids. By day 92, PUFAs only accounted for 6% of total fatty acids. Saturated fatty acids also decreased from 41 to 32% of the total acids during the incubation period.

Neutral lipids, including phytol and sterols, occured in lower concentrations than fatty acids in the algal assemblage, but showed similar decreases during degradation. Phytol concentrations decreased initially, but stabilized between the days 5 and 13 and days 20 and 25 sampling time points (Fig. 5.4). In the 2002 ice algal assemblage, the overwhelmingly dominant sterol (~79 % of total sterols) was 24-methylcholesta-5,24(28)-dien-3β-ol ($C_{28}\Delta^{5,24(28)}$), which decreased overall, but remained at detectable concentrations throughout the entire experimental period.. This sterol represented 76% of the total sterol concentration at the end of the degradation experiment.

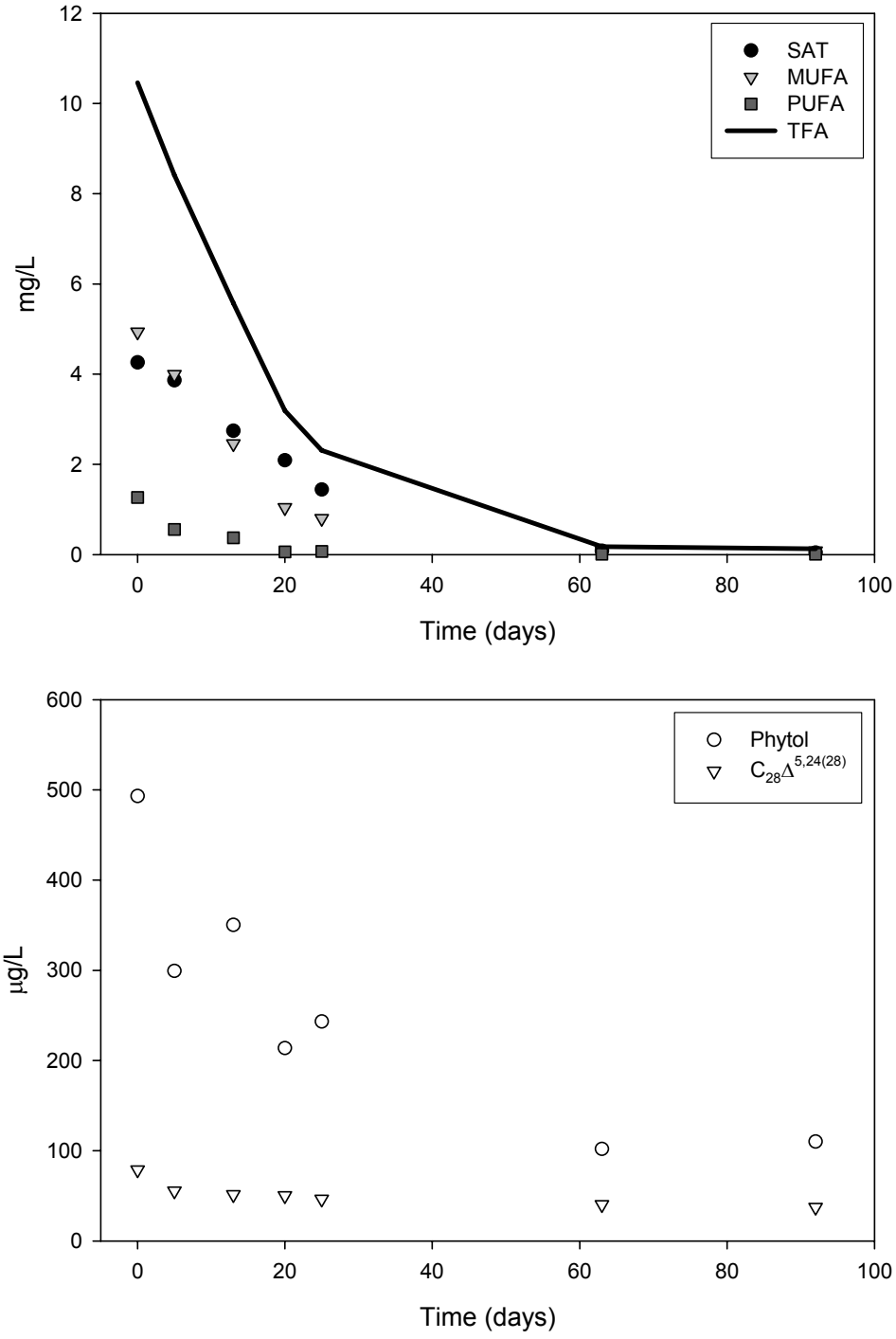

Figure 5.4. A) Concentrations of saturated (SAT), monounsaturated (MUFA), polyunsaturated (PUFA), and total (TFA) fatty acids (in mg/L) and B) concentrations of phytol and 24-methylcholesta-5,24(28)-dien-3β-ol ($C_{28}\Delta^{5,24(28)}$) (in µg/L) throughout the 2002 92-day ice-algae degradation experiment.

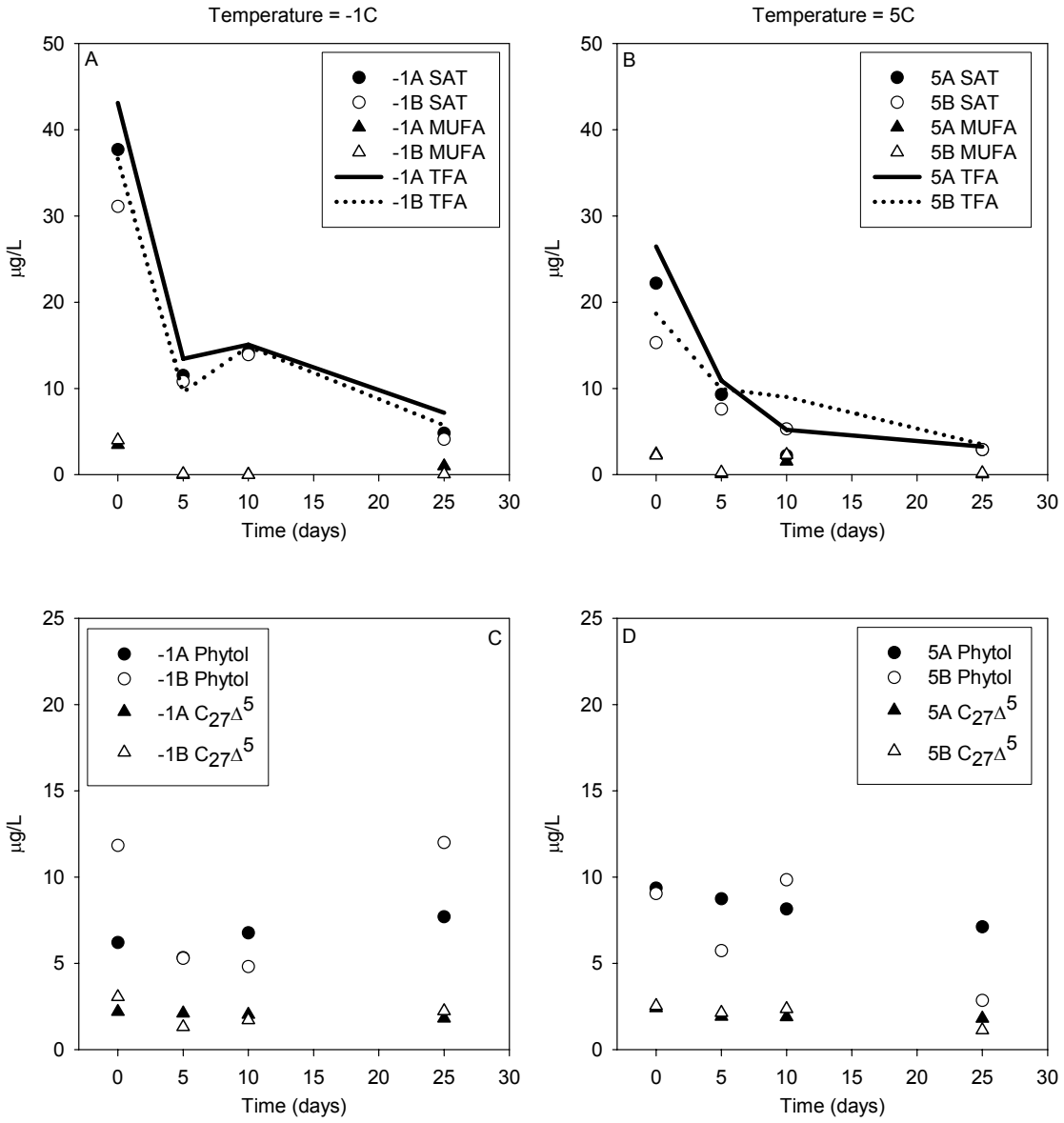

Figure 5.5. Concentrations (µg/L) of saturated (SAT), monounsaturated (MUFA), and total (TFA) fatty acids in replicate -1°C (A) and 5°C (B) and concentrations of phytol and cholest-5-en-3b-ol ($C_{27}\Delta^5$) in replicate -1°C (C) and 5°C (D) 25-day ice-algae degradation experiments.

In both the -1°C and 5°C *M. arctica* incubations of 2007, total fatty acids decreased over the shorter 25-day time span (Fig. 5.5). Saturated fatty acid losses mirrored total fatty acid losses for replicates (denoted as A and B) at both temperatures. In contrast to the algae utilized in 2002, the *M. arctica* used as the marine organic carbon substrate was characterized by largely saturated fatty acids, with low concentrations of MUFAs and PUFAs seen principally as the C16:1ω9, C16:1ω7 and C20:5ω3. Concentrations of C_{16} MUFAs decreased rapidly in the -1 °C incubation, with largely undetectable levels after day 5. In the 5 °C incubation, however, MUFA concentrations decreased initially for the first 5 days, but increased at day 10. Detection of the C20:5ω3 PUFA occurred sporadically resulting from very low concentrations in all 2007 incubations.

Phytol concentrations varied considerably between microcosms (Fig. 5.5). In carboy -1A, phytol increased over the 25 day incubation. In the -1B carboy, contrastingly, phytol concentrations decreased for the first ten days, followed by a sharp increase at day 25. Carboy 5A was the only microcosm in which phytol concentrations continually decreased over time. In carboy 5B, an initial decrease from day 0 to 5 was followed by an increase to initial concentrations by day 10, with a subsequent sharp decline to the end of the incubation. Cholesterol ($C_{27}\Delta^5$) was the dominant (83% of total sterol concentration) sterol in the *M. arctica* substrate, similar to that previously reported (Belicka, 2002); however, all sterols were low in concentration throughout the experiment (Fig. 5.5).

The kinetics of the loss of particulate organic carbon, total fatty acids, and grouped and individual lipids (in mg or μg per L) were investigated by using least squares regression techniques to determine rate constants. A first-order equation where

the concentration of each parameter (summed or individual lipids) at a given time is equal to the product of its original concentration (C_o) and the first-order decay constant (k) (equation 1).

$$y = C_o e^{-kx} \qquad (1)$$

In general, exponential decay curves fit the data observations quite well (Table 5.2), as noted by the high r^2 values, especially for total and grouped fatty acid components. For both the 2002 and 2007 incubations at -1°C, unsaturated fatty acids degraded faster than their saturated counterparts. This trend was not seen in the 5°C incubation, however, as the increase in MUFAs at day 10 resulted in a poor fit for the exponential decay (r^2 of 0.48 and 0.52 for treatments A and B, respectively) and a lower calculated rate constant (Table 5.2). Rates for lipid degradation were markedly higher during the 2007 incubations than the previous trial in 2002. C_{12}-C_{22} saturated fatty acids in the 2002 incubation displayed turnover times ($\tau = 1/k$) on the order of 24 days; however the same compounds had an average turnover time of only 7.8 days in the 2007 incubation.

The effect of temperature on degradation rate constants was found to be inconsistent. Although the two microcosms incubated at -1 °C resulted in similar rate constants for grouped and individual lipids, rates for the 5B microcosm lagged considerably behind those found for the 5A microcosm. Degradation rates in 5A for total and saturated fatty acids were notably higher than those in the -1 °C treatment; conversely, rates in 5B were slower than those in the -1 °C treatment.

Table 5.2. Experimentally determined first-order rate constants (k, yr^{-1}), regression coefficients (r^2), and turnover times (τ, days) for particulate organic carbon (POC), total fatty acids (TFA) and major grouped and individual lipids during oxic decay of marine organic matter substrates.

	2002			2007											
	Algae -1°C			Algae A -1°C			Algae B -1°C			Algae A 5°C			Algae B 5°C		
	k (yr^{-1})	r^2	τ (days)	k (yr^{-1})	r^2	τ (days)	k (yr^{-1})	r^2	τ (days)	k (yr^{-1})	r^2	τ (days)	k (yr^{-1})	r^2	τ (days)
POC	3	0.80	120	-	-	-	-	-	-	-	-	-	-	-	-
TFA	21	0.99	17.7	52	0.85	7.1	50	0.78	7.3	60	0.97	6.1	28	0.94	12.9
SAT	15	0.99	24.4	51	0.86	7.2	40	0.84	9.1	69	0.96	5.3	38	0.94	9.7
MUFA	24	0.98	15.1	193	0.84	1.9	282	0.99	1.3	50	0.48	7.3	19	0.52	19.4
PUFA	46	0.98	8.0	-	-	-	-	-	-	-	-	-	-	-	-
Phytol	8	0.84	44.2	-	-	-	41	0.91	8.9	4	0.99	90.9	-	-	-
Sterol[a]	3	0.65	134	3	0.89	130	-	-	-	4	0.59	95.2	10	0.83	36.2

[a]Represents rate calculated for dominant sterol in substrate algal assemblage: 24-methylcholesta-5,24(28)-dien-3β-ol for 2002 experiment, cholest-5-en-3β-ol for 2007 experiment.

Notably, rate constants for all marine organic matter incubations either paralleled or exceeded those found for similar oxic degradation of labile marine organic matter at higher temperatures (Harvey and Macko, 1997; Harvey et al., 1995).

5.4.2. Terrestrial organic matter degradation

Particulate organic carbon and particulate nitrogen increased over the 69 day time span of the snow-debris incubation (Fig. 5.6). Correspondingly, the atomic C:N ratio also increased, from 10.98 to 14.9. Due to this increase in POC over the time course of the experiment, lipid concentrations were normalized to total organic carbon content. Total fatty acids initially decreased over the first 37 days, but increased substantially by day 63, indicating growth of organisms in the microcosm despite the dark conditions (Fig. 5.7). This increase in fatty acids was largely due to increasing concentrations of short-chain saturates (SCFA) and monounsaturated fatty acids (MUFA). Long-chain saturated fatty acids (LCFA) were the only group of fatty acids to decrease throughout the entire degradation time span (Fig. 5.7).

In combination with incubation experiments carried out in 2004 to investigate the response of bacterial lipid synthesis and bacterial community structure to the availability of organic matter substrates (Dyda, 2005), a recalcitrant terrestrial organic matter substrate (peat/woody debris collected from the banks of the Ikpikpuk River) was investigated both initially and after an 82-day degradation experiment in the presence of natural Arctic microbial assemblages. Over the span of the incubation, the peat substrate was observed to increase in carbon content, with a corresponding small enrichment in $\delta^{13}C$ composition.

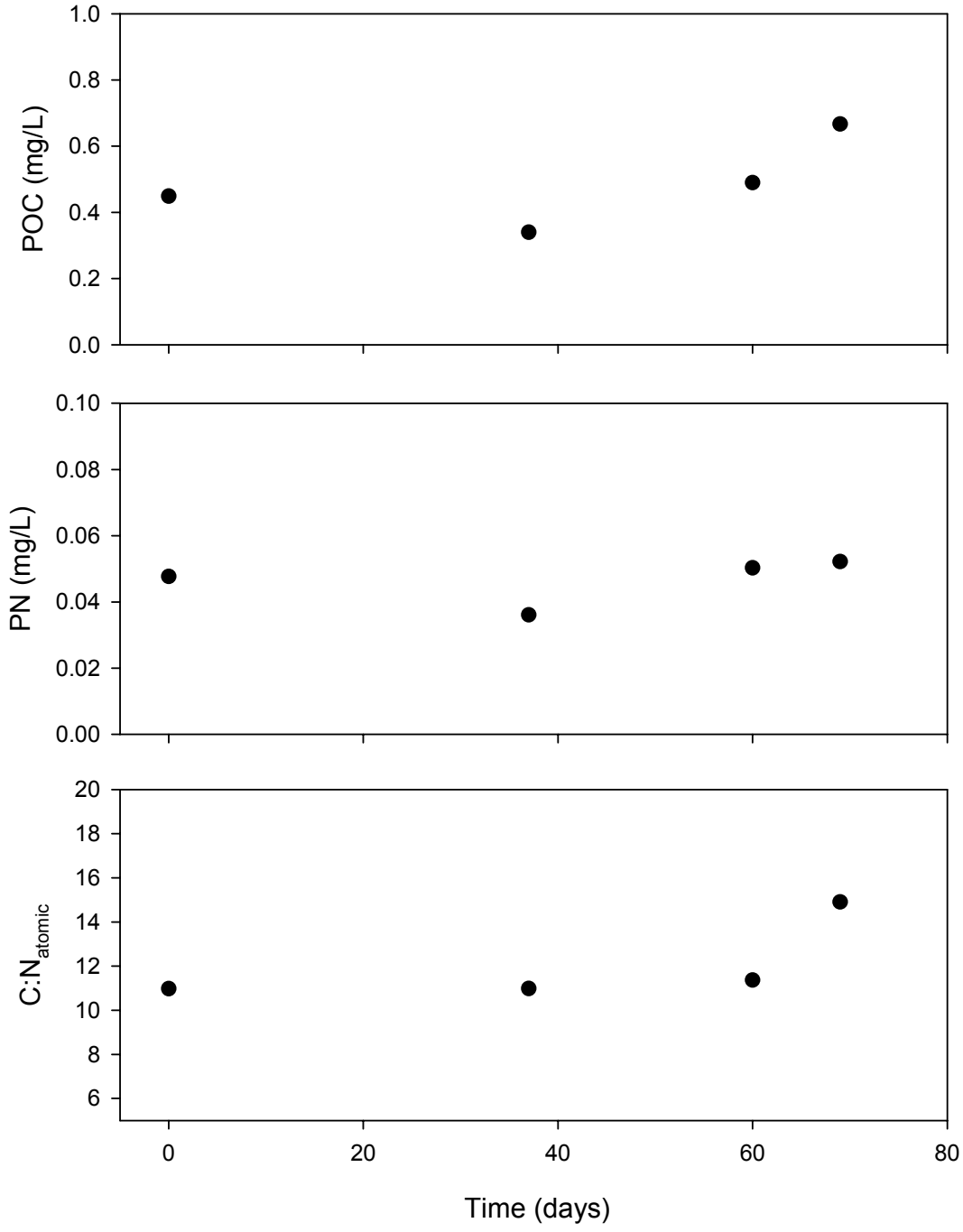

Figure 5.6. Particulate organic carbon (POC) and particulate nitrogen (PN) in mg/L and atomic C:N ratio throughout the 69-day snow debris incubation experiment.

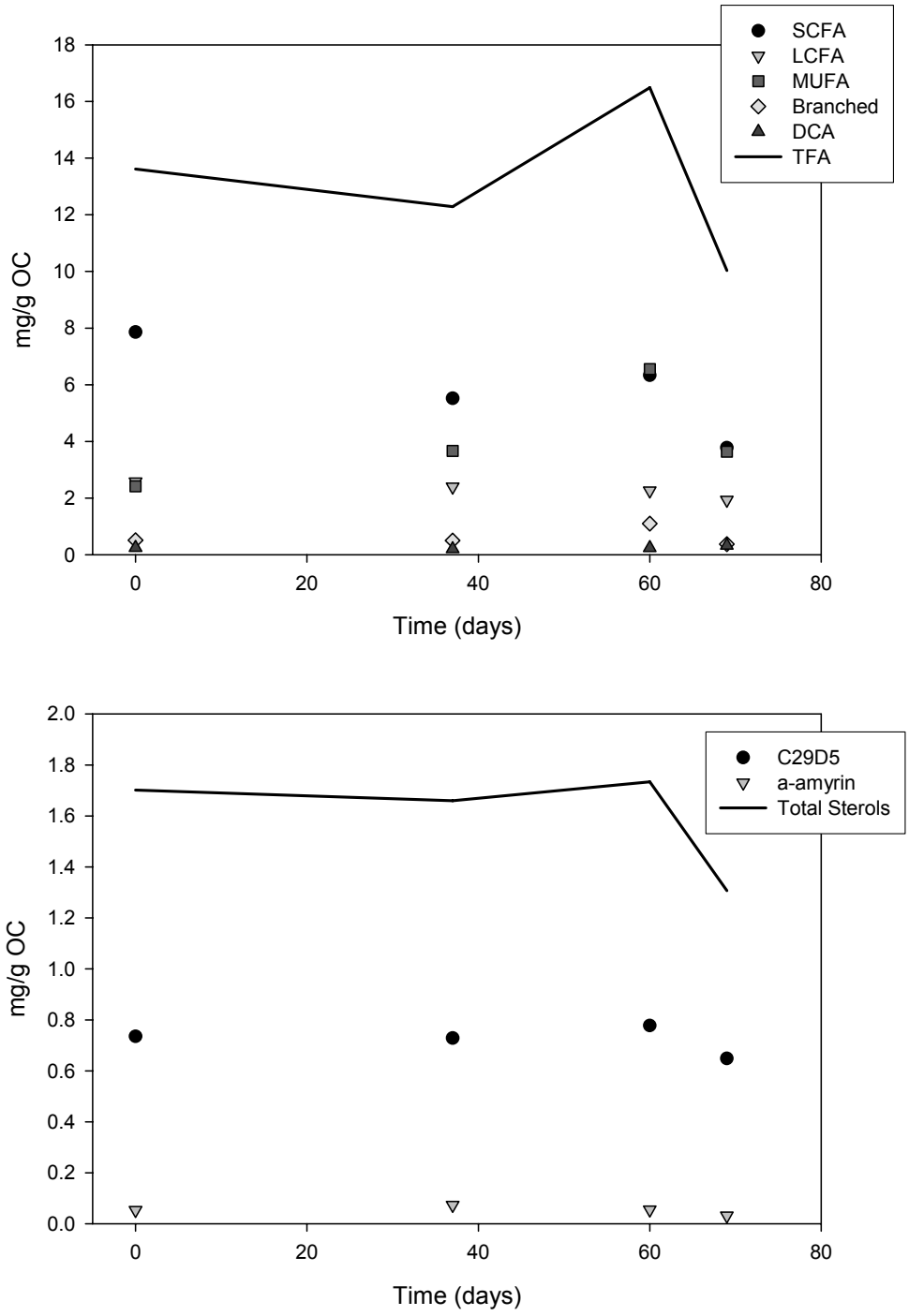

Figure 5.7. The concentrations (mg/g OC) of short chain (C_{14}-C_{22}) saturated (SAT), monounsaturated (MUFA), branched, mid- to long-chain (C_{18}-C_{26}) dicarboxylic, and total (TFA) fatty acids and concentrations of 24-ethylcholest-5-en-3b-ol ($C_{29}\Delta^5$), total sterols, and the triterpenoid α-amyrin in the -1°C 69-day snow debris degradation experiment.

Interestingly, the average radiocarbon age ($\Delta^{14}C$) of the substrate material nearly doubled over the 82-day experiment (Table 5.3). In addition to these bulk alterations, compositional changes in the organic matter (i.e., lipids, amino acids, and carbohydrates) were also investigated. Total carbohydrates and total hydrolysable amino acids (THAA) per dry weight of substrate decreased over the time span of the incubation while total lipid content and distribution remained relatively unchanged. This resulted in a proportional decrease in the relative abundance of amino acids and carbohydrates in the final peat, and a subsequent slight increase in the relative abundance of the lipid pool (Fig. 5.8). In spite of the total decrease in amino acid concentrations, the distribution of amino acids did not substantially change—serine and glutamic acid decreased in relative abundance while threonine, methionine, and phenyl alanine increased slightly (Fig. 5.9).

Table 5.3. Bulk parameters of Ikpikpuk River peat substrate before and after the 82-day incubation in the presence of natural Arctic Ocean microbial assemblages.

	OC (%)	TN (%)	C:N	$\delta^{13}C$ (‰)	f_m	$\Delta^{14}C$ (‰)	Age (^{14}C Years)	NOSAMS Accession #
Initial	32.1	1.1	33.7	-28.23	0.6502	-353.9	3460± 25	OS-39574
Final	37.4	1.2	35.7	-27.95	0.3893	-613.3	7580± 40	OS-48405

In conjunction with the 2007 marine organic matter experiment presented above, Ikpikpuk River peat and a mixture of Ikpikpuk River Peat and *Melosira arctica* (sea-ice algae) were incubated at -1 °C and 5 °C in the presence of natural Bering Sea microbial fauna. In order to simulate the natural delivery of terrestrial organic matter to the marine environment through processes including coastal erosion or river flow, we did not homogenize or sort the peat substrate, but rather added it to the microcosms intact, as a mixture of small wood-like sticks in a finer-grained matrix of peat-mossy sediment.

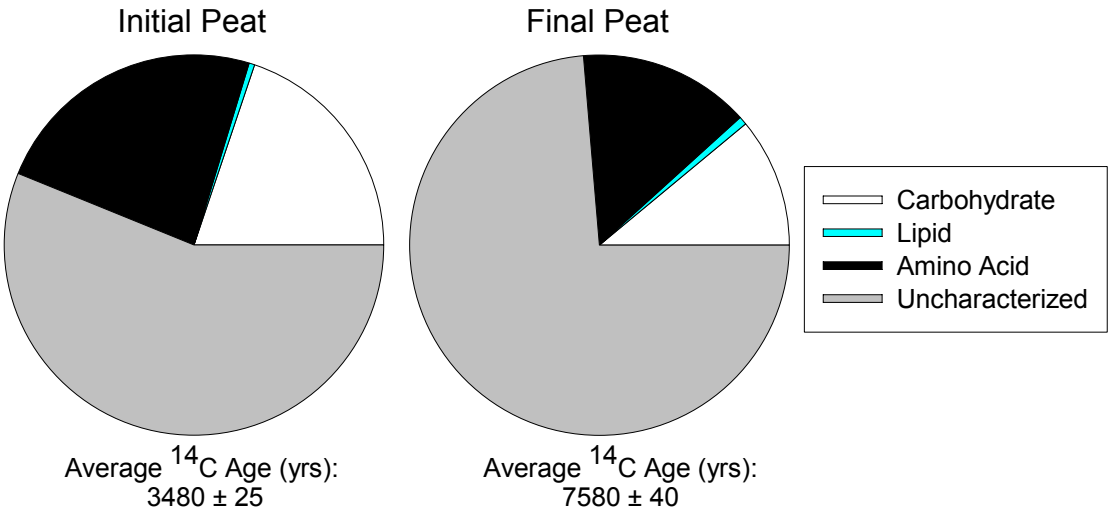

Figure 5.8. Relative distribution of major organic matter components before and after 82-day incubation of Ikpikpuk River Peat in the presence of natural Arctic microbial assemblages.

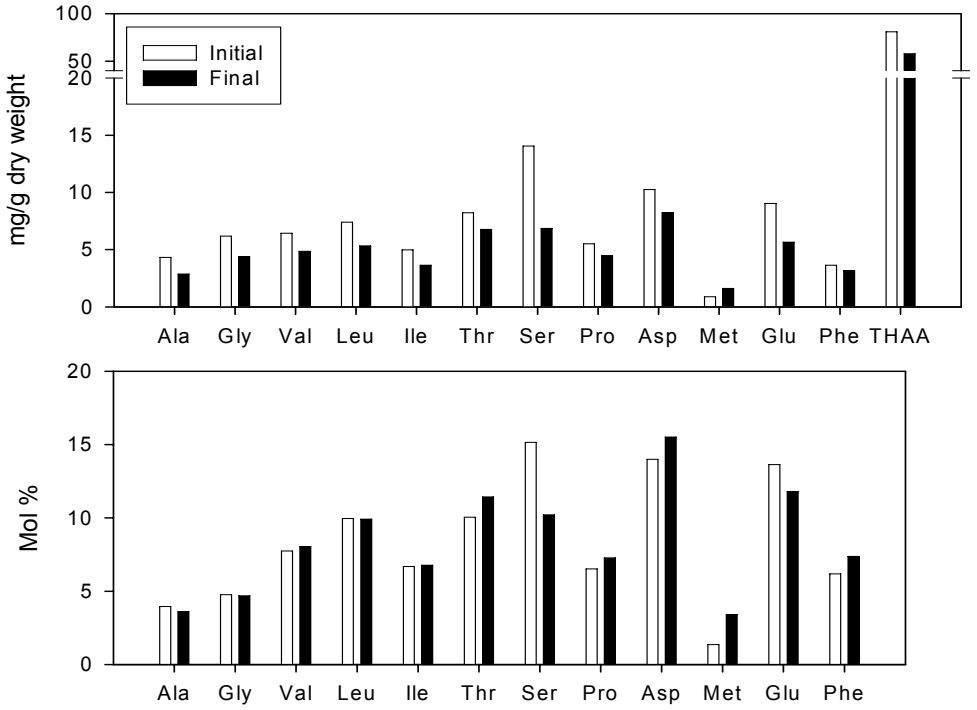

Figure 5.9. Amino acid concentrations (mg/g dry weight peat) and distribution (mol % of total amino acids) before and after the 82-day incubation of Ikpikpuk River peat in the presence of natural Arctic microbial assemblages.

Unfortunately, the heterogeneity of the substrate created irresolvable difficulties for quantification throughout the experiment. Obtaining an even distribution of substrate material for a given water volume filtered during the sampling time points was not achievable. An attempt at remedying this problem by normalizing all data to the mass of substrate on the filter also was not successful because the mass of substrate on the filter post-collection was smaller than the average difference in mass of blank filters. Because this problem was not anticipated, the blank filters were not pre-weighed, rendering mass normalization of the samples an ineffective solution. Finally, an attempt was made to normalize all data to the concentration of a highly recalcitrant marker. For this approach, several compounds known to be highly resistant to degradation (i.e., α-amyrin, long-chain saturated fatty acids) were assumed to remain at constant concentration throughout the degradation experiment. Because the initial loadings of these compounds were easily calculated (both the lipid distribution and the total mass of substrate added to the carboy were known), the concentrations of all other biomarkers present in the POM were scaled such that the concentration of the recalcitrant marker remained constant over time. However, due to the extreme heterogeneous nature of the substrate, this normalization process also failed. Thus, the results of the total POC and lipid distributions for the peat and mixed substrate additions for the 2007 experiment are not presented, although DOC concentrations, which were not affected by the substration quantification issue, are presented in Table A5.1. We repeated the incubation in 2008 with a homogenized and sieved (<600 μm) peat substrate from the Colville River.

Over a time-span of twenty-three days, total particulate organic carbon in the Colville River peat incubation microcosm oscillated around the initial loading of 4mg/L

(Fig. 5.10). Initially particulate organic matter increased, followed by a sharp decline between days 7 and 14. By day 23, total organic carbon increased back to initial concentrations (Fig. 5.10). Incubations at 1.7 °C followed similar trends as those conducted at 5 °C, with no obvious patterns or differences between the two. Particulate nitrogen followed a similar trend, oscillating between 0.2 and 0.3 mg/L. In spite of this oscillation, the atomic C:N ratio decreased slightly (Fig. 5.10).

Total fatty acids in the 1.7 °C microcosm were lowest at the day 14 time point, which, notably, closely corresponded to the day 13 temperature anomaly within the environmental chamber in which the incubation took place (Fig. 5.11). By day 23, concentrations of total fatty acids were back to initial levels. Several groups of fatty acids (short-chain saturated, long-chain saturated, and monounsaturated) also decreased in concentration over the first 14 days of the experiment (Fig. 5.11). In contrast, grouped and total fatty acids remained unchanged throughout the 23-day incubation at 5 °C. Concentrations of neutral lipids derived from terrestrial matter, including the $C_{29}\Delta^5$ sterol, α-amyrin, and friedelin decreased slightly over the first 14 days of the 1.7 °C incubation (Fig. 5.12). Similar to the fatty acid concentrations, a slight increase in concentration of all lipid compounds was noticed at the final sampling point (day 23) in the 1.7 °C microcosm. In the 5 °C incubation, no net loss of terrestrial organic biomarkers was evident over the 23-day time-span. First-order rate constants were determined, as described above, for individual or grouped lipids that decreased over the time-span of the various terrestrial organic matter incubation experiments (Table 5.4).

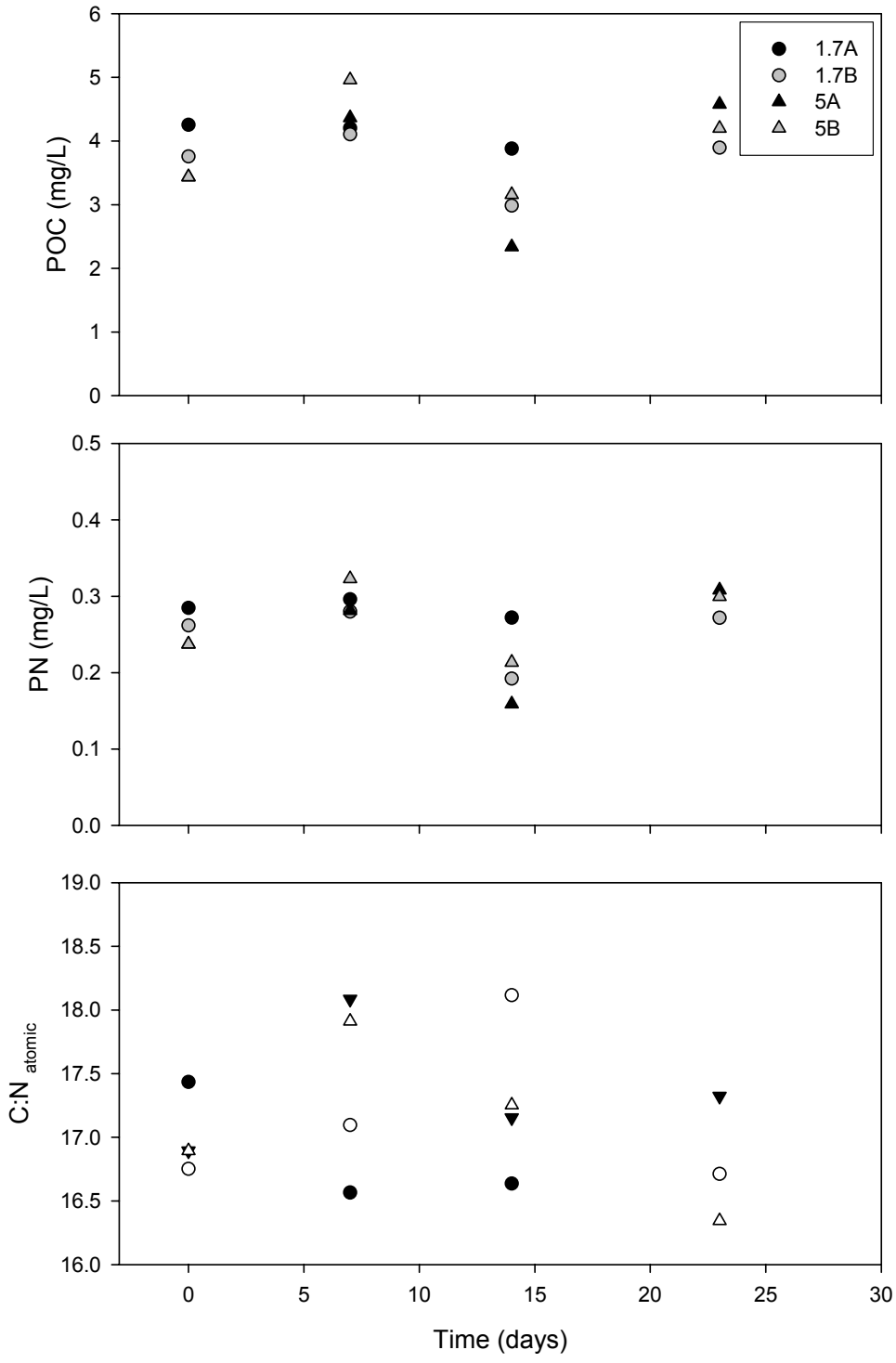

Figure 5.10. Particulate organic carbon and nitrogen (mg/L) and atomic C:N ratio throughout the 2008 23-day degradation of Colville River peat.

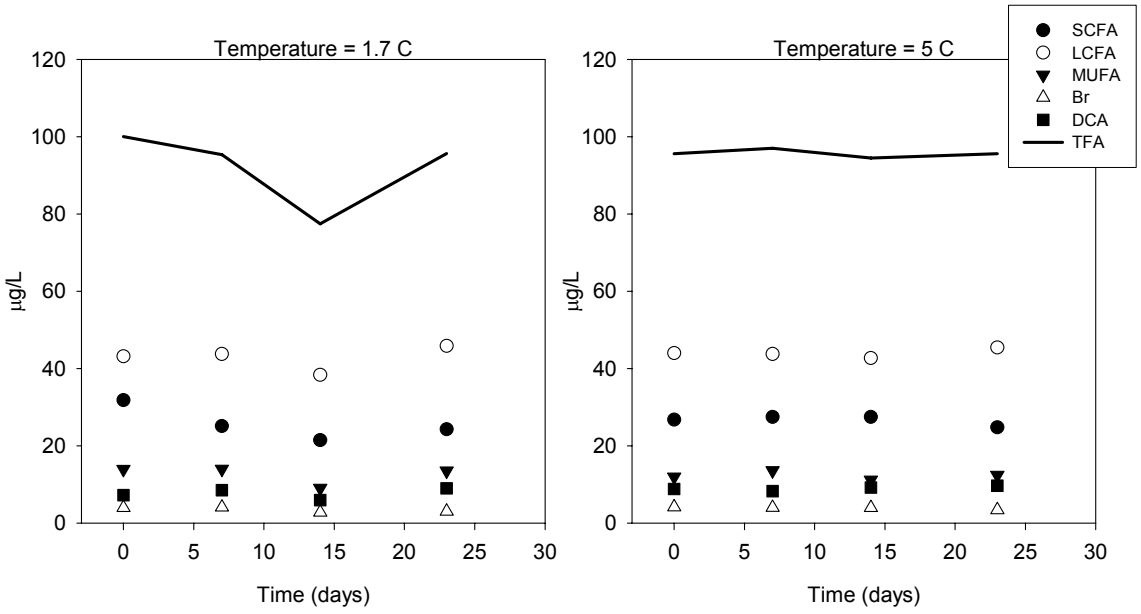

Figure 5.11. Concentrations (µg/L) of short-chain (C_{14}-C_{22}) saturated (SCFA), long-chain (C_{23}-C_{28}) saturated (LCFA), monounsaturated (MUFA), branched (Br), mid- to long-chain dicarboxylic (DCA), and total fatty acids (TFA) during degradation of Colville River peat at 1.7 and 5°C.

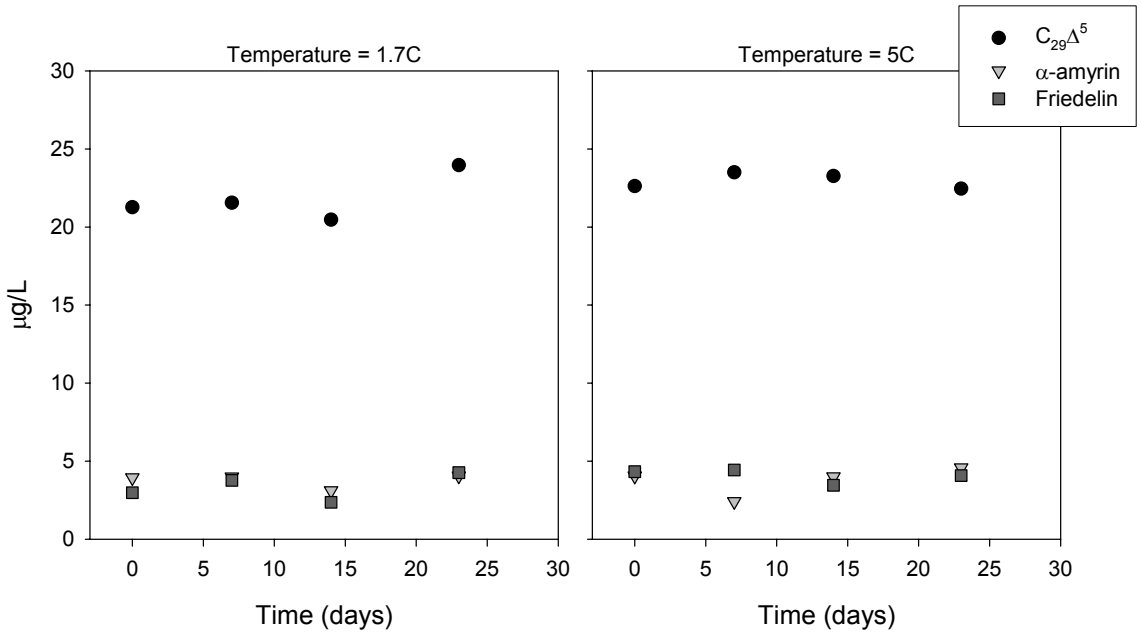

Figure 5.12. Concentrations of selected terrestrial lipid biomarkers (24-ethylcholest-5-en-3β-ol: $C_{29}\Delta^5$, α-amyrin, and friedelin) over a 23-day incubation of Colville River peat in the presence of natural assemblages of Bering Sea microbes.

Only two of the experimental trials—the 2004 69-day incubation of snow-debris and the 2008 incubation of Colville River peat at 1.7°C—resulted in decreasing lipid marker concentrations over time. Both of these incubation experiments underwent considerable warming due to problems with the shipboard environmental chambers, which likely affected the rates of degradation of organic matter. As temperature increases would tend to cause more rapid degradation, the rates presented here are likely overestimates of the rates found in polar and sub-polar environments. In the snow-debris experiment, only the long-chain fatty acids did not increase over time throughout the incubation, and the loss of these compounds was very slow (Table 5.4), with a turnover time of nearly 300 days. Loss rates of terrestrial organic compounds were also very slow in the Colville Peat degradation, with turnover times ranging from 35-369 days. The shortest turnover times (i.e., fastest rates) were expressed by short-chain and monounsaturated fatty acids (Table 5.4). The rate of loss of long-chain fatty acids was approximately 1.5 times faster in the 2008 incubation, but still lagged behind the rates for fatty acid degradation found in all marine organic matter incubations.

Table 5.4. Experimentally determined first-order rate constants (k, yr^{-1}), regression coefficients (r^2), and turnover times (τ, days) for grouped and individual lipids during oxic decay of terrestrial organic matter substrates.

	2004 Snow-Debris -1 °C			2008 Colville River Peat[a] 1.7 °C		
	k (yr^{-1})	r^2	τ (days)	k (yr^{-1})	r^2	τ (days)
Short-Chain Fatty Acids (C_{14}-C_{22})	-	-	-	10.5	0.99	34.6
Long-Chain Fatty Acids (C_{23}-C_{28})	1.2	0.80	296.4	2.9	0.64	125.0
Monounsaturated Fatty Acids	-	-	-	9.7	0.69	37.5
Total Fatty Acids	-	-	-	6.3	0.88	57.8
$C_{29}\Delta^5$	-	-	-	1.0	0.51	369.1
α-amyrin	-	-	-	5.6	0.68	65.0

[a]Rates calculated for the 2008 Colville River peat incubation over the first 14 days of the degradation.

5.5. Discussion

This comparison of two dominant organic carbon source materials in polar and sub-polar environments demonstrates the differences in lability between marine and terrestrial organic matter substrates during microbial degradation. Although differences in degradation rates were found among similar substrates and among the various individual components of similar substrates (Tables 5.2 and 5.4), is it apparent that marine organic matter was considerably more labile than that from terrestrial sources.

Particulate organic carbon (POC) from an Arctic sea-ice algal assemblage degraded at a rate of 3 yr^{-1}, which resulted in a turnover time of 120 days (Table 5.2). Although slower than that found for marine algal POC water column degradation in more temperate regions, with rate constants ranging from 1.4-99 yr^{-1} for marine systems (Emerson and Hedges, 1988; Harvey et al., 1995) and even faster rates of 83 yr^{-1} in lacustrine systems (Lehmann et al., 2002), this rate still implies a near complete loss of algal organic carbon on seasonal timescales. During the 2007 incubation of *M. arctica*, a net loss of POC over the 25-day experiment was not observed and consequently, rate constants for total organic carbon remineralization were not calculated. This is attributed to the short length of the incubation, compared to the 92-day timespan in 2002. Ideally, the incubation would have been continued, but research cruise length was limited in 2007.

During the 2002 incubation, total POC concentrations fluctuated greatly over the first 20 days, with exponential decreases only apparent after day 20. It is conceivable that despite the dark conditions present in the microcosm incubations, the algal cells, having just been collected and immediately added to the experimental microcosms,

continued to survive throughout the early time points of the experiments. If this is the case, the changes in organic matter over the first several time points could be indicative of cellular responses to the changing environmental conditions as opposed to degradation (Harvey and Macko, 1997). If we assume that day 20 represents the point of cellular death and the beginning of degradation, the rate of loss of POC slightly increases to 4.5 yr^{-1} (τ = 81 days). This issue is not of concern for the 2007 incubation, as the *M. arctica* utilized as the marine carbon substrate was collected in 2004 and frozen at -70°C until use in 2007. A twenty-day time interval until cellular death appears long in comparison to similar degradation experiments with temperate diatoms, in which cellular death occurred after five days (Harvey and Macko, 1997), and lipid loss in both the 2002 and 2007 incubations began immediately, arguing for rapid cell death in the 2002 incubation.

Early diagenesis of organic matter is typically thought to result in increasing C:N ratios, as more labile, nitrogen-rich components such as proteins are rapidly utilized (Hedges et al., 1988a; Lehmann et al., 2002). Conflicting results were observed between the 2002 and 2007 incubations with respect to the C:N ratio. In the 2002 algal incubation the atomic C:N ratio decreased throughout the experiment; conversely, in the 2007 incubation of *Melosira arctica*, the C:N ratio increased over the 25-day time-span. Differences in the original biochemical composition of the substrate could be responsible for the discrepancy between the 2002 and 2007 incubations; however, it is also conceivable that the different timescales of the incubations is causative. Considering the high lability of the algal material, loss of nitrogenous material is likely very rapid, and a corresponding increase in C:N ratio may be missed by the coarse sampling timescale in 2002. The decrease in C:N ratio over the entire 92-day experiment likely represents a

divergence from early, widespread loss of nitrogenous compounds to subsequent degradation of carbon-rich lipids.

A wide range in degradation rates was observed for individual and grouped lipids both within and between incubations (Table 5.2). On average, lipid degradation rates were slower for the 2002 incubation, but whether this is due to biochemical differences in the substrate itself or differences in the natural microbial community between the Arctic (2002) and Bering Sea (2007) cannot be determined here. Differences in the lipid composition between algal assemblages were evident prior to degradation—the sea-ice alga utilized in 2002 contained nearly equal concentrations of monounsaturated and saturated fatty acids and also contained a diverse suite of C_{16} and C_{20} PUFAs, while the 2007 *M. arctica* substrate was largely characterized by short-chain saturated fatty acids and cholesterol, although the few monounsaturated and polyunsaturated structures present initially in the 2007 substrate did undergo rapid recycling (Table 5.2). However, substantially higher rates of degradation for the saturated lipid compounds in the 2007 incubation compared to the same suite of saturated compounds in 2002 suggest that the variation in lipid composition is not controlling the observed rate differences.

Overall, both experimental incubations demonstrated that marine algal lipids were rapidly recycled, with total fatty acid turnover times ranging from 6-18 days (Table 5.2), a result consistent with previous estimates that >99% of marine organic matter is recycled prior to sedimentary burial (Berner, 1989; Hedges and Keil, 1995), and the results of Chapter 3, where the lipid composition of POM with depth reflected a loss of labile material. In spite of this, the presence of marine organic matter, comprising perhaps 57-88% of the organic carbon in surface sediments (Chapter 2), argues for a chemical,

physical, and/or biological protection mechanism operating in the western Arctic system to ensure burial of at least some component of this naturally labile material. Both biochemical and physical mechanisms have been proposed as controlling factors of organic matter degradation (Eglinton and Logan, 1991). Biochemical models of degradation include a mechanism via the selective preservation of recalcitrant components of organic matter as the remineralization removes the intrinsically labile components (Boudreau and Ruddick, 1991; De Leeuw and Largeau, 1993; Westrich and Berner, 1984), proposed random repolymerization and condensation reactions which result in the depolymerized compounds representing a larger proportion of the remaining organic matter through time (Killops and Killops, 1993), as well the resistance of terrestrial organic matter to degradation due to complex lignin or cellulosic structures which are affected by a smaller number of microorganisms than polysaccharides (De Leeuw and Largeau, 1993). Mechanisms of physical processes, such as adsorption onto particulate (clay, mineral surfaces, etc.) matrices (Hedges and Keil, 1995; Mayer, 1994; Rothman and Forney, 2007), or the availability of electron acceptors and exposure to O_2 (Middelburg and Meysman, 2007), also likely exert some degree of control on organic matter degradation. For this region, a decoupling of primary and secondary producers and the wide, shallow shelf regions likely enhance marine organic matter burial (Grebmeier, 1993; Moran et al., 2005; Wassmann et al., 2004).

An important observation in several of these incubations is that temperature had no statistically significant effect on the rate of degradation, as the duplicate microcosms incubated at the higher temperature responded in an opposite manner. The Algae 5B carboy, incubated at 5 °C, exhibited substantially slower fatty acid degradation rates than

those at -1 °C, while the companion microcosm (Algae 5A) exhibited much faster rates of degradation for saturated compounds that observed at -1 °C (Table 5.2). While we cannot statistically confirm this based on the inconsistent results of the replicate incubations presented here, overall however, we would argue that the positive response of carboy 5A would be a more typical response of microbial respiration to temperature. The response of microbial populations in Arctic waters to temperature was investigated by Kirchman et al. (2005), and in direct contrast to the Wiebe-Pomeroy hypothesis, the impact of the addition of dissolved organic matter to bacterial growth rates was the same or greater at higher temperatures, not lower temperatures. Furthermore, the response of bacteria to increasing temperatures was similar to that found in temperate latitude climates (Kirchman et al., 2005).

The incubations of terrestrial organic matter substrates provide a stark contrast to the rapid recycling of marine organic material. Particulate organic matter and lipid concentrations in most microcosms remained nearly stable throughout the incubations. These results suggest that recycling of terrigenous organic matter occurs on much longer timescales than represented by the simulated incubations conducted here. Lipids in the 1.7 °C Colville River incubation demonstrated losses over the first 14 days of the incubation, and, because of the warming of the environmental chamber to room temperature as described above, likely represent maximum estimates of terrestrial organic matter degradation rates. Even considering that this temperature anomaly affected the apparent rate, the degradation of short-chain fatty acids demonstrated for the first 14 days of the 2008 Colville Peat incubation, with a turnover time of 35 days, was still 1.5-6.6 times slower than rates for the same short-chain compounds derived from sea-ice algae.

The apparent discrepancy between rates for identical compounds derived from the marine and terrigenous substrates argues for a physical protection mechanism in the terrestrial substrate, although biochemical differences, such as high concentrations of lignin or cellulose, may also provide a biochemical resistance, protecting lipids and polysaccharides from degradation (De Leeuw and Largeau, 1993). Rothman and Forney (2007) proposed a mathematical physical-exclusion model whereby the apparent decrease in degradation rates of algal material over time is explained by the diffusion of hydrolytic enzymes away from a microbe where their ability to attack organic matter is subsequently hindered by a sediment matrix. Indeed, the terrestrial substrates contained abundant matrix material as noted by visible mineral grains and detrital material under microscopic examination, and physical protection due to adsorption likely contributes to the slower degradation found for the terrestrial material. Yet, while this physical model may aid in understanding the differences in degradation rates for *similar* lipid compounds between marine and terrestrial organic matter substrates, clearly their biochemical differences also play a role in their overall relative labilities. The peat substrates were, on average, 30% organic carbon by weight, and contained considerably less nitrogenous material (initial C:N of ~11 and 17 for the snow-debris and Colville River peat, respectively) in comparison to the algal substrates (initial C:N between 6-8). The high degree of refractory compounds, such as lignin, would be expected to afford protection from microbial degradation of the peat material (Tegelaar et al., 1989). For example, lipids associated with cutin tend to survive degradation compared to epicuticular waxes (De Leeuw and Largeau, 1993; Wannigama et al., 1981).

In spite of the physical and chemical controls on degradation processes, soil organic matter, in the form of aged woody peat debris, did contain susceptible components when exposed to natural Arctic microbial assemblages during the 82-day degradation in 2004. Carbohydrates and amino acids comprised a smaller fraction of organic carbon in the final substrate (Fig. 5.8); however, losses are difficult to tightly constrain due to the nature of the experiment. Because the primary function of this incubation was to explore the changes in the bacterial community to varying organic matter substrate additions (Dyda, 2005), total POC over time in the experiment was not monitored, so we can only consider the losses of amino acids and carbohydrates in terms of the carbon content of the substrate initially and post-incubation. Bacterial abundances and cell volumes were greatest when incubated with more labile substrates, yet *Sulfitobacter*, a member of the *Alphaproteobacteria* common in Arctic systems (Brinkmeyer et al., 2003), responded significantly in the latter portions of the peat incubation (Dyda, 2005) and could be a key player in the degradation of land-derived materials in the Arctic Ocean. Together with the doubling of the average radiocarbon age of the substrate over the 82-day time-span of the incubation, the relative losses in amino acids and carbohydrates clearly suggest that "pre-aged" terrestrial organic substrates contain labile components that can be respired to CO_2 on timescales similar to marine organic matter. This result is particularly relevant for the global carbon cycle when considered from the perspective that Arctic soils contain as much as 600 Gt organic carbon (Ping et al., 2008), nearly double previous estimates, and the fact that surface air temperature and hydrological changes are linked to increasing mobilization of permafrost-bound organic carbon (Frey and Smith, 2005).

The strong increase in relative age of the peat substrate suggests that only labile components were respired, a result consistent with microbial degradation of Arctic soil organic matter at in situ temperatures (Biasi et al., 2005). However, Biasi et al. (2005) found that with increasing temperatures, heterotrophs shifted respiration from labile to more recalcitrant substrates in identical organic matter. This temperature-dependent shift was not evident in the degradation rates calculated for groups of lipids from the Colville River Peat at 1.7 °C and 5 °C. It is possible that the short timescale of the experiment masks small differences in the observed degradation rates, as the timescale of the experiment can have a significant impact on the calculated degradation rates (Hedges and Keil, 1995). Additionally, the difference in incubation temperature (1.7 °C versus 5 °C) is less significant for the Bering Sea, where the 2008 experiment was conducted, than the Arctic Ocean. Summer water temperatures in the Bering Sea are commonly as high as 10 °C (Hare et al., 2007) but were about 5.8 °C during the 2008 experiment. In contrast, throughout the summer in the western Arctic Ocean, the majority of temperatures ranged between and -2 °C and 0 °C, with only a few stations reaching maximum temperatures of 3 °C (Codispoti et al., 2005). Thus, the 3 °C temperature difference in the 2008 Bering Sea incubations would not appear great enough to affect rates of bacterial degradation of organic matter. The design of these experiments do not allow direct determination of the amount of labile material respired during the peat degradation experiment, however, the loss of modern material and retention of relatively labile components in the "pre-aged" peat substrate reflects the complexity of evaluating the impact of increasing inputs of land-derived material for the Arctic carbon cycle.

Although terrestrial material contains a spectrum of organic matter components from labile to highly refractory, the incubations presented here demonstrate that land-derived material degrades on much longer timescales compared to fresh marine inputs. While this suggests that increasing amounts of the terrigenous component would be preserved in oceanic sediments, it is important to note the difficulty in extrapolating from such empirical studies (and their difficulties) to long-term preservation. As noted by Hedges and Keil (1995), degradation and preservation tend to be opposing processes, and the reactions involved in the early diagenesis of organic matter may not be useful for describing the specific characteristics of organic carbon responsible for long-term preservation after the relatively short period of early diagenesis. While perhaps less important than the effect of compaction or increasing temperatures from deep burial on preservation (Eglinton and Logan, 1991), the composition of organic matter clearly plays a large role on the type of organic matter reaching surface sediments.

5.6. Conclusions

In summary, the lipid component of organic matter from marine algae in the Arctic Ocean was highly labile, with turnover times ranging from 1-130 days. Algal particulate organic carbon exhibited complete loss on timescales equivalent to spring and summer seasons (120 days). In contrast, the timescales for turnover of lipids from terrestrial organic matter were 1.5-6.6 times slower than for identical compounds from marine organic substrates. The biochemical differences in carbon substrates, as well as physical protection mechanisms, likely enhance preservation of land-derived material. Elevated temperatures did not consistently affect marine or terrestrial organic carbon

degradation rates; however, aged terrigenous organic matter contains labile, easily recycled components. The potential effects of a warmer Arctic on the recycling of relict organic matter, as well as changes in Arctic microbial community structure, should be focus areas for future research.

Chapter 6: The Influence of Land-Derived Material on the Organic Carbon Cycle of the Western Arctic Ocean: Carbon Budgets and Concluding Perspectives

The purpose of this dissertation was to explore the role of land-derived material in the organic carbon cycle of the western Arctic Ocean. Tracking the origin of organic matter is of utmost importance for a complex system like the Arctic, where strong inputs of terrigenous material from rivers and erosion are imprinted over highly seasonal marine organic inputs from primary productivity. Given the biochemical differences between these two sources of organic matter and the likely alterations in the inputs of each with continued climate warming, accurate estimations of the inventory sizes and turnover rates of the marine and terrestrial components are necessary for regional carbon budgets and predictions on the impacts of climate change. Below, a summary model is presented which utilizes the findings gained from this dissertation together with published data to provide insight into the cycling of organic carbon in the western Arctic Ocean. This model parallels previously developed organic carbon box models of Arctic regions included in Macdonald et al. (1998) for the Beaufort Sea Shelf, Naidu et al. (2004) for the North Bering-Chukchi Sea, and Stein and Fahl (2004) for the Laptev and Kara Seas, with an added focus on the shelf-basin exchange of organic carbon.

6.1. Applications of this Research to Western Arctic Organic Carbon Budgets

Organic carbon budgets provide a descriptive model of the transfer of organic matter between various storage reservoirs, estimates of the fractions lost to

remineralization, and an understanding of the processes that lead to accumulation of material over long time scales. Here, we combine literature values with estimated remineralization rates (Chapter 5) and estimated burial rates of marine and terrestrial organic matter (Chapters 2 and 4) to explore the transfer and accumulation of organic matter in the western Arctic Ocean.

A simple box-model describing the sources and sinks of marine and terrestrial organic matter was created using the Simulistics, Ltd. Simile v5.3p2 software package. The Simile software, which is available at http://www.simulistics.com in three formats including the free evaluation edition utilized here, was specifically designed to provide a visual modeling and simulation environment for expressing complex systems in the earth, environmental, and life sciences (Muetzelfeldt and Massheder, 2003). The Simile package is capable of creating many types of models, including matrix, differential/difference equation, and population dynamics models; here, we focus on a basic systems dynamics scheme that relies on compartments (i.e., organic carbon storage reservoirs), flows and variables (i.e., fluxes of organic matter into or out of a reservoir), and influences between fluxes and variables to describe a given system (Muetzelfeldt and Massheder, 2003).

The developed box-model focuses on the western Arctic region encompassed by the NSF-sponsored Shelf-Basin Interactions (SBI) Program region (Fig. 6.1). The region was divided into shelf and basin reservoirs for the model, as one of the main goals of the SBI Program was to evaluate the exchange of organic matter between shallow and deep environments. For simplicity, organic matter reservoirs were aggregated into four compartments for both the marine and terrestrial components of the box-model, including

shelf and basin suspended and/or sinking water column particulate organic matter (Shelf POC, Basin POC) and shelf and basin sediments. This partitioning allowed for an examination of the exchange of organic carbon between shallow and deep Arctic environments. Sources and sinks for each reservoir were defined based on established values in the primary literature or taken from results gained through this dissertation (Table 6.1).

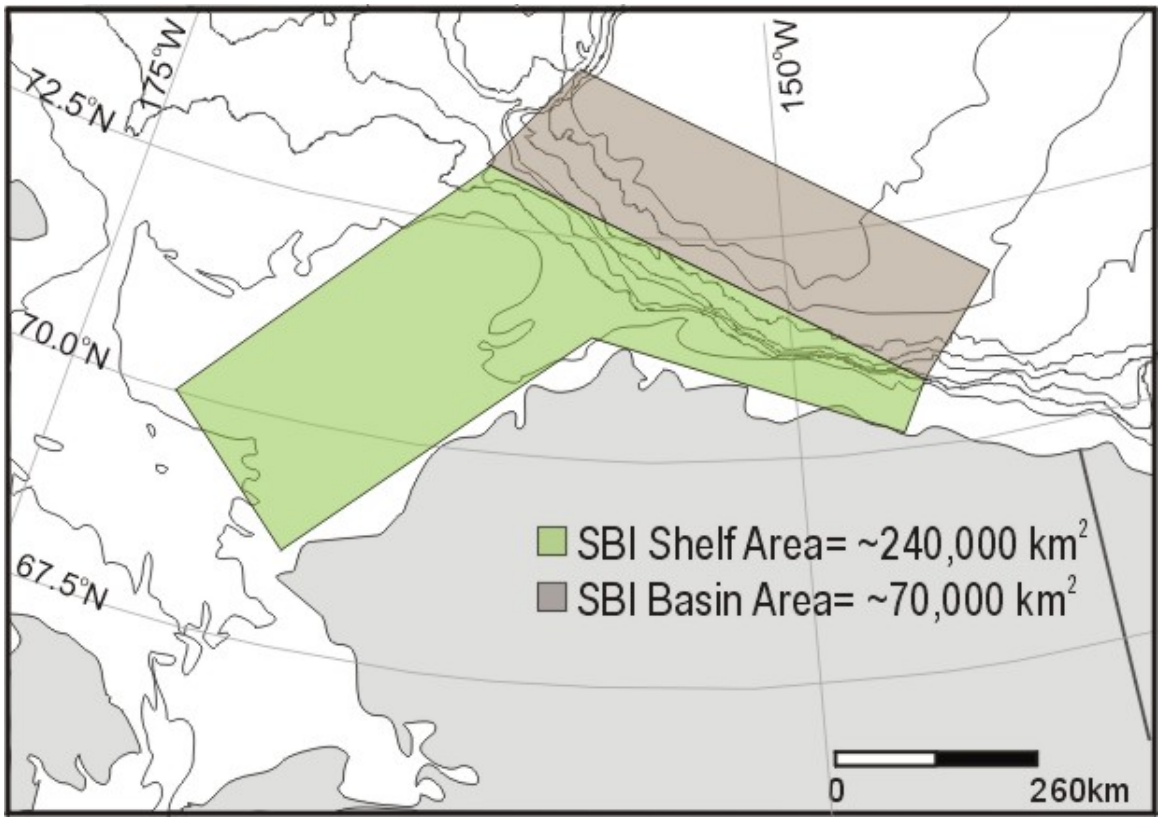

Figure 6.1. Map of the western Arctic study region with approximate shelf and basin areas classified into two regions as outlined in the text. These regions were used to define areas for the generalized box-model.

Table 6.1. Summary of sources (+) and sinks (-), in 10^6 t yr^{-1}, of organic carbon to reservoirs in the marine and terrestrial components of a simplified Arctic Ocean carbon cycle box model.

Reservoir	Sources or Sinks	Value	References and Comments[a]
Marine Organic Matter			
Shelf POC	Water/Sea-ice PP[b]	+16.92/+2.45	Hill and Cota (2005); Gosselin et al. (1997)
	Accumulation	-2.4	Chapters 2 and 4; see text for calculation
	Remineralization	-16.97	Calculated by difference
Basin POC	Water/Sea-Ice PP[b]	+1.39/+0.75	Hill and Cota (2005); Gosselin et al. (1997)
	Accumulation	-0.187	Chapters 2 and 4; see text for calculation
	Remineralization	-1.953	Calculated by difference
Shelf Sediments	Accumulation	+2.4	Equal to shelf POC accumulation
	Remineralization	-1.25 (52%)	Naidu et al. (2004)
	Down-slope Transport	-0.24 (10%)	See text
Basin Sediments	Accumulation	+0.187	Equal to basin POC accumulation
	Down-slope Transport	+0.24	Equal to down-slope inputs from shelf
	Remineralization	-0.188 (44%)	Naidu et al. (2004)
Terrestrial Organic Matter			
Shelf POC	Aeolian	+0.07	Stein and Macdonald (2004a)
	Erosion	+0.80	Stein and Macdonald (2004a)
	Rivers	+0.255	Derived from Colville River delta budget in Macdonald et al. (2004); see text
	Export to Basin	-0.068	Eicken et al. (2005); Belicka and Harvey (unpublished data)
	Accumulation	-0.719	Chapters 2 and 4; see text for calculation
	Remineralization	-0.338 (30%)	By difference; Chapter 5
Basin POC	Aeolian	+0.013	Stein and Macdonald (2004a)
	Export from Shelf	+0.068	Equal to export to basin
	Remineralization	-0.024 (30%)	Chapter 5; Equal to shelf remineralization rate
	Accumulation	-0.057	By difference; see text
Shelf Sediments	Accumulation	+0.719	Equal to shelf POC accumulation
	Down-slope Transport	-0.06	See text
Basin Sediments	Accumulation	+0.057	Equal to basin POC accumulation
	Down-slope Transport	+0.06	Equal to down-slope transport from shelf

[a]Primary references, please see text for conversions and full parameter derivation descriptions; [b]PP: primary production.

6.1.1. Model Parameterizations

Hill and Cota (2005) determined daily net primary productivity in the SBI region to average 70.5 g C m^2 yr^{-1} on the shelf and 19.8 g C m^2 yr^{-1} at the edge of the basin. Using the average spatial extent of the SBI shelf and basin regions (Fig. 6.1), we

determined that water column primary production resulted in inputs of 16.92 Mt C yr^{-1} and 1.39 Mt C yr^{-1} for the shelf and basin regions, respectively (Fig. 6.2). Similarly, we utilized the estimated daily primary production from shelf and basin sea-ice algae (0.028 g C m^2 day^{-1} on Chukchi Shelf; 0.002-0.057 g C m^2 day^{-1} in Chukchi Basin for average of 0.0295) from Gosselin et al. (1997) to calculate inputs to the shelf and basin marine POC reservoirs from sea-ice algae of 2.45 and 0.75 Mt C yr^{-1}, respectively (Table 6.1, Fig. 6.2). These annual averages do not take into account the highly seasonal nature of primary production and are likely be underestimates, as they are derived from sampling on cruises in between the spring bloom and also do not include observed patches of extremely high production (reaching up to 8 g C m^{-2} day^{-1}; Hill and Cota (2005)). However, these estimates are similar to those found for the southern Chukchi Sea and Gulf of Anadyr (Hill and Cota, 2005 and references therein) and provide the most comprehensive estimates for annual primary productivity in the SBI region.

Several terrestrial organic matter inputs were similarly assigned constant values (Table 6.1, Fig. 6.2). The Colville River is the largest river in the SBI region, estimated to deliver 170,000 t OC yr^{-1} to the Alaskan Beaufort Shelf region (Macdonald et al., 2004a), but many other small rivers, including the Ikpikpuk, Meade, Utukok, Kokolik, and Kuparuk also drain into the Chukchi/Beaufort region. Estimates for the total delivery from these smaller rivers are sparse, so an estimate that when combined, they would delivery approximately 50% more than the Colville alone was assumed, resulting in a total annual river delivery to the shelf of 0.255 Mt C (Fig. 6.2). This flux estimate is not well constrained; however, it does not appear greatly inflated since, as defined, this input is only about 10% of the total particulate organic carbon delivery assumed from the

Mackenzie River (Macdonald et al., 1998). Inputs from coastal erosion were set at 0.8 Mt yr^{-1} (Stein and Macdonald, 2004a). Aeolian annual inputs were determined to reach 0.11 Mt yr^{-1} in the Chukchi Sea and 0.03 Mt yr^{-1} in the Beaufort Sea (Stein and Macdonald, 2004a); as a result, an average of 0.07Mt yr^{-1} for the shelf region was utilized in the SBI region box-model. Aeolian inputs to deeper Arctic regions are more difficult to constrain and have not been widely reported. Here, we utilized the reported central Arctic value of 0.809 Mt yr^{-1} over a total area of 4.5 km^2 (Stein and Macdonald, 2004a). Once extrapolated to the SBI basin area of 70,000 km^2, aeolian input to the basin is very low (0.013 Mt yr^{-1}).

Next, the mass accumulation rate of sediment was estimated based on ^{210}Pb data in the EB-2 shelf core as described in Baskaran and Naidu (1995). Although not tightly constrained given the active sedimentary mixing in our core, this method provides an estimate of 113.2 mg cm^{-2} yr^{-1}, which compares well with previously reported values for the North Bering and Chukchi Seas (Baskaran and Naidu, 1995; Naidu et al., 2004). Similarly, we obtained an average mass accumulation rate of 31.18 mg cm^{-2} yr^{-1} for the basin using ^{210}Pb concentration in the EB-7 core (Chapter 4). It is important to note that this is a first approximation which likely overestimates basin accumulation, as diffusional processes exert a strong influence on the ^{210}Pb profile in the deep basin. For all sediments collected from locations in <200 m of water, total organic carbon content in the surface (0-1cm) sediments averaged 1.15% (Chapter 2). Given the SBI shelf area of 240000 km^2 and an average shelf accumulation rate of 113.2 mg cm^{-2} yr^{-1}, this results in a total accumulation of organic carbon on the shelf of 3.12 Mt yr^{-1}. Similarly, using the average basin surface sediment organic carbon content of 1.30% (Chapter 2) and the SBI

basin area of 70,000 km^2, we obtain an average basin organic carbon accumulation of 0.284 Mt OC yr^{-1}. Results obtained from biomarker analysis and PCA found that shelf sediments contained an average of 23% terrestrial organic carbon while basin sediments averaged 34% terrestrial organic carbon (Chapter 2). This suggests annual average initial accumulations of 0.719 Mt terrestrial OC and 2.401 Mt marine organic carbon to shelf sediments, and 0.097 Mt terrestrial organic carbon and 0.187 Mt marine organic carbon to basin sediments.

For marine organic matter, the accumulation rates of 2.4 Mt and 0.187 Mt must be balanced by total water column sources minus losses to remineralization. This was accomplished by setting the amount of organic matter remineralized in the water column of the shelf and basin as the difference between the defined inputs from primary production and the calculated amounts of initial accumulation in sediments (Table 6.1). For the shelf environment, this oxidation rate was calculated to be 87.6% of total primary production inputs, while in the basin it was slightly higher at 91.3%. These rates are somewhat low compared to the 99.9% usually stated as the rate of loss of marine organic matter (Berner, 1989; Hedges, 1992); however, the high seasonal export fluxes of POC (up to 37% in summer) demonstrated by Moran et al. (2005) for the SBI region, as well as the strong sedimentary metabolism noted in the East Barrow shelf core (Chapter 4), suggest that water column loss rates in these shallow systems do not approach 99.9%. The degradation experiments in Chapter 5 suggested an average turnover time of marine particulate organic matter on the order of 120 days, which supports the contention that some component of the marine POM will survive sinking through the average 50 m water depth prior to degradation. Through the investigations in Chapter 4, it is clear that

remineralization of the labile components of organic matter is also active in shelf and slope sediments. While we could not directly quantify this process, we utilize values of 52% for sediments underlying highly productive regions and 44% for sediments underlying less productive regions given by Naidu et al. (2004) for calculation of losses of marine organic matter in sediments in the shelf and basin, respectively (Table 6.1). Organic carbon transport downslope in the Laptev Sea region is estimated to reach 30-48% of total inputs (Stein and Fahl, 2004), however for the SBI region this flux is poorly constrained and in the absence of quantitative data we take a conservative approach and assume that only 10% of the shelf accumulation rates of marine organic matter, a total of 0.24 Mt OC yr^{-1}, are transported to the basin by gravity flows (Table 6.1). Based on the proportions of marine and terrestrial organic matter found in shelf sediments (Chapter 2), and on an assumption that the down-slope transport processes would not discriminate between marine or terrestrial organic carbon, this translates to an approximate delivery of terrestrial organic matter of 0.06 Mt OC yr^{-1}, since shelf sediments were, on average, 20% terrestrial OC.

In the terrestrial organic matter model, the accumulation rate of terrestrial organic matter on the shelf was similarly set equal to that approximated above from accumulation rates (0.719 Mt, Table 6.1). An attempt was also made to estimate the amount of terrestrial organic matter lost to the basin through sea-ice export. Eicken et al. (2005) estimated that during 2002 approximately 4 Mt of sediment were transported in sea-ice in the SBI region. One sample of this ice-rafted debris was collected for organic carbon compositional analysis, and determined that it contained 1.7% organic carbon (Belicka and Harvey, unpublished data). By assuming that it was entirely terrestrial in origin, this

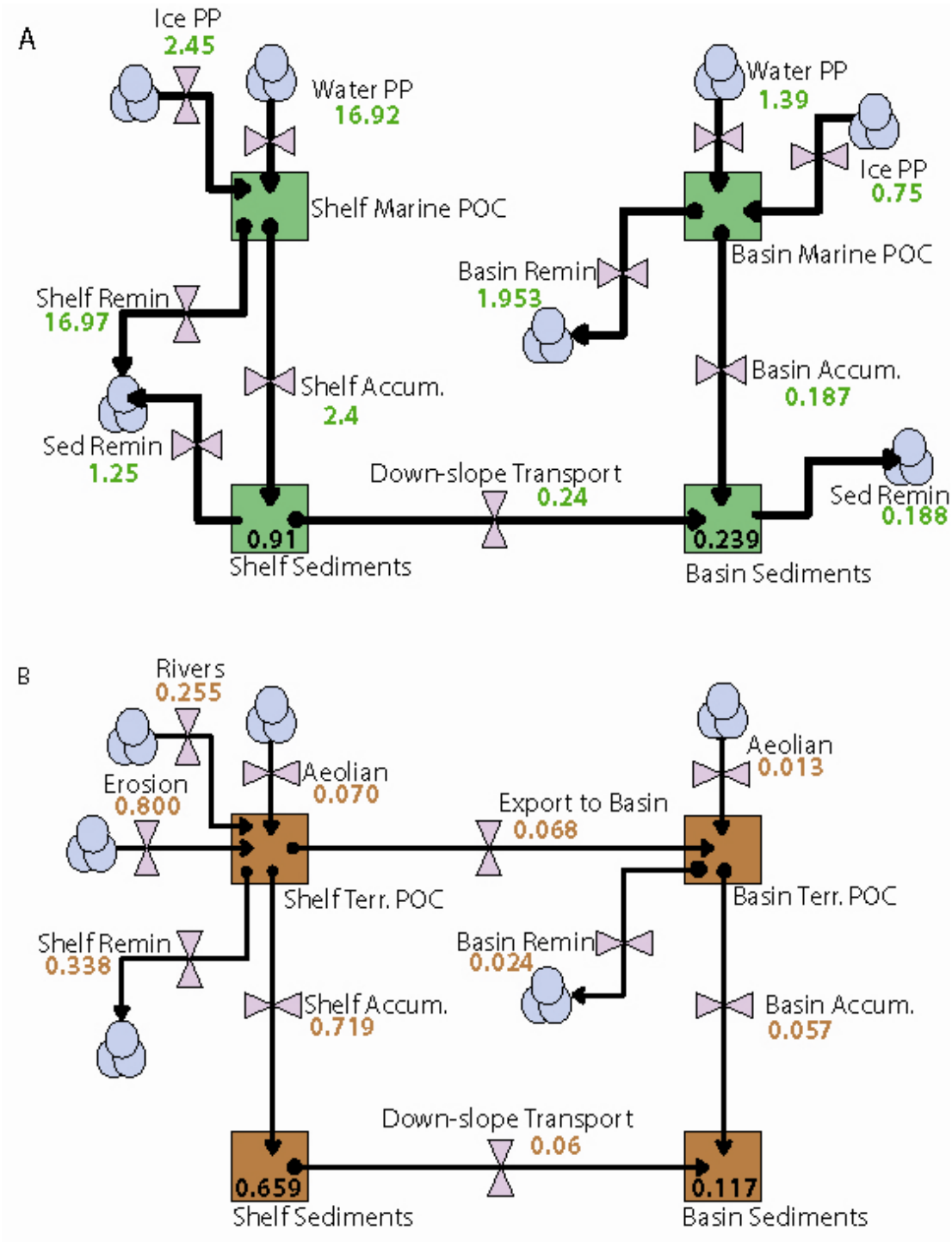

Figure 6.2. Inputs and outputs (in Mt C yr^{-1}) of marine (A) and terrestrial (B) organic carbon in the Chukchi and Alaskan Beaufort Sea regions of the western Arctic Ocean. See text and Table 6.1 for model parameterization. The rectangular boxes represent reservoirs of organic carbon. Fluxes are represented by the bowtie (valve) pattern beginning or ending from either a source or sink (triple circle pattern) or between reservoirs.

results in a suggested export to the basin of 0.068 Mt yr^{-1}(Table 6.1). So, in the shelf region, the inputs of land-derived material were balanced by an export to the basin of 0.068 Mt, a sedimentary accumulation of 0.719 Mt, and a remaining loss, by difference, of 0.338 Mt through water column oxidation. This oxidation equals 30% of the initial inputs, which corresponds well to previous estimates of 35% (Ittekkot, 1988) as well as findings that components of terrestrial organic matter turned over 1-6x slower than marine organic matter (Chapter 5). In the basin, however, the suggested accumulation of 0.097 Mt yr^{-1} could not be utilized, as this suggested accumulation is greater than the estimated aeolian and sea-ice rafting inputs (Table 6.1, Fig. 6.2). Thus, the remineralization of terrestrial organic matter in the water column of the basin was defined as 30%, resulting in an average sedimentary accumulation of 0.057 Mt yr^{-1} (Fig. 6.2).

Given the parameterization as described above, this simplistic box model suggests that approximately 0.91 Mt of marine OC and 0.66 Mt of terrestrial OC (total of 1.57 Mt) are buried per year in the shelf region of the Chukchi and Alaskan Beaufort Seas. An additional 0.24 Mt of marine OC and 0.12 Mt of terrestrial OC, for a total of 0.36 Mt OC, are buried in the basin. These values closely correspond to preserved estimates of *terrestrial* organic carbon through previous attempts at Chukchi and Beaufort Sea carbon budgets (Stein and Macdonald, 2004b), but suggest substantially greater preservation of marine organic matter (3-9 times as much from previous budgets). This discrepancy is likely a result of the lower water column degradation rates (~90%) suggested for the highly productive SBI region, as evidenced by high seasonal POC export fluxes (Moran et al., 2005) and ungrazed algal material in sediments (Coyle and Cooney, 1988; Grebmeier, 1993). Previous studies may have alternatively underestimated the impacts

of POC export fluxes and a decoupling between benthic and pelagic systems—for example, Moran et al. (2005) found that despite high export fluxes of organic matter to the benthos, approximately 18% of this export remained unconsumed and was seasonally exported to deeper waters and sediments. Future efforts focusing on constraining small river inputs and the lateral transport, either through sea-ice, oceanic currents, or gravity flows, of both marine and terrestrial organic matter to the basin would greatly improve the validity of this carbon budget.

6.2. Summary of the Key Findings from this Dissertation

6.2.1. A comparison of geochemical proxies for the estimation of preserved organic matter components in sediments and implications for regional carbon budgets

The first segment of my research compared established approaches for quantifying organic matter preservation in contemporary marine sediments to determine if estimates of the preserved terrestrial fraction for a given sedimentary environment were consistent (Chapter 2). The results demonstrated that each method had considerable variation in the estimated terrestrial organic component for identical sediment samples, and this lack of consistency limits our ability to incorporate such estimates into pan-Arctic carbon budgets. Two techniques, the two end-member $\delta^{13}C$ mixing model and the ALKOC ratio were found to be inappropriate for the western Arctic, due to the difficulty in constraining a marine $\delta^{13}C$ end-member and the abundant, but patchy, influx of terrestrial organic carbon from coastal erosion. A further difficulty is that these established proxies may target different fractions of the terrestrial component--the BIT index, for example, appears to represent peat or soil organic matter inputs compared to more traditional lipids such as *n*-alkanes or long-chain fatty acids which measure higher

plant wax inputs. Along similar lines, unless the lipid fraction is wholly representative of the bulk organic carbon, quantified values utilizing preserved lipid material (PCA, BIT index, ALKOC) may skew quantifications if selected markers are better preserved relative to bulk organic matter. Despite the absolute differences between approaches, overall average terrestrial organic matter inputs to surface sediments in the Chukchi and western Beaufort Seas ranged between 12-43%, highlighting the importance of terrestrial organic matter in Arctic Ocean sediments, even on non-river dominated continental margins.

6.2.2. The sources and transformation of water column POM in the western Arctic

The second component of this research addressed the character and composition of suspended particulate organic matter in shelf, halocline and deep waters of the western Arctic shelf and basin, with an emphasis on determining the balance of marine and terrestrial sources of POM and the changing chemical composition of POM during transit through the water column. Suspended particles from upper regions of the shelf and basin water column were dominated by lipid markers of marine origin, but extreme spatial heterogeneity was observed, stressing the strong control that nutrient availability and sea-ice cover exert on the region. Evidence of terrestrial organic matter inputs was rare in surface and intermediate depth POM, suggesting a disconnect between the abundant terrestrial OC in sedimentary material (Chapter 2) and shallow suspended POM. However, deep water particles contained high concentration of terrestrial organic markers, as well as the oldest average radiocarbon age. This implies that as organic matter sinks and is transported laterally to from the shelf to deeper basin environments,

labile marine components are recycled quickly, and recalcitrant, land-derived organic matter remains for sedimentation.

6.2.3. Trace element and molecular markers of organic carbon dynamics

The third component of this research focused on an analysis coupling lipid biomarkers with redox-sensitive elements to understand the sources and recycling of carbon in Arctic sediments (Chapter 4). Results demonstrated that sediments along the shelf-to-basin continuum in the western Arctic Ocean receive sufficient labile organic matter inputs to consume available O_2. Intense metabolism of organic matter, indicated by high levels of AVS, was present in shelf sediments, likely due to important inputs of highly labile sea-ice algal material. In addition to this labile marine organic carbon, additional terrestrial inputs, possibly both of modern, vascular plant material and older, recently remobilized permafrost material, were evidenced by the abundance of long-chain *n*-alkanes, *n*-alcohols, and *n*-alkanoic acids in shelf sediments. Sedimentary metabolism of organic matter was less intense on the continental slope, which, when coupled with the strong hydrodynamic forces leading to focusing of organic matter, may be leading to greater preservation of organic matter to support the rich benthic community found there. Despite the physical limitations that sea-ice cover and water depth exert on carbon fluxes to the benthos in the deep Arctic basin, redox-elements suggest that labile material does occasionally reach the sedimentary floor. In addition, strong signals of terrestrial organic matter inputs were also found in the basin sediments, corroborating recent evidence for abundant land-derived organic carbon in locations far removed from coastlines. ^{210}Pb did not prove useful for sedimentation rate calculations in the western Arctic Ocean. On the

shelf and slope, substantial mixing of the sediments precluded development of an age model. The basin sediments exhibited accumulation at slow rates inconsistent with the capability of a short-lived radioisotope such as ^{210}Pb.

6.2.4. Experimental investigations on the lability of marine and terrestrial organic carbon

Chapter 5 detailed research on the differential kinetics between the microbial degradation of marine and terrestrial organic matter substrates in polar and sub-polar waters. The goals were two-fold: (1) to determine the timescales of degradation of recalcitrant terrestrial organic matter and how these compare with the turnover of labile marine organic sources; and (2) to determine if predicted temperature increased for the Arctic region impact turnover times of the land-derived organic material. The results of these experiments show that marine organic matter was recycled very quickly, at rates comparable to, and in some cases greater than, those found for diatomaceous material microbially recycled at temperatures of mid-latitude environments. Furthermore, experiments suggest that marine organic carbon inputs are remineralized completely on spring and summer season timescales (120 days). In contrast, the timescales for turnover of terrestrial organic matter were substantially longer than the timescales measured for labile marine organic matter. Although most experimental trials did not demonstrate loss of total terrestrial particulate organic carbon, several classes of lipids were found to decay, albeit at rates 1.5-6.6 times slower than for identical compounds from marine organic substrates. This discrepancy argues for a physical protection mechanism within the terrestrial organic matter that enhances preservation. An increase in temperature of 3.3-6.0 °C was not found to consistently influence degradation rates for either marine or

terrestrial organic matter. Although this implies that predicted temperature changes for Arctic regions may not directly affect the rate of respiration of organic matter back to CO_2, temperature could have an indirect effect by increasing the abundances of this material produced and delivered to Arctic regions.

6.2.5. Concluding Remarks

Based on a simple box model of marine and terrestrial organic matter inputs (Chapter 6), an estimated 0.91 Mt marine organic carbon and 0.24 Mt terrestrial organic carbon are accumulating in shelf sediments. This model corresponds well to the sedimentary material analyzed in this dissertation (Chapters 2 and 4), and together with the particulate organic matter analysis, demonstrates that although marine organic matter predominates in both water column particles and sediments, terrestrial organic carbon still plays a strong role in organic carbon dynamics. In terms of total inputs, only 4.7% of the marine primary productivity on the shelf is ultimately preserved in shelf sediments, while approximately 58.6% of terrestrial organic matter inputs become sequestered. The balance between these two main sources of organic carbon is likely to be altered with climate change, which may affect the average burial rates of each, as well as the potential recycling of these types of organic matter eventually to atmospheric CO_2. With respect to the sensitivity of the Arctic Ocean to climate change, future efforts should focus on the following two themes in order to more fully understand the implications of climate change on regional and global scales: 1) improving the ability to constrain marine and terrestrial organic components preserved in sediments through the use of geochemical proxies; and 2) refining the results gained here to improve quantification of the transport of organic matter through sea-ice, ocean currents, and sediment slumping.

Appendices

Table A2.1. Concentration of C_{17}-C_{31} *n*-alkanes (as µg/g OC) in surface sediment samples (0-1 cm) in the western Arctic Ocean

	STN 1	STN 2	WHS-2	WHS-5	WHS-6	WHS-7	WHS-12	EHS-4	EHS-6	EHS-9	EHS-11	EHS-12	BC-3	BC-4	BC-5	BC-7	EB-2	EB-4	EB-7
C_{17}	1.0	0.5	3.9	3.7	nf	1.8	2.9	nf	2.8	2.3	0.5	3.2	9.3	4.9	6.6	5.6	3.3	4.2	2.5
C_{18}	1.7	1.7	4.7	7.4	3.1	2.9	6.5	1.3	6.9	4.1	2.3	7.7	11.3	6.3	9.3	8.8	4.5	6.1	4.9
C_{19}	2.8	3.8	8.1	9.4	5.3	5.0	10.9	5.4	12.8	7.5	6.1	14.7	55.4	15.8	17.3	14.3	8.9	10.6	11.5
C_{20}	2.3	3.1	7.8	11.5	8.6	4.6	11.3	2.4	14.5	6.0	6.5	14.8	18.9	9.0	15.0	15.2	5.3	9.1	7.6
C_{21}	4.9	5.6	17.8	15.6	36.6	5.9	15.4	3.8	31.7	7.2	8.1	20.9	40.7	15.0	23.4	24.5	11.1	20.8	12.9
C_{22}	4.0	6.0	16.9	16.4	64.6	5.7	14.5	3.3	43.9	5.3	7.1	19.1	39.2	11.3	19.5	22.6	7.9	15.1	11.3
C_{23}	11.3	12.1	33.7	23.4	86.3	9.0	21.9	6.8	60.0	9.2	Nf	28.8	74.3	25.5	42.6	42.2	14.0	35.6	21.5
C_{24}	5.0	6.5	21.8	17.0	89.7	8.4	14.0	3.7	51.3	5.3	7.1	19.4	40.2	13.3	25.4	26.7	3.9	15.0	10.2
C_{25}	13.3	14.6	43.5	24.9	89.0	9.9	20.5	8.1	66.3	6.7	9.0	26.8	66.9	25.4	42.2	43.0	12.2	38.8	22.4
C_{26}	4.0	6.2	25.8	12.1	82.2	9.3	10.2	3.0	44.6	3.5	5.3	13.9	28.0	9.5	18.8	20.8	5.1	11.7	8.5
C_{27}	20.8	21.7	65.2	32.0	75.9	13.1	24.5	10.3	70.8	7.3	9.3	33.8	72.0	32.2	41.4	59.8	16.9	54.3	33.3
C_{28}	3.8	4.7	12.0	6.5	57.7	11.5	4.8	2.5	26.6	3.1	4.3	7.0	15.3	8.8	11.7	8.8	0.7	9.5	7.7
C_{29}	11.7	13.5	54.2	24.6	51.5	12.7	21.7	6.4	50.2	4.7	6.8	32.0	53.5	18.6	17.9	56.3	14.0	43.1	32.2
C_{30}	2.3	0.4	6.4	3.7	31.0	8.8	2.9	nf	20.6	0.5	1.8	3.5	7.0	1.9	0.2	7.5	3.2	5.6	4.9
C_{31}	7.8	15.7	45.2	23.2	30.6	2.6	22.7	4.8	57.3	5.5	5.2	23.2	61.0	13.0	25.1	39.2	15.1	33.5	29.1

Station locations as defined in Table 2.1. nf: not found in sediment sample.

Table A2.2. Concentration of C_{14}-C_{28} *n*-alcohols (in µg/g OC) in surface sediment samples (0-1 cm) in the western Arctic Ocean

	STN 1	STN 2	WHS-2	WHS-5	WHS-6	WHS-7	WHS-12	EHS-4	EHS-6	EHS-9	EHS-11	EHS-12	BC-3	BC-4	BC-5	BC-7	EB-2	EB-4	EB-7
C_{14}	8.4	3.7	14.7	4.4	nf	1.6	4.4	1.9	6.2	2.4	1.3	5.3	nf	5.5	6.3	9.5	13.6	17.5	3.6
C_{15}	6.5	1.4	7.9	4.7	nf	nf	nf	1	5.1	nf	nf	3.5	3.1	1.8	1.9	7.0	6.0	12.0	3.1
C_{16}	27.3	16.4	61.5	17.7	8.9	4.2	14.6	10.5	47	8.4	7.7	19.3	7.8	30.3	32.0	44.3	35.5	60.7	22.5
C_{17}	3.2	2.5	17.8	3	6.8	nf	nf	3.1	13	1.7	1.6	3.2	4.2	9.2	10.2	9.2	13.2	24.9	4.8
C_{18}	11.3	8.7	37.2	14.3	9.1	3.8	10.6	5.8	25.9	5.1	6.1	14.1	4.4	18.1	26.6	28.9	22.0	41.4	13.7
C_{19}	2.1	2.0	9.3	6.7	nf	nf	nf	1.7	9.1	1.4	1.5	3.2	2.6	3.3	5.2	8.1	3.6	8.6	3.4
C_{20}	27.1	18	73.1	23.7	9.5	7.1	19	11.8	48.2	13.1	13.6	24.6	13.1	60.6	61.9	70.3	27.6	80.7	35.9
C_{21}	1.3	5.6	20.1	7.2	3.8	1.5	5.4	3.5	13.3	2.8	2.6	7.5	4.5	11.9	15.1	17.5	6.8	17.6	8.0
C_{22}	63.5	39.8	186.1	57.7	24.3	10.2	47.8	27.5	124.9	20.4	16.8	64.4	32.2	99.0	114.5	146.9	50.6	131.6	76.4
C_{23}	11.4	7.3	33.9	11.8	5.1	2.8	8.7	4.7	21.9	3.4	3.5	11.5	5.2	13.8	20.7	27.4	9.8	26.4	12.1
C_{24}	44.8	31.8	148.9	47.5	20.0	5.2	40.3	18.1	92.9	11.4	8.7	53.1	19.3	63.2	77.1	110.5	40.5	103.5	59.7
C_{25}	3.1	nf	26.6	10.3	5.5	nf	8.5	0.4	15.3	2.0	1.9	11.9	4	2.7	4.6	25.3	6.8	15.6	8.8
C_{26}	36.9	31.1	154.5	63.9	31.0	4.4	60.3	15.2	106.8	10.0	7.1	79.9	23.2	46.2	78.1	136.2	38.6	98.9	65.1
C_{27}	6.5	nf	26.2	6.9	7.8	nf	6.4	nf	18.3	nf	nf	8.0	2.0	nf	4.7	24.9	7.4	15.8	10.3
C_{28}	34.2	32.3	99.6	45.5	26.2	2.4	53.6	12.8	80.7	7.6	5.3	5.5	22.2	34.8	64.7	109.6	38.1	99.5	64.4

Station locations as defined in Table 2.1. nf: not found in sediment sample.

Table A2.3. Concentration of selected sterols, phytol, and a-amyrin (in μg/g OC) in surface sediment samples (0-1 cm) among the 19 sites of the western Arctic Ocean

	STN 1	STN 2	WHS2	WHS5	WHS6	WHS7	WHS-12	EHS-4	EHS-6	EHS-9	EHS-11	EHS-12	BC-3	BC-4	BC-5	BC-7	EB-2	EB-4	EB-7
$C_{26}\Delta^{5,22}$	23.3	23.0	73.7	21.6	26.0	0.7	12.1	26.6	41.0	3.3	1.7	20.1	10.1	25.1	32.0	42.5	9.8	17.0	5.9
$C_{26}\Delta^{22}$	9.0	6.8	21.5	4.2	3.7	1.6	nf	5.0	15.1	2.0	1.9	3.4	5.1	9.0	9.4	11.0	3.6	6.7	4.1
$C_{27}\Delta^{5,22}$	29.0	20.0	64.9	12.1	7.6	2.7	7.1	28.4	39.4	6.4	4.6	5.5	6.5	30.4	50.4	36.1	46.7	74.7	19.4
$C_{27}\Delta^{22}$	13.2	6.4	20.1	5.1	3.0	0.9	4.5	6.5	17.0	2.0	1.9	2.7	11.8	9.6	11.2	14.9	6.7	12.6	4.2
$C_{27}\Delta^{5}$	119.7	52.8	214.0	40.0	16.6	7.1	47.3	157.2	128.0	17.0	11.6	13.8	24.0	130.6	377.3	80.7	190.3	251.9	59.3
$C_{28}\Delta^{5,22}$	98.4	55.5	172.6	18.0	8.2	3.6	7.8	65.1	68.5	10.7	6.5	14.7	24.2	93.6	83.4	67.4	169.8	234.0	48.5
$C_{28}\Delta^{22}$	19.0	8.9	46.2	5.8	nf	nf	3.5	10.7	19.8	2.7	nf	5.5	nf	19.1	13.8	18.2	12.6	23.4	13.6
$C_{28}\Delta^{5,24(28)}$	82.5	29.3	97.4	20.8	8.3	4.1	8.7	38.1	53.2	10.2	6.6	20.7	17.9	46.3	70.6	63.1	163.5	200.8	35.5
$C_{28}\Delta^{5}$	93.9	34.0	134.9	12.8	8.9	3.9	8.2	35.0	41.3	7.8	5.4	9.8	21.2	56.1	95.5	32.8	73.2	72.9	78.0
$C_{29}\Delta^{5}$	94.2	94.3	122.6	45.5	17.1	12.0	37.3	50.1	86.9	29.2	26.7	38.2	52.1	169.2	191.6	150.5	161.1	419.4	141.2
$C_{29}\Delta^{5,24(28)Z}$	23.8	18.6	42.4	9.1	3.0	1.1	5.3	11.3	25.5	3.1	2.0	7.5	22.4	25.0	29.5	51.4	nf	75.6	0.0
$C_{29}\Delta^{7}$	0.3	3.3	nf	0.9	nf	0.1	nf	3.3	2.1	0.1	0.1	0.6	3.1	6.8	4.6	5.1	8.8	29.9	8.6
$C_{30}\Delta^{22}$	21.5	15.4	51.2	12.4	3.4	2.5	6.5	13.7	30.0	6.1	nf	9.7	14.8	23.5	31.5	33.2	23.0	38.2	31.2
$C_{30}\Delta^{5,24(28)}$	5.1	9.3	25.1	4.6	2.1	0.4	3.5	9.0	9.2	2.1	1.1	2.6	16.8	9.4	9.6	17.4	7.6	17.2	9.8
$C_{30}\Delta^{8(14)}$	11.7	6.3	32.3	3.7	2.8	nf	1.5	9.1	16.7	nf	nf	2.4	5.1	11.7	8.5	16.3	31.3	47.7	19.1
α-Amyrin	4.1	3.6	14.1	4.4	1.9	0.6	2.3	1.7	5.5	1.2	1.5	4.4	3.9	14.6	12.0	18.0	54.0	56.9	19.1
Phytol	256.1	96.0	434.6	42.5	26.7	6.2	13.2	61.3	154.6	22.0	11.7	24.5	41.5	100.2	126.0	176.7	408.5	609.4	83.6

Station locations as defined in Table 2.1. Sterol abbreviations as defined in Table 2.2. nf: not found in sediment sample.

Table A2.4. Concentrations of fatty acids (in μg/g OC) in surface sediment samples (0-1 cm) among the 19 sites of the western Arctic Ocean

	STN 1	STN 2	WHS-2	WHS-5	WHS-6	WHS-7	WHS-12	EHS-4	EHS-6	EHS-9	EHS-11	EHS-12	BC-3	BC-4	BC-5	BC-7	EB-2	EB-4	EB-7
14:0n	473	463	580	84	45	9	65	254	231	49	24	83	665	413	220	190	1079	1838	100
15:0n	130	29	177	26	13	5	18	11	46	15	38	22	161	74	53	51	162	198	28
16:0n	1009	1192	1433	313	161	64	226	693	713	208	173	287	1404	995	936	691	2134	2927	356
17:0n	50	51	66	19	13	6	13	21	31	9	10	18	58	28	38	35	46	54	14
18:0n	96	131	201	64	40	53	53	65	114	27	30	63	206	82	276	126	149	178	64
20:0n	37	67	107	39	18	10	38	16	69	14	18	50	153	57	77	95	47	89	42
21:0n	10	21	29	14	8	4	12	5	21	6	7	16	46	16	30	30	10	20	11
22:0n	59	107	162	55	37	16	65	26	104	24	20	76	310	93	154	148	53	109	59
23:0n	23	53	59	24	16	5	21	11	42	12	11	29	139	33	83	58	19	39	21
24:0n	98	208	254	96	66	17	79	43	179	43	26	108	545	119	279	187	61	144	80
25:0n	21	51	62	28	24	4	25	10	50	11	5	33	110	23	67	38	12	24	15
26:0n	57	135	160	68	54	10	60	27	146	25	15	80	303	53	150	76	29	62	39
27:0n	9	24	26	14	11	2	13	4	29	5	6	18	46	7	25	11	4	7	5
28:0n	22	50	52	27	21	4	23	8	63	7	10	33	129	17	52	tr	11	23	14
16:1ω9	162	58	177	19	5	nf	19	27	75	5	nf	28	136	102	41	190	108	nf	38
16:1ω7	2206	904	2214	133	26	1	285	622	795	36	2	228	2238	2189	426	736	6089	10172	552
16:1ω5	160	74	184	29	7	nf	32	40	87	8	55	42	108	89	54	191	160	184	55
17:1ω8	94	33	83	9	9	nf	10	15	22	2	nf	15	70	40	16	34	114	100	15
17:1ω6	72	31	68	26	9	2	19	14	47	8	nf	28	49	35	18	80	67	69	18
18:1ω9	281	199	443	73	68	5	87	173	199	32	23	99	297	272	201	238	695	388	79
18:1ω7	691	565	691	93	46	1	140	162	317	30	4	145	473	406	257	537	466	393	156
20:1ω9	33	76	43	36	15	20	8	8	58	11	36	12	137	66	78	37	173	41	12
20:1ω7	57	31	53	7	4	3	12	21	13	5	6	6	44	57	22	20	102	60	10
16:2	153	33	80	8	4	1	6	25	29	4	nf	5	38		27	26	nf	nf	17
18:2	60	49	83	nf	13	nf	9	16	35	6	nf	10	80	66	32	59	118	132	21
18:2	71	24	45	7	8	nf	7	10	18	2	2	6	26	14	2	21	33	27	11
20:4	94	46	148	nf	nf	nf	4	16	48	nf	nf	3	279	115	12	48	422	235	38
20:5	636	75	623	nf	nf	nf	11	62	78	nf	nf	10	1060	365	43	61	2907	3822	207
14:0i	49	50	64	22	12	2	9	20	31	12	6	12	42	21	14	39	33	40	7
15:0i	123	138	163	85	43	15	37	65	103	57	47	49	95	69	80	160	83	92	29

Table A2.4. (cont.) Concentrations of fatty acids (in μg/g OC) in surface sediment samples (0-1 cm) among the 19 sites of the western Arctic Ocean.

	STN 1	STN 2	WHS-2	WHS-5	WHS-6	WHS-7	WHS-12	EHS-4	EHS-6	EHS-9	EHS-11	EHS-12	BC-3	BC-4	BC-5	BC-7	EB-2	EB-4	EB-7
15:0a	299	236	328	109	58	23	57	138	147	83	64	78	168	122	113	219	141	146	47
16:0i	39	63	55	26	14	7	14	18	3	17	16	18	11	41	32	66	nf	429	13
17:0br	59	32	64	48	nf	14	23	30	42	26	27	32	19	22	47	42	16	23	8
17:0i	25	45	33	14	8	4	9	15	21	9	8	11	40	20	36	38	50	32	11
17:0a	25	56	52	19	12	7	15	20	24	13	13	18	44	29	35	46	51	40	13
C20 DCA	3	6	10	4	5	1	3	nf	3	1	3	3	16	8	9	9	2	5	4
C21 DCA	nf	3	6	5	4	1	3	nf	4	nf	1	4	6	2	4	6	nf	nf	nf
C22 DCA	7	14	20	13	6	1	4	3	12	3	10	6	43	15	21	17	4	8	5
C23 DCA	nf	4	6	5	1	nf	2	nf	5	nf	nf	4	8	2	5	7	nf	nf	nf
C24 DCA	3	10	17	8	6	2	4	nf	10	2	3	8	31	5	12	12	nf	2	2
C25 DCA	nf	nf	7	20	7	1	4	nf	14	1	nf	6	12	3	6	1	nf	nf	1
C26 DCA	2	6	11	6	5	nf	4	1	8	1	9	8	20	3	8	8	nf	nf	nf

Station locations as defined in Table 2.1. DCA: dicarboxylic acid, ω: double bond position counted from terminal methyl end, listed where determined, i: iso, a: anteiso, br: branched, nf: not found in sediment sample, tr: <1 μg/g OC.

Table A2.5. Concentration of five major glycerol dialkyl glycerol tetraether lipids (in μg/g OC) in surface sediment samples (0-1 cm) in the western Arctic Ocean and calculated BIT index.

	STN 1	WHS-2	WHS-5	WHS-6	WHS-7	WHS-12	EHS-4	EHS-6	EHS-9	EHS-11	EHS-12	BC-3	BC-4	BC-5	BC-7	EB-2	EB-4	EB-7
I (1022)	0.4	1.0	0.1	0.1	0.4	0.3	0.1	0.3	0.4	0.6	0.1	1.4	1.2	0.5	0.3	0.4	0.7	0.3
II (1036)	0.8	1.7	0.1	0.1	0.4	0.1	0.1	0.3	0.5	0.8	0.1	3.0	2.3	0.8	0.4	0.7	1.6	0.1
III (1050)	0.7	2.6	0.2	0.1	0.6	0.2	0.2	0.5	0.7	0.9	1.2	2.8	2.0	0.6	0.4	0.6	1.4	0.1
IV (1292)	12.0	104.9	10.8	3.0	14.8	0.7	7.4	36.6	39.3	43.2	9.5	33.5	44.6	13.6	27.0	7.4	9.6	3.8
V (1302)	14.4	102.2	15.8	5.4	29.9	1.6	8.8	54.4	59.3	73.5	4.3	41.6	52.9	25.2	46.2	11.1	20.2	6.7
BIT	0.13	0.05	0.03	0.07	0.09	0.46	0.05	0.03	0.04	0.05	0.13	0.18	0.11	0.12	0.04	0.19	0.28	0.11

Station names as defined in Table 2.1. Tetraether structures are presented in figure 2.2. STN 2 did not have adequate sediment amounts for analysis and is excluded.

Table A3.1. Distribution (%) and total concentration of fatty acids in western Arctic POM samples.

Fatty Acid	EHS-12 50m	EHS-12 524m	EHS-12 1000m	EHS-12 3669m	ACW-1 10m	ACW-1 38m	ACW-2 10m	ACW-2 28m	BC-1 15m	BC-1 60m	BC-2 15m	BC-2 50m
14:0n	8.4	3.7	3.6	4.4	6.8	13.1	5.1	9.1	10.7	6.3	7.1	7.8
15:0n	0.5	1.8	2.3	2.8	1.4	1.2	0.8	3.1	0.7	0.8	0.5	0.7
16:0n	14.3	24.4	29.4	33.0	26.2	27.2	37.1	38.3	25.1	25.4	22.0	23.6
17:0n	0.2	1.2	1.8	1.9	1.1	1.0	2.5	2.5	0.2	0.4	0.1	0.3
18:0n	1.5	11.8	18.3	20.7	4.9	3.6	8.6	8.8	1.1	2.9	0.8	3.1
16:1ω9	--	2.1	3.1	4.0	0.7	0.6	0.9	2.9	0.2	0.4	0.1	0.3
16:1ω7	13.0	12.4	3.9	2.7	16.5	11.4	18.2	11.0	44.3	37.0	46.9	40.6
16:1ω5	1.2	0.4	0.2	0.3	3.4	5.3	3.4	3.9	1.0	1.3	0.6	1.4
17:1ω8	0.1	1.0	0.8	0.8	0.1	0.5	0.7	0.9	0.2	0.4	0.1	0.4
17:1ω6	0.04	0.1	0.1	0.1	0.2	0.1	0.2	0.1	0.1	0.2	0.1	0.2
18:1ω9	6.2	26.3	15.1	17.1	6.8	4.5	5.6	5.8	2.7	3.9	1.8	3.5
18:1ω7	2.7	9.5	9.5	5.5	6.0	7.8	5.2	2.1	1.7	3.8	0.9	3.3
16:4	1.2	--	--	--	0.8	0.4	--	0.3	1.1	0.7	2.2	0.9
18:4	6.4	--	--	--	3.0	2.1	1.6	1.6	1.4	2.1	3.2	2.1
18:2	3.6	3.0	2.5	3.3	2.7	3.0	1.9	1.0	0.8	1.9	1.0	1.1
18:2	0.3	0.8	1.3	1.1	0.8	--	1.8	1.3	0.3	--	0.1	--
20:5	16.6	2.9	0.9	0.6	2.9	4.7	--	--	5.4	8.6	10.2	7.1
15:0i	0.6	0.6	0.6	0.6	1.7	1.4	0.9	0.8	0.5	0.6	0.1	0.6
15:0a	0.3	0.6	0.6	0.7	1.3	1.0	1.0	0.9	0.2	0.4	0.1	0.5
17:0i	0.3	0.3	0.3	0.4	0.3	0.2	0.2	0.5	0.2	0.4	0.4	0.2
17:0a	0.2	0.5	0.6	0.6	0.1	0.1	0.2	0.5	0.1	0.2	--	0.1
Total (μg/mg OC)	452	161	60	54	68	70	35	147	80	51	151	55

Table A3.1. (cont.) Distribution (%) and total concentration of fatty acids in western Arctic POM samples.

Fatty Acid	BC-3 24m	BC-3 65m	BC-3 150m	BC-4 22m	BC-4 100m	BC-6 25m	BC-6 50m	BC-6 170m	BC-6 300m	BC-6 800m	BC-6 1500m	BC-7 42m
14:0n	10.1	--	6.8	12.9	8.5	11.8	9.6	5.6	4.9	2.1	6.7	13.8
15:0n	0.5	--	0.8	0.6	1.7	0.6	1.2	1.2	2.0	2.5	3.5	0.7
16:0n	20.2	26.2	27.0	25.2	25.9	22.9	25.4	26.1	52.7	29.8	29.2	26.1
17:0n	0.1	0.6	0.5	0.1	0.9	0.1	0.5	0.5	2.2	1.5	1.3	0.3
18:0n	0.6	5.7	2.6	1.0	6.0	1.2	0.1	4.0	15.8	12.0	7.6	2.3
16:1ω9	--	0.3	0.7	0.3	3.4	--	1.9	1.3	--	12.9	16.0	0.5
16:1ω7	46.7	23.7	40.6	43.1	26.4	38.7	26.8	26.3	0.3	4.6	4.8	32.8
16:1ω5	0.5	1.8	1.0	1.1	1.4	1.4	2.1	1.7	0.1	0.3	0.4	1.3
17:1ω8	0.1	0.5	0.5	0.2	0.8	0.1	0.5	0.6	2.7	1.9	1.8	0.2
17:1ω6	0.1	0.2	0.2	0.1	0.2	0.1	0.3	0.2	0.8	0.2	0.2	0.1
18:1ω9	1.7	10.2	2.7	2.3	5.2	3.0	4.7	5.1	1.6	16.6	11.5	2.0
18:1ω7	0.9	5.9	2.9	1.7	4.2	1.6	4.0	5.1	--	2.3	1.9	2.0
16:4	2.4	--	0.8	1.0	0.6	1.1	1.6	0.4	--	0.1	0.1	0.6
18:4	2.3	3.2	1.8	1.7	1.7	1.8	2.7	1.9	0.8	1.6	1.7	1.7
18:2	1.2	5.0	1.5	1.7	1.3	2.1	1.6	1.2	1.4	2.6	1.3	3.5
18:2	--	1.1	--	--	0.6	0.2	0.5	0.7	--	1.6	0.4	0.5
20:5	10.4	12.1	6.8	4.4	5.5	8.0	10.1	6.1	--	--	1.1	7.7
15:0i	0.1	--	0.4	0.3	1.0	0.3	0.9	1.0	1.1	0.7	1.2	0.4
15:0a	0.1	--	0.3	0.2	0.9	0.2	0.6	0.7	1.1	0.6	1.1	0.3
17:0i	0.3	0.3	0.4	0.2	0.2	0.2	0.3	0.3	0.6	0.3	0.4	0.2
17:0a	--	0.2	0.1	0.1	0.3	0.1	0.2	0.2	--	0.3	0.3	0.1
Total (μg/mg OC)	207	38	65	170	38	238	52	32	8	68	82	105

Table A3.1. (cont.) Distribution (%) and total concentration of fatty acids in western Arctic POM samples.

Fatty Acid	BC-7 90m	BC-7 170m	BC-7 1000m	BC-7 2000m	BC-7 3000m	BRS-1 15m	BRS-5 15m	EB-1 14m	EB-1 35m	EB-2 25m	EB-2 90m	EB-3 35m
14:0n	2.5	1.4	3.8	4.4	2.9	1.6	4.2	4.3	3.9	5.0	4.5	7.5
15:0n	1.2	0.7	3.7	2.9	2.1	0.8	0.6	0.7	0.9	1.5	0.8	1.6
16:0n	34.3	26.6	39.3	29.4	29.9	41.0	19.5	17.3	23.6	22.2	22.9	31.8
17:0n	1.0	1.0	2.6	1.7	1.4	1.6	0.3	0.4	0.4	--	--	0.8
18:0n	6.9	9.5	16.5	9.7	13.4	13.8	2.2	1.6	2.9	8.5	3.2	7.4
16:1ω9	3.3	2.2	4.4	12.6	8.2	1.0	0.6	0.6	0.6	--	--	2.5
16:1ω7	17.5	20.8	3.8	1.9	6.6	8.5	19.3	12.5	21.7	12.6	23.6	18.3
16:1ω5	3.2	1.7	0.8	0.2	0.8	3.1	1.1	5.1	3.8	7.6	4.4	3.1
17:1ω8	1.2	0.8	1.1	1.1	1.2	0.7	0.3	0.5	0.6	0.2	0.4	0.7
17:1ω6	0.4	0.5	0.4	0.2	--	0.4	0.1	0.1	0.2	0.6	0.5	0.1
18:1ω9	7.6	16.5	6.8	18.6	14.6	10.5	5.0	1.7	6.2	6.3	4.1	5.8
18:1ω7	5.4	7.8	2.0	2.8	5.0	9.7	6.6	3.2	7.8	10.0	6.7	5.9
16:4	--	--	0.1	--	--	--	1.5	0.8	0.2	--	--	0.4
18:4	--	--	0.6	--	--	--	3.0	16.5	1.7	--	--	1.1
18:2	1.9	1.4	0.6	3.2	1.9	3.0	1.8	3.1	1.4	2.3	2.1	1.7
18:2	1.7	2.2	0.9	0.8	1.0	--	0.2	0.3	2.2	--	0.6	0.5
20:5	4.5	--	--	--	--	--	15.8	11.3	8.6	7.9	11.3	1.2
15:0i	0.6	0.5	0.9	1.0	0.9	0.3	0.6	--	--	1.0	1.0	1.2
15:0a	0.6	0.6	1.0	0.9	0.9	0.5	0.4	--	--	0.2	1.0	0.9
17:0i	0.5	0.4	0.5	0.5	0.4	0.5	0.3	--	--	0.3	0.7	0.2
17:0a	0.4	0.3	0.5	0.5	0.5	0.5	0.2	--	--	1.0	0.5	0.2
Total (µg/mg OC)	24	12	61	139	43	57	38	49	76	70	83	113

Table A3.1. (cont.) Distribution (%) and total concentration of fatty acids in western Arctic POM samples.

Fatty Acid	EB-3 80m	EB-3 120m	EB-4 20m	EB-4 120m	EB-5 30m	EB-5 113m	EB-5 170m	EB-5 300m	EB-5 800m	EB-6 15m	EB-6 30m	EB-6 45m
14:0n	7.6	4.2	2.1	5.6	12.9	3.7	2.8	2.7	3.6	15.9	12.3	10.9
15:0n	1.3	1.1	0.5	0.8	0.8	1.1	0.9	1.4	1.2	0.6	0.8	1.2
16:0n	32.1	23.7	20.9	28.7	27.8	31.2	32.1	29.2	30.0	25.6	23.6	26.9
17:0n	0.8	1.4	--	--	0.4	1.1	2.0	1.6	2.5	0.1	0.3	0.6
18:0n	2.4	3.2	2.4	2.4	1.0	3.9	7.6	5.8	8.7	1.0	1.1	1.3
16:1ω9	0.9	0.3	--	--	0.5	0.4	1.0	5.1	1.8	0.0	0.5	1.0
16:1ω7	25.7	19.4	22.6	29.3	28.6	28.0	21.7	28.3	27.9	43.5	34.3	39.1
16:1ω5	4.5	1.6	3.3	1.6	3.5	2.7	1.9	2.0	1.7	0.8	1.9	2.3
17:1ω8	0.5	2.1	0.5	0.5	0.2	0.3	0.8	1.3	1.0	0.0	0.1	0.2
17:1ω6	0.1	0.3	1.0	1.3	0.1	0.2	0.3	0.4	0.3	0.0	0.1	0.1
18:1ω9	3.3	5.3	6.3	5.5	2.8	4.3	5.9	8.3	7.4	1.7	3.6	2.3
18:1ω7	8.1	8.1	7.8	6.8	2.7	5.8	6.7	4.5	4.6	1.1	2.8	3.6
16:4	0.4	0.3	0.4	--	0.8	1.1	0.2	0.3	0.2	0.5	1.9	1.2
18:4	0.6	0.4	1.4	0.6	0.8	1.6	1.5	1.0	0.7	1.5	2.1	0.8
18:2	0.9	2.4	5.6	1.3	0.6	1.5	2.1	1.5	1.0	4.2	2.0	0.7
18:2	1.1	0.3	3.9	--	0.9	0.5	0.6	0.5	2.1	0.2	0.2	0.9
20:5	--	5.6	8.5	4.3	5.4	3.3	2.3	--	--	1.4	6.3	--
15:0i	1.3	0.8	0.5	--	0.6	1.0	0.6	0.7	0.5	0.2	0.6	1.3
15:0a	1.0	0.5	0.8	1.8	0.4	0.6	0.4	0.5	0.5	0.2	0.4	0.9
17:0i	0.3	1.0	0.5	0.5	0.1	0.6	0.4	0.5	0.2	0.1	0.2	0.2
17:0a	0.1	0.3	0.9	1.0	--	0.2	0.3	0.3	0.2	--	0.1	0.1
Total (μg/mg OC)	125	99	46	81	116	80	31	96	21	472	142	156

Table A3.1. (cont.) Distribution (%) and total concentration of fatty acids in western Arctic POM samples.

Fatty Acid	EB-6 133m	EB-6 500m	EB-7 30m	EB-7 130m	EB-7 800m
14:0n	5.9	6.8	11.9	--	1.1
15:0n	1.0	2.3	0.9	2.3	1.4
16:0n	26.9	25.1	18.3	45.9	39.4
17:0n	1.0	0.6	--	--	5.0
18:0n	1.9	5.3	3.0	4.4	23.8
16:1ω9	0.9	5.5	--	--	0.9
16:1ω7	34.8	31.9	35.0	--	4.9
16:1ω5	2.2	1.4	4.3	--	1.0
17:1ω8	0.2	0.9	0.2	21.8	1.6
17:1ω6	0.3	0.1	0.4	7.0	0.8
18:1ω9	4.3	11.0	3.4	5.5	8.7
18:1ω7	5.7	4.4	4.6	5.3	5.5
16:4	1.0	0.1	--	--	--
18:4	1.8	0.6	--	--	--
18:2	1.0	1.5	1.5	--	1.1
18:2	1.6	--	3.4	--	1.3
20:5	2.5	--	6.5	--	--
15:0i	1.2	--	0.2	--	0.4
15:0a	0.8	--	1.1	--	0.6
17:0i	0.6	--	0.3	--	--
17:0a	0.2	--	0.3	2.8	--
Total (µg/mg OC)	68	241	135	34	10

Table A3.2. Distribution (% of total sterols) and total concentration (mg/g OC) of sterols in western Arctic POM samples.

Sterol	EHS-12 50m	EHS-12 524m	EHS-12 1000m	EHS-12 3669m	ACW-1 10m	ACW-1 38m	ACW-2 10m	ACW-2 28m	BC-1 15m	BC-1 60m	BC-2 15m	BC-2 50m
$C_{26}\Delta^{5,22}$	10.2	4.0	2.7	--	14.4	12.5	2.9	4.4	11.4	16.6	15.9	13.8
$C_{26}\Delta^{22}$	0.5	1.1	2.0	--	2.2	1.7	--	1.0	0.7	1.1	0.6	1.2
$C_{27nor}\Delta^{5,22}$	1.6	1.7	1.5	--	2.1	5.6	0.8	--	0.7	1.4	0.6	1.2
$C_{27}\Delta^{5,22}$	8.3	10.7	6.2	1.9	12.7	7.4	6.8	3.8	7.6	9.4	4.8	7.8
$C_{27}\Delta^{5}$	12.4	51.0	43.2	58.9	25.1	20.1	21.2	49.0	14.5	12.9	17.0	29.0
$C_{27}\Delta^{0}$	--	--	--	--	3.1	1.5	1.5	4.8	0.5	0.9	0.4	1.6
$C_{28}\Delta^{5,22}$	20.2	6.0	5.8	3.5	11.7	11.8	12.2	8.8	22.5	18.8	21.2	13.9
$C_{28}\Delta^{22}$	1.5	1.5	3.1	3.4	0.0	2.0	2.1	1.3	0.8	1.3	0.5	1.1
$C_{28}\Delta^{5,24(28)}$	25.7	9.1	7.7	8.1	17.8	13.4	25.2	15.9	28.7	17.7	28.7	13.8
$C_{28}\Delta^{5}$	--	5.8	--	--	--	2.2	1.8	--	2.2	4.2	1.8	2.5
$C_{28}\Delta^{0}$	--	--	--	--	--	1.9	--	--	0.6	1.0	0.7	0.8
$C_{29}\Delta^{5,22}$	--	--	--	--	--	--	1.5	--	0.7	1.1	0.4	0.7
$C_{29}\Delta^{5}$	1.9	10.8	20.6	19.9	3.6	3.0	4.1	2.9	3.2	4.2	2.0	4.0
$C_{29}\Delta^{5,24(28)Z}$	11.0	2.8	4.4	--	7.3	10.1	9.6	6.8	2.0	4.4	2.0	3.3
Dinosterol	--	--	--	--	--	3.1	1.5	--	0.5	1.1	0.5	0.9
Total Sterols (μg/mg OC)	21.6	12.2	4.3	6.0	2.5	2.9	4.7	2.5	3.0	2.3	3.3	2.8

Table A3.2. (cont.) Distribution (% of total sterols) and total concentration (mg/g OC) of sterols in western Arctic POM samples.

Sterol	BC-3 24m	BC-3 65m	BC-3 150m	BC-4 22m	BC-4 100m	BC-6 25m	BC-6 50m	BC-6 170m	BC-6 300m	BC-6 800m	BC-6 1500m	BC-7 42m
$C_{26}\Delta^{5,22}$	12.2	22.7	22.5	13.4	15.7	19.3	20.7	32.8	12.9	4.2	2.5	15.8
$C_{26}\Delta^{22}$	0.5	1.7	2.0	0.8	0.9	1.3	1.3	1.4	5.0	1.9	0.7	1.8
$C_{27nor}\Delta^{5,22}$	0.6	1.7	1.4	0.7	1.1	0.9	0.9	1.4	1.5	3.7	1.4	0.8
$C_{27}\Delta^{5,22}$	5.2	10.5	10.0	4.9	8.1	7.9	7.6	12.4	9.0	2.1	0.9	6.4
$C_{27}\Delta^{5}$	11.3	20.7	23.7	10.0	33.9	16.4	16.9	14.0	28.2	71.3	79.8	11.2
$C_{27}\Delta^{0}$	0.3	2.1	1.7	0.4	1.5	0.9	1.0	1.2	2.7	3.3	1.7	0.9
$C_{28}\Delta^{5,22}$	19.4	13.2	15.4	16.1	12.3	14.1	18.9	11.5	14.6	3.0	2.0	30.1
$C_{28}\Delta^{22}$	0.4	1.2	--	0.8	0.8	1.3	2.1	1.1	--	--	0.6	1.8
$C_{28}\Delta^{5,24(28)}$	40.2	10.4	11.4	35.2	8.4	24.0	13.7	8.2	8.6	2.2	1.8	7.1
$C_{28}\Delta^{5}$	2.8	6.7	8.0	2.1	3.6	6.3	5.3	4.9	6.7	0.6	0.8	1.9
$C_{28}\Delta^{0}$	0.7	--	--	0.8	0.9	--	1.5	1.2	3.3	0.9	0.3	1.6
$C_{29}\Delta^{5,22}$	0.4	--	--	0.9	0.8	--	1.5	1.5	1.3	0.7	0.5	1.9
$C_{29}\Delta^{5}$	2.4	4.0	4.0	1.7	3.9	5.1	4.1	4.8	3.8	2.2	1.8	4.8
$C_{29}\Delta^{5,24(28)Z}$	1.5	3.8	--	2.8	2.9	2.6	2.9	3.0	2.3	0.6	0.9	7.4
Dinosterol	0.2	1.4	--	0.8	1.5	--	--	--	--	--	--	1.9
Total Sterols (μg/mg OC)	2.8	2.2	1.1	4.4	2.8	4.1	2.2	2.4	0.8	4.7	6.6	3.2

Table A3.2. (cont.) Distribution (% of total sterols) and total concentration (mg/g OC) of sterols in western Arctic POM samples.

Sterol	BC-7 90m	BC-7 170m	BC-7 1000m	BC-7 2000m	BC-7 3000m	BRS-1 15m	BRS-5 15m	EB-1 14m	EB-1 35m	EB-2 25m	EB-2 90m	EB-3 35m
$C_{26}\Delta^{5,22}$	16.6	11.5	3.3	3.6	--	13.1	10.0	13.9	12.2	9.9	8.2	9.8
$C_{26}\Delta^{22}$	0.7	1.0	0.7	0.9	--	1.2	0.5	1.1	1.2	--	--	0.6
$C_{27nor}\Delta^{5,22}$	1.4	2.3	1.3	1.0	--	4.3	1.6	0.8	1.0	1.0	--	0.6
$C_{27}\Delta^{5,22}$	6.7	8.5	1.8	0.5	3.1	8.2	4.8	7.3	9.8	6.4	4.5	5.5
$C_{27}\Delta^{5}$	26.4	27.1	68.4	79.1	80.8	23.0	35.5	9.3	21.0	17.1	9.0	25.9
$C_{27}\Delta^{0}$	1.2	1.4	2.0	1.3	3.0	2.3	1.5	--	1.2	0.6	--	1.0
$C_{28}\Delta^{5,22}$	12.7	11.9	3.6	1.1	5.6	12.4	21.2	12.5	19.4	11.2	10.5	9.9
$C_{28}\Delta^{22}$	1.6	1.5	0.5	0.4	--	0.7	0.8	--	--	1.4	--	0.9
$C_{28}\Delta^{5,24(28)}$	8.3	7.4	3.4	1.3	3.5	9.2	11.0	22.0	12.9	14.7	9.0	17.8
$C_{28}\Delta^{5}$	1.6	1.9	1.1	0.6	--	1.2	2.5	--	1.5	1.0	--	1.4
$C_{28}\Delta^{0}$	0.9	1.0	0.6	0.2	--	0.7	0.2	--	1.0	0.9	--	1.1
$C_{29}\Delta^{5,22}$	1.5	1.7	1.3	0.5	--	0.8	0.4	0.6	1.2	1.4	1.6	2.9
$C_{29}\Delta^{5}$	5.4	6.7	3.0	2.4	4.0	4.2	2.7	4.7	3.5	3.4	1.3	3.9
$C_{29}\Delta^{5,24(28)Z}$	5.6	4.5	1.0	0.4	--	15.2	3.8	26.1	4.9	4.1	1.9	3.5
Dinosterol	2.5	2.3	0.6	0.4	--	1.4	0.4	1.6	1.0	0.8	4.7	1.2
Total Sterols (μg/mg OC)	1.8	1.1	5.6	11.7	2.4	4.9	2.2	4.1	12.8	3.4	1.3	9.3

Table A3.2. (cont.) Distribution (% of total sterols) and total concentration (mg/g OC) of sterols in western Arctic POM samples.

Sterol	EB-3 80m	EB-3 120m	EB-4 20m	EB-4 120m	EB-5 30m	EB-5 113m	EB-5 170m	EB-5 300m	EB-5 800m	EB-6 15m	EB-6 30m	EB-6 45m
$C_{26}\Delta^{5,22}$	12.3	7.8	--	22.8	10.4	17.1	17.6	6.5	5.9	12.8	11.5	14.9
$C_{26}\Delta^{22}$	0.9	0.7	--	--	0.7	0.9	0.8	0.7	0.5	0.7	0.5	0.7
$C_{27nor}\Delta^{5,22}$	0.8	2.0	--	1.8	0.7	1.4	1.3	1.0	1.3	1.2	0.5	1.0
$C_{27}\Delta^{5,22}$	7.2	12.1	--	10.3	4.6	7.7	9.3	5.0	6.4	7.4	5.6	7.4
$C_{27}\Delta^{5}$	12.6	30.3	--	20.1	7.5	11.9	22.7	52.5	37.8	10.4	11.0	12.9
$C_{27}\Delta^{0}$	0.8	1.0	--	1.0	0.5	0.9	1.4	2.2	2.0	0.9	0.7	0.8
$C_{28}\Delta^{5,22}$	15.2	28.9	42.9	17.3	12.2	15.1	15.0	10.5	13.5	15.9	18.0	18.8
$C_{28}\Delta^{22}$	1.0	1.1	--	--	1.1	1.2	1.1	0.7	1.4	1.5	1.5	1.2
$C_{28}\Delta^{5,24(28)}$	15.2	7.7	23.1	10.5	39.1	12.5	11.1	5.8	9.2	21.3	32.1	20.0
$C_{28}\Delta^{5}$	2.9	1.4	--	5.2	1.1	3.5	3.5	1.9	4.9	1.5	1.5	2.5
$C_{28}\Delta^{0}$	1.8	0.4	--	2.5	0.8	1.8	1.4	0.0	2.2	0.8	1.0	1.1
$C_{29}\Delta^{5,22}$	2.8	0.3	--	--	1.4	2.0	1.6	1.5	2.5	1.4	1.0	1.8
$C_{29}\Delta^{5}$	4.1	0.6	8.0	--	2.6	7.3	4.8	4.0	1.7	6.8	6.4	2.3
$C_{29}\Delta^{5,24(28)Z}$	4.9	2.2	17.2	3.3	2.6	5.6	3.1	2.2	1.8	7.0	4.3	4.3
Dinosterol	1.0	0.5	--	2.8	1.5	2.6	2.2	2.2	2.5	1.8	--	1.0
Total Sterols (μg/mg OC)	6.8	30.2	0.1	1.9	16.3	6.5	3.5	4.6	1.6	5.8	8.0	6.5

Table A3.2. (cont.) Distribution (% of total sterols) and total concentration (mg/g OC) of sterols in western Arctic POM samples.

Sterol	EB-6 133m	EB-6 500m	EB-7 30m	EB-7 130m	EB-7 800m
$C_{26}\Delta^{5,22}$	28.7	4.0	12.3	14.5	4.2
$C_{26}\Delta^{22}$	2.1	4.1	--	0.8	2.3
$C_{27nor}\Delta^{5,22}$	1.3	--	1.3	1.3	3.3
$C_{27}\Delta^{5,22}$	11.1	3.1	7.1	10.5	7.0
$C_{27}\Delta^{5}$	12.0	76.3	11.8	22.6	36.3
$C_{27}\Delta^{0}$	1.1	--	0.4	1.8	1.7
$C_{28}\Delta^{5,22}$	14.8	9.4	13.2	11.5	9.0
$C_{28}\Delta^{22}$	--	--	1.5	1.7	--
$C_{28}\Delta^{5,24(28)}$	11.0	3.0	12.8	10.1	6.5
$C_{28}\Delta^{5}$	5.6	--	1.6	2.3	3.6
$C_{28}\Delta^{0}$	--	--	1.6	1.0	1.6
$C_{29}\Delta^{5,22}$	--	--	2.2	2.7	2.0
$C_{29}\Delta^{5}$	4.4	--	4.1	6.6	10.1
$C_{29}\Delta^{5,24(28)Z}$	4.8	--	4.9	3.2	2.1
Dinosterol	3.1	--	1.3	2.8	1.8
Total Sterols (μg/mg OC)	4.5	5.0	6.7	6.4	1.6

Table A4.1. Fatty acid distribution (% of total fatty acids) in EB-2 sediments.

	Depth (cm)														
	0-1	**1-2**	**2-3**	**3-4**	**4-5**	**5-6**	**6-7**	**7-8**	**8-9**	**9-10**	**10-12**	**12-14**	**14-16**	**16-18**	**18-20**
***n*-saturates**															
12:0	0.2	--	--	0.3	0.2	0.3	0.4	0.2	0.2	0.5	0.8	0.6	0.7	0.6	0.4
14:0	6.0	7.8	6.2	6.1	5.8	6.2	6.4	7.1	5.6	6.4	5.1	4.5	4.4	2.5	1.9
15:0	0.9	2.0	2.1	1.7	1.7	2.0	2.3	3.0	2.5	2.5	2.1	1.6	2.4	1.0	0.9
16:0	11.9	13.6	15.1	14.4	14.2	11.7	16.4	17.2	15.9	16.4	15.1	14.7	15.4	13.1	11.1
17:0	0.3	0.6	0.7	0.6	0.6	0.7	1.2	1.4	1.2	1.0	0.9	0.8	1.0	1.0	0.9
18:0	0.8	1.6	1.8	1.6	1.6	2.3	3.2	2.7	3.3	3.3	4.0	3.6	4.2	4.9	4.9
20:0	0.3	1.5	1.3	0.8	0.8	1.9	2.2	1.7	2.7	2.2	3.5	3.2	3.8	5.2	6.1
21:0	0.1	0.2	0.2	0.2	0.2	0.5	0.4	0.3	0.5	0.5	0.9	0.9	1.1	1.3	1.4
22:0	0.3	1.2	1.2	1.0	0.9	3.3	2.8	2.4	3.9	3.4	6.4	6.0	7.3	9.6	11.3
23:0	0.1	0.4	0.4	0.5	0.3	1.5	1.1	1.0	1.6	1.5	3.3	3.4	4.0	5.4	5.6
24:0	0.3	1.5	1.7	1.8	1.1	7.2	4.3	4.2	6.3	6.1	12.6	13.0	15.4	21.6	22.9
25:0	0.1	0.3	0.3	0.3	0.2	1.4	1.1	0.8	1.1	1.2	2.8	3.0	3.4	5.2	5.4
26:0	0.2	0.7	0.5	0.8	0.5	4.3	2.4	1.9	3.8	3.1	6.9	7.5	8.3	13.1	13.6
27:0	tr	--	0.1	0.1	0.1	0.5	0.3	0.2	0.4	0.4	1.0	1.0	1.1	1.9	1.9
28:0	0.1	--	0.2	0.2	0.3	1.3	0.7	0.4	1.4	1.2	2.7	3.0	3.1	5.3	5.5
Monounsaturates (MUFA)															
15:1	0.3	0.7	0.5	0.4	0.4	0.4	0.6	0.6	0.3	0.6	0.3	0.3	--	--	--
16:1n-9	0.6	1.1	1.0	0.8	0.8	0.9	1.2	1.2	1.0	1.0	0.5	0.5	0.3	--	--
16:1n-7	34.1	25.0	22.4	26.3	27.0	12.9	18.6	20.1	14.4	15.5	6.3	9.0	4.0	0.4	0.2
16:1n-5	0.9	3.1	2.4	1.9	1.6	1.9	2.4	3.0	2.1	2.0	0.8	0.7	0.6	0.1	tr
17:1n-8	0.6	1.0	0.9	0.7	0.8	0.6	0.8	0.8	1.0	0.8	0.3	0.3	0.2	0.1	--
17:1n-6	0.4	0.7	0.7	0.6	0.6	0.5	0.5	0.7	0.8	0.6	0.3	0.2	0.2	0.1	0.1
18:1n-9	3.9	2.8	3.4	2.8	2.8	3.1	3.1	3.6	3.5	3.6	2.4	2.2	1.8	0.4	0.3
18:1n-7	2.6	3.2	4.6	3.7	4.8	3.1	3.3	2.9	2.5	2.4	2.6	2.4	1.7	0.7	0.3
18:1n-5	0.2	--	0.4	0.4	0.4	0.3	0.6	0.4	0.2	0.2	0.1	0.1	0.1	--	--
20:1n-9	1.0	1.3	1.2	0.8	0.6	0.3	1.0	0.2	0.7	0.7	0.5	0.6	0.3	tr	0.1
20:1n-7	0.6	1.2	1.2	0.7	0.8	0.5	0.6	0.1	0.3	0.3	0.4	0.6	0.6	0.1	--
22:1	0.1	--	0.2	0.1	0.2	0.4	0.2	0.2	0.5	0.2	0.5	0.3	0.2	--	--
Polyunsaturates (PUFA)															
16:4	3.9	1.5	1.4	1.4	1.3	1.5	0.9	0.9	0.9	1.2	0.1	0.2	0.1	--	--
16:2	1.7	1.0	0.9	0.9	0.8	0.6	0.7	0.2	0.6	0.7	tr	0.1	0.1	--	--
16:2	--	3.2	1.4	1.0	0.8	0.8	1.7	2.2	1.1	1.2	2.5	3.2	1.4	0.5	tr
18:4	1.7	0.8	0.8	0.8	0.8	0.5	0.5	0.4	0.6	0.1	0.2	0.2	tr	--	--
18:2	0.7	0.7	1.0	0.9	1.1	0.7	0.6	0.3	1.0	0.9	0.6	0.6	0.6	0.2	0.1
18:2	0.2	--	0.5	0.7	0.8	0.3	1.1	0.6	0.6	0.5	0.8	0.7	0.4	0.3	0.1
20:4	2.4	0.7	1.3	0.7	1.0	1.3	0.4	0.4	0.5	0.3	0.2	0.2	0.1	--	--

Table A4.1. (cont.) Fatty acid distribution (% of total fatty acids) in EB-2 sediments.

	Depth (cm)														
	0-1	**1-2**	**2-3**	**3-4**	**4-5**	**5-6**	**6-7**	**7-8**	**8-9**	**9-10**	**10-12**	**12-14**	**14-16**	**16-18**	**18-20**
20:5	16.3	11.0	10.3	10.8	11.0	10.5	3.0	5.5	4.7	5.4	1.6	1.8	1.4	--	--
20:3	0.1	--	--	0.5	0.4	--	1.2	--	0.9	--	0.3	0.3	0.2	--	--
20:4	0.4	--	0.8	0.7	0.7	0.6	1.6	--	0.4	--	0.6	0.4	0.4	0.1	--
20:5	0.2	--	0.5	0.5	0.5	0.4	1.1	--	--	--	0.4	0.4	0.4	--	--
20:2	0.2	--	0.4	0.4	0.3	0.5	--	--	--	--	0.4	0.3	0.3	--	--
20:5	tr	--	0.4	0.5	0.5	0.6	--	--	--	--	--	tr	tr	tr	tr
22:6	1.5	0.4	0.6	0.7	1.0	0.7	0.2	0.1	0.3	0.2	0.2	0.2	0.2	--	--
22:2	0.1	0.5	0.3	0.2	0.4	0.7	0.2	--	--	0.2	0.4	0.3	0.2	--	--
Branched															
14:0i	0.2	0.4	0.4	0.5	0.4	0.5	0.5	0.6	0.7	0.6	0.6	0.4	0.5	0.4	0.3
15:0i	0.5	1.2	1.2	1.3	1.1	1.2	1.3	1.7	1.5	1.7	1.1	1.0	1.2	1.0	0.8
15:0a	0.8	2.8	3.0	2.4	2.3	3.2	3.6	5.2	4.1	4.6	2.8	2.1	2.7	1.3	1.0
16:0i	--	0.9	0.8	0.8	0.7	0.7	0.7	0.7	0.6	0.6	0.4	0.4	0.5	0.4	0.3
17:0br	0.1	0.3	0.4	0.3	0.2	0.4	0.4	0.5	0.5	0.4	--	--	--	--	--
17:0i	0.3	0.7	0.5	1.1	1.0	0.7	0.4	0.3	0.5	0.5	0.5	0.6	0.4	0.4	0.3
17:0a	0.3	0.7	0.8	0.8	0.9	0.8	0.3	0.6	0.7	0.6	0.6	0.5	0.5	0.3	0.3
18:0br	0.1	0.3	--	--	0.1	0.1	--	0.3	--	0.5	--	--	--	--	--
Total % Saturated	21.6	31.5	32.0	30.6	28.6	45.2	45.5	44.6	50.7	49.9	68.4	67.0	76.1	91.7	94.0
Total % MUFA	45.6	40.6	39.3	39.9	41.5	25.5	33.5	34.4	27.9	28.5	15.2	17.6	10.2	1.9	1.0
Total % PUFA	30.3	20.0	21.1	21.7	22.6	20.8	13.5	10.5	11.9	11.1	8.7	9.2	5.9	1.2	0.3
Total % DCA	tr	--	--	--	--	0.5	--	--	0.2	0.4	1.2	0.9	1.5	1.0	1.3
Total % Branched	2.4	7.9	7.6	7.9	7.4	8.0	7.6	10.5	9.3	10.1	6.5	5.3	6.3	4.2	3.3
Total mg/g OC	17.9	3.8	4.5	9.3	7.3	1.4	1.9	1.1	2.8	2.3	4.3	3.4	2.1	1.4	1.9
Total µg/g dry wt.)	164.7	40.8	52.9	107.1	68.8	13.7	19.3	10.3	27.9	22.1	31.4	29.0	19.6	13.0	19.6

Station location is shown in Fig. 4.1. Individual fatty acids with relative abundances <0.5% throughout the core are omitted for brevity. Key: tr: <0.1%, br: branched, i: iso; a: anteiso, w: double bond position counted from terminal methyl group, listed where determined, --: not detected. Total % rows include omitted data.

Table A4.2. Fatty acid distribution (% total fatty acids) in EB-4 sediments.

	Depth (cm)													
	0-1	**1-2**	**2-3**	**3-4**	**4-5**	**6-7**	**7-8**	**8-9**	**9-10**	**10-12**	**12-14**	**14-16**	**16-18**	**18-20**
***n*-saturates**														
12:0	0.2	0.1	0.1	0.4	0.3	0.5	0.5	0.2	0.3	0.5	0.5	0.8	0.6	0.6
14:0	7.5	7.1	5.9	6.5	5.9	6.5	6.5	5.6	5.4	6.6	7.2	7.1	6.8	7.3
15:0	0.8	1.0	0.9	1.3	1.6	1.9	2.5	2.1	2.2	2.7	3.2	3.1	3.4	3.9
16:0	11.9	12.1	11.3	9.6	10.3	10.9	11.8	11.2	11.8	12.3	12.6	14.0	14.2	14.2
17:0	0.2	0.3	0.3	0.4	0.5	0.5	0.6	0.6	0.7	0.6	0.6	0.8	0.8	0.7
18:0	0.7	0.9	1.1	1.3	1.6	1.7	1.7	1.7	2.0	1.7	1.6	2.1	2.2	1.8
20:0	0.4	0.6	0.8	1.0	1.3	0.9	1.4	1.5	2.1	1.4	1.4	1.9	1.9	1.5
21:0	0.1	0.2	0.2	0.3	0.4	0.3	0.4	0.4	0.7	0.4	0.4	0.6	0.6	0.5
22:0	0.4	1.3	1.5	1.5	2.8	1.5	2.8	2.7	4.5	2.9	2.5	3.7	3.7	3.0
23:0	0.2	0.5	0.7	0.5	1.2	0.6	1.2	1.1	1.8	1.3	1.0	1.5	1.6	1.3
24:0	0.6	2.1	2.5	2.0	4.7	2.3	4.4	4.0	6.7	4.5	3.5	5.5	5.9	4.7
25:0	0.1	0.3	0.5	0.4	0.9	0.4	0.8	0.7	1.2	0.8	0.6	1.0	1.0	0.9
26:0	0.3	0.9	1.2	0.8	2.0	0.9	1.7	1.5	2.7	1.8	1.4	2.3	2.6	2.1
28:0	0.1	0.2	0.4	0.3	0.6	0.3	0.5	0.4	0.8	0.6	0.5	0.8	1.0	0.8
Monounsaturates (MUFA)														
Σ15:1	0.3	0.3	0.3	0.5	0.5	0.5	0.7	0.6	0.6	0.5	0.5	0.5	0.5	0.6
16:1n-9	--	0.6	0.5	1.1	1.1	0.9	1.0	1.0	1.3	1.9	1.7	1.5	1.2	1.6
16:1n-7	41.4	34.2	32.2	29.6	22.5	26.0	21.2	23.1	19.0	21.3	20.5	14.0	16.0	15.9
16:1n-5	0.7	0.8	0.8	1.0	1.2	1.0	1.2	1.1	1.4	1.4	1.4	1.6	1.5	1.4
17:1n-8	0.4	0.5	0.5	0.6	0.6	0.8	1.0	0.9	1.0	1.0	0.9	0.8	0.9	0.9
17:1n-6	0.3	0.3	0.3	0.4	0.5	0.5	0.5	0.5	0.6	0.6	0.6	0.5	0.6	0.5
18:1n-9	1.6	2.0	2.2	2.5	3.0	2.4	2.9	2.8	2.9	3.7	4.1	3.7	4.2	3.7
18:1n-7	1.6	3.0	2.6	2.9	2.9	3.7	2.7	2.6	2.3	2.7	2.9	3.6	3.5	3.2
20:1n-9	0.2	0.2	0.3	0.4	0.3	0.6	0.4	0.4	0.2	0.3	0.3	0.5	0.4	0.5
20:1n-7	0.2	0.4	0.4	0.5	0.4	0.6	0.5	0.5	0.3	0.2	0.2	0.3	0.3	0.2
Polyunsaturates (PUFA)														
16:4	3.8	2.2	2.6	3.1	2.2	2.7	2.0	2.3	1.5	1.6	1.8	0.5	0.6	0.6
16:2	--	0.1	--	--	--	--	0.3	0.2	0.6	0.8	0.8	0.3	0.3	0.3
16:2	--	--	--	--	--	--	0.5	--	--	1.1	1.9	6.8	2.9	6.4
18:3	0.1	tr	tr	0.1	0.1	0.1	tr	tr	0.5	tr	--	--	tr	--
18:4	1.8	1.4	1.5	1.2	0.9	0.9	0.8	1.0	0.8	0.7	0.6	0.3	0.5	0.4
18:2	0.5	1.1	0.7	0.8	1.0	0.7	0.9	0.8	0.9	0.9	1.1	0.9	0.9	0.9
18:2	0.1	0.2	0.2	0.2	0.2	0.2	0.2	0.2	0.2	0.2	0.4	1.0	0.6	0.8
20:4	1.0	2.3	1.7	2.1	2.3	1.9	1.6	1.7	1.5	1.4	1.0	0.5	0.7	0.6
20:5	15.5	14.8	17.2	16.6	14.6	16.2	13.8	15.6	10.0	10.8	11.2	3.3	5.3	4.4
20:3	0.1	0.1	0.1	0.1	0.1	0.2	0.1	0.1	--	0.3	0.4	0.6	0.4	0.9

Table A4.2. (continued). Fatty acid distribution (% total fatty acids) in EB-4 sediments.

	Depth (cm)													
	0-1	**1-2**	**2-3**	**3-4**	**4-5**	**6-7**	**7-8**	**8-9**	**9-10**	**10-12**	**12-14**	**14-16**	**16-18**	**18-20**
20:4	0.3	0.3	0.4	0.4	0.4	0.4	0.4	0.4	0.3	0.1	0.3	1.2	0.4	1.5
20:5	0.2	0.1	0.2	0.2	0.1	0.1	0.2	0.2	--	0.4	0.6	0.9	0.6	1.2
20:2	0.1	0.1	0.1	0.1	0.1	0.2	0.1	0.2	0.1	0.2	0.4	1.1	0.3	1.3
22:6	1.1	1.5	1.7	1.6	1.4	1.4	1.0	1.1	0.7	0.7	0.7	0.3	0.5	0.3
22:5	0.2	0.3	0.3	0.4	0.3	0.5	0.3	0.3	0.2	0.1	0.1	0.1	0.1	0.1
22:2	0.1	0.2	0.2	0.2	0.2	0.5	0.2	0.3	0.1	tr	tr	0.1	tr	0.1
Dicarboxylic Acids (DCA)														
22:0	tr	0.1	0.2	0.2	0.4	0.2	0.3	0.3	0.5	0.3	0.3	0.4	0.4	0.3
Branched														
14:0i	0.2	0.2	0.2	0.3	0.4	0.3	0.5	0.3	0.4	0.6	0.5	0.8	0.7	0.6
15:0i	0.4	0.4	0.5	0.6	0.8	0.7	0.9	0.7	1.0	1.1	1.1	1.4	1.4	1.2
15:0a	0.6	0.7	0.8	1.2	1.5	1.3	1.9	1.6	2.1	2.5	2.6	3.3	3.1	2.7
16:0i	1.7	1.3	1.4	1.6	1.3	1.5	1.3	1.4	1.1	0.4	0.4	0.5	0.5	0.5
17:0br	0.1	0.1	0.1	0.2	0.3	0.2	0.3	0.3	0.8	0.3	--	--	--	--
17:0a	0.2	0.2	0.2	0.3	0.4	0.5	0.4	0.4	0.5	0.3	0.5	0.5	0.5	0.5
Total % Saturated	23.5	27.9	27.6	26.5	34.7	29.5	37.1	34.2	43.3	38.8	37.6	45.8	46.9	43.8
Total % MUFA	47.2	42.8	40.6	40.2	33.8	37.7	32.8	34.3	30.3	34.3	33.9	27.6	29.9	29.1
Total % PUFA	25.7	25.6	27.7	27.9	24.8	26.8	23.1	25.3	18.1	20.0	22.0	18.1	14.6	20.1
Total % DCA	0.1	0.2	0.6	0.7	1.4	0.7	0.9	0.9	1.7	0.9	0.9	1.2	1.3	0.9
Total % Branched	3.5	3.4	3.5	4.8	5.3	5.3	6.0	5.4	6.6	6.0	5.7	7.4	7.3	6.1
Total mg/g OC	24.6	28.0	20.2	7.0	7.2	7.4	5.7	4.0	2.8	4.6	5.4	6.0	6.5	6.2
Total μg/g dry wt.)	460.0	485.5	349.9	123.2	121.8	127.2	99.6	59.0	43.7	80.8	89.6	90.7	109.8	115.0

Station location is shown in Fig. 4.1. Individual fatty acids with relative abundances <0.5% throughout the core are omitted for brevity. Key: tr: <0.1%, br: branched, i: iso; a: anteiso, w: double bond position counted from terminal methyl group, listed where determined, --: not detected. Total % rows include omitted data.

Table A4.3. Fatty acid distribution (% total fatty acids) in EB-7 sediments.

	Depth (cm)														
	0-1	**1-2**	**2-3**	**3-4**	**4-5**	**5-6**	**6-7**	**7-8**	**8-9**	**9-10**	**10-12**	**12-14**	**14-16**	**16-18**	**18-20**
***n*-saturates**															
12:0	--	0.2	--	0.2	0.1	0.1	0.2	0.2	0.3	--	0.2	0.4	1.0	0.7	0.3
13:0	0.1	0.1	0.1	0.2	0.1	0.1	0.3	0.2	0.3	--	0.2	0.6	0.6	0.5	0.4
14:0	4.2	3.7	2.5	2.9	3.2	2.9	4.8	3.8	4.6	2.6	3.6	4.8	5.5	4.5	3.8
15:0	1.2	1.2	1.4	1.5	1.8	1.3	2.1	1.7	1.9	1.5	1.7	1.9	2.2	1.8	3.3
16:0	14.9	14.2	15.5	13.9	17.3	13.9	21.3	19.0	19.6	18.7	18.2	22.5	21.4	19.1	20.5
17:0	0.6	1.0	1.1	0.9	1.4	1.5	1.4	1.5	1.4	1.5	1.2	1.4	1.4	1.2	1.3
18:0	2.7	2.4	3.4	3.5	3.9	3.8	3.5	3.3	3.7	3.8	3.9	4.7	4.7	4.2	4.9
20:0	1.8	1.8	2.1	3.6	3.1	3.3	3.2	3.4	3.4	3.6	3.3	4.0	4.1	4.1	4.9
21:0	0.5	0.6	0.6	1.2	1.1	1.1	0.9	1.0	1.0	1.1	1.2	1.5	1.4	1.4	1.9
22:0	2.5	3.5	3.6	11.7	6.4	7.5	6.3	7.4	6.6	7.3	6.4	8.4	6.7	7.3	8.3
23:0	0.9	1.7	1.5	3.3	3.2	3.4	2.6	3.2	2.7	3.4	2.8	3.1	3.4	3.4	4.3
24:0	3.3	6.6	6.1	14.0	13.1	15.1	11.4	14.4	12.3	14.5	11.0	11.4	12.7	13.3	15.8
25:0	0.6	1.7	1.4	3.0	3.0	3.8	2.9	3.1	2.9	3.4	2.6	2.6	3.0	3.0	3.5
26:0	1.6	4.0	3.2	7.7	7.9	10.2	6.5	8.1	6.8	8.3	6.6	6.1	7.2	7.2	8.5
27:0	0.2	0.6	0.5	1.1	1.2	1.8	1.0	1.1	1.0	1.2	1.1	1.1	1.2	1.2	1.4
28:0	0.6	1.2	0.9	2.3	2.8	4.2	2.7	2.7	2.5	2.4	2.2	1.9	2.2	2.3	2.5
Monounsaturates (MUFA)															
Σ15:1	0.5	0.4	0.5	0.2	0.3	0.3	0.7	0.2	0.4	0.1	0.2	0.1	0.2	0.2	--
16:1n-9	1.6	1.5	2.1	0.7	0.7	0.7	0.5	0.6	0.5	0.6	0.7	0.2	0.4	0.5	tr
16:1n-7	23.1	15.2	15.5	6.1	6.9	4.5	8.7	5.4	7.0	5.7	4.6	1.5	2.6	4.1	0.2
16:1n-5	2.3	2.7	3.3	1.5	1.9	1.5	2.1	1.4	1.3	1.8	1.3	0.5	0.6	1.1	--
17:1n-8	0.6	0.6	0.7	0.5	0.6	0.5	0.5	0.4	0.4	0.6	0.5	0.3	0.2	0.3	0.1
17:1n-6	0.7	1.1	1.4	0.6	0.8	0.6	0.5	0.4	0.4	0.7	0.6	0.6	0.4	0.4	0.1
18:1n-9	3.3	3.3	3.4	1.7	2.3	2.3	2.6	2.3	2.8	2.4	2.5	1.6	1.4	2.0	0.4
18:1n-7	6.5	6.8	9.9	2.7	2.5	1.8	1.8	1.5	1.7	2.4	2.1	1.4	1.0	1.7	0.4
18:1n-5	0.3	0.6	0.9	0.2	0.2	0.4	0.2	0.1	0.3	--	0.1	--	0.1	0.1	--
20:1n-9	0.5	1.1	0.7	0.3	0.2	0.2	0.1	0.4	0.2	0.1	0.3	0.2	0.3	0.2	--
20:1n-7	0.4	0.5	0.4	0.2	0.2	0.2	--	0.2	0.2	--	0.1	0.1	0.1	0.2	0.1
22:1	1.2	0.4	0.1	0.4	0.5	0.3	0.3	0.4	0.4	0.2	0.2	0.1	--	0.2	--
22:1	0.3	0.3	0.2	0.7	0.8	0.7	0.6	0.8	0.8	0.5	0.5	0.3	0.4	0.7	0.4
Polyunsaturates (PUFA)															
16:2	0.7	1.1	1.4	0.5	0.7	1.0	--	1.1	0.7	1.3	0.3	--	0.2	0.3	--
18:4	1.0	0.5	0.5	0.2	0.1	0.3	--	--	0.2	--	tr	--	tr	--	0.1
18:2	0.9	0.7	0.4	0.6	0.8	0.3	0.7	0.3	0.5	0.2	7.8	0.8	0.7	0.7	0.7
18:2	0.4	0.9	--	0.3	0.2	0.4	0.5	0.3	0.3	0.2	0.2	0.1	0.1	0.2	0.1
20:4	1.6	0.8	0.4	0.4	0.3	0.2	0.2	0.2	0.3	0.2	0.1	--	0.1	0.1	--

Table A4.3. (cont.) Fatty acid distribution (% total fatty acids) in EB-7 sediments.

	Depth (cm)														
	0-1	**1-2**	**2-3**	**3-4**	**4-5**	**5-6**	**6-7**	**7-8**	**8-9**	**9-10**	**10-12**	**12-14**	**14-16**	**16-18**	**18-20**
20:5	8.7	4.2	2.6	0.8	1.0	1.1	1.6	1.7	1.8	0.9	0.6	--	0.3	0.4	--
22:6	1.6	0.9	0.4	0.1	0.2	0.1	--	0.2	0.1	--	0.1	--	0.1	0.1	--
22:5	0.4	0.8	1.0	0.1	0.1	--	--	0.1	--	--	--	--	--	--	--
Dicarboxylic Acids (DCA)															
20C DCA	0.2	0.3	0.2	0.5	0.3	0.4	0.2	0.3	0.3	0.1	0.3	0.3	0.3	0.3	0.5
22C DCA	0.2	0.5	0.3	1.0	0.5	0.7	0.3	0.6	0.5	0.4	0.4	0.5	0.4	0.5	0.6
24C DCA	0.1	0.3	0.1	0.5	0.3	0.1	0.3	0.3	0.3	0.3	0.2	0.2	0.2	0.2	0.4
Branched															
12:0i	--	0.5	0.4	tr	--	--	--	--	--	--	--	--	0.1	0.1	--
13:0A	0.1	0.1	0.1	0.1	0.1	0.1	0.1	0.1	0.1	--	0.2	0.4	0.5	0.4	0.2
14:0I	0.3	0.4	0.5	0.4	0.4	0.3	0.5	0.3	0.5	0.4	0.6	1.0	0.9	0.9	0.5
15:0I	1.2	1.7	2.2	1.0	1.1	0.8	1.2	0.9	1.0	1.2	1.3	2.0	1.5	1.3	1.8
15:0A	2.0	2.4	3.1	2.2	3.0	2.6	3.6	2.4	2.5	4.1	4.4	7.5	4.7	4.0	4.2
16:0i	0.5	0.8	0.7	0.4	0.5	0.5	0.4	0.4	0.4	0.4	0.5	0.7	0.5	0.5	0.5
17:0br	0.3	0.7	0.4	0.6	0.6	0.5	--	0.4	0.4	0.9	0.8	1.1	0.6	0.6	0.6
17:0I	0.5	0.6	0.6	0.6	0.5	0.6	0.3	0.4	0.3	0.4	0.4	0.5	0.4	0.4	0.4
17:0A	0.5	0.6	0.6	0.4	0.5	0.5	0.4	0.4	0.4	0.6	0.7	0.8	0.6	0.6	0.6
18:0br	--	0.3	0.2	0.1	0.2	0.5	--	0.3	--	--	--	--	--	--	0.3
Total % SAT	35.5	44.4	43.8	71.0	69.5	73.9	70.9	74.3	71.0	73.2	66.0	76.2	78.5	75.2	85.3
Total %MUFA	41.3	34.8	39.2	16.0	18.0	14.0	18.7	14.1	16.4	15.0	13.8	6.9	7.8	11.8	1.7
Total %PUFA	16.9	11.0	7.1	3.6	3.7	3.3	3.0	4.6	4.7	2.8	9.3	0.9	1.7	1.8	1.0
Total %DCA	0.7	1.6	1.0	3.2	1.9	2.1	0.9	1.4	2.1	0.8	1.7	1.7	1.7	2.0	2.7
Total % Branched	5.5	8.1	9.0	6.1	6.9	6.6	6.5	5.6	5.8	8.1	9.3	14.3	10.3	9.2	9.3
Total mg/g OC	2.4	1.7	1.0	2.8	2.1	1.7	0.9	1.5	1.4	1.0	1.0	0.5	1.0	0.6	0.5
Total μg/g dry wt.)	38.0	22.6	13.1	38.1	29.7	25.2	13.6	19.3	17.2	12.0	13.6	6.5	10.6	7.8	4.7

Station location is shown in Fig. 4.1. Individual fatty acids with relative abundances <0.5% throughout the core are omitted for brevity. Key: tr: <0.1%, br: branched, i: iso; a: anteiso, w: double bond position counted from terminal methyl group, listed where determined, --: not detected. Total % rows include omitted data.

Table A4.4. Distribution of *n*-alkanes (% of total *n*-alkane concentration) and *n*-alcohols (% total of *n*-alcohol concentration) in EB-2 sediments.

	Depth (cm)														
	0-1	**1-2**	**2-3**	**3-4**	**4-5**	**5-6**	**6-7**	**7-8**	**8-9**	**9-10**	**10-12**	**12-14**	**14-16**	**16-18**	**18-20**
***n*-alkanes**															
C17	2.2	--	0.6	1.9	2.5	1.3	1.7	0.6	1.7	3.3	1.4	1.1	1.8	2.7	0.6
C18	3.1	--	--	1.2	2.2	2.1	2.0	1.6	1.2	1.7	2.3	1.9	2.4	2.7	1.7
C19	6.1	--	0.6	3.0	3.2	1.4	1.4	0.1	1.3	3.2	4.5	3.5	4.2	4.5	3.5
C20	3.6	--	1.2	3.1	2.6	3.7	1.9	2.1	2.9	3.0	3.9	3.2	3.8	4.0	3.4
C21	7.7	--	2.3	3.3	6.3	5.0	4.0	4.1	6.7	5.6	6.2	5.1	6.0	6.0	5.6
C22	5.5	--	4.1	4.0	4.4	4.4	4.1	3.5	4.7	4.5	4.8	4.2	4.8	4.7	4.5
C23	9.6	23.8	11.6	9.9	11.1	11.6	12.9	10.4	10.3	10.9	10.8	9.6	10.6	10.0	9.9
C24	2.7	5.4	4.3	4.3	4.0	4.8	5.7	5.8	5.0	4.2	5.0	5.4	6.2	4.7	5.9
C25	8.4	12.1	12.3	10.1	10.4	10.1	12.7	10.4	11.1	10.5	11.4	11.2	11.4	10.3	10.5
C26	3.5	5.1	3.5	3.4	3.1	3.5	4.0	3.6	3.0	2.9	3.2	4.1	4.1	3.1	4.0
C27	11.6	12.1	14.9	15.8	16.3	17.2	18.0	19.6	13.4	13.1	15.4	15.5	15.0	13.8	14.7
C28	0.5	2.6	2.2	2.5	1.7	1.6	2.7	1.9	2.2	2.2	2.6	3.6	2.5	2.4	2.3
C29	9.6	9.3	15.3	14.8	13.4	14.0	11.4	15.3	12.9	13.1	13.5	13.6	12.6	13.4	14.5
C30	2.2	3.3	1.2	1.3	1.1	1.6	1.1	1.0	1.3	1.3	1.1	1.5	0.9	1.1	0.8
C31	10.4	1.4	10.4	9.2	10.2	11.0	6.0	10.3	9.0	9.7	9.5	10.2	9.1	10.7	11.0
C32	5.7	7.5	4.8	4.3	1.5	1.0	3.5	3.3	5.1	4.0	1.6	3.0	2.4	2.8	2.8
C33	7.7	17.4	10.5	7.8	5.9	5.8	7.2	6.6	8.2	6.7	2.7	3.3	2.2	3.3	4.3
***n*-alcohols**															
C14	4.3	--	0.8	1.0	0.7	0.6	0.7	0.6	0.9	1.2	1.0	0.8	0.9	0.9	0.5
C15	1.9	8.1	1.2	1.2	1.2	0.8	0.8	0.7	0.8	0.9	0.6	0.3	0.3	0.3	0.0
C16	11.1	12.2	6.6	7.6	6.0	6.2	5.4	5.0	6.0	6.2	3.8	4.7	4.9	3.6	3.3
C17	4.1	2.7	0.5	0.6	1.1	0.5	0.3	0.3	0.8	0.8	0.5	0.4	0.2	0.2	0.0
C18	6.9	6.1	4.0	4.8	4.6	4.9	4.6	3.8	4.3	4.1	2.9	3.6	4.0	3.8	3.6
C19	1.1	1.0	0.9	1.0	1.0	0.7	0.9	0.8	0.9	0.9	0.5	0.7	0.6	0.7	0.6
C20	8.6	13.4	10.2	10.7	12.6	9.9	10.4	10.2	11.2	10.8	8.8	9.8	10.6	9.3	9.4
C21	2.1	2.1	2.1	2.2	2.3	2.0	2.0	2.0	2.2	2.2	2.1	1.3	1.5	1.3	0.9
C22	15.8	16.3	19.9	18.8	22.9	20.8	20.4	20.4	21.4	20.5	20.2	22.2	22.2	22.2	23.6
C23	3.1	3.9	2.7	3.5	3.9	3.1	3.3	3.1	3.4	3.3	3.1	3.5	3.5	3.7	3.6
C24	12.7	15.5	15.6	13.0	13.1	14.1	15.9	17.0	16.3	15.1	17.1	17.5	17.1	17.1	18.3
C25l	2.1	4.7	3.1	2.6	3.2	2.8	2.7	3.1	3.2	2.9	1.2	0.5	0.6	0.6	0.4
C26	12.1	11.1	19.6	19.9	17.3	19.1	20.1	19.1	21.0	17.9	20.8	19.8	18.9	22.0	22.4
C27	2.3	1.3	1.2	1.1	1.1	1.2	1.1	1.1	1.5	1.3	0.9	0.6	0.6	0.5	0.1
C28	11.9	1.5	11.8	12.1	9.0	13.4	11.4	13.1	6.2	11.7	16.4	14.4	14.0	13.8	13.4
Total *n*-alkanes (ug/g OC)	145	33	171	401	222	115	174	81	406	396	720	675	509	552	555
Total *n*-alcohols (ug/g OC)	320	107	403	753	207	265	426	184	868	684	714	972	763	755	863

Table A4.5. Distribution of *n*-alkanes (% of total *n*-alkane concentration) and *n*-alcohols (% total of *n*-alcohol concentration) in EB-4 sediments.

	Depth (cm)													
	0-1	**1-2**	**2-3**	**3-4**	**4-5**	**6-7**	**7-8**	**8-9**	**9-10**	**10-12**	**12-14**	**14-16**	**16-18**	**18-20**
***n*-alkanes**														
C17	1.2	0.6	0.6	0.4	0.3	0.4	0.8	0.3	0.6	2.7	2.5	1.9	1.3	1.9
C18	1.7	1.5	1.7	1.7	0.8	1.7	1.8	0.9	1.2	2.8	2.7	2.3	2.0	2.4
C19	3.0	2.7	2.9	2.9	2.4	3.9	4.1	3.0	3.1	5.1	5.4	4.5	4.2	4.2
C20	2.6	2.6	3.1	3.1	2.7	3.2	3.2	3.0	2.9	3.7	3.6	3.3	3.4	3.3
C21	5.8	6.0	6.9	7.4	5.5	7.0	6.6	6.7	7.2	7.0	7.0	6.4	6.5	6.5
C22	4.2	4.4	4.7	4.6	4.5	4.7	4.9	5.0	4.9	5.5	5.3	5.0	5.3	5.1
C23	10.0	10.8	12.0	11.5	10.7	10.7	11.2	11.4	11.4	12.9	12.4	12.4	12.3	12.3
C24	4.2	4.5	5.2	5.7	5.1	4.1	5.2	5.7	5.2	5.9	6.8	5.4	4.8	5.2
C25	10.9	11.0	11.0	11.0	11.8	10.3	11.4	11.4	10.8	11.8	11.5	11.8	11.3	11.4
C26	3.3	3.7	3.8	3.9	3.8	3.3	3.8	3.8	3.6	3.7	4.5	3.8	3.5	3.7
C27	15.3	14.6	14.7	13.8	15.6	13.1	14.2	13.9	13.2	14.4	13.9	15.0	14.5	14.7
C28	2.7	3.2	3.5	2.5	3.4	2.7	2.7	2.3	2.3	1.9	2.2	2.9	2.4	2.6
C29	12.1	12.3	12.8	10.1	13.0	10.2	11.3	11.6	12.1	9.6	8.5	11.3	10.4	11.1
C30	1.6	2.6	1.6	3.3	2.1	3.2	2.1	1.7	1.9	1.0	1.1	1.2	1.2	1.2
C31	9.4	10.7	5.5	7.7	12.0	9.5	9.0	8.8	9.4	7.3	7.7	8.3	11.6	9.1
C32	5.2	0.9	1.0	1.8	0.9	0.8	1.2	1.5	1.2	2.9	2.8	2.5	2.5	2.7
C33	6.9	8.0	8.8	8.8	5.5	11.1	6.5	8.9	8.9	1.8	2.0	2.0	2.8	2.6
***n*-alcohols**														
C14	2.3	1.4	1.9	1.2	1.0	1.3	1.2	0.8	0.8	2.3	3.0	2.5	2.6	3.2
C15	1.6	1.3	1.5	1.3	1.0	1.5	1.2	1.2	1.1	0.7	0.8	0.5	0.5	0.7
C16	8.0	7.9	8.8	7.9	6.4	7.3	6.6	6.2	6.5	8.5	9.4	8.8	9.9	9.9
C17	3.3	2.5	2.5	2.3	1.5	2.1	1.9	1.8	1.6	1.0	1.2	1.0	0.9	1.4
C18	5.5	5.0	5.0	4.7	4.0	4.6	4.2	4.4	4.1	4.9	5.0	4.6	5.3	4.7
C19	1.1	0.9	0.9	0.9	0.7	0.8	0.9	1.0	0.9	0.8	1.2	1.2	1.3	1.0
C20	10.7	10.3	10.8	13.4	11.2	12.1	11.7	13.0	13.2	15.2	15.1	14.4	14.4	13.7
C21	2.3	2.1	2.0	2.2	2.1	2.1	2.3	2.4	2.4	0.9	0.7	0.5	0.6	0.6
C22	17.4	16.3	16.6	19.7	19.0	18.4	18.6	20.0	19.8	23.6	22.9	23.1	22.6	22.6
C23	3.5	2.9	2.9	3.2	2.7	3.0	3.0	3.1	2.8	3.6	3.5	3.5	3.4	3.6
C24	13.7	12.0	12.4	13.6	13.7	13.1	13.7	14.1	13.9	14.8	14.0	14.7	14.6	14.7
C25	2.1	2.1	2.1	1.8	2.1	1.9	2.2	2.1	1.8	0.6	0.6	0.5	0.5	0.5
C26	13.1	16.9	16.1	14.3	16.5	15.2	15.3	14.9	15.1	10.2	9.4	10.9	10.8	10.7
C27	2.1	1.8	1.4	1.2	1.5	1.4	1.6	1.3	1.4	0.9	0.8	0.8	1.0	0.5
C28	13.2	16.7	15.0	12.1	16.6	15.1	15.5	13.5	14.4	12.1	12.3	13.2	11.4	12.1
Total *n*-alkanes (ug/g OC)	356	674	589	263	352	322	400	281	287	286	348	484	499	349
Total *n*-alcohols (ug/g OC)	755	1670	1483	597	977	690	855	589	626	512	654	917	878	693

Table A4.6. Distribution of *n*-alkanes (% of total *n*-alkane concentration) and *n*-alcohols (% total of *n*-alcohol concentration) in EB-7 sediments.

	Depth (cm)														
	0-1	**1-2**	**2-3**	**3-4**	**4-5**	**5-6**	**6-7**	**7-8**	**8-9**	**9-10**	**10-12**	**12-14**	**14-16**	**16-18**	**18-20**
***n*-alkanes**															
C17	1.0	--	--	0.7	1.2	1.3	0.5	0.6	0.8	1.7	1.3	3.1	1.3	4.0	2.7
C18	1.9	1.1	--	1.6	2.4	1.9	0.7	1.1	1.7	2.1	2.4	4.0	2.5	4.0	3.8
C19	4.6	4.0	2.5	3.9	4.8	4.0	2.9	2.6	3.6	4.2	5.2	7.7	5.9	7.1	7.5
C20	3.0	3.6	2.5	3.2	3.2	3.1	2.7	2.8	3.1	3.6	4.5	5.7	4.8	5.1	5.7
C21	5.1	7.5	5.7	5.8	5.9	6.0	6.6	6.2	6.2	7.4	7.2	8.2	7.5	7.7	8.2
C22	4.5	4.9	5.5	5.0	4.6	4.6	5.6	4.9	4.9	5.4	6.0	6.1	6.0	5.9	6.4
C23	8.6	10.4	11.4	10.3	9.8	10.5	11.0	10.6	10.8	11.0	12.3	11.5	12.4	12.2	12.2
C24	4.1	5.1	4.9	4.7	4.3	5.3	5.2	4.4	4.8	4.8	6.2	6.1	6.4	6.1	6.8
C25	8.9	10.4	10.3	11.0	10.2	10.7	10.7	10.6	10.3	10.4	12.6	10.6	11.8	11.2	10.8
C26	3.4	3.5	4.1	3.7	3.3	4.1	3.9	3.5	3.4	3.6	4.5	4.0	4.3	4.1	5.2
C27	13.3	13.4	13.5	15.0	14.1	14.7	14.1	14.4	13.5	12.9	14.5	10.6	13.0	12.0	11.3
C28	3.1	2.5	3.5	2.8	2.6	2.6	3.4	2.5	3.6	2.5	2.9	2.5	2.5	2.3	2.6
C29	12.8	10.2	13.3	12.2	11.7	10.7	10.6	11.2	10.3	9.6	8.9	6.3	7.7	6.8	6.1
C30	2.0	3.4	1.9	1.8	1.9	1.7	1.9	2.8	2.5	2.9	0.7	0.7	0.8	0.7	0.5
C31	11.6	9.5	9.4	10.5	10.5	9.9	10.0	9.8	9.1	8.8	6.2	6.6	6.9	5.3	5.6
C32	4.8	0.0	0.6	0.4	0.3	1.5	0.7	0.6	0.6	0.0	2.8	4.2	4.2	3.7	3.1
C33	7.3	10.5	10.8	7.3	9.1	7.3	9.6	11.3	10.9	9.0	1.5	1.9	2.1	1.8	1.6
***n*-alcohols**															
C14	0.9	0.9	0.4	0.8	1.1	0.9	0.4	0.8	0.9	1.0	1.1	2.2	1.2	2.0	1.7
C15	0.8	0.9	0.5	0.8	0.9	0.8	0.7	1.0	0.9	0.9	0.4	0.9	0.4	0.5	0.6
C16	5.7	7.1	6.3	5.6	6.1	6.1	5.2	5.8	5.7	6.5	6.3	7.4	6.6	6.5	6.8
C17	1.2	1.5	1.5	1.2	1.4	1.2	1.5	1.5	1.4	1.4	0.6	0.8	0.6	0.6	0.6
C18	3.5	4.3	5.2	4.1	4.5	4.1	4.0	3.9	3.8	4.2	4.3	4.6	4.1	4.0	4.1
C19	0.9	0.8	1.0	0.9	0.8	0.8	0.8	0.9	1.0	0.9	1.0	1.3	1.0	1.2	1.1
C20	9.2	9.5	11.2	9.5	9.3	9.7	10.5	10.0	10.7	10.0	11.1	12.5	11.1	11.9	12.3
C21	2.0	1.9	2.3	2.3	2.2	2.2	2.3	2.2	2.3	2.4	0.8	0.5	0.5	0.7	0.6
C22	19.5	19.6	21.6	19.5	18.6	19.8	21.0	19.7	20.6	21.4	24.8	26.4	24.3	26.7	27.4
C23	3.1	2.9	3.3	3.2	3.0	3.3	3.2	3.4	3.3	3.4	4.0	4.9	4.4	4.1	4.2
C24	15.2	14.0	14.3	14.8	14.0	15.2	15.5	15.0	14.8	14.7	16.5	14.8	16.2	16.6	16.1
C25l	2.2	2.5	0.5	2.5	2.5	2.6	2.4	2.5	2.5	2.5	0.8	1.3	1.5	0.9	1.0
C26	16.6	17.3	16.7	16.8	17.2	16.3	16.2	16.4	16.9	15.7	13.6	10.0	13.1	11.9	11.2
C27	2.6	1.8	2.0	2.0	2.2	2.1	1.6	1.9	1.9	1.8	0.9	1.1	1.0	1.0	1.1
C28	16.4	14.9	13.2	16.1	16.2	14.9	14.8	15.0	13.4	13.3	13.6	11.3	13.9	11.3	11.1
Total *n*-alkanes (ug/g OC)	251	142	93	444	393	303	159	276	271	205	219	146	281	167	142
Total *n*-alcohols (ug/g OC)	392	279	178	903	720	625	362	569	547	403	308	188	410	253	191

Table A4.7. Distribution of sterols (as % of total sterol concentration) and selected triterpenoid concentrations in EB-2 sediments.

	Depth (cm)														
	0-1	**1-2**	**2-3**	**3-4**	**4-5**	**5-6**	**6-7**	**7-8**	**8-9**	**9-10**	**10-12**	**12-14**	**14-16**	**16-18**	**18-20**
C26Δ5,22	0.7	2.1	1.5	1.1	0.9	0.8	1.4	1.6	1.2	0.9	1.8	1.6	1.1	0.3	
C26Δ22	0.3	0.1	0.7	0.6	0.4	0.4	1.1	0.8	0.8	0.8	1.3	1.5	1.0	1.2	1.3
27norC26Δ5,22	0.8	0.8	1.8	1.8	1.4	1.6	1.9	2.0	2.0	2.0	0.9	1.5	1.2	1.9	1.4
C27Δ5,22	3.6	3.4	3.3	3.4	3.5	3.0	2.2	2.0	2.5	2.6	2.1	2.2	1.7	1.7	0.9
C27Δ22	0.5	0.5	0.8	0.6	0.7	0.7	0.6	0.7	1.0	0.9	--	0.5	0.7	1.7	1.4
C27Δ5	14.5	16.0	12.4	17.8	23.6	1.2	10.9	7.1	8.6	8.6	17.6	6.7	21.7	4.2	3.7
C27Δ0	2.2	3.6	3.5	3.0	3.4	2.7	3.1	3.4	3.2	3.1	2.3	2.7	3.0	2.3	1.9
C27Δ5,24	0.6	1.3	1.9	1.3	1.8	2.1	1.9	2.4	1.9	1.8	--	--	--	--	--
C28Δ5,22	12.9	17.0	11.2	10.0	8.1	14.9	9.5	8.5	6.7	9.1	6.3	5.1	3.4	2.8	2.6
C28Δ22	1.0	2.7	2.4	1.5	1.5	2.2	1.4	2.7	2.8	2.3	1.7	1.8	1.5	1.9	1.4
C27Δ7	9.2	1.3	0.5	0.4	0.6	0.4	0.4	0.4	1.1	0.7	0.6	0.5	0.4	0.5	0.3
C28Δ5,7,22	2.0	0.5	0.7	1.0	0.9	2.1	1.1	0.8	0.8	1.5	--	--	--	--	--
C28Δ5,24(28)	12.5	6.3	5.6	6.7	6.3	4.6	5.0	4.5	4.5	4.8	4.3	4.5	3.3	2.2	3.1
C28Δ5	5.6	3.6	4.3	4.4	5.5	4.6	4.6	6.1	4.4	3.5	6.8	7.1	8.1	4.3	5.0
C28Δ24(28)	0.8	0.9	0.9	3.9	1.1	1.5	0.9	1.8	1.3	1.0	2.0	2.7	2.0	3.1	2.9
C28Δ0 + dMeΔ5,22	2.7	4.1	4.7	0.6	3.7	4.2	4.6	5.0	5.0	5.0	3.0	3.9	4.1	3.1	2.7
C29Δ5,22	2.6	3.6	3.7	3.1	3.0	3.4	3.7	3.8	5.0	4.3	2.9	3.8	2.9	3.5	3.1
C29Δ22 + dMeΔ22	1.6	1.1	1.4	1.4	0.9	3.1	1.6	2.6	2.1	1.7	0.7	0.8	1.0	1.9	--
C29Δ5	12.3	15.9	19.1	19.1	18.3	20.1	26.5	20.2	26.3	27.1	25.2	28.7	22.0	32.8	36.4
C29Δ0	2.2	2.7	0.7	0.8	0.6	6.6	1.0	1.1	1.2	1.2	10.3	10.9	9.8	8.5	17.6
C29Δ5,24(28)Z	coel	3.1	3.1	3.6	2.6	2.8	1.8	1.2	2.9	2.5	4.9	4.8	3.7	12.1	5.2
Dinosterol	1.8	2.6	3.9	3.5	2.3	4.1	4.7	4.6	5.5	5.6	2.4	2.4	2.0	2.3	1.4
C29Δ7	0.7	1.2	1.2	1.4	0.3	1.3	1.6	2.5	1.5	1.2	--	--	--	--	--
tMeΔ8(14)	2.4	2.5	6.2	4.7	5.5	3.6	3.9	5.2	2.5	1.6	1.4	1.7	2.0	--	1.0
C30Δ5,24(28)	0.6	--	1.0	0.8	0.7	1.1	0.8	1.8	1.8	2.0	1.6	0.9	0.7	4.5	3.3
tMeSΔ0	0.8	1.8	1.8	1.6	1.1	1.4	1.6	2.5	1.5	1.9	--	1.5	1.1	1.1	1.2
tMeRΔ0	1.2	1.3	2.0	1.7	1.3	1.6	2.1	2.4	2.0	2.4	--	2.0	1.7	2.0	1.9
Total Sterols (µg/g OC)	1311	357	635	1180	421	290	368	192	723	552	809	586	606	329	317
a-amyrin (µg/g OC)	54.0	9.4	18.3	39.0	4.4	10.9	17.7	10.8	24.2	25.4	27.9	17.1	18.3	8.8	14.6
Tetrahymanol (µg/g OC)	10.7	3.6	5.3	11.8	1.2	2.7	4.6	2.7	6.9	8.3	6.9	4.9	5.5	3.4	2.6

Abbreviations: --: not detected; coel: coeluted with compound above; C26Δ5,22: 24-norcholesta-5,22-dien-3b-ol; C26Δ22: 24-nor-5a-cholest-22-en-3b-ol; 27norC26Δ5,22: 27-nor-24-cholesta-5,22-dien-3b-ol; C27Δ5,22: cholesta-5,22-dien-3b-ol; C27Δ22: 5a-cholest-22-dien-3b-ol; C27Δ5: cholest-5-en-3b-ol; C27Δ0: 5a-cholestan-3b-ol; C27Δ5,24: cholesta-5,24-dien-3b-ol; C28Δ5,22: 24-methylcholesta-5,22-dien-3b-ol; C28Δ22: 24-methylcholest-22-en-3b-ol; C27Δ7: cholest-7-en-3b-ol; C28Δ5,7,22: 24-methylcholesta-5,7,22-trien-3b-ol; C28Δ5,24(28): 24-methylcholesta-5,24(28)-dien-3b-ol; C28Δ5: 24-methylcholest-5-en-3b-ol; C28Δ24(28): 24-methylcholest-24(28)-en-3b-ol; C28Δ0 + dMeΔ5,22: chromatographically unresolved mixture of 24-methylcholestan-3b-ol + 4a,24-dimethylcholesta-5,22-dien-3b-ol; C29Δ5,22: 24-ethylcholesta-5,22-dien-3b-ol; C29Δ22 + dMeΔ22: unresolved mixture of 24-ethylcholest-22-en-3b-ol + 4a,24-dimethylcholest-22-en-3b-ol; C29Δ5: 24-ethylcholest-5-en-3b-ol; C29Δ0: 24-ethylcholestan-3b-ol; C29Δ5,24(28)Z: 24-ethylcholesta-5,24(28)Z-dien-3b-ol; Dinosterol: 4a,23,24-trimethylcholest-22-en-3b-ol; C29Δ7: 24-ethylcholest-7-en-3b-ol; tMeΔ8(14): 4a,23,24-trimethylcholest-8(14)-en-3b-ol; C30Δ5,24(28): 24-propylcholesta-5,24(28)-dien-3b-ol; tMeSΔ0: 4a,23S,24R-trimethylcholestan-3b-ol; tMeRΔ0: 4a,23R,24R-trimethylcholestan-3b-ol.

Table A4.8. Distribution of sterols (as % of total sterol concentration) and selected triterpenoid concentrations in EB-4 sediments.

	Depth (cm)													
	0-1	**1-2**	**2-3**	**3-4**	**4-5**	**6-7**	**7-8**	**8-9**	**9-10**	**10-12**	**12-14**	**14-16**	**16-18**	**18-20**
C26Δ5,22	0.8	0.9	0.8	1.0	0.1	0.8	0.8	0.8	0.6	1.6	1.7	1.7	1.8	2.1
C26Δ22	0.3	0.3	0.2	0.3	0.2	0.3	0.3	0.3	0.3	1.2	1.5	1.3	1.4	1.5
27norC26Δ5,22	1.6	1.3	1.2	1.2	1.2	1.1	1.2	1.1	1.0	1.0	1.0	0.9	1.0	1.2
C27Δ5,22	3.4	3.7	3.3	2.6	2.6	2.4	2.3	2.1	2.0	2.9	3.1	3.7	3.3	2.4
C27Δ22	0.6	0.6	0.6	0.8	0.7	0.7	0.9	0.8	0.8	1.4	2.2	1.6	1.4	1.6
C27Δ5	11.6	12.5	12.3	10.5	9.4	9.5	8.1	8.7	6.6	9.8	8.5	12.0	10.4	8.1
C27Δ0	1.8	2.0	1.4	2.5	2.6	2.4	2.9	2.6	2.9	4.0	1.0	5.6	5.0	4.4
C27Δ5,24	0.4	0.5	0.6	0.8	0.8	0.7	0.9	0.7	0.9	1.0	1.0	0.7	0.4	0.5
C28Δ5,22	10.7	11.0	9.5	8.8	8.3	9.2	6.3	6.3	5.9	7.4	7.8	6.5	6.6	6.8
C28Δ22	1.1	1.7	0.9	1.9	1.9	1.2	2.0	1.9	2.0	2.7	2.9	2.5	2.9	3.1
C27Δ7	2.9	2.8	3.1	3.7	2.8	6.9	3.8	3.2	1.5	2.4	2.7	1.8	1.9	1.5
C28Δ5,7,22	1.3	0.8	1.0	1.0	1.1	1.2	1.0	1.2	1.2	1.2	1.4	0.8	1.2	0.7
C28Δ5,24(28)	9.2	7.5	7.0	5.3	5.4	4.6	4.8	4.6	4.0	4.9	5.1	4.7	5.4	5.3
C28Δ5	3.3	6.4	8.7	4.7	8.7	4.6	5.7	4.0	5.3	9.2	9.8	8.7	9.8	11.9
C28Δ24(28)	5.1	0.9	0.2	1.3	1.3	1.4	0.8	1.2	1.0	2.0	1.6	1.4	1.9	2.5
C28Δ0 + dMeΔ5,22	3.7	3.0	3.0	3.0	2.9	2.8	3.0	3.2	3.2	3.6	4.3	4.1	4.5	5.7
C29Δ5,22	3.5	3.3	3.4	3.8	3.6	3.5	3.7	4.0	4.3	4.2	4.5	4.0	4.3	4.3
C29Δ22 + dMeΔ22	1.6	1.5	1.3	2.1	1.4	2.0	1.9	2.0	2.2	--	--	--	--	--
C29Δ5	19.2	19.7	19.7	20.0	20.4	19.0	22.2	23.1	27.2	21.7	21.2	19.4	19.8	20.3
C29Δ0	2.4	3.1	3.5	3.6	3.5	4.6	1.5	6.1	7.0	7.3	7.4	7.2	6.1	5.4
C29Δ5,24(28)Z	3.5	3.0	3.0	3.6	3.1	2.5	6.4	2.5	2.2	3.4	3.8	4.3	4.2	3.5
Dinosterol	1.8	3.0	2.9	3.1	3.4	3.2	4.2	3.7	3.6	2.6	3.0	2.6	2.8	3.0
C29Δ7	1.4	0.8	1.3	1.9	1.9	2.0	2.0	2.1	2.0	--	--	--	--	--
tMeΔ8(14)	2.2	1.7	1.7	2.1	2.5	2.4	1.9	2.0	1.6	2.5	2.9	2.3	2.0	1.6
C30Δ5,24(28)	0.8	0.7	0.6	0.9	1.2	0.8	1.6	1.5	1.4	0.9	1.1	1.4	2.0	1.7
tMeSΔ0	0.9	0.8	1.0	1.0	1.3	1.2	1.5	1.3	1.1	--	--	--	--	--
tMeRΔ0	1.3	1.8	2.1	2.0	2.3	2.2	2.3	2.2	2.4	1.0	0.7	0.5	0.0	0.6
Total Sterols (µg/g OC)	2180	2880	2676	1205	1740	1426	1267	945	822	783	1047	1392	1175	900
a-amyrin (µg/g OC)	56.9	89.9	75.5	44.2	62.5	62.4	32.6	41.5	38.2	13.6	21.1	17.9	26.8	14.4
Tetrahymanol (µg/g OC)	16.5	16.0	23.6	9.8	11.5	10.1	8.4	7.8	7.9	6.2	9.5	11.5	8.4	8.4

Abbreviations: See Table A4.7.

Table A4.9. Distribution of sterols (as % of total sterol concentration) and selected triterpenoid concentrations (µg/g OC) in EB-7 sediments.

	Depth (cm)														
	0-1	**1-2**	**2-3**	**3-4**	**4-5**	**5-6**	**6-7**	**7-8**	**8-9**	**9-10**	**10-12**	**12-14**	**14-16**	**16-18**	**18-20**
C26Δ5,22	0.8	0.4	0.7	0.8	0.9	0.7	0.9	0.7	1.1	0.8	1.6	1.4	1.3	1.3	1.3
C26Δ22	0.6	--	0.8	0.6	0.6	0.5	0.5	0.4	0.7	0.5	1.5	1.3	1.4	1.4	1.4
27norC26Δ5,22	0.4	1.2	1.2	1.6	1.4	1.8	1.5	1.5	1.6	1.9	1.0	1.1	1.2	1.0	1.5
C27Δ5,22	2.7	2.6	2.5	2.5	2.1	2.3	2.0	1.9	2.1	2.4	2.1	2.2	1.8	1.5	2.2
C27Δ22	0.6	0.9	0.8	0.5	0.9	1.1	0.8	0.8	0.9	1.2	--	--	--	--	--
C27Δ5	8.4	18.9	15.4	7.3	6.8	6.1	6.4	5.5	5.8	6.6	6.6	7.1	6.4	5.8	7.1
C27Δ0	2.1	2.6	2.6	2.9	2.8	2.9	2.8	2.4	2.6	3.5	--	--	--	--	--
C27Δ5,24	1.3	1.1	1.1	1.7	1.6	1.7	1.8	1.3	1.4	1.5	1.0	1.5	0.9	1.2	0.8
C28Δ5,22	6.9	5.9	4.7	5.7	5.4	5.6	5.0	4.7	4.8	5.5	5.5	4.5	5.0	4.9	5.2
C28Δ22	1.9	1.4	1.6	2.0	2.0	2.2	2.0	2.0	2.0	2.4	2.7	2.9	1.6	2.3	2.6
C27Δ7	0.6	--	0.4	0.8	0.9	0.6	0.6	0.6	0.9	0.6	--	0.5	0.3	--	--
C28Δ5,7,22	0.4	--	0.6	0.8	0.7	0.9	0.7	0.8	0.7	0.6	--	--	--	--	--
C28Δ5,24(28)	5.0	4.1	4.0	4.7	4.3	4.5	4.2	4.0	4.3	4.6	4.5	4.7	4.5	4.3	4.1
C28Δ5	11.0	5.7	6.0	11.8	16.3	12.2	13.9	18.7	10.5	5.7	21.6	10.1	22.2	19.5	16.5
C28Δ24(28)	1.0	1.5	1.5	1.2	0.0	1.2	0.0	0.0	1.8	1.4	--	4.1	--	--	--
C28Δ0 + dMeΔ5,22	4.4	3.7	3.9	4.9	5.0	4.8	4.9	4.5	4.7	5.2	5.1	6.3	5.5	5.9	5.7
C29Δ5,22	4.9	4.1	4.2	4.7	4.7	4.1	4.3	4.1	4.7	4.6	4.1	5.5	4.9	5.3	4.4
C29Δ22 + dMeΔ22	1.6	2.2	2.1	1.9	1.7	1.6	1.9	2.4	2.1	2.2	--	--	--	--	--
C29Δ5	20.0	16.8	16.7	17.0	15.6	15.6	15.5	14.0	15.5	17.5	19.9	19.7	18.9	20.2	21.4
C29Δ0	7.6	3.5	4.6	4.5	7.2	4.5	7.8	4.5	5.4	5.6	10.0	4.6	4.3	3.6	6.4
C29Δ5,24(28)Z	--	3.7	2.5	3.0	--	3.2	--	3.3	3.0	2.6	--	5.8	5.1	5.7	4.5
Dinosterol	4.4	5.0	5.0	6.0	5.2	6.2	5.7	5.3	6.0	5.8	4.9	6.1	5.2	5.9	5.9
C29Δ7	1.2	1.4	2.1	1.1	1.2	1.8	1.4	1.6	1.6	1.6	--	--	--	--	--
tMeΔ8(14)	2.7	2.0	2.0	1.4	2.0	2.9	3.1	2.3	2.5	2.6	1.9	2.9	2.6	2.9	1.7
C30Δ5,24(28)	1.4	1.4	1.8	1.4	1.5	1.4	1.9	1.8	2.1	1.9	0.8	1.9	1.8	1.8	1.3
tMeSΔ0	1.9	2.2	2.9	1.7	2.0	2.7	2.6	2.3	2.5	2.6	2.4	2.5	2.2	2.5	2.7
tMeRΔ0	2.5	2.3	3.2	2.1	2.0	2.6	2.7	2.3	2.6	2.6	2.8	3.1	2.8	3.0	3.2
Total Sterols (µg/g OC)	707	477	288	890	1023	760	483	852	776	509	271	197	402	233	160
a-amyrin (µg/g OC)	19.1	13.0	10.8	29.4	29.2	25.8	15.0	27.3	25.0	13.9	8.0	6.8	10.3	7.3	5.1
Tetrahymanol (µg/g OC)	7.5	4.0	2.6	11.3	13.7	10.1	8.5	13.2	9.6	8.7	3.9	3.3	4.5	2.3	2.2

Abbreviations: See Table A4.7.

Table A4.10. Trace metal content in shelf, slope, and basin sediments in the Alaskan Beaufort Sea.

	Al %	Fe %	Mg %	Ca %	Ba µg/g	Mn µg/g	Cd µg/g	Mo µg/g	U µg/g	As µg/g	Ag µg/g	Co µg/g	Cr µg/g	Ni µg/g	Cu µg/g	Zn µg/g	Pb µg/g	Re ng/g	AVS µmol/g
EB-2 (Shelf)																			
0-1	5.25	3.14	1.36	1.49	607	271	0.341	2.660	2.035	15.33	0.23	25.8	66.7	37.8	18.5	98.3	21.1	4.783	6
1-2	4.93	3.02	2.34	3.69	489	236	0.223	1.383	2.386	10.43	0.13	12.8	50.3	29.9	16.2	81.3	9.6	5.206	59
2-3	6.34	3.70	1.53	1.87	615	296	0.295	1.868	2.850	13.18	0.31	17.6	59.9	39.6	21.1	103.5	10.6	6.521	42
3-4	6.17	3.53	1.51	2.08	604	308	0.287	2.369	2.895	12.88	0.32	17.4	62.9	37.5	21.5	98.6	13.0	6.582	82
4-5	5.90	4.03	1.96	2.83	542	301	0.273	2.169	2.635	18.32	0.32	16.2	69.6	35.0	18.6	94.2	9.5	5.319	206
5-6	6.72	3.90	1.56	2.20	636	343	0.325	3.186	2.897	13.23	0.33	16.4	65.9	42.7	25.4	109.8	10.2	6.147	145
6-7	6.67	3.99	1.52	2.45	623	380	0.318	2.666	2.765	13.04	0.34	17.8	70.7	45.9	27.3	111.5	11.8	6.425	280
7-8	6.96	4.15	1.58	2.94	642	423	0.353	2.762	3.198	9.97	0.42	21.0	66.5	46.4	28.3	117.1	12.4	6.078	72
8-9	6.45	3.87	1.48	2.30	603	319	0.265	2.639	2.791	10.38	0.32	17.7	66.5	40.2	22.8	107.2	9.8	5.574	591
9-10	6.76	4.13	1.59	3.02	622	350	0.238	2.020	2.526	11.72	0.32	18.4	75.2	44.4	26.4	112.1	12.1	4.216	423
10-12	6.55	3.89	1.52	2.54	610	319	0.269	1.971	2.594	10.01	0.32	16.8	67.5	41.5	24.6	108.3	13.3	5.121	222
12-14	6.70	4.10	1.59	3.21	617	336	0.277	1.904	2.772	13.91	0.37	18.6	80.9	43.5	27.4	111.9	13.1	4.159	78
14-16	7.09	4.18	1.56	3.47	644	420	0.312	1.393	2.747	12.82	0.41	19.4	72.2	44.5	29.3	117.5	12.4	4.930	286
16-18	7.46	4.53	1.54	4.55	643	619	0.442	1.142	2.697	13.24	0.41	20.1	71.4	50.9	33.7	129.5	9.6	4.608	167
18-20	7.50	4.73	1.59	4.98	656	665	0.414	1.320	2.199	12.78	0.34	19.3	74.9	52.2	33.7	131.9	13.7	4.299	155
EB-4 (Slope)																			
0-1	6.42	4.27	1.54	2.00	586	416	0.11	3.4	1.8	23.5	0.18	15.5	61.8	39.3	19.0	118	16.9	3.2	0.44
1-2	6.06	4.02	1.56	1.94	568	463	0.19	6.1	2.2	22.8	0.37	16.3	103	39.5	18.6	120	14.1	3.5	0.39
2-3	6.55	4.24	1.53	2.11	607	372	0.00	4.3	1.8	21.2	0.14	16.8	83.2	40.7	20.1	123	11.2	2.7	0.79
3-4	6.61	4.32	1.54	2.07	607	406	0.08	5.3	2.0	21.9	0.24	16.6	80.3	39.2	19.7	123	13.2	3.6	0.46
4-5	6.50	4.18	1.44	1.97	586	344	0.06	3.6	2.2	22.7	0.21	17.5	86.8	38.5	21.4	120	14.5	3.6	1.2
5-6	6.62	4.26	1.47	2.01	601	353	0.06	3.3	2.2	20.5	0.21	17.2	95.9	40.8	19.8	128	13.4	3.7	2.1
6-7	7.17	4.51	1.54	2.02	636	363	0.07	4.6	2.1	18.5	0.20	16.9	104	44.0	22.3	130	14.9	3.8	4.7
7-8	6.98	4.35	1.47	1.96	617	345	0.08	3.5	2.3	18.4	0.22	17.4	97.7	42.5	22.2	130	16.2	3.7	4.3
8-9	7.57	4.56	1.51	2.05	646	373	0.09	5.2	2.6	19.2	0.26	18.7	74.8	45.3	24.6	135	15.2	4.1	6.4
9-10	7.39	4.50	1.48	2.02	636	367	0.11	3.8	2.7	18.8	0.28	18.1	103	44.5	24.8	133	15.2	4.1	6.0
10-12	7.03	4.38	1.48	1.73	622	344	0.07	4.1	2.4	17.7	0.23	18.7	91.8	41.8	21.0	129	15.6	4.4	30.5
12-14	6.79	4.30	1.47	1.63	610	331	0.09	4.1	2.4	20.1	0.23	17.8	94.2	39.3	19.8	125	15.5	4.3	42.0
14-16	7.49	4.70	1.60	1.79	675	360	0.06	4.4	2.1	20.9	0.96	19.1	107	43.6	21.6	136	15.2	3.5	19.9
16-18	6.50	4.23	1.46	1.63	610	305	0.10	0.9	2.2	6.35	0.33	16.7	78	37.5	19.7	107	9.2	4.6	3.1
18-20	6.06	3.96	1.35	2.40	396	299	0.09	1.4	2.1	3.54	0.30	15.7	85	35.3	18.4	99	4.5	4.6	26.2
EB-7 (Basin)																			
0-1	6.86	4.45	1.50	1.02	618	1461	0.36	4.10	2.07	21.2	0.17	18.2	92.9	38.2	20.5	114	16.0	3.37	0.43
1-2	7.00	4.62	1.47	0.97	640	1453	0.36	6.55	2.28	21.8	0.17	19.9	97.7	37.0	20.1	111	14.5	3.29	0.42
2-3	6.83	4.58	1.43	0.93	638	1733	0.34	7.84	2.04	24.4	0.53	21.9	93.0	37.0	19.8	107	13.3	2.71	0.02
3-4	6.53	4.45	1.43	0.95	619	428	0.35	3.35	1.98	27.2	1.18	15.8	78.7	36.7	20.5	109	9.8	3.24	0.17
4-5	7.09	4.62	1.50	1.04	644	357	0.38	4.22	2.13	34.4	0.25	15.8	95.6	36.2	20.3	113	15.6	3.51	0.42
5-6	7.01	4.36	1.50	1.03	645	361	0.33	4.86	2.50	24.6	0.21	15.9	69.2	36.6	20.9	112	13.0	5.60	1.15
6-7	7.14	4.11	1.51	1.06	651	355	0.33	6.28	3.32	13.9	0.71	18.5	88.9	38.5	22.0	131	13.1	10.58	48.50

Table A4.10 (cont.) Trace metal content in shelf, slope, and basin sediments in the Alaskan Beaufort Sea.

	Al	Fe	Mg	Ca	Ba	Mn	Cd	Mo	U	As	Ag	Co	Cr	Ni	Cu	Zn	Pb	Re	AVS
	%	%	%	%	µg/g	µg/g	µg/g	µg/g	µg/g	µg/g	µg/g	µg/g	µg/g	µg/g	µg/g	µg/g	µg/g	ng/g	µmol/g
7-8	6.85	4.03	1.47	1.14	630	368	0.34	11.82	2.96	13.3	0.25	19.9	90.7	38.4	21.6	127	14.1	8.03	129.34
8-9	7.06	4.23	1.50	1.09	660	400	0.34	9.12	2.64	10.3	0.22	20.7	96.3	40.3	23.1	129	13.5	5.76	71.76
9-10	7.07	5.14	1.49	1.00	668	496	0.30	4.71	2.28	60.9	0.43	22.4	97.3	39.4	21.9	129	17.1	3.93	21.07
10-12	6.89	5.12	1.46	0.94	659	473	0.21	2.18	2.08	55.1	0.33	22.2	88.8	37.5	21.4	117	7.4	4.66	8.66
12-14	7.08	5.32	1.49	0.87	671	508	0.25	2.37	2.19	62.9	0.38	21.4	106.8	53.2	25.5	211	11.0	4.53	1.74
14-16	7.07	4.60	1.48	0.92	665	381	0.17	1.18	2.69	14.1	0.35	20.8	83.4	37.3	21.6	114	15.4	4.48	5.98
16-18	6.88	4.20	1.46	1.01	653	350	0.21	1.10	2.67	12.8	0.34	19.4	83.7	36.4	21.6	111	9.6	3.95	4.18
18-20	7.12	4.70	1.48	0.90	671	369	0.17	0.71	2.51	15.4	0.31	20.0	87.9	37.6	21.1	115	13.8	4.00	2.38
22	6.85	6.62	1.44	1.12	639	709	0.23	3.86	2.30	28.3	0.27	18.6	91.3	35.6	15.0	107	13.6	3.68	2.24

Table A5.1. Average (n=2) dissolved organic carbon concentrations (mg/L) from experimental microcosms throughout 2007 degradation experiments.

							DOC (mg/L)								
	Treatment	Control	Control	Algae	Algae	Algae	Algae	Peat	Peat	Peat	Peat	Mix	Mix	Mix	Mix
	Carboy	-1	5	-1A	-1B	5A	5B	-1A	-1B	5A	5B	-1A	-1B	5A	5B
Time (days)															
0		1.48	1.58	1.40	1.59	1.43	1.24	1.19	1.46	1.56	1.65	1.33	1.44	1.57	1.59
5		1.23	1.10	1.35	1.53	1.50	1.46	1.34	1.13	1.10	1.40	1.68	1.34	1.46	1.48
10		1.16	1.39	1.65	2.01	1.20	1.48	1.21	1.57	1.58	1.98	1.59	1.29	1.80	2.19
25		1.25	1.42	1.35	1.66	1.63	1.51	1.36	1.79	1.81	1.88	1.42	1.34	1.59	1.58

Bibliography

Allen, H.E., Fu, G.M. and Deng, B.L., 1993. Analysis of acid-volatile sulfide (AVS) and simultaneously extracted metals (SEM) for the estimation of potential toxicity in aquatic sediments. Environmental Toxicology and Chemistry, 12(8): 1441-1453.

Are, F., Reimnitz, E., Grigoriev, M.N., Hubberten, H.-W. and Rachold, V., 2008. The influence of cryogenic processes on the erosional Arctic shoreface. Journal of Coastal Research, 24(1): 110-121.

Arnarson, T.S. and Keil, R.G., 2005. Influence of organic-mineral aggregates on microbial degradation of the dinoflagellate *Scripsiella trochoidea*. Geochimica et Cosmochimica Acta, 69(8): 2111-2117.

Arnosti, C., Finke, N., Larsen, O. and Ghobrial, S., 2005. Anoxic carbon degradation in Arctic sediments: microbial transformations of complex substrates. Geochimica et Cosmochimica Acta, 69(9): 2309-2320.

Balino, B.M., Fasham, M.J.R. and Bowles, M.C., (eds.), 2001. Ocean Biogeochemistry and Global Change: JGOFS Research Highlights 1988-2000, 2. International Geosphere-Biosphere Programme, Stockholm, 32 pp.

Barrett, S.M., Volkman, J.K., Dunstan, G.A. and LeRoi, J.M., 1995. Sterols of 14 Species of Marine Diatoms (Bacillariophyta). Journal of Phycology, 31: 360-369.

Baskaran, M. and Naidu, A.S., 1995. ^{210}Pb-derived chronology and the fluxes of ^{210}Pb and ^{137}Cs isotopes into continental shelf sediments, East Chukchi Sea, Alaskan Arctic. Geochimica et Cosmochimica Acta, 59(21): 4435-4448.

Bates, N.R., Best, M.H.P. and Hansell, D.A., 2005a. Spatio-temporal distribution of dissolved inorganic carbon and net community production in the Chukchi and Beaufort Seas. Deep-Sea Research II, 52: 3303-3323.

Bates, N.R., Hansell, D.A., Moran, S.B. and Codispoti, L.A., 2005b. Seasonal and spatial distribution of particulate organic matter (POM) in the Chukchi and Beaufort Seas. Deep-Sea Research II, 52: 3324-3343.

Behrenfeld, M.J. and Falkowski, P.G., 1997. Photosynthetic rates derived from satellite-based chlorophyll concentration. Limnology and Oceanography, 42(1): 1-20.

Belchansky, G.I., Douglas, D.C. and Platonov, N.G., 2004. Duration of the Arctic sea ice melt season: regional and interannual variability, 1979-2001. Journal of Climate, 17: 67-80.

Belicka, L.L., 2002. Biochemical markers of carbon source and transport in the western Arctic Ocean, The University of Maryland, College Park, 137 pp.

Belicka, L.L., Macdonald, R.W. and Harvey, H.R., 2002. Sources and transport of organic carbon to shelf, slope, and basin surface sediments of the Arctic Ocean. Deep-Sea Research I, 49: 1463-1483.

Belicka, L.L., Macdonald, R.W., Yunker, M.B. and Harvey, H.R., 2004. The role of depositional regime on carbon transport and preservation in Arctic Ocean sediments. Marine Chemistry, 86: 65-88.

Belyaeva, A.N. and Eglinton, G., 1997. Lipid biomarker accumulation in the Kara Sea sediments. Oceanology, 37(5): 634-642.

Berner, R.A., 1989. Biogeochemical cycles of carbon and sulfur and their effect on atmospheric oxygen over Phanerozoic time. Palaeogeography, Palaeoclimatology, Palaeoecology, 73: 97-122.

Biasi, C. et al., 2005. Temperature-dependent shift from labile to recalcitrant carbon sources of arctic heterotrophs. Rapid Communications in Mass Spectrometry, 19: 1401-1408.

Birgel, D., Stein, R. and Hefter, J., 2004. Aliphatic lipids in recent sediments of the Fram Strait/Yermak Plateau (Arctic Ocean): composition, sources, and transport processes. Marine Chemistry, 88: 127-160.

Bischof, J.F. and Darby, D.A., 1997. Mid- to Late Pleistocene ice drift in the western Arctic Ocean: evidence for a different circulation in the past. Science, 277: 74-78.

Bligh, E.G. and Dyer, W.J., 1959. A rapid method of total lipid extraction and purification. Canadian Journal of Biochemistry and Physiology, 37(8): 911-917.

Booth, B.C. and Horner, R.A., 1997. Microalgae on the Arctic Ocean Section, 1994: species abundance and biomass. Deep-Sea Research II, 44(8): 1607-1622.

Bordowskiy, O.K., 1965. Sources of organic matter in marine basins. Marine Geology, 3: 5-31.

Boucsein, B., Knies, J. and Stein, R., 2002. Organic matter deposition along the Kara and Laptev Seas continental margin (eastern Arctic Ocean) during last deglaciation and Holocene: evidence from organic-geochemical and petrographical data. Marine Geology, 183: 67-87.

Boudreau, B.P. and Ruddick, B.R., 1991. American Journal of Science, 291: 507.

Bouloubassi, I. et al., 1997. Carbon sources and cycle in the western Mediterranean--the use of molecular markers to determine the origin of organic matter. Deep-Sea Research II, 44(3-4): 781-799.

Brinkmeyer, R. et al., 2003. Diversity and structure of bacterial communities in Arctic versus Antarctic pack ice. Applied and Environmental Microbiology, 69: 6610-6619.

Budge, S.M. and Parrish, C.C., 1998. Lipid biogeochemistry of plankton, settling matter, and sediments in Trinity Bay, Newfoundland. II. Fatty acids. Organic Geochemistry, 29(5-7): 1547-1559.

Canuel, E., 2001. Relations between river flow, primary production and fatty acid composition of particulate organic matter in San Francisco and Chesapeake Bays: A multivariate approach. Organic Geochemistry, 32(4): 563-583.

Canuel, E. and Zimmerman, A.R., 1999. Composition of particulate organic matter in the southern Chesapeake Bay: Sources and reactivity. Estuaries, 22(4): 980-994.

Cavalieri, D.J., Goersen, P., Parkinson, C.L., Comiso, J.C. and Zwally, H.J., 1997. Observed hemispheric asymmetry in global sea ice changes. Science, 278: 1104-1106.

Coachman, L.K. and Aagaard, K., 1966. On the water exchange through Bering Strait. Limnology and Oceanography, 11(1): 44-59.

Codispoti, L.A., Flagg, C., Kelly, V. and Swift, J.H., 2005. Hydrographic conditions during the 2002 SBI process experiments. Deep-Sea Research II, 52: 3199-3226.

Cooper, L.W., Larsen, I.L., Grebmeier, J.M. and Moran, S.B., 2005. Detection of rapid deposition of sea ice-rafted material to the Arctic Ocean benthos using the cosmogenic tracer ^{7}Be. Deep-Sea Research II, 52: 3452-3461.

Coyle, K.O. and Cooney, R.T., 1988. Estimating carbon flux to pelagic grazers in the ice-edge zone of the eastern Bering Sea. Marine Biology, 98: 299-306.

Crusius, J. and Kenna, T.C., 2007. Ensuring confidence in radionuclide-based sediment chronologies and bioturbation rates. Estuarine, Coastal, and Shelf Science, 71: 537-544.

Dalsgaard, J., St. John, M., Kattner, G., Muller-Navarra, D. and Hagen, W., 2003. Fatty acid trophic markers in the pelagic environment, Advances in Marine Biology. Academic Press Ltd., London.

Darby, D.A., Bischof, J.F. and Jones, G.A., 1997. Radiocarbon chronology of depositional regimes in the western Arctic Ocean. Deep-Sea Research II, 44: 1745-1757.

Davidson, E., Trumbore, S.E. and Amundson, E., 2000. Soil warming and organic carbon content. Nature, 408: 789-790.

De Leeuw, J.W. and Largeau, C., 1993. A review of macromolecular organic compounds that comprise living organisms and their role in kerogen, coal, and petroleum formation. In: M.H. Engel and S.A. Macko (Editors), Organic Geochemistry. Plenum Press, New York.

Dibb, J.E., 1992. The accumulation of 210Pb at Summit, Greenland since 1885. Tellus, 44B: 72-79.

Drenzek, N.J., Montlucon, D.B., Yunker, M.B., Macdonald, R.W. and Eglinton, T.I., 2007. Constraints on the origin of sedimentary organic carbon in the Beaufort Sea from coupled molecular ^{13}C and ^{14}C measurements. Marine Chemistry, 103: 146-162.

Dunton, K.H., Goodall, J.L., Schonberg, S.V., Grebmeier, J.M. and Maidment, D.R., 2005. Multi-decadal synthesis of benthic-pelagic coupling in the western arctic: Role of cross-shelf advective processes. Deep-Sea Research II, 52: 3462-3477.

Dyda, R.Y., 2005. Linking Phylogeny and Lipid Composition of Natural Bacterial Communities in Arctic Waters., University of Maryland, College Park, 156 pp.

Eglinton, G. and Hamilton, R.J., 1969. Leaf epicuticular waxes. Science, 156: 1322-1334.

Eglinton, G. and Logan, G.A., 1991. Molecular preservation. Philosophical Transactions of the Royal Society of London Series B--Biological Sciences, 333: 315-328.

Eicken, H., 2004. The role of Arctic Sea Ice in Transporting and Cycling Terrigenous Organic Matter. In: R. Stein and R.W. Macdonald (Editors), The Organic Carbon Cycle in the Arctic Ocean. Springer-Verlag, Berlin, pp. 45-52.

Eicken, H. et al., 2005. Sediment transport by sea ice in the Chukchi and Beaufort Seas: Increasing importance due to changing ice conditions? Deep-Sea Research II, 52(24-26): 3281-3302.

Emerson, S. and Hedges, J.I., 1988. Processes controlling the organic carbon content of open ocean sediments. Paleoceanography, 3: 621-634.

Fahl, K. and Nöthig, E.-M., 2007. Lithogenic and biogenic particle fluxes on the Lomonosov Ridge (central Arctic Ocean) and their relevance for sediment accumulation: Vertical versus lateral transport. Deep-Sea Research I, 54: 1256-1272.

Fahl, K. and Stein, R., 1997. Modern organic carbon deposition in the Laptev Sea and the adjacent continental slope: surface water productivity versus terrigenous input. Organic Geochemistry, 26(5/6): 379-390.

Fahl, K. and Stein, R., 1999. Biomarkers as organic-carbon-source and environmental indicators in the Late Quaternary Arctic Ocean: problems and perspectives. Marine Chemistry, 63: 293-309.

Falk-Petersen, S. et al., 1998. Lipids and fatty acids in ice algae and phytoplankton from the Marginal Ice Zone in the Barents Sea. Polar Biology, 20: 41-47.

Feder, H.M. et al., 1994. The northeastern Chukchi Sea: benthos-environmental interactions. Marine Ecology Progress Series, 111: 171-190.

Fernandes, M.B. and Sicre, M.-A., 2000. The importance of terrestrial organic carbon inputs on Kara Sea shelves as revealed by *n*-alkanes, OC and d13C values. Organic Geochemistry, 31: 363-374.

Fogel, M.L. and Cifuentes, L.A., 1993. Isotope fractionation during primary production. In: M.H. Engel and S.A. Macko (Editors), Organic Geochemistry. Plenum Press, New York, pp. 73-98.

Freeman, C., Evans, C.D., Monteith, D.T., Reynolds, B. and Fenner, N., 2001. Export of organic carbon from peat soils. Nature, 412: 785.

Frey, K.E. and Smith, L.C., 2005. Amplified carbon release from vast West Siberian peatlands by 2100. Geophysical Research Letters, 32(9): L09401,doi:10.1029/2004GL022025.

Gaye, B. et al., 2007. Particulate matter fluxes in the southern and central Kara Sea compared to sediments: Bulk fluxes, amino acids, stable carbon and nitrogen isotopes, sterols, and fatty acids. Continental Shelf Research, 27: 2570-2594.

Goad, L.J., Holz, G.G. and Beach, D.H., 1983. Identification of (24S)-24-methylcholesta-5,22-dien-3beta-ol as the major sterol of a marine cryptophyte and a marine prymnesiophyte. Phytochemistry, 22(2): 475-476.

Gobeil, C., Macdonald, R.W., Smith, J.N. and Beaudin, L., 2001. Atlantic water flow pathways revealed by lead contamination in Arctic basin sediments. Science, 293: 1301-1304.

Goericke, R. and Fry, B., 1994. Variations of marine plankton $\delta^{13}C$ with latitude, temperature, and dissolved CO2 in the world ocean. Global Biogeochemical Cycles, 8: 85-90.

Goñi, M.A., Yunker, M.B., Macdonald, R.W. and Eglinton, T.I., 2000. Distribution and sources of organic biomarkers in arctic sediments from the Mackenzie River and Beaufort Shelf. Marine Chemistry, 71: 23-51.

Gordeev, V.V., Martin, J.M., Sidorov, I.S. and Sidorova, M.V., 1996. A reassessment of the Eurasian river input of water, sediment, major elements, and nutrients to the Arctic Ocean. American Journal of Science, 296: 664-691.

Gordon, E.S. and Goñi, M., 2004. Controls on the distribution and accumulation of terrigenous organic matter in sediments from the Mississippi and Atchafalaya river margin. Marine Chemistry, 92: 331-352.

Gosselin, M., Levasseur, M., Wheeler, P.A., Horner, R.A. and Booth, B.C., 1997. New measurements of phytoplankton and ice algal production in the Arctic Ocean. Deep-Sea Research II, 44(8): 1623-1644.

Gradinger, R., in press. Sea ice algae: major contributors to primary production and algal biomass in the Chukchi and Beaufort Sea during May/June 2002. Deep-Sea Research II.

Grantz, A., Phillips, R.L. and Jones, G.A., 1999. Holocene pelagic and turbidite sedimentation rates in the Amerasian Basin, Arctic Ocean from radiocarbon age-depth profiles in cores. Geological Research Forum, 5: 209-222.

Grebmeier, J.M., 1993. Studies of pelagic-benthic coupling extended onto the Soviet continental shelf in the northern Bering and Chukchi seas. Continental Shelf Research, 13(5/6): 653-668.

Grebmeier, J.M. and Harvey, H.R., 2005. The western Arctic Shelf-Basin Interactions (SBI) project: An overview. Deep-Sea Research II, 52: 3109-3115.

Grebmeier, J.M., Smith, W.O.J. and Conover, R.J., 1995. Biological processes on arctic continental shelves: ice-ocean biotic interactions. In: W.O.J. Smith and J.M. Grebmeier (Editors), Arctic Oceanography: Marginal Ice Zones and Continental Shelves. American Geophysical Union, Washington, D.C., pp. 231-261.

Grutters, M., van Raaphorst, W. and Helder, W., 2001. Total hydrolysable amino acid mineralisation in sediments across the northeastern Atlantic continental slope (Goban Spur). Deep-Sea Research I, 48: 811-832.

Guo, L. and Macdonald, R.W., 2006. Source and transport of terrigenous organic matter in the upper Yukon River: evidence from isotope (d13C, D14C, and d15N) composition of dissolved, colloidal, and particulate phases. Global Biogeochemical Cycles, 20(GB2011): doi:10.1029/2005GB002593.

Guo, L., Ping, C.-L. and Macdonald, R.W., 2007. Mobilization Pathways of organic carbon from permafrost to arctic rivers in a changing climate. Geophysical Research Letters, 34(L13603): doi:10.1029/2007GL030689.

Guo, L. et al., 2004. Characterization of Siberian Arctic coastal sediments: implications for terrestrial carbon export. Global Biogeochemical Cycles, 18: GB1036.

Han, J., McCarthy, E.D., Calvin, M. and Benn, M.H., 1968. Hydrocarbon constituents of blue-green algae Nostoc muscorum, Anacystis nidulans, Phormidium luridum, and Chlorogloea fritschii. Journal of the Chemical Society C-Organic, 22: 2785.

Hare, C.E. et al., 2007. Consequences of increase temperature and CO2 for phytoplankton community structure in the Bering Sea. Marine Ecology Progress Series, 352: 9-16.

Harper, J.R., 1990. Morphology of the Canadian Beaufort Sea coast. Marine Geology, 91(1-2): 75-91.

Harvey, H.R., Dyda, R.Y. and Kirchman, D.L., 2006. Impact of DOM composition on bacterial lipids and community structure in estuaries. Aquatic Microbial Ecology, 42(2): 105-117.

Harvey, H.R. and Johnston, J.R., 1995. Lipid composition and flux of sinking and size-fractionated particles in Chesapeake Bay. Organic Geochemistry, 23(8): 751-764.

Harvey, H.R. and Macko, S.A., 1997. Kinetics of phytoplankton decay during simulated sedimentation: changes in lipids under oxic and anoxic conditions. Organic Geochemistry, 27(3/4): 129-140.

Harvey, H.R., Tuttle, J.H. and Bell, J.T., 1995. Kinetics of phytoplankton decay during simulated sedimentation: changes in biochemical composition and microbial activity under oxic and anoxic conditions. Geochimica et Cosmochimica Acta, 59(16): 3367-3377.

Hedges, J.I., 1992. Global biogeochemical cycles: progress and problems. Marine Chemistry, 39: 67-93.

Hedges, J.I., Clark, W.A. and Cowie, G.L., 1988a. Fluxes and reactivities of organic matter in a coastal marine bay. Limnology and Oceanography, 33: 1137-1152.

Hedges, J.I., Clark, W.A. and Cowie, G.L., 1988b. Organic matter sources to the water column and surficial sediments of a marine bay. Limnology and Oceanography, 33: 1116-1136.

Hedges, J.I. et al., 1986. Composition and fluxes of particulate organic material in the Amazon River. Limnology and Oceanography, 31: 717-738.

Hedges, J.I. and Keil, R.G., 1995. Sedimentary organic matter preservation: an assessment and speculative synthesis. Marine Chemistry, 49: 81-115.

Hedges, J.I., Keil, R.G. and Benner, R., 1997. What happens to terrestial organic matter in the ocean? Organic Geochemistry, 27(5/6): 195-212.

Herfort, L. et al., 2006. Characterization of transport and deposition of terrestrial organic matter in the southern North Sea using the BIT index. Limnology and Oceanography, 51(5): 2196-2205.

Hermanson, M.H., 1990. 210Pb and 137Cs chronology of sediments from small shallow Arctic lakes. Geochimica et Cosmochimica Acta, 54: 1443-1451.

Hill, V. and Cota, G., 2005. Spatial patterns of primary production on the shelf, slope, and basin of the Western Arctic in 2002. Deep-Sea Research II, 52: 3344-3354.

Hill, V., Cota, G. and Stockwell, D., 2005. Spring and summer phytoplankton communities in the Chukchi and Eastern Beaufort Seas. Deep-Sea Research II, 52: 3369-3385.

Hilmer, M. and Lemke, P., 2000. On the decrease of Arctic sea ice volume. Geophysical Research Letters, 27(22): 3751-3754.

Holmes, M.R. et al., 2002. A circumpolar perspective on fluvial sediment flux to the Arctic Ocean. Global Biogeochemical Cycles, 16(4): 10.1029/2002GB001920.

Hopmans, E.C. et al., 2004. A novel proxy for terrestrial organic matter in sediments based on branched and isoprenoid tetraether lipids. Earth and Planetary Science Letters, 224: 107-116.

Huh, C.-a., Pisias, N.G., Kelley, J.M., Maiti, T.C. and Grantz, A., 1997. Natural radionuclides and plutonium in sediments from the western Arctic Ocean: sedimentation rates and pathways of radionuclides. Deep-Sea Research II, 44(8): 1725-1743.

Hwang, J., Eglinton, T.I., Krishfield, R.A., Manganini, S.J. and Honjo, S., 2008. Lateral organic carbon supply to the deep Canada Basin. Geophysical Research Letters, 35: doi:10.1029/2008GL034271, 2008.

Ittekkot, V., 1988. Global trends in the nature of organic matter in river suspensions. Nature, 332: 436-438.

Jakobsson, M., 2002. Hypsometry of the Arctic Ocean and its constituent seas. Geochemistry Geophysics Geosystems, 3(5).

Jakobsson, M., Backman, J., Murray, A. and Lovlie, R., 2003. Optically stimulated luminescence dating supports central Arctic Ocean cm-scale sedimentation rates. Geochemistry Geophysics Geosystems, 4(2): 1016, doi:10.1029/2002GC000423, 2003.

Johannessen, O.M., Shalina, E.V. and Miles, M.W., 1999. Satellite evidence for an Arctic sea ice cover in transformation. Science, 286(5446): 1937-1939.

Johnson, K.M. and Sieburth, J.M., 1977. Dissolved carbohydrates in seawater. I. A precise spectrophotometric analysis for monosaccharides. Marine Chemistry, 5: 1-13.

Jones, E.P. and Anderson, L.G., 1986. On the origin of chemical properties of the Arctic Ocean halocline. Journal of Geophysical Research, 91: 10759-10767.

Killops, S.D. and Killops, V.J., 1993. An Introduction to Organic Geochemistry. John Wiley & Sons, Inc., New York, 265 pp.

Kirchman, D.L., Malmstrom, R.R. and Cottrell, M.T., 2005. Control of bacterial growth by temperature and organic matter in the western Arctic. Deep-Sea Research II, 52: 3386-3395.

Knies, J. and Stein, R., 1998. New aspects of organic carbon deposition and its paleoceanographic implications along the northern Barents Sea margin during the last 30,000 years. Paleoceanography, 13(4): 384-394.

Kristensen, E. and Holmer, M., 2001. Decomposition of plank materials in marine sediment exposed to different electron acceptors (O2, NO3-, and SO42-), with emphasis on substrate origin, degradation kinetics, and the role of bioturbation. Geochimica et Cosmochimica Acta, 65(3): 419-433.

Lantuit, H. and Pollard, W.H., 2008. Fifty years of coastal erosion and retrogressive thaw slump activity on Herschel Island, southern Beaufort Sea, Yukon Territory, Canada. Geomorphology, 95(1-2): 84-102.

Laws, E.A., Popp, B.N., Bidigare, R.R., Kennicutt, M.C. and Macko, S.A., 1995. Dependence of phytoplankton carbon isotopic composition on growth rate and [CO2]aq: theoretical considerations and experimental results. Geochimica et Cosmochimica Acta, 59(6): 1131-1138.

Lee, C., 1992. Controls on organic carbon preservation: the use of stratified water bodies to compare intrinsic rates of decomposition in oxic and anoxic systems. Geochimica et Cosmochimica Acta, 56: 3323-3335.

Lehmann, M.F., Bernasconi, S.M., Barbieri, A. and McKenzie, J.A., 2002. Preservation of organic matter and alteration of its carbon and nitrogen isotope composition during simulated and in situ early sedimentary diagenesis. Geochimica et Cosmochimica Acta, 66(20): 3573-3584.

Lepore, K., Moran, S.B. and Smith, J.N., in press. ^{210}Pb as a tracer of shelf-basin transport and sediment focusing in the Chukchi Sea. Deep-Sea Research II.

Macdonald, R.W., Naidu, A.S., Yunker, M.B. and Gobeil, C., 2004a. The Beaufort Sea: Distribution, Sources, Fluxes, and Burial of Organic Carbon. In: R. Stein and R.W. Macdonald (Editors), The Organic Carbon Cycle in the Arctic Ocean. Springer-Verlag, Berlin.

Macdonald, R.W., Sakshaug, E. and Stein, R., 2004b. The Arctic Ocean: Modern Status and Recent Climate Change. In: R. Stein and R.W. Macdonald (Editors), The Organic Carbon Cycle in the Arctic Ocean. Springer, Berlin.

Macdonald, R.W. et al., 1998. A sediment and organic carbon budget for the Canadian Beaufort Shelf. Marine Geology, 144: 255-273.

Maslanik, J.A., Serreze, M.C. and Barry, R.G., 1996. Recent decreased in Arctic summer ice cover and linkages to atmospheric circulation anomalies. Geophysical Research Letters, 23(13): 1677-1680.

Maslowski, W., Newton, B., Schlosser, P., Semtner, A. and Martinson, D., 2000. Modeling recent climate variability in the Arctic Ocean. Geophysical Research Letters, 27(22): 3743-3746.

Mayer, L.M., 1994. Relationships between mineral surfaces and organic carbon concentrations in soils and sediments. Chemical Geology, 114: 347-363.

Meyers, P.A., 1997. Organic geochemical proxies of paleoceanographic, paleolimnologic, and paleoclimatic processes. Organic Geochemistry, 27(5/6): 213-250.

Middelburg, J.J. and Meysman, F.J.R., 2007. Burial at Sea. Science, 316: 1294-1295.

Moore, R.M. and Smith, J.N., 1986. Disequilibria between 228Ra, 210Pb, and 210Po in the Arctic Ocean and the implications for chemical modification of the Pacific water inflow. Earth and Planetary Science Letters, 77: 285-292.

Moran, S.B. et al., 2005. Seasonal changes in POC export flux in the Chukchi Sea and implications for water column-benthic coupling in Arctic shelves. Deep-Sea Research II, 52: 3427-3451.

Muetzelfeldt, R. and Massheder, J., 2003. The Simile visual modelling environment. European Journal of Agronomy, 18: 345-358.

Naidu, A.S. et al., 2000. Organic carbon isotope ratios (d13C) of Arctic Amerasian continental shelf sediments. International Journal of Earth Sciences, 89: 522-532.

Naidu, A.S., Cooper, L.W., Grebmeier, J.M., Whitledge, T.E. and Hameedi, J.M., 2004. The Continental Margin of the North-Bering-Chukchi Sea: Concentrations, Sources, Fluxes, Accumulation, and Burial Rates of Organic Carbon. In: R. Stein and R.W. Macdonald (Editors), The Organic Carbon Cycle in the Arctic Ocean. Springer-Verlag, Berlin.

Naidu, A.S., Finney, B.P. and Baskaran, M., 1999. 210Pb- and 137Cs-based sediment accumulation rates in inner shelves and coastal lakes of subarctic and arctic Alaska: A synthesis. In: P. Bruns and H.C. Hass (Editors), On the Determination of Sediment Accumulation Rates, GeoResearch Forum 5. Trans Tech Publications, Switzerland, pp. 185-196.

Naidu, A.S. et al., 1993. Stable organic carbon isotopes in sediments of the north Bering-south Chukchi seas, Alaskan-Soviet Arctic Shelf. Continental Shelf Research, 13(5/6): 669-691.

Naraoka, H. and Ishiwatari, R., 2000. Molecular and isotopic abundances of long-chain *n*-fatty acids in open marine sediments of the western North Pacific. Chemical Geology, 165: 23-36.

NSIDC, 2008. Arctic Sea Ice News. National Snow and Ice Data Center.

O'Brien, M.C., Macdonald, R.W., Melling, H. and Iseki, K., 2006. Particle fluxes and geochemistry on the Canadian Beaufort Shelf: implications for sediment transport and deposition. Continental Shelf Research, 26: 41-81.

Opsahl, S., Benner, R. and Amon, R.M.W., 1999. Major flux of terrigenous dissolved organic matter through the Arctic Ocean. Limnology and Oceanography, 44(8): 2017-2023.

Osterkamp, T.E. and Romanovsky, V.E., 1999. Evidence for warming and thawing of discontinuous permafrost in Alaska. Permafrost and Periglacial Processes, 10(1): 17-37.

Ostrom, P.H. and Fry, B., 1993. Sources and Cycling of Organic Matter within Modern and Prehistoric Food Webs. In: M.H. Engel and S.A. Macko (Editors), Organic Geochemistry. Plenum Press, New York, pp. 785-798.

Pakulski, J.D. and Benner, R., 1992. An improved method for the hydrolysis and MBTH analysis of dissolved and particulate carbohydrates in seawater. Marine Chemistry, 40: 143-160.

Ping, C.-L. et al., 2008. High stocks of soil organic carbon in the North American Arctic region. Nature Geoscience, 1(9): 615-619.

Pirtle-Levy, R.S., Grebmeier, J.M., Cooper, L.W. and Larsen, I.L., in press. Chlorophyll *a* in Arctic sediments implies long persistence of algal pigments. Deep-Sea Research II.

Prahl, F.G. and Carpenter, R., 1984. Hydrocarbons in Washington coastal sediments. Estuarine, Coastal, and Shelf Science, 18: 703-720.

Prahl, F.G., Ertel, J.R., Goni, M., Sparrow, M.A. and Eversmeyer, B., 1994. Terrestrial organic carbon contributions to sediments on the Washington margin. Geochimica et Cosmochimica Acta, 58(14): 3035-3048.

Preiss, N., Melieres, M. and Pourchet, M., 1996. A compliation of data on lead 210 concentration in surface air and fluxes at the air-surface and water-sediment interfaces. Journal of Geophysical Research, 101: 28847-828862.

Rachold, V. et al., 2004. Modern Terrigenous Organic Carbon Input to the Arctic Ocean. In: R. Stein and R.W. Macdonald (Editors), The Organic Carbon Cycle in the Arctic Ocean. Springer-Verlag, Berlin, pp. 33-55.

Reimnitz, E., Barnes, P.W. and Weber, W.S., 1993. Particulate matter in pack ice of the Beaufort Gyre. Journal of Glaciology, 39: 186-198.

Rigor, I.G., Wallace, J.M. and Colony, R., 2002. Response of sea ice to the Arctic Oscillation. Journal of Climate, 15: 2648-2663.

Roach, A.T. et al., 1995. Direct measurements of transport and water properties through Bering Strait. Journal of Geophysical Research, 100: 18443-18457.

Rothman, D.H. and Forney, D.C., 2007. Physical model for the decay and preservation of marine organic carbon. Science, 316: 1325-1328.

Rothrock, D.S., Yu, Y. and Maykut, G.A., 1999. Thinning of the Arctic sea-ice cover. Geophysical Research Letters, 26(23): 3469-3472.

Sargent, J.R., Gatten, R.R. and Henderson, R.J., 1981. Marine Wax Esters. Pure and Applied Chemistry, 53(4): 867-871.

Schubert, C.J. and Calvert, S.E., 2001. Nitrogen and carbon isotopic composition of marine and terrestrial organic matter in Arctic Ocean sediments: implications for nutrient utilization and organic matter composition. Deep-Sea Research I, 48: 789-810.

Schubert, C.J. and Stein, R., 1996. Deposition of organic carbon in Arctic Ocean sediments: terrigenous supply versus marine productivity. Organic Geochemistry, 24(4): 421-436.

Schubert, C.J. and Stein, R., 1997. Lipid distribution in surface sediments from the eastern central Arctic Ocean. Marine Geology, 138: 11-25.

Schubert, C.J., Stein, R. and Calvert, S.E., 2001. Tracking nutrient and productivity variations over the last deglaciation in the Arctic Ocean. Paleoceanography, 16(2): 199-211.

Siegenthaler, U. and Sarmiento, J.L., 1993. Atmospheric carbon dioxide and the ocean. Nature, 365: 119-125.

Simoneit, B.R.T., 1989. Organic matter of the troposphere--V. Application of molecular marker analysis to biogenic emissions into the troposphere for source reconciliations. Journal of Atmospheric Chemistry, 8: 251-275.

Sinninghe Damsté, J.S., Schouten, S., Hopmans, E.C., Van Duin, A.C.T. and Geenevasen, J.A.J., 2002. Crenarchaeol: the characterisitic core glycerol dibiphytanyl glycerol tetraether membrane lipid of cosmopolitan pelagic crenarchaeota. Journal of Lipid Research, 43: 1641-1651.

Smith, D., 1998. Recent increase in the length of the melt season of perennial Arctic sea ice. Geophysical Research Letters, 25: 655-658.

Smith, J.N., Moran, S.B. and Macdonald, R.W., 2003. Shelf-basin interactions in the Arctic Ocean based on ^{210}Pb and Ra isotope tracer distributions. Deep-Sea Research I, 50: 397-416.

Stein, R. et al., 2004. Arctic (palaeo) river discharge and environmental change: evidence from the Holocene Kara Sea sedimentary record. Quaternary Science Reviews, 23: 1485-1511.

Stein, R. and Fahl, K., 2000. Holocene accumulation of organic carbon at the Laptev Sea continental margin (Arctic Ocean): sources, pathways, and sinks. Geo-Marine Letters, 20: 27-36.

Stein, R. and Fahl, K., 2004. The Laptev Sea: Distribution, Sources, Variability and Burial of Organic Carbon. In: R. Stein and R.W. Macdonald (Editors), The Organic Carbon Cycle in the Arctic Ocean. Springer-Verlag, Berlin, pp. 213-237.

Stein, R., Fahl, K., Niessen, F. and Siebold, M., 1999. Late Quaternary organic carbon and biomarker records from the Laptev Sea continental margin (Arctic Ocean): implications for organic carbon flux and composition. In: H. Kassens et al. (Editors), Land-Ocean Systems in the Siberian Arctic: Dynamics and History. Springer-Verlag, Berlin, pp. 635-655.

Stein, R., Grobe, H. and Wahsner, M., 1994a. Organic carbon, carbonate, and clay mineral distributions in eastern central Arctic Ocean surface sediments. Marine Geology, 119: 269-285.

Stein, R. and Macdonald, R.W., 2004a. Organic Carbon in Arctic Ocean Sediments: sources, variability, and paleoenvironmental significance. In: R. Stein and R.W. Macdonald (Editors), The Organic Carbon Cycle in the Arctic Ocean. Springer-Verlag, Berlin, pp. 170-314.

Stein, R. and Macdonald, R.W., (eds.), 2004b. The Organic Carbon Cycle in the Arctic Ocean. Springer-Verlag, Berlin, 363 pp.

Stein, R. et al., 1994b. The last deglaciation event in the eastern central Arctic Ocean. Science, 264: 692-695.

Stein, R., Schubert, C.J., Vogt, C. and Futterer, D.K., 1994c. Stable isotope stratigraphy, sedimentation rates, and salinity changes in the Latest Pleistocene to Holocene eastern central Arctic Ocean. Marine Geology, 119: 333-355.

Stein, R. and Stax, R., 1996. 22. Organic carbon and *n*-alkane distribution in late Cenozoic sediments of Arctic Gateways sites 909 and 911 and their paleoenvironmental implications: preliminary results. In: J. Thiede, A.M. Myhre, J.V. Firth, G.L. Johnson and W.F. Ruddiman (Editors), Proceedings of the Ocean Drilling Program, Scientific Results. Ocean Drilling Program, College Station, TX.

Stuiver, M. and Polach, H.A., 1977. Discussion, reporting of ^{14}C data. Radiocarbon, 19: 355-363.

Sun, M.-Y., Lee, C. and Aller, R.C., 1993. Laboratory studies of oxic and anoxic degradation of chlorophyll-*a* in Long Island Sound sediments. Geochimica et Cosmochimica Acta, 57: 147-157.

Tegelaar, E.W., de Leeuw, J.W., Derenne, S. and Largeau, C., 1989. A reappraisal of kerogen formation. Geochimica et Cosmochimica Acta, 53: 3103-3106.

Tolosa, I. et al., 2003. Distribution of sterol and fatty alcohol biomarkers in particulate matter from the frontal structure of the Alboran Sea (S.W. Mediterranean Sea). Marine Chemistry, 82: 161-183.

Tremblay, J.-E., Michel, C., Hobson, K.A., Gosselin, M. and Price, N.M., 2006. Bloom dynamics in early opening waters of the Arctic Ocean. Limnology and Oceanography, 51(2): 900-912.

Volkman, J.K., 1986. A Review of Sterol Markers for Marine and Terrigenous Organic Matter. Organic Geochemistry, 9(2): 83-99.

Volkman, J.K., 2006. Lipid markers for marine organic matter. In: J.K. Volkman (Editor), Handbook of Environmental Chemistry. Springer-Verlag, Berlin Heidelberg.

Volkman, J.K. et al., 1998. Microalgal biomarkers: a review of recent research developments. Organic Geochemistry, 29(5-7): 1163-1179.

Volkman, J.K., Barrett, S.M., Dunstan, G.A. and Jeffrey, S.W., 1993. Geochemical significance of the occurrence of dinosterol and other 4-methyl sterols in a marine diatom. Organic Geochemistry, 20(1): 7-15.

Volkman, J.K., Farmer, C.L., Barrett, S.M. and Sikes, E.L., 1997. Unusual dihydroxysterols as chemotaxonomic markers for microalgae from the order Pavlovales (Haptophyceae). Journal of Phycology, 33(6): 1016-1023.

Volkman, J.K., Jeffrey, S.W., Nichols, P.D., Rogers, G.I. and Garland, C.D., 1989. Fatty acid and lipid composition of 10 species of microalgae used in mariculture. Journal of Experimental Marine Biology and Ecology, 128: 219-240.

Wakeham, S.G., 1999. Monocarboxylic, dicarboxylic and hydroxy acids released by sequential treatments of suspended particles and sediments of the Black Sea. Organic Geochemistry, 30: 1059-1074.

Wakeham, S.G. and Beier, J.A., 1991. Fatty acid and sterol biomarkers as indicators of particulate matter source and alteration processes in the Black Sea. Deep-Sea Research I, 38(Supplement 2): S943-S968.

Wakeham, S.G. et al., 1980. Organic matter fluxes from sediment traps in the equatorial Atlantic Ocean. Nature, 286: 798-800.

Walsh, J.J. et al., 2005. A numerical model of seasonal primary production within the Chukchi/Beaufort Seas. Deep-Sea Research II, 52: 3541-3576.

Walsh, J.J. et al., 1989. Carbon and nitrogen cycling within the Bering/Chukchi seas: source regions for organic matter effecting AOU demands of the Arctic Ocean. Prog. Oceanogr., 22: 277-359.

Wang, J., Cota, G. and Comiso, J., 2005. Phytoplankton in the Beaufort and Chukchi Seas: Distribution, dynamics, and environmental forcing. Deep-Sea Research II, 52(24-26): 3355-3368.

Wannigama, G.P., Volkman, J.K., Gillan, F.T., Nichols, P.D. and Johns, R.B., 1981. A comparison of lipid components of fresh and dead leaves and pneumatophores of the mangrove *Avicennia marina*. Phytochemistry, 20: 659-666.

Wassmann, P. et al., 2004. Particulate organic carbon flux to the Arctic Ocean sea floor. In: R. Stein and R.W. Macdonald (Editors), The Organic Carbon Cycle in the Arctic Ocean. Springer-Verlag, Berlin.

Weijers, J.W.H., Schouten, S., Spaargaren, O.C. and Sinninghe Damsté, J.S., 2006. Occurrence and distribution of tetraether membrane lipids in soils: Implications for the use of the TEX_{86} proxy and the BIT index. Organic Geochemistry.

Weijers, J.W.H., Schouten, S., van den Donker, J.C., Hopmans, E.C. and Sinninghe Damsté, J.S., 2007. Environmental controls on bacterial tetraether membrane lipid distribution in soils. Geochimica et Cosmochimica Acta, 71: 703-713.

Weingartner, T.J. et al., 2005. Circulation on the north central Chukchi Sea shelf. Deep-Sea Research II, 52: 3150-3174.

Westrich, J.T. and Berner, R.A., 1984. The role of sedimentary organic matter in bacterial sulfate reduction: the G model tested. Limnology and Oceanography, 29: 236-249.

Wheeler, P.A. et al., 1996. Active cycling of organic carbon in the central Arctic Ocean. Nature, 380: 697-699.

Woodgate, R., Aagaard, K. and Weingartner, T.J., 2005. A year in the physical oceanography of the Chukchi Sea: Moored measurements from autumn 1990-1991. Deep-Sea Research II, 52: 3116-3149.

Yamamoto, M., Okino, T., Sugisaki, S. and Sakamoto, T., 2008. Late Pleistocene changes in terrestrial biomarkers in sediments from the central Arctic Ocean. Organic Geochemistry, 39: 754-763.

Yunker, M.B., Backus, S.M., Graf Pannatier, E., Jeffries, D.S. and Macdonald, R.W., 2002. Sources and significance of alkane and PAH hydrocarbons in Canadian Arctic rivers. Estuarine, Coastal, and Shelf Science, 55: 1-31.

Yunker, M.B., Belicka, L.L., Harvey, H.R. and Macdonald, R.W., 2005. Tracing the inputs and fate of marine and terrigenous organic matter in Arctic Ocean sediments: a multivariate analysis of lipid biomarkers. Deep-Sea Research II, 52(24-26): 3478-3508.

Yunker, M.B., Macdonald, R.W., Cretney, W.J., Fowler, B.R. and McLaughlin, F.A., 1993a. Alkane, terpene, and polycyclic aromatic hydrocarbon geochemistry of the Mackenzie River and Mackenzie Shelf: riverine contributions to Beaufort Sea coastal sediment. Geochimica et Cosmochimica Acta, 57: 3041-3061.

Yunker, M.B., Macdonald, R.W., Veltkamp, D.J. and Cretney, W.J., 1995. Terrestrial and marine biomarkers in a seasonally ice-covered Arctic estuary--integration of multivariate and biomarker approaches. Marine Chemistry, 49: 1-50.

Yunker, M.B., Macdonald, R.W. and Whitehouse, B.G., 1993b. Phase associations and lipid distributions in the seasonally ice-covered Arctic estuary of the Mackenzie Shelf. Organic Geochemistry, 22(3-5): 651-669.

Yunker, M.B., Macdonald, R.W. and Whitehouse, B.G., 1994. Phase associations and lipid distributions in the seasonally ice-covered Arctic estuary of the Mackenzie Shelf. Organic Geochemistry, 22: 651-669.